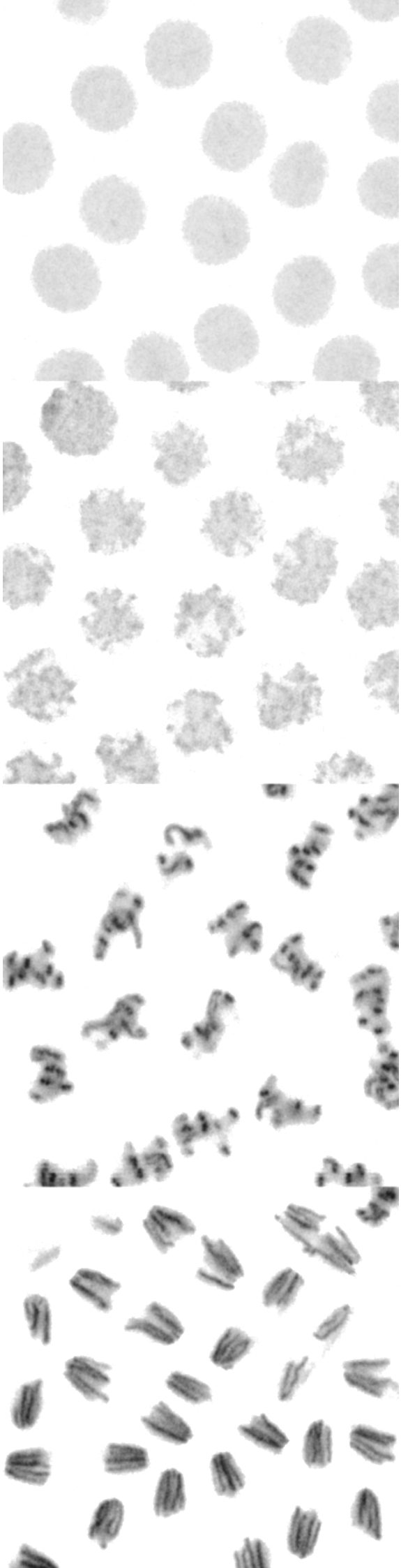

Condensins and mitotic chromosome structure:

functional and dynamic analysis in *Drosophila melanogaster*

Raquel Aguiar Cardoso de Oliveira

Dissertação de candidatura ao grau de Doutor em Bioquímica, especialidade de Biologia Molecular, submetida à Faculdade de Ciências e Tecnologia, Universidade de Coimbra

Orientador - Professor Doutor Claudio E. Sunkel

Coimbra 2007

Este trabalho teve o apoio financeiro da Fundação para a Ciência e Tecnologia (SFRH/BD/9683/2002), co-financiada pelo POCI2010 e pelo FSR.

A referida bolsa foi atribuída no âmbito do Programa Doutoral em Biologia Experimental e Biomedicina, Centro de Neurociências e Biologia Celular, Universidade de Coimbra.

UNIÃO EUROPEIA
Fundo Social Europeu

FCT Fundação para a Ciência e a Tecnologia
MINISTÉRIO DA CIÊNCIA E DA TECNOLOGIA
Portugal

Ciência.Inovação 2010
Programa Operacional Ciência e Inovação 2010
MINISTÉRIO DA CIÊNCIA, TECNOLOGIA E ENSINO SUPERIOR

PhD Programme
Biologia Experimental e Biomedicina
University of Coimbra

De acordo com o disposto no nº 2 do Artº 8º do Decreto-Lei nº 388/70, nesta dissertação foram utilizados resultados das publicações abaixo indicadas. No cumprimento do disposto no referido Decreto-Lei, a autora desta dissertação declara que interveio na concepção e na execução do trabalho experimental, na interpretação dos resultados e na redacção dos manuscritos publicados, sob o nome de Oliveira, R.A.:

Oliveira, R.A., Coelho, P.A., and Sunkel, C.E. (2005). The condensin I subunit Barren/CAP-H is essential for the structural integrity of centromeric heterochromatin during mitosis. *Mol Cell Biol* 25(20): 8971-8984.

Oliveira, R.A., Heidmann, S., and Sunkel, C.E. (2007). Condensin I binds chromatin early in prophase and displays a highly dynamic association with *Drosophila* mitotic chromosomes. *Chromosoma*, in press.

Acknowledgments/Agradecimentos

Serão estas as últimas palavras a ser escritas nesta tese. Contudo, serão certamente as mais importantes. Porque raramente um doutoramento é um percurso solitário, e neste caso certamente não o foi, guardo este espaço para expressar a minha enorme gratidão a todos aqueles que de uma forma ou de outra contribuíram para que esta tese fosse possível.

Ao Professor Claudio E. Sunkel, por me ter aceite como sua aluna de doutoramento e me apresentar o fantástico mundo do ciclo celular e das moscas. Pela orientação, pelas construtivas discussões, pela confiança, e também pela liberdade científica que serviu de estímulo à minha criatividade.

A todos os que ao longo destes anos fizeram parte "dos cromossomas". De uma forma muito especial, à Paula Coelho, presença constante durante todo este trabalho, pela imprescindível ajuda, dedicação, entusiasmo e espírito crítico. Agradeço também ao Søren Steffensen pela sua contribuição neste trabalho.

Ao Helder Maiato e à Elsa Logarinho, com quem dei os primeiros passos no laboratório.

À Carla Lopes e ao Nicolas Malmanche, pela imprescindível ajuda nas moscas, espírito crítico e sugestões.

Ao André Maia, pelas produtivas discussões, pela companhia nos congressos e pela amizade que foi crescendo ao londo destes anos.

À Rita Reis, pela genuidade, pelas gargalhadas e por sem saber, me ter tornado uma pessoa melhor.

À Susana Gouveia, à Augusta Monteiro, à Filipa Sousa e ao Bernardo Orr, pelos bons momentos, dentro e fora do laboratório, que alegraram estes anos.

À Adelaide Santos, à Maria João Falcão e à Susana Aveiro, pela preciosa ajuda.

A todos os outros que fizeram parte do "Sunkel lab" durante estes anos, e que aqui não enunciei em particular. Aos "mais velhos", pelo exemplo, pelas boas sugestões e espírito crítico e por toda a ajuda e disponibilidade. Aos "mais novos", pelo estímulo, pela paciência e por apesar da pouca experiência terem o entusiasmo de contribuir com novas ideias e sugestões (não é Torcato?!).

Aos BEB1, companheiros desta primeira maratona bébica, pelos bons tempos em Coimbra e pelo companheirismo ao longo destes anos. A todos os responsáveis pelo Programa Doutoral em Biologia Experimental e Biomedicina, pela oportunidade. Em particular, ao Professor Carlos Faro, pelas palavras positivas, sempre na altura certa.

I want to thank everyone at Lehner's lab for the warm welcome to the cold German winter. In particular, I thank Christian Lehner, for accepting me as part of his lab and for the constructive criticism and ideas. Very special thanks go to Stefan Heidmann, for all the teachings, the enthusiasm, the "German perfectionism" and for being so easy to work with. More personally, I thank Sebastian Heeger for the (not only!) scientific discussions, for the trips across Germany and for the great fun.

I especially thank Volker Nussgräber, for the fantastic cover design and for much more.

A todos os meus amigos, simplesmente por o serem.

Aos meus pais por tudo o que aquilo que não pode ser aqui escrito, e por nesta fase, sem saberem ao certo o que são cromossomas nem porque é que se trabalha com moscas, terem sempre acreditado em mim. À minha irmã Gabriela por toda a ajuda durante a realização desta tese e acima de tudo, pelo exemplo que ao longo dos anos tive o prazer de (tentar) seguir. Ao meu irmão Tiago, pela alegria. À Salomé, simplesmente por existir.

Por fim, ao Nuno, por todo o amor e carinho, pela companhia, pelo incondicional apoio, e por durante estes anos, perdoar os "15 minutos" de laboratório. E porque tudo teria sido bem mais difícil sem ti, esta tese também é tua!

A todos, um sincero MUITO OBRIGADA!

Contents

PART II – EXPERIMENTAL WORK

Chapter 1 – Role of Condensin I in mitotic chromosome architecture and structural integrity of the centromere

Chapter 2 – Dynamics of condensin I association with mitotic chromatin in *Drosophila*

Chapter 3 – Preliminary studies on the Condensin II complex of *Drosophila melanogaster*

Summary

The condensed state of mitotic chromosomes is crucial for the faithful segregation of the genome during cell division. Chromosome condensation not only allows the physical compaction of chromatin but also promotes the resolution of topological problems such as intertwines between sister chromatids and different chromosomes. Key factors implicated in the formation of mitotic chromosomes are the condensin I and II complexes. However, the exact contribution of these complexes and the molecular mechanisms involved are far from being understood. The work reported in this thesis aims to further our understanding on the role of condensins in the structure of mitotic chromosome in *Drosophila melanogaster*. The first part of the thesis describes the phenotypic analysis of S2 cells in which the condensin I subunit Barren/CAP-H was depleted. The results showed that mitotic chromosomes are able to condense but fail to resolve sister chromatids. Additionally, Barren/CAP-H-depleted cells show chromosome congression defects that are not associated to abnormal kinetochore-microtubule interaction. Instead, the centromeric and pericentromeric heterochromatin of Barren/CAP-H-depleted chromosomes shows severe structural abnormalities. The data suggests that centromeric heterochromatin organized in the absence of Barren/CAP-H cannot withstand the forces exerted by the mitotic spindle and undergoes irreversible distortion. The second part of the thesis reports the *in vivo* analysis of the dynamic behavior of condensin I during early embryonic divisions. We find that Barren-EGFP associates with chromatin early in prophase concomitantly with the initiation of chromosome condensation. Barren-EGFP loading starts at the centromeric region from where it spreads distally reaching maximum accumulation at metaphase/early anaphase. Furthermore, FRAP analysis indicates that most of the bound protein exchanges rapidly with the cytoplasmic pool during mitosis. In the third the role of condensin II specific subunits was addressed. The results, although preliminary, indicate that this complex does not seem to be involved in mitotic chromosome structure. Taken together, the results elucidate a new function for the condensin I complex in the maintenance of pericentromeric chromatin rigidity. In addition, the dynamic chromatin association of condensin I reveals that this complex cannot be trapping chromatin loops statically, as proposed in some of the current models but supports a model in which the assembly and maintenance of the mitotic chromosome involves a highly dynamic behavior of condensin I.

Resumo

O estado condensado dos cromossomas mitóticos é fundamental para uma eficiente segregação do genoma durante a mitose. A condensação dos cromossomas permite não só a compactação física da cromatina mas também a resolução de problemas topológicos como concatâmeros existentes entre as cromátidas irmãs e entre diferentes cromossomas. Os complexos condensina I e II são importantes factores envolvidos na formação dos cromossomas mitóticos. Contudo, a sua exacta contribuição, bem como os mecanismos moleculares envolvidos, não são ainda completamente compreendidos. O trabalho apresentado nesta tese teve como principal objectivo alargar o conhecimento do papel dos complexos condensina na estrutura dos cromossomas mitóticos em *Drosophila melanogaster*. A primeira parte da tese descreve a análise fenotípica de células de cultura S2, nas quais a subunidade do complexo condensina I Barren/CAP-H foi depletada. Os resultados mostram que os cromosomas mitóticos são capazes de condensar, mas não de resolver as cromátidas irmãs. Células depletadas de Barren/CAP-H apresentam defeitos na congressão para a placa metafásica os quais não se devem a uma incorrecta ligação dos cromosomas ao fuso mitótico mas sim a problemas estruturais na heterocromatina centromérica e pericentromérica. Após o estabelecimento de ligação bipolar, a cromatina centromérica, organizada na ausência de Barren/CAP-H, é incapaz de resistir às forças exercidas pelo fuso e sofre distorção irreversível. A segunda parte da tese reporta a análise *in vivo* do comportamento dinâmico do complexo condensina I durante as divisões sinciciais do embrião de *Drosophila*. Esta análise mostra que a proteina de fusão Barren-EGFP se associa à cromatina durante a profase, concomitantemente com o início da condensação dos cromossomas. A associação ocorre inicialmente na região centromérica, e posteriormente estende-se para os braços dos cromossomas, atingindo um máximo de acumulação durante metaphase/anaphase. Análises de FRAP indicam que a maior parte da proteina associada à cromatina se encontra em contínua troca de subunidades com o conteúdo citoplasmático durante prometafase/metaphase. A terceira parte descreve uma análise preliminar sobre a função do complexo condensina II em *Drosophila* a qual sugere que este complexo não está envolvido na organização dos cromosomas mitóticos. Os resultados apresentados revelam uma nova função para o complexo condensina I na manutenção da rigidez da cromatina pericentromérica. Adicionalmente, a dinâmica associação do complexo condensina I aos cromossomas demonstra que este complexo não se encontra estaticamente aprisionando a cromatina, como proposto em alguns modelos, e sugere um modelo no qual a formação dos cromossomas mitóticos envolve um comportamento altamente dinâmico do complexo condensina I.

Résumé

L'état condensé des chromosomes mitotique est essentiel pour la ségrégation du génome durant la division cellulaire. La condensation des chromosomes n'assure pas seulement la compaction de la chromatine, mais aussi permet la résolution de problèmes topologiques tels que les concatomeres des chromatides sœur ou entre les chromosomes Les éléments clefs implique dans la formation des chromosomes mitotiques sont les complexes condensin I et II. Cependant la contribution de ces complexes et le mécanisme moléculaire impliques sont loin d'être compris. Le travail présenté dans cette thèse apporte une meilleure compréhension pour le rôle des complexes condensin durant la formation des chromosomes mitotiques chez *Drosophila melanogaster*. La première partie décrit l'analyse phénotypique dans les cellules S2 de la déplétion de la sous-unite Barren/CAP-H présente dans le complexe condensin I. Les résultats montrent que les chromosomes mitotiques peuvent condenser mais ne sont pas capable de résoudre les chromatides sœurs. De plus, les cellules S2 déplétées de Barren/CAP-H présentent des défauts durant la congression des chromosomes indépendamment de l'interaction entre les microtubules et les kinetechores mais l'heterochromatine centroméric et peri-centromeric présentent de sérieux défauts structuraux. Nos résultats suggèrent que l'heterochromatin centroméric ne puisse soutenir les forces exercer par le spindle et subit une distorsion irréversible. La deuxième partie décrit l'analyse *in vivo* du comportement du complexe condensin I durant les divisions embryonnaires précoces. Nous montrons que Barren/CAP-H s'associe avec la chromatine durant le debout de la prophase, au moment de l'initiation de la condensation des chromosomes. Son association débute dans la région centroméric, et s'associe dans les régions distales avec une accumulation maximum a la métaphase/début de l'anaphase. De plus, l'analyse par FRAP indique que le majeur parti de la protéine Barren/CAP-H associée avec la chromatine est échangée de manière rapide avec la protéine cytoplasmique durant la mitose. La troisième partie présente des résultats préliminaires concernant le complexe Condensin II. Nos résultats indiquent que ce complexe ne semble pas être implique dans la structure des chromosomes mitotiques. Les résultats présentés ici élucident une nouvelle fonction du complexe Condensin I dans la maintenance de la rigidité de la chromatine peri-centromeric. De plus, l'étude de l'association dynamique du complexe Condensin I indique qu'il ne peut piéger les boucles de chromatine d'une manière statique, comme suggère dans certain modèle actuel. Nos résultats supportent un modèle dans lequel l'assemblage et le maintient des chromosomes mitotiques impliquent un comportement extrêmement dynamique du complexe condensin I.

PART I

GENERAL INTRODUCTION

1 – The Cell Division Cycle

The cell division cycle is a central process in Cell Biology that has fascinated scientist for centuries. Since the consolidation of the cell theory, which brought the concept that all the living organisms are made by cells, and the discovery that every cell is derived from pre-existing cells ("*omnis cellulla e cellulla*") (Rudolf Virshaw), extensive research aiming to understand how cells divide has been carried out. In 1879 Walter Flemming reports the first full description of cell division (reedited in Flemming 1965). He described that cells found in a resting state, undergo a particular sequence of changes in the nucleus that can be observed during each nuclear division. He showed that the threads (later called chromosomes) shorten and organize at the cell centre, in an equatorial plate, and split longitudinally into two halves, each half moving to opposite sides of the cell. He named this process of nuclear division mitosis (from the Greek, division of the threads).

1.1 – The cell division cycle – a general description

The cell division cycle is nowadays defined as the complete series of events in a cell between one cell division and the next. Through cell division, one parental cell gives rise to two genetically identical daughter cells and at each cell division cycle, cells are able to proliferate, grow and eventually differentiate. Therefore, the cell division cycle is a universal process by which a fertilized oocyte ultimately develops into a complex multicellular organism and by which the mature organism is maintained by continuous cell renewal.

The cell division cycle is a highly ordered and strictly regulated process. The eukaryotic cell cycle can be divided in two fundamental parts (Fig. 1): a long phase, called interphase, which comprises the period between two cell division events and where cells continuously grow and synthesize all essential cellular components, and a shorter stage, named mitosis, where the nuclear division takes place. After nuclear division, the formation of the two daughter cells is ultimately achieved the division of the cytoplasm, known as cytokinesis.

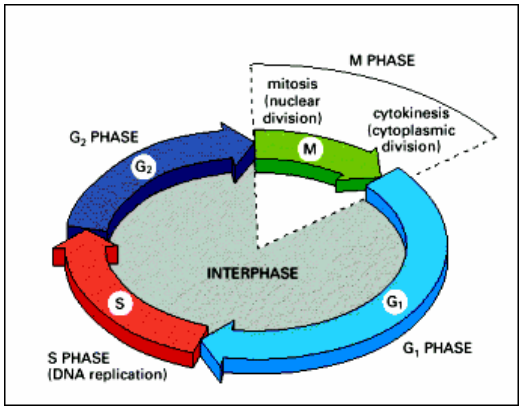

Figure 1. The eukaryotic cell cycle. The relative duration of each phase is variable in length and depends on the cell type, organism and developmental stage. While in G1, cells can exit the cycle into a G0 stationary phase and later return to G1. In later stages of G1, the cell becomes committed to cell division and begins DNA synthesis, which occurs in S phase. During G2 the cell prepares for mitosis, when the genetic material is segregated and the cell divides. After nuclear and cytoplasmic divisions, the cell re-enter in G1 for a new cycle (adapted from Alberts et al. 2002).

In interphase, most cells are morphologically indistinguishable with the chromatin dispersed within the nucleus and where individual chromosomes are not clearly discerned. Despite the absence of morphological changes, interphase can be further divided into different phases given that at each particular stage, cells have a distinct set of specialized biochemical processes that prepare them for the following stage. In G1 phase (Gap 1), the cell carries on its metabolic activities and is receptive to extracellular signals, such as soluble growth factors and intracellular contact. According to these signals cells have three possibilities: 1) to exit the cell cycle and enter a non-proliferative stage, G0, 2) to enter a differentiating pathway and express tissue specific factors or 3) to enter the cell cycle and proliferate once more. Cells in G0 can re-enter the cell cycle program after a long period of time, and do so by going back to G1. For cells committed to proliferation, the later events of the G1 phase are related to the preparation for the subsequent stage, DNA replication. These preparations often include a massive growth by increasing the amount of cytoplasm and important cellular organelles such as mitochondria, membrane, endoplasmatic reticulum, ribosomes and most cellular proteins, including the enzymatic machinery required for DNA synthesis. During S-phase (S=synthesis) cells synthesize an exact replica of the genome DNA, so that in the following nuclear division, each chromosome is composed of two identical sister chromatids. During S phase, cells also replicate their centrosomes (in animal cells centrosomes define the major microtubule organizing center -MTOC) but these remain together until the onset of mitosis. Once DNA replication is complete, cells enter a second Gap phase, G2, in which cells

continue to grow and prepare themselves for the subsequent nuclear division, mitosis, a process where cells separate their duplicated genome into two identical halves.

1.2 – Mitosis

Mitosis is a continuous and dynamic process by which cells equally separate their duplicated genome. For purposes of description, this process is conventionally divided into five sub-stages, based on the major structural changes that take place: prophase, prometaphase, metaphase, anaphase and telophase (Fig. 2).

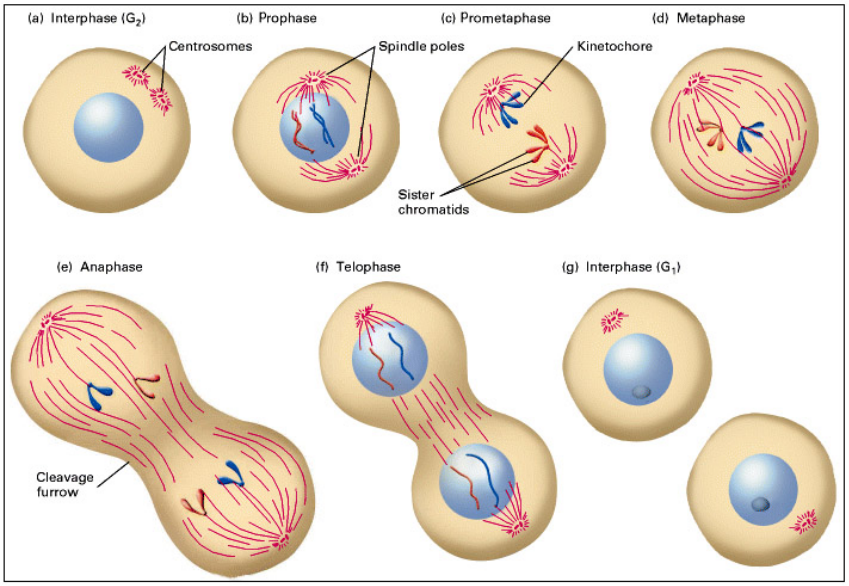

Figure 2. The stages of mitosis and cytokinesis in an animal cell. While in G2 (a) the chromosomes, each containing a sister chromatid, are dispersed and not visible as distinct structures. As prophase is initiated (b) the centrosomes begin to move towards opposite poles of the cell and the chromosomes start to be seen as long threads. When nuclear envelope breakdown, prometaphase (c) starts where chromosome condensation is completed and each visible chromosome structure is composed of two chromatids held together at their centromeres. Chromosomes are captured by microtubules growing from opposite poles, which contribute to chromosome congression and alignment at the metaphase plate (d). At anaphase onset (e) the two sister chromatids separate into independent chromosomes and segregate to opposite poles of the cell. By the end of mitosis, in telophase (f), the chromosomes decondense and the nuclear membrane re-forms around the daughter nuclei. Cytoplasm division, or cytokinesis, occurs concomitantly with the later mitosis stages, giving rise to two daughter cells (g) (Adapted from Lodish et al. 2000).

During prophase, dramatic chromatin morphological changes occur. The replicated DNA starts to progressively condense into a highly ordered thread like structures, known as chromosomes, and different chromosomes become distinct from each other. Prophase

chromosomes consist in a pair of sister chromatids that are joined throughout their length and contain each a kinetochore mostly located at the primary constriction.

Concomitantly with the nuclear changes replicated centrosomes migrate to opposite poles of the cell and start to nucleate microtubules, re-organizing the interphase microtubule array into the mitotic spindle, a microtubule-based bipolar structure responsible for chromosome movements during mitosis. In higher eukaryotes, the end of prophase and consequent beginning of prometaphase is dictated by the breakdown of the nuclear envelope (NEBD). As NEBD occurs, microtubules emanating from opposite centrosomes start to overlap in the equatorial region of the cell and give rise to the interpolar microtubules which help to stabilize the bipolar configuration of the mitotic spindle. In addition, astral microtubules grow from the MTOC towards the cell cortex which is thought to provide physical support for this highly dynamic structure. Simultaneously, the loss of the structural barrier between the nucleus and the cytoplasm allows for the first time a physical contact of mitotic chromosomes with microtubules from the mitotic spindle.

Thus, the chromosomes can attach to the spindle microtubules by a process known as “search and capture” (Kirschner and Mitchison 1986; for review see Maiato and Sunkel 2004). Microtubules are nucleated at the MTOCs in a random direction, forming large asters where each microtubule can either grow or shrink. This highly dynamic behavior allows microtubules to explore the cytoplasmic space and eventually encounter individual kinetochores. The chromosome initially becomes attached to a single pole and is said to be mono-oriented. This helps to orient the kinetochore of the other sister chromatid so that it now faces the other pole and microtubules growing from the opposite pole ultimately reach the free kinetochore. Once both sister chromatids of a chromosome are correctly attached to microtubules from opposite spindle poles the chromosome is said to have established a bipolar attachment. The microtubules that attach kinetochores are known as kinetochore microtubules and are responsible for the forces that drive chromosome congression, a process by which the chromosomes are pulled back and forth to finally reach an equilibrium position (chromosome alignment) midway between the poles at a stage called metaphase.

When every kinetochore is attached to a kinetochore fibber and the chromosomes have been properly aligned at the metaphase plate, the cell can proceed the final events of chromosome segregation that involve the separation of sister chromatids and their migration to opposite poles in a process called anaphase. The initial events of anaphase, anaphase A,

include the loss of the link between sister chromatid and their rapid movement to opposite poles as kinetochore microtubules shorten. Later, during anaphase B, the overall mitotic spindle elongates, pushing centrosomes further away of each other to opposite ends of the cells. Finally, during telophase, each set of chromatids decondenses while the nuclear envelope re-forms, giving rise to two daughter nuclei. Cytokinesis or cytoplasm division occurs concomitantly with the later events of nuclear division. In animal cells, a process known as cleavage takes place, in which the cytoplasm constricts at the cell centre through the formation of a ring of actin and myosin microfilaments until the two cells eventually separate.

1.3 – Cell cycle transitions and cell cycle checkpoints

In order to ensure a faithful segregation of the genome, cells have to guarantee that cell cycle progression occurs unidirectionally and that every time the genome is fully replicated, segregation of sister chromatids during mitosis. This is ensured by several cell cycle control mechanisms which are composed of a series of biochemical switches that trigger the events of the cycle in the proper order.

The main effectors of this system are the cyclin-dependent kinases (Cdks) and their regulators which participate in a versatile regulatory network that controls the order and timing of cell-cycle events. Higher eukaryotes have several Cdk homologues but Cdk1 and Cdk2 appear to be the major regulators of cell cycle transitions (for review see Morgan 1997). As the cell progresses through the cycle, regulation of Cdks activity depends primarily on corresponding oscillations in levels of the regulatory subunits known as cyclins, which bind tightly to Cdks and stimulate their catalytic activity. Different cyclin types are produced at different cell-cycle stages (e.g. cyclin E and cyclin D are more abundant during interphase whereas cyclin A and cyclin B reach a maximum during mitosis), resulting in the formation of a series of cyclin–Cdk complexes. Additionally, Cdk phosphorylation by Cdk-activating enzyme (CAK) also acts as a positive regulator of Cdk activity, by promoting the catalytic activity of Cdks. Moreover, negative regulation can be achieved by Cdk inhibitor proteins (CKIs) or through inhibitory phosphorylation at specific residues. As a result of these combined regulatory processes, particular cyclin-Cdk complexes are activated at different times during the cell cycle which are then responsible for changes in the biochemical status of cell division machinery in order to activate specific factors that carry out each cell cycle event.

Cell cycle progression is also controlled by ubiquitin-dependent proteolysis of specific cell cycle regulators, through the addition of ubiquitin-polymeric chains to specific proteins which is sufficient to target them for proteolytic degradation by an abundant protease complex - the 26S proteasome. Ubiquitination of a substrate requires an ubiquitin enzyme-shuttle using an ubiquitin-activating enzyme (E1), an ubiquitin conjugating enzyme (E2) and an ubiquitin-ligase enzyme (E3). The specificity of this destruction system is mainly governed by the E3 ubiquitin ligase enzyme. Two major E3 enzymes are involved in degradation of cell cycle regulators: the SCF complexes (containing Skp1, Cullin and F-Box proteins), which is constitutively active during interphase, and the Anaphase-Promoting Complex/Cyclosome (APC/C) which depends on activator proteins (Cdc20/Fizzy or Cdh1/Hct1/Fizzy-related) for substrate recognition. These pathways are responsible for the degradation of several substrates such as cyclins, thereby regulating Cdk activity and securin, triggering sister chromatid separation at the anaphase onset.

Additionally, cell cycle control is also coordinated by a balance between nuclear import and export of the components of the cell cycle machinery (reviewed by Pines 1999). Thus, proteins can be sequestered in the cytoplasm until they are required to act in the nucleus, or vice versa. Other proteins, such as CyclinB1-Cdk1 in animal cells, constantly shuttle between the nucleus and the cytoplasm during interphase. There are even examples of proteins that have different functions in the nucleus and in the cytoplasm.

During G1 phase, mitotic Cdks are kept inactive by both the APC/C^{cdh1} and cyclin dependent kinase inhibitors (CKIs). G1 cyclins are generally not an APC/C^{cdh1} substrate which allows their accumulation. At the restriction point ("start point" in yeast), G1/S-Cdk becomes active which induces APC/C^{cdh1} inactivation and CKIs destruction via SCF proteolytic pathway. This restriction point is the point of the cell cycle at which commitment to cell division occurs. G1/S-Cdk then activates S-Cdk complex which in turn triggers DNA replication at the onset of S phase. Moreover, S-Cdk complex inhibits the re-assembly of the pre-replication complex (pre-RC) after S-phase entry which ensures that only once per cycle each origin of replications if fired to initiate DNA synthesis (reviewed by Diffley 2004).

Completion of S-phase results in the activation of M-Cdk and subsequent entry into mitosis. Mitosis entry is mainly governed by Cdk1, whose activation depends not only on binding to Cyclin A/B but also on the removal of two inhibitory phosphates at the ATP binding site (for recent review see Stark and Taylor 2006). This occurs at the G2/M transition

when activity of the phosphatase Cdc25C exceeds that of the opposing kinases Wee1 and Myt1. Activated cyclin-Cdk1 complexes phosphorylate numerous downstream targets including nuclear lamins, kinesin-related motors and other microtubule-binding proteins, condensins and golgi matrix components modifying their behavior. In this way, Cdk1 activity controls the majority of the events required at the early stages of mitosis like the nuclear envelope breakdown, centrosome separation, spindle assembly, chromosome condensation and Golgi fragmentation. In addition to Cdk1, other mitotic kinases (Polo, Aurora, NIMA, BubR1 and Mps1 kinases) regulate the orchestrated events of nuclear division (for review see Nigg 2001). Later mitotic events include sister-chromatid separation which is triggered by APC/C^{cdc20} activation at the metaphase-to-anaphase transition. APC/C^{cdc20} activity also induces the destruction of S and M cyclins and thus the inactivation of Cdks, and additionally promotes Cdc20 degradation inducing the activation of APC/C^{cdh1}. This later promotes the completion of mitosis and cytokinesis. APC/C^{cdh1} activity is maintained in G1 until G1/S–Cdk activity rises again and commits the cell to the next cycle.

Besides a unidirectional sequence of events, successful progression through the cycle additionally requires that these events are not initiated until successful completion of the previous event. This is ultimately achieved by several checkpoint controls which through signal transduction pathways are able to monitor if different cell functions have been properly completed. If the processes or functions are incomplete, the checkpoints prevent or delay initiation of subsequent processes.

The DNA damage checkpoint detects DNA lesions (single strand DNA, ssDNA, or DNA doublestrand breaks, DSB), arrests cell cycle progression and triggers DNA repair. These DNA lesions act as signals that activate specific kinases. DSB usually activate a checkpoint pathway mediated by ATM kinase whereas ssDNA activates a checkpoint pathway that contains ATR kinase. In response to DNA damage, the biochemical outcome of activating ATM/ATR and their downstream targets (Chk2/Chk1 kinases among others) depends on the cell cycle stage. In G1, DNA damage checkpoint arrests cell cycle through the block of Cdk2/Cyclin E (required for S phase entry) via a p53 and p21 mediated pathway. During S-phase, this checkpoint inhibits Cdk2 by enhancing Cdc25A degradation, thus maintaining Cdk2 inhibitory phosphorylation. During G2, in response to DNA damage, Chk1 and Chk2 kinases prevent mitosis entry through the inactivation of Cdc25C, while upregulate Wee1 and Myt1 kinases. Consequently, activation of these pathways inhibits Cdk1/cyclin B activation and mitosis entry.

The replication checkpoint ensures the fidelity of replication and monitors proper S-phase progression, delaying DNA replication in response replication block, i.e. impaired progression of the replication forks either by physical constrains or malformation of the replication machinery (*stalled* replication fork) (for further reading see Nyberg et al. 2002; Branzei and Foiani 2005). The biochemical outcome of replication checkpoint activation results in the stabilization of stalled replication forks and inhibition of further origin firing. These tasks are primarily mediated by the ATR kinase which is actively recruited to the sites of replication block. As mentioned above, during S-phase the cell is also responsive to DNA damage. Moreover, the formation of stalled replication forks leads to the exposure of ssDNA and therefore the molecular players of the DNA damage are common to the replication checkpoint. This leads to the proposal that these two pathways can be integrated into a single one, termed simply the S-phase checkpoint.

The spindle assembly checkpoint is a surveillance mechanism that ensures that anaphase onset is only triggered when all the chromosome are bipolarly attached and have been properly aligned at the metaphase plate, a pre-requisite for equal distribution of the genome. Thus, the presence of unattached kinetochores and/or the absence of tension at the kinetochores is able to trigger this checkpoint by emitting a global "wait anaphase" signal that prevents exit from mitosis.

The downstream target of the spindle checkpoint is the APC/C. Anaphase onset is directly dependent on APC/C^{cdc20} activity as once APC/C^{cdc20} is active it triggers degradation of the securin, the separase inhibitor. Consequently, active separase cleaves scc1 cohesin subunit and releases the link between sister chromatids, triggering the anaphase onset (for review see Yanagida 2000). Moreover, APC/C^{cdc20} induces degradation of mitotic cyclins and consequent mitotic exit (reviewed by Irniger 2002).

The core spindle checkpoint proteins include Mad1, Mad2, BubR1 (Mad3 in yeast), Bub1, Bub3 and Mps1. The Mad (for mitotic-arrest deficient) and Bub (for budding uninhibited by benzimidazole) genes were initially identified in yeast by genetic screens for mutants that failed to arrest in response to spindle damage (Hoyt et al. 1991; Li and Murray 1991). Subsequently, Mps1 (monopolar spindle), was also identified as a component of the checkpoint pathway (Weiss and Winey 1996). These proteins were later on shown to be conserved among eukaryotes (for review see Musacchio and Hardwick 2002). All these key checkpoint components are essential for the checkpoint response in different organisms and

were shown to localize to the outer kinetochore early in mitosis kinetochores and accumulate strongly on unattached kinetochores. Thus, the checkpoint proteins are ideally placed to monitor kinetochore-spindle interactions. Current models have therefore propose that the kinetochores serve as sensors for MT-kinetochore attachment and tension acting as catalytic sites for the "wait anaphase" signal (reviewed in Musacchio and Hardwick 2002).

Whether kinetochore sense microtubules occupancy accomplished by attachment to the spindle or tension across the sister kinetochores is still a matter of debate (Pinsky and Biggins 2005). Several studies clearly reveal that spindle checkpoint components respond differently to both situations, suggesting that distinct spindle checkpoint proteins monitor different aspects of kinetochore interaction with the spindle. For example, studies in *Drosophila* tissue culture cells have revealed that Bub1 and Mad2 leave the kinetochore as soon as attachment is fulfilled whereas Bub3 and BubR1 remain at attached kinetochores lacking tension (Logarinho et al. 2004). However, Mad2 and Mad1 are required for checkpoint activation in response to lack of tension (Shannon et al. 2002) which strongly suggests the two sensing mechanisms might ultimately converge into a single pathway.

The signal transduction pathways involved in this checkpoint are far from being understood, however, it is clear that spindle checkpoint proteins can inhibit anaphase onset through the formation of inhibitory complexes with Cdc20, an activator of APC/C. It has been postulated that unattached kinetochores would provide a site for the assembly of these inhibitory complexes (reviewed by May and Hardwick 2006). Because a single unattached kinetochore is able to activate the checkpoint, this inhibitory signal must be amplified throughout the cell (Rieder et al. 1995). Indeed, it was recently reported that some checkpoint proteins display a highly dynamic behavior at the kinetochores which has been proposed to account for the amplification of the signal (Howell et al. 2004; Shah et al. 2004).

2 – The Chromosome Cycle

A faithful segregation the genome DNA is the major purpose of each cell division. In eukaryotic cells, the four main events of the chromosome cycle (duplication, cohesion, condensation and separation) are temporally separated and occur at discrete stages of the cell cycle. Accordingly, throughout the cell division cycle, chromosomes undergo dramatic functional and structural changes, according to cell cycle phase. During G1 the cell is highly

transcriptionally active and therefore chromatin is found to be in a more diffused conformation and DNA-associated proteins related to transcription processes are highly abundant. As cells enter the cell division program, a complete replica of the genome DNA is produced and cohesion between the two sister chromatids is established during S-phase. At the onset of mitosis, chromosome condensation starts in a gradual process throughout prophase and prometaphase. Concomitantly with chromosome condensation, resolution of the sister chromatids at the chromosome arms is established. Final separation of the two sisters occurs only at the anaphase onset, leading to equal segregation of each sister chromatid.

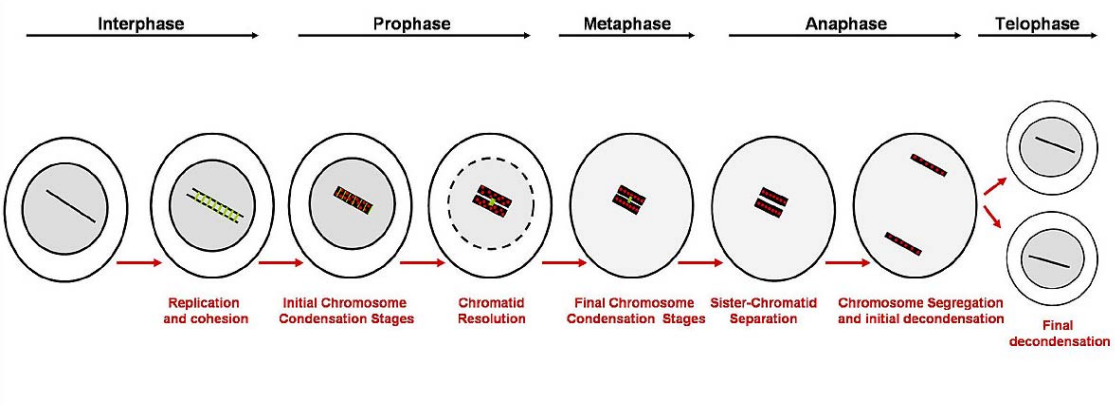

Figure 3. The Chromosome Cycle. As chromosomes replicate during S phase, cohesion between sister-chromatids is established (cohesion factors are represented by green bars). In higher eukaryotes, chromosomes begin to condense into discernible threads early in prophase (condensation factors as represented by red circles). During later prophase stages, the two sister chromatids start to resolve and distinct sister chromatids become visible and are held together at their centromeric region. Chromosomes continue to condense reaching final levels of condensation during metaphase. Cohesion is dissolved at the metaphase/anaphase transition, allowing the chromosomes to be segregated by the mitotic spindle. At the end of mitosis, chromatin decondenses as the nuclear envelopes are reformed.

2.1 DNA replication

Once cell commit to cell division the first crucial event is the synthesis of a replica of its genetic material. This occurs through a semiconservative replication process where, due the antiparallel and complementary nature of the DNA strands, each one serves as a template for the reproduction of the opposite strand. DNA replication is initiated at multiple sites within chromatin called origin of replication. Whereas in yeast origins of replication are short consensus sequences in metazoan, origin of replication exhibit virtually no sequence-specificity (Cvetic and Walter 2005). However, initiation events do not occur randomly and are determined by the assembly of the origin recognition complex (ORC), a six-subunit

protein complex that acts on the recruitment of cdc6 and cdt1. These proteins, in turn, are responsible for the recruitment of MCM2-7 complex, which is believed to be the replicative helicase (Labib and Diffley 2001), and all together form the pre-replication complex, pre-RC, which is assembled during G1. Loading of MCM helicase is referred to as DNA replication licensing since only these replication origins can initiate DNA synthesis. This ensures that one and only one duplication of the genome prior to cell division occurs (for review see DePamphilis et al. 2006). The initiation of DNA synthesis is triggered by the Cdk-dependent loading of cdc45 and cdc45-mediated association of DNA polymerases to the initiation complex. At this stage, the helicase activity of the MCM complex is activated resulting in the unwinding of the DNA duplex at the origin, which exposes single stranded DNA template for priming and DNA synthesis. Synthesis of a new DNA strand is catalyzed by DNA holoenzymes (DNA polymerase III in prokaryotes and DNA polymerase δ and DNA pol ε in eukaryotes), a complex of proteins that act together in the polymerization of nucleotides complementary to the template strand.

Each part of the genome replicates at characteristic time within S phase but the mechanisms that control replication timing are not well understood (for further reading see MacAlpine and Bell 2005). They appear to involve the control of crucial activating kinases (Henneke et al. 2003) as well as effects on chromatin structure (Vogelauer et al. 2002; Aparicio et al. 2004). Accordingly, early studies of metazoan replication noted that heterochromatic regions were consistently replicated later than their euchromatic counterparts (Stambrook and Flickinger 1970).

From one origin of replication two replication forks progress in opposite directions along the DNA fiber. Due to the double helical structure of DNA, progression of replication forks generates strains and supercoiling which cause intertwining of the two replicated regions. These are dissipated by the topoisomerases activities, enzymes that interconvert different topological states of DNA. Type I enzymes pass a single-stranded region of DNA through a break in the opposite strand whereas type II topoisomerases pass a region of double-stranded DNA through a break in a second duplex (inter- or intra-molecularly). Nonetheless, some links between newly synthesized sister chromatids persist until metaphase.

2.2 Sister chromatid cohesion and separation

The end-product of DNA replication is a set of two sister chromatids that must remain tightly associated until they segregate at the metaphase-anaphase transition of the subsequent mitosis. Cohesion is established during replication by the topological links between sister chromatids and through the deposition of a multisubunit protein complex called cohesin. Its maintenance until the initiation of anaphase is a prerequisite for accurate distribution of the genome between the two daughter cells.

In the cohesin complexes, two Structural Maintenance of Chromosomes proteins, SMC1 and SMC3, associate with two non-SMC protein Scc1/Rad21 and Scc3/SA (reviewed in Nasmyth and Haering 2005). Components of the cohesin complex were first isolated out of two independent screens in *S. cerevisiae* where it became obvious their requirement for accurate chromosome segregation, even though the physiological function was not understood at this time (Guacci et al. 1997; Michaelis et al. 1997). Functional hints arose first from localization studies which revealed that chromatin localization of cohesin was observed shortly before S phase until the onset of anaphase, fully consistent with its role in the maintenance of sister chromatids cohesion (Michaelis et al. 1997). Moreover, its precise removal at the metaphase-anaphase transition was shown to be APC/C dependent (Ciosk et al. 1998) and separase-mediated cleavage of scc1 was later shown to trigger anaphase onset (Uhlmann et al. 1999; Uhlmann et al. 2000), which clearly revealed that cohesin was indeed responsible for sister chromatid cohesion.

Homologues for budding yeast cohesin subunits were found in all eukaryotes studied so far and the requirement of cohesin for proper sister chromatid cohesion has been confirmed either by mutations, antibody mediated depletion or RNA interference in several species including in *Xenopus* egg extracts (Losada et al. 1998; Losada et al. 2000), in *Drosophila melanogaster* (Vass et al. 2003), in *C. elegans* (Mito et al. 2003), in *Arabidopsis thaliana* (Bhatt et al. 1999) and in chicken and mammalian tissue culture cells (Sumara et al. 2000; Sonoda et al. 2001). The majority of these studies have confirmed that loss of cohesin causes precocious sister chromatid separation (before APC/C activation) and defects in the biorientation of sister chromatids during mitosis which results in a prometaphase spindle checkpoint-dependent arrest/delay. Reciprocally, non-cleavable forms of scc1 either prevent or delay sister chromatin separation in *S. cerevisiae* (Uhlmann et al. 1999), *S. pombe* (Tomonaga et al. 2000) and HeLa cells (McGuinness et al. 2005).

Cohesin has been proposed to form a ring-shaped multiprotein structure that holds sister chromatids together by embracing two DNA duplexes within its coiled-coil arms (Haering et al. 2002; Gruber et al. 2003). EM studies on purified cohesin complex further support this ring shaped complex assembly (Anderson et al. 2002) and this model can nicely explain how proteolytic cleavage of scc1 subunit induces the opening of the ring and thereby triggers sister chromatid separation (Uhlmann et al. 1999). In *S. cerevisiae*, the release of chromatin-bound cohesin occurs in a single step at anaphase onset. Once spindle checkpoint is inactivated, APC/C targets the separase inhibitor, securin, for proteasome destruction and activated separase cleaves scc1 subunit from the cohesin complex. In higher eukaryotes, however, cohesin was shown to be released in a two step process. The bulk of cohesin dissociates from chromosome arms during prophase through a mechanism that does not involve proteolytic cleavage of scc1 by separase (Losada et al. 1998; Sumara et al. 2000; Waizenegger et al. 2000; Warren et al. 2000). Centromeric cohesin is resistant to this first step of release, possibly by Shugoshin/MeiS332-mediated protection mechanism (Watanabe 2005), and persist at the centromeres until the anaphase onset. The prophase cohesin release step appears to be mediated by Polo-like kinase (PLK) and Aurora B kinases (Losada et al. 2002; Sumara et al. 2002; Gimenez-Abian et al. 2004) whereas the remaining centromeric cohesin is released only at the anaphase onset by separase cleavage, a process dependent on spindle checkpoint inactivation.

2.3 Mitotic chromosome condensation

At the onset of mitosis, a highly dynamic process of chromosome condensation begins which ensures that entangled chromatin fibbers present in interphase nuclei are resolved and packed into individualized structures, the mitotic chromosomes. The condensed state of mitotic chromosomes is crucial for faithful genome segregation. Interphase chromosomes are generally much longer than the length of the dividing cell. Accordingly, without chromosome condensation proper chromatid segregation could not occur during anaphase and portions of chromosomes would often cross the plane of cell division and would be cleaved or entrapped by cytokinesis. Thus, chromosome condensation physically compacts chromatin in such a way that makes nuclear division feasible within the cell space. However, chromosome condensation is not a mere process of linear chromatin fibers compaction as, besides compaction, other topological problems need to be solved. As a result of the replication

process and chromatin diffusion events that occur during interphase, several chromatin tangles between sister chromatids and even between neighboring chromosomes arise. Accordingly, chromosome condensation helps to individualize different chromosomes and to resolve sister chromatids in order to eliminate these DNA intertwines. Additionally, the process of chromatin compaction *per se* leads to an increase in chromosome rigidity which is extremely important for the physical resistance to the mechanical stress of mitotic chromosomes as throughout nuclear division, chromosomes are subjected to both pulling and pushing forces exerted by the mitotic spindle during congression and segregation movements.

At each nuclear division, mitotic chromosomes fold into an invariant structure. Mitotic chromosomes in a given cell-type have a characteristic and reproducible length and each mitotic chromosome has signature pattern of bands after staining with specific dyes like Giemsa. In further support of an invariant folding process, FISH analysis reveal that specific DNA sequences occupy a reproducible position along the long and transverse axes of the chromosome (Baumgartner et al. 1991). The invariant folding implies that chromosome condensation is not a random process and that extrinsic or intrinsic mechanisms underlie chromosome condensation assembly in such a way that at the onset of mitosis the interphase chromatin is properly converted into a folded rod-shaped structure. However, despite extensive research in the field, the molecular mechanisms involved in the process of chromosome condensation remain poorly understood. A more detailed description of what is known relatively to the mitotic chromosome assembly process is presented in the next section.

3 – Chromosome Condensation

Mitotic chromosomes were one of the first sub-cellular structures to be observed. The first reports were made by Karl Wilhelm von Nägeli in 1842, while studying plant cells, and independently in *Ascaris* worms by Edouard Van Beneden. A detailed description of their behavior during nuclear division was beautifully described by Walther Flemming, in 1882, where he described that as cells enter in mitosis, interphase chromatin condensed into thin threads that organized at the cell centre and eventually split longitudinally (reedited in Flemming 1965). The word chromosome was invented later by Heinrich von Waldeyer in 1888 based on the stained properties of the thread-like structures after fuchsin staining. Etymologically, the word chromosome comes from the Greek χρώμα (chroma, color) and σώμα (soma, body).

Ever since their discovery, scientists have tried to understand how mitotic chromosomes are assembled. While extensive progress has been made in unraveling the lower levels of chromatin compaction, the mechanisms underlying the establishment of higher order levels of chromatin organization remain to be unveiled. Both histone modification and non-histone protein factors have been implicated in the establishment of proper mitotic chromosome architecture. However, the exact contribution of each molecular event in the mitotic chromosome assembly is still controversial and most likely other yet unidentified players might have a pivotal role in this process.

3.1 Interphase chromosome structure

The structure of interphase chromosomes is of extreme importance to conceptually understand the mechanism of chromosome condensation as they are the initial substrate of this process. The lowest level of chromatin compaction are the nucleosomes, where 1.67 left-handed super-helical turns of the DNA molecule (~147 bp) is wrapped around an octamer, composed of four identical pairs of core histones, H2A, H2B, H3 and H4 (Davey et al. 2002). Binding of the linker histone H1/H5 organizes additional 20 bp to complete and stabilize the nucleosome (Zhou et al. 1998). Linker DNA, of variable lengths according to each cell type and species, connects adjacent elements of this repetitive unit (Widom 1992). The first level of nucleosome organization is called “11 nm fiber” and accounts for 6 to 7 fold compaction (Fig. 4). This organization was first revealed by Electron Microcopy (EM) studies of chromatin under low ionic strength conditions, which showed that nucleosomes are arranged as 11 nm beads on a string (Oudet et al. 1975; Thoma and Koller 1977). With increased ionic strength this fiber was shown to convert into a higher order of organization of about 30nm, the “30nm fiber”, which accounts for further 6 to 7 fold compaction, with a total packing ratio of ~ 40 (Suau et al. 1979) (Fig. 4). In agreement, EM analysis on thin section of HeLa cells metaphase chromosomes showed thick fibers with a diameter of ~ 30 nm (Marsden and Laemmli 1979), whose integrity was dependent on high ionic strength an the presence of linker histone H1 (Thoma et al. 1979).

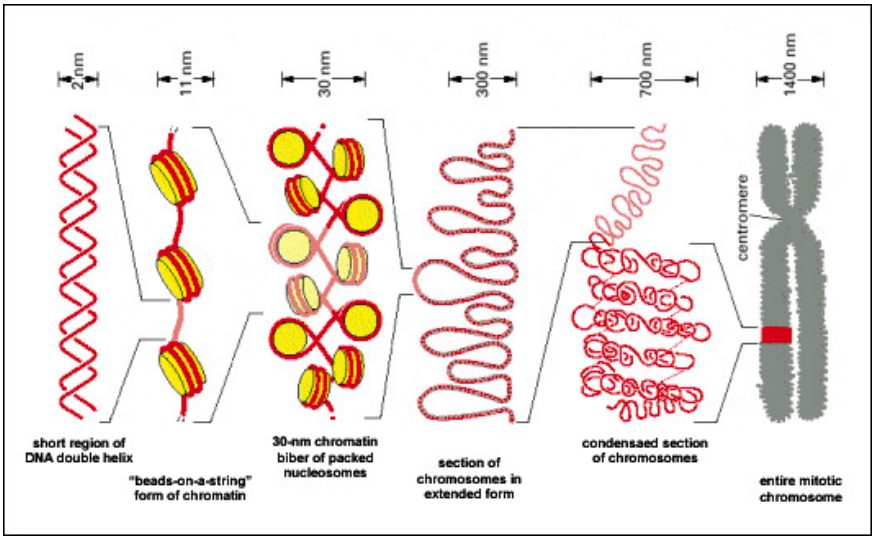

Figure 4. Distinct levels of chromatin compaction. Liner DNA is about 2 nm thick and is folded around nucleosomes (yellow rods). This beads-on-a-string chromatin arrangement folds into the so called 30-nm fiber. Higher levels of chromatin organization are hypothetically achieved by extra folding of the fibers reaching a maximum of compactness during mitosis. Mitotic chromosomes are ~10.000 fold shorter than the linear DNA molecule (adapted from Alberts et al., 2002).

The mechanism underlying the formation of the 30 nm fiber is quite controversial (Robinson and Rhodes 2006). The "one-start solenoidal helix" model, proposes that a linear array of nucleosomes is coiled (Finch and Klug 1976) whereas the "two-start helix" model argues that nucleosomes are assembled in a zigzag ribbon that twists or supercoils (Woodcock et al. 1984; Williams et al. 1986). Despite that several indirect observations supporting both models can be found in the literature, a crystal structure of a tetranucleosome was recently solved, providing strong evidence in support of the two-start helix model (Schalch et al. 2005). Above the 30 nm fiber level, the structure of the chromatin is poorly understood but secondary and tertiary chromatin structure are thought to be formed in a protein-mediated manner (Luger and Hansen 2005).

The interphase chromatin has to fulfill two opposing requirements. In one hand chromatin must be physically compacted to fit within the nucleus but on the other, chromatin compaction needs to be flexible enough to allow ready access of DNA to transcription, repair and replication machineries. On average, in mammalian cells, interphase chromatin is about 200 to 1000 fold more compacted than linear DNA (Lawrence et al. 1990) but different levels of chromatin compaction are present in the interphase chromosomes. Mechanisms that potentially alter the levels of chromatin compaction have an inherent role in the regulation of DNA accessibility. These mechanisms involve mainly (but not only) modifications on

histones, either by post-translational modifications on histone tails and histone cores or by the introduction of histone variants.

Numerous histone tail modifications have been already reported and were shown to influence chromatin structure in several ways (Luger 2006). Histone tail modifications such as acethylation and phosphorylation can alter the charge of the tails and, therefore, may influence chromatin structure through electrostatic mechanisms. Moreover, tail modifications are known to modulate "docking sites" for other non-histone proteins binding to the chromatin and also to affect DNA accessibility by altering protein-DNA interactions. Additionally, histone tail modifications were shown to alter nucleosome-nucleosome interaction, which directly modulates the formations of higher-order structures of compaction.

Core histone modifications have been also shown to alter solute accessible face, histone lateral surface and also histone-histone interphase and therefore affect chromatin structure by modulating DNA-histone and also intranucleosomal interactions (Mersfelder and Parthun 2006).

The replacements of histones H2A or H3 with their corresponding variants can have several outcomes on chromatin structure (Chakravarthy et al. 2005). Indeed, histone variant containing nucleosomes were reported to display distinct properties that can account for altered chromatin structure in these regions. These include alterations in the DNA binding properties, changes in nucleosome sliding and chromatin remodeling behavior, alterations in the nucleosomal surface width and changes in the available sites for post-translational modifications within the tails.

In addition to histone modifications, remodeling factors, histone chaperones, and chromatin-binding proteins all contribute in a combinatorial manner to the structural changes that are necessary to allow (or not) access to the DNA template (Luger 2006). Based on these different structural changes, chromatin can be subdivided into two structural and functional compartments, euchromatin and heterochromatin. This distinction was originally cytological, as stained nuclei revealed abundant light stained regions (euchromatin) in contrast to dark stained regions (heterochromatin). Nowadays, this distinction is coming more and more refined at the molecular level. The bulk of the transcribed genome resides within euchromatin, which partially decondenses in interphase chromosomes, whereas the more compacted heterochromatin is typically regarded as transcriptionally inert and participates critically in the

formation of chromosomal structures, like the centromeres and telomeres, essential for proper chromosome function.

Interphase chromatin is not randomly diffused and several studies have shown that the chromosomes as well as the other components inside the nucleus are highly organized. A certain degree of chromosomal order results from the configuration that the chromosomes always have at the end of mitosis. During anaphase movement the centromeres are moved ahead whereas the distal arms (terminating in the telomeres) lag behind. The chromosomes in some nuclei tend to retain this so-called Rabl orientation throughout interphase, with their centromeres facing one pole of the nucleus and their telomeres pointing toward the opposite pole (Comings 1980). This orientation is particularly frequent in very short interphases such as in the *Drosophila* syncytial embryos (Foe and Alberts 1985). Most cells have a longer interphase, and this presumably gives their chromosomes time to assume a different conformation. Nevertheless, chromosomes in the cell nucleus are organized as chromosome territories (CTs), where the structure of each CT is strongly correlated with its functional state. In the past decade, accumulating evidence has supported the view that the nuclear architecture provides another level of epigenetic gene regulation and several models have been developed aiming to understand the architecture of the CTs (for further reading see Cremer et al. 2006). The position of each CT is governed by attachments to distinct structures such the nuclear envelope, nucleoli, nuclear bodies and the controversial nuclear matrix (reviewed by Foster and Bridger 2005). Moreover, differences in the chromatin compaction level and reposition of each CT have been shown to be implicated in the differentiation process (Foster and Bridger 2005).

3.2 Mitotic chromosome structure

As cells enter prophase, at the onset of mitosis, the most striking morphological changes in chromatin structure are initiated. Even though interphase chromatin is already highly compacted, mitotic chromatin condenses much further in order to achieve a final 10.000-20.000 fold linear compaction present in metaphase chromosomes.

Extensive work can be found in the literature with detailed characterization of metaphase chromosomes using different cytological approaches. Different models for mitotic chromosome assembly have therefore emerged. In the **folded-fiber model** the chromosomes

are thought to result from a random fiber folding which occurs repeatedly transversely and longitudinally, with no intermediate levels of compaction (DuPraw 1965; DuPraw 1966; Comings 1972; DuPraw 1972). However, it is nowadays well accepted that mitotic chromosomes fold into a reproducible structure every mitosis ruling out a random process of chromosome assembly.

An alternative model proposes that metaphase chromosomes are the result of helical coiling events. The **helical-coiling model** supports that the nucleohistone fiber is coiled up into a helix which may be hierarchically wound up into a larger helix to achieve the compactness of the mitotic chromosome (Ohnuki 1968; Bak et al. 1977; Sedat and Manuelidis 1978). Subsequent studies using a three-dimensional-oriented structural approach have in fact revealed that mitotic chromosomes showed a consistent size hierarchy of discrete structural domains with specific cross-sectional diameters (from 120 to 1000 Å) (Belmont et al. 1987). Metaphase-arrested chromosomes show a larger-structural organization in the range of 1.300-3.000- Ǻ size. This study supports a **hierarchical folding model** for chromosome assembly, which is to some extent consistent with the helical-coil driven compaction. However, the nonsymmetric intrachromatid orientation of the higher-order structures observed in this study is incompatible with a simple helical folding suggesting a more complex chromosome assembly in which other non-helical folding events might additionally occur.

A different view of the metaphase chromosome emerged when Paulson and Laemmli (1977) reported the EM structure of histone-depleted chromosomes. They described a scaffold or core which has the shape of the metaphase chromosomes and is surrounded by loops of chromatin attached to this central core (Fig. 5). Interestingly, after nuclease digestion and histone removal, the remaining scaffolding structure retains the shape of the mitotic chromosomes (Adolph et al. 1977; Earnshaw and Laemmli 1983). These and subsequent studies lead to the consolidation of the **scaffold/radial-loop model** which argues that radial DNA loops extend out from a protein element or scaffold positioned along the central axis of the chromatid. Specific AT-rich DNA sequences were later found to be the main attachment sites of the chromatin loops to the central core and were therefore called Scaffold Attachment Regions (SARs) (Mirkovitch et al. 1984; Gasser and Laemmli 1987).

It is important to refer that the radial loop model does not exclude a helical organization of the domains (Marsden and Laemmli 1979; Adolph 1980). In fact, radial loops and helical

coils were reported to co-exist in metaphase chromosomes and a helical arrangement of the loops in metaphase chromosomes was suggested (Rattner and Lin 1985).

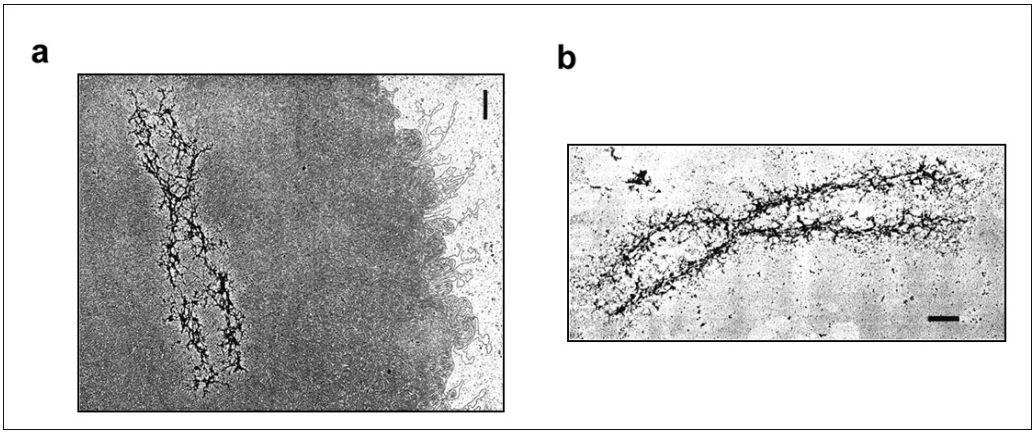

Figure 5. The scaffold of mitotic chromosomes (a) Electron micrograph of histone-depleted mitotic chromosome revealing chromatin loops extended out of a central protein matrix (scaffold). (b) Electron micrograph of the scaffold obtained from metaphase chromosomes after histone removal and nuclease digestion. In the absence of chromatin, a scaffold structure remains and retains the shape of mitotic chromosomes (adapted from Laemmli et al. 1978).

An alternative approach to understand the structure of mitotic chromosomes is the analysis of their biophysical properties. Several studies have shown that chromosomes display a highly elastic behavior as they can be stretched several times their original length and still relax to their original shape (Nicklas 1983; Houchmandzadeh et al. 1997; Marshall et al. 2001; Poirier et al. 2002; Poirier and Marko 2002). However, divergent data has arisen in attempts to understand the structural components responsible for this elastic behavior. Poirier and Marko (2002) have demonstrated that the elastic response of mitotic chromosomes is lost when after DNA digestion and concluded that the chromatin is the mechanical contiguous component of the mitotic chromosome. Moreover, after mild protease treatment of mitotic chromosomes the chromosomes retain a reversible elastic response upon successive stretch-relax cycles, despite a progressively reduced force constant (Pope et al. 2006). Thus, these authors suggest the **chromatin-network model** where it is proposed that the mitotic chromosome is essentially a "network" of chromatin and rule out the possibility that the chromatin is attached to a mechanical continuous protein scaffold. In contrast, other studies reveal that the elastic response of mitotic chromosomes is consistent with the existence of a rigid thin core inside the chromosome (Houchmandzadeh and Dimitrov 1999). Furthermore, extensive protease digestion of mitotic chromosomes leads to loss of structural integrity and

the intermediate "melted" chromosome does not exhibit any detectable elastic response (Almagro et al. 2004). Interestingly, one of the major components of the chromosomal scaffold (SMC proteins) were shown to be associated with chromosomal regions that exhibit higher elastic response (Almagro et al. 2004). Thus, these later studies strongly support that the elastic behavior of mitotic chromosomes depends not only on DNA continuity, but also on the presence of protein scaffold components.

The classical cytological studies and the elasticity assays have concentrated their attention in the analysis of already formed metaphase chromosome. It has become clear that an important contribution into the understanding of mitotic chromosome structure will come from a detailed analysis of the assembly process during early mitotic stages. Therefore, several studies have concentrated their attention in the detailed characterization of prophase chromosomes structure as well as in the *in vivo* analysis of the condensation process in living cells.

Pioneer work was the microinjection of calf thymus histone (H2A ad H2B) conjugated with rhodamine into *Drosophila* embryos (Hiraoka et al. 1989) followed by 3D confocal imaging. This study revealed that chromosomal regions on the nuclear envelope, distinct from the centromeres and telomeres, serve as foci for the condensation process of mitotic chromosomes. Moreover, the relative positions of the late decondensation sites at the beginning of interphase appear to correspond to the early condensation sites at the subsequent prophase. This strongly suggests that specific regions on the chromosome might act as *cis*-acting sites that serve as landmark to direct condensation. Live imaging of labeled late-replicating heterochromatin reveals that these chromatin foci remain at the same position throughout prophase and do no move considerably, as chromosomes are formed (Manders et al. 1999). Most chromatin shortening and movement occurs during prometaphase.

Further supporting a sequential chromosome condensation process, a detailed analysis of prophase chromosomes in fixed HeLa cells revealed a hierarchical chromosome condensation process (Kireeva et al. 2004). Early prophase nuclei are distinguished from G2 interphase nuclei by the resolution and further compaction of local chromatin aggregates into more clearly defined linear chromatids. Middle prophase cells contain chromosomes that are well defined liner structures of about 0.4-0.5 μm diameter whereas later prophase cells contain sorter chromosomes ~0.8-1.0 μm thick. In agreement, quantitative time-resolved analysis of live cells expressing GFP-histone H2B reveals that chromosome condensation in

C. elegans is biphasic (Maddox et al. 2006). The first phase involves the conversion of diffuse chromatin into discrete linear chromosomes whereas the second condensation event further compacts these chromosomes to shorter bar-shaped structures.

All together, these recent studies reveal that chromosome condensation is a gradual process and thereby intermediate condensed states can be found during prophase and prometaphase until chromosome reach a rod-shape structure present in metaphase chromosomes. Additionally, the presence of these intermediate condensed states strongly supports a hierarchical folding of the mitotic chromosome and argues against the scaffold/radial loop model. The scaffold/radial-loop model has been recently directly questioned by a study in which engineered labeled chromosome regions flanked by scaffold-associated region (SAR) were analyzed (Strukov et al. 2003). This study reports no evident differential targeting of SAR sequences to a chromosome axis within native chromosomes and a higher density of SAR sequences in a particular chromosomal region does not affect chromosome compaction. Notably, the visualization of chromosomes containing tandem labeled insertions reveal that this chromosomal region assembles into a ~250-nm diameter folding subunit. This arrangement is compatible with a hierarchical folding assembly and inconsistent with the scaffold/radial-loop model. In addition to this study, detailed analysis of prophase chromosome from HeLa cells reveals that topoisomerase II and SMC2 (the two major scaffold components) do not form an axial staining pattern until late prophase, when chromosome compaction is nearly complete (Kireeva et al. 2004). However, a well defined chromosome axis could be already observed in middle prophase chromosomes which strongly suggest that axial localization of scaffold components might not required for the initial formation of the chromosome axis.

3.2.1 Centromeres and kinetochores

The centromere, initially described cytologically as the primary constriction region on chromosomes, plays an essential role in chromosome segregation. First, it underlies the organization of the kinetochore and thereby the attachment and movement of chromosomes along spindle microtubules. Second, it ensures sister chromatid cohesion until metaphase-anaphase transition. In that way centromeres contribute to bipolar attachment of chromosomes and to ensure a proper partitioning of the genome.

Centromeric DNA is extremely diverse among species. The "point" centromeres found in *Saccharomyces cerevisiae* are short and simple, and consist of common sequence elements that span just 125 bp (Fitzgerald-Hayes et al. 1982). In contrast, most eukaryotes have complex centromeres that are in general composed by long stretches of repetitive DNA but are highly divergent between different species. The best-characterized complex centromeres are those of the fission yeast *Schizosaccharomyces pombe.* A central core of several kilobases that is rather dissimilar between chromosomes is surrounded by inverted "inner" repeats which are, in turn, surrounded by outer repeats (Mellone and Allshire 2003).

Centromeres in metazoan species are more complex than those in yeast. In *Drosophila melanogaster*, mapping and large scale sequencing have identified several islands of complex sequence within a long otherwise contiguous region of simple repetitive DNA in a total of ~ 500 bp centromeric chromatin (Sun et al. 1997; Sun et al. 2003). Human centromeres contain large arrays of tandemly repeated 171-bp α-satellite DNA that can span several megabases (Sullivan 2001).

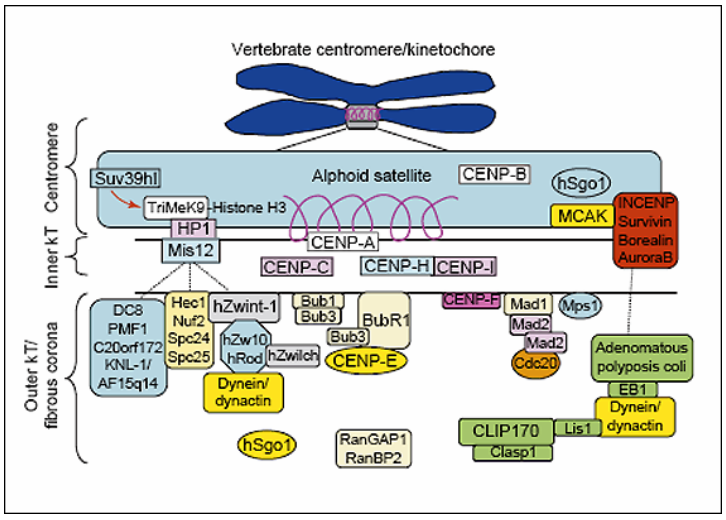

Figure 6. The vertebrate centromere/kinetochore. Schematic representation of the spatial distribution of centromeric and kinetochore proteins. The coil at the centromere depicts the proposed helical path organization of the chromatin fiber, where CENP-A-bearing nucleosomes are exposed as repeat subunits at the inner plate of the kinetochore. The majority of the kinetochore proteins reside at the outer kinetochore and include spindle checkpoint proteins, proteins involved in the kinetochore MT-binding proteins (depicted in yellow) and proteins that regulated microtubule dynamics (in green) (adapted from Chan et al. 2005)).

Despite the differences in size and sequence of centromeric DNA, the architecture and composition of centromeric chromatin is quite conserved between different species.

Accordingly, in functional centromeres, histone H3 is replaced by the H3 variant Cenp-A which has a histone-fold domain at its C-terminus similar to that of histone H2, but its N-terminal region is variable (Sullivan et al. 1994). Cenp-A containing nucleosomes is a particular feature of all centromeres analyzed so far (reviewed by Sullivan 2001) and its depletion leads to the mis-localization of other kinetochore proteins (Meluh et al. 1998; Howman et al. 2000; Blower and Karpen 2001; Oegema et al. 2001).

One of the most important features of a functional centromere is its ability to assemble a kinetochore, a pre-requisite for proper chromosome segregation. Classical electron microscopy studies reveal that mammalian kinetochores appear as a trilaminar stack of plates situated on opposite sites of the centromeric heterochromatin of mitotic chromosomes (Brinkley and Stubblefield 1966; Jokelainen 1967; Rieder 1982; McEwen et al. 1993). In non-attached kinetochores, a meshwork of fibers, termed fibrous corona, can be seen extended from the surface of the outer plate, extending ~0.1-0.3 μm away from the outer plate (Ris and Witt 1981). The electron-dense inner plate is approximately 20-40 nm wide and is located on the surface of the centromeric heterochromatin where Cenp-A-bearing nucleosomes are exposed as repeat units. In addition to Cenp-A, other centromere proteins act as a constitutive "kinetochore foundation" unit through a hierarchical and co-dependent assemble onto centromeric DNA (Cenp-C, Cenp-B, Cenp-C, Cenp-H, Cenp-I and Mis12) (for review see Amor et al. 2004).

The outer-plate is approximately 35-40 nm wide structure, composed of regular and irregular 10-20 nm thick fibrillar components, and is separated from the inner plate by a region of loosely organized fibrillar material (inner plate) whose protein composition is unknown. The fibrous corona and the outer plate contain the majority of the known kinetochore proteins, including proteins involved in the microtubule kinetochore attachment (e.g.CENP-E, CLIP170, Lis1, CLASP1, APC, EB1) (reviewed by Maiato et al. 2004) as well as proteins that monitor the attachment state and activate the spindle checkpoint (e.g. Bub1, BubR1, Bub3, Mad1, Mad2, Mps1, Nuf2, HEC1, Zwint-1, ZW10, Roughdeal) (for review see Musacchio and Hardwick 2002).

Cenp-A containing chromatin is usually embedded within a large domain of heterochromatin, called pericentric heterochromatin. Heterochromatin is closely associated with repeat sequences but the 'heterochromatic state' is ultimately specified by epigenetic

mechanisms (for review see Wallace and Orr-Weaver 2005). Histone flexible N-termini (tails) are modified (e.g. di- or trimethylation of histone H3 at lysine 9, monomethylation of Histone H3 at lysine 27 and hypoacetilation) an this modifications mediate the binding of Heterochromatin Protein 1 (HP1). Additionally, modifications on the DNA molecule (cytosine methylation) also dictate the heterochromatic state. Pericentric heterochromatin is required for centromere function due to its role in the recruitment and maintenance of cohesin complex to centromeric regions, essential for accurate chromosome segregation. In *S. pombe*, mutants for Swi6 (HP1 homologue) are unable to recruit cohesin subunit Rad21 and fail to maintain centromeric cohesion (Bernard et al. 2001; Nonaka et al. 2002). Moreover, cell lines that lack Su(var)3-9, the enzyme responsible for K9 H3 methylation, fail to recruit HP1 to pericentric heterochromatin and cohesin between pericentric regions of sister chromatids is lost (Guenatri et al. 2004).

3.3 Protein factors of chromosome condensation

As structural changes of chromatin during interphase are largely governed by histone modifications, for many years the studies on chromosome condensation mechanisms were concentrated on the hypothesis that histone modifications would modulate the higher levels of chromatin compaction present in the mitotic chromosomes. Indeed, several histones modifications have been shown to correlate with chromosome condensation but the exact contribution of those to the condensation process remains until now very controversial.

For decades the analysis on chromosome structure remained mainly cytological. However, the isolation of the protein "scaffold" from histone-depleted and nuclease digested mitotic chromosomes together with the development of chromatin assembly *in vitro* assays using *Xenopus* egg extracts started to reveal the non-histone protein components involved in mitotic chromosomes structure. These studies allowed the identification of Topoisomerase II and Condensin complexes as the major non-histone structural players in the assembly of mitotic chromosomes. In parallel, genetic studies have largely contributed to clarify the role of these (and other) proteins in the maintenance of chromosomes structure.

3.3.1 Histones and histone modifications

The role of histones and histone modifications in mitotic chromosome condensation is quite controversial. Initial studies proposed that histone H1 would have a determinant compacting activity in mitotic chromosome assembly as the 11 nm fiber is converted to a more condensed conformation (the 30 nm fiber) by addition of histone H1 (Thoma and Koller 1977). Moreover, histone H1 is hyperphosphorylated at the onset of mitosis (Fischer and Laemmli 1980; Boggs et al. 2000). However, several subsequent studies have suggested that Histone H1 is dispensable for mitotic chromosome condensation. Chromosomes can condense in the absence of H1 hyper-phosphorylation (Guo et al. 1995), metaphase-arrested *Xenopus* egg extracts, in which histone H1 was immunodepleted, are able to properly assemble unreplicated sperm chromatids (Ohsumi et al. 1993) and H1 gene disruption in *Tetrahymena* does not perturb mitotic condensation (Shen et al. 1995). All these data strongly suggests that histone H1 is not involved in mitotic chromosome condensation at all. An alternative model has been proposed suggesting that H1 hyperphosphorylation reduces its affinity for DNA and might allow the access of condensing factors to the chromatin (Roth and Allis 1992). The debate has been recently re-opened when replicated chromosomes (instead of unreplicated chromatin) were used as substrate for chromatin *in vitro* assembly by histone H1 depleted extracts. In this assay chromosomes exhibited significant structural defects as they were thinner and 50% longer than control chromosomes (Maresca et al. 2005). Moreover, EM analysis of chromatin isolated from H1 knockout mouse embryonic stem cells lacking 50% of endogenous H1 reveal dramatic chromatin structure changes, including decreased global nucleosome spacing (Fan et al. 2005).

Also subject to controversy is the role of histone H3 phosphorylation in mitotic chromosome condensation (reviewed by Prigent and Dimitrov 2003). Histone H3 is phosphorylated at serine-10 during mitosis (Paulson and Taylor 1982), by the mitotic kinase Aurora-B (Hsu et al. 2000; Giet and Glover 2001; Murnion et al. 2001; Crosio et al. 2002). Mitosis-specific phosphorylation of histone H3 also occurs at Ser 28, also by Aurora-B (Goto et al. 1999; Goto et al. 2002) and at threonine 11 (Thr 11), this later predominantly at the centromeres (Preuss et al. 2003).

Ser10 phosphorylation has been shown to be temporally correlated with chromosome condensation (Hendzel et al. 1997; Wei et al. 1998). Additionally, detectable levels of phosphorylated H3 Ser28 start to be only detectable at the onset of mitosis, in strict

correlation with the initiation of chromosome condensation (Goto et al. 2002). In agreement with these correlations, classical cell fusion experiments reveal that when mammalian interphase cell are fused with mitotic cells, premature chromosome condensation (PCC) is accompanied by a significantly increased levels of H3 phosphorylation (Johnson and Rao 1970; Hanks et al. 1983). Accordingly, induction of Histone H3 phosphorylation in interphase has been shown to promote chromosome condensation prior to mitosis and reciprocally, premature dephosphorylation during mitosis results in chromosome decondensation (Ajiro et al. 1996a; Ajiro et al. 1996b). Moreover, studies in *Tetrahymena* showed that this modification is indeed required for proper chromosome condensation and segregation (Wei et al. 1999). All together, these studies have raised the possibility that histone H3 phosphorylation is involved in chromosome condensation either by acting directly in the recruitment of condensation factors or indirectly, by reducing its affinity to the DNA inducing a more open chromatin conformation, which would then be accessible to condensation factors. In support of this last model, it has been shown that phosphorylation of the H3 histone tail during mitosis, induces chromatin rearrangements leading to a higher accessibility of antibodies against the histone H3 tail, when compared to the accessibility detected in interphase nuclei (Sauve et al. 1999). Interestingly, histone H3 phosphorylation was shown to be required for the onset of chromosome condensation but not for maintenance of the condensed state, once condensation is completed (Van Hooser et al. 1998). Other genetic data, however, suggests that histone H3 phosphorylation is not a pre-requisite for chromosome condensation. Mutations is Ser10 (S10A) do not result in major defects in mitotic or meiotic chromosome transmission in *S. cerevisiae* (Hsu et al. 2000) and mutation in both Ser10 and Ser28 do not affect mitotic chromosome structure in this organism (Lavoie et al. 2002). Competition experiments using reconstituted chimeric nucleosomes reveal that the N-terminus of histone H2B, but not of H3 or its phosphorylation, is required for chromosome condensation in *Xenopus* egg extracts (de la Barre et al. 2001). Furthermore, chromosomes are properly assembled in aurora B-depleted *Xenopus* egg extracts, without phosphorylated histone H3 (MacCallum et al. 2002). Additionally, in *Drosophila*, there is a weak correlation between the levels of histone H3 phosphorylation and the degree of chromosome compaction (Adams et al. 2001). Finally, H3 phosphorylation in plant mitotic cells, was reported to occur very late in prophase, whereas dramatic changes in chromosome morphology are detected much earlier (Kaszas and Cande 2000). Thus, the specific role of histone H3 phosphorylation in mitotic chromosome condensation remains a controversial issue.

Other histone modifications have been hypothesized to participate in chromosome organization. Approximately 6-7% of total H2A and H2B proteins were shown to be ubiquitinated during interphase and prophase but these ubiquitinated proteins are completely absent in metaphase chromosomes (Mueller et al. 1985). The authors propose that removal of ubiquitin molecules from these core histones is a final event of chromosome condensation, during metaphase and that re-ubiquitination of these histones occurs as cells exit mitosis, while chromosomes decondense. They do not argue that this modification would be *per se* a condensation factor but rather that this would serve as labelling probe for specific chromosomal regions. Interestingly, a deubiquininating enzyme (Ubp-M), when mutated in its active site, associates with mitotic chromosomes and blocks cell growth (Cai et al. 1999). An interpretation of this result is that the mutant form of this enzyme is trapped onto chromosomal substrates (possibly histone H2A and H2B) and suggests the existence of a deubiquitination-dependent mechanism involved in chromosome dynamics. This is still a very speculative interpretation of the data as so far, there is not direct evidence that histone ubiquitination/deubiquitination might play a role in mitotic chromosome condensation.

3.3.2 Topoisomerase II

As in the case of histone modifications, the role of topoisomerase II in the structure of mitotic chromosomes remains quite controversial. TopoII is an ATP-dependent DNA-strand passing enzyme that is able to create a transient double-strand break in a DNA molecule, which allows the passage of one DNA strand through another, and then reseals the break (Wang 2002). This catalytic activity has already been demonstrated to participate in several cellular processes such as DNA replication and transcription by the reduction of DNA superhelicity through the removal of DNA interwines that naturally arise from these processes. Although Topoisomerase I can also remove superhelicity within one DNA molecule, only TopoII can resolve intertwines between two catenated DNA molecules. Accordingly, this function of TopoII is consensually seen as a prerequisite for proper chromosome segregation. In several organisms, mutations or drugs that block TopoII decatenating activity severely affect chromosome segregation as the concatamers between sister chromatids physically constrain their segregation (Holm et al. 1985; Uemura et al. 1987; Clarke et al. 1993; Gorbsky 1994; Gimenez-Abian et al. 1995). Overall depletion of TopoII either by genetic means (Uemura et al. 1987) or by RNAi depletion of the protein (Chang et

al. 2003; Savvidou et al. 2005) further reveals failures in segregation of sister chromatids during anaphase.

In addition to its catalytic activity, TopoII has been proposed to play a structural role in the architecture of mitotic chromosomes. TopoII was found to be one of the major components of the residual scaffold structure obtained by differential protein extraction from isolated mitotic chromosomes (Earnshaw et al. 1985) and it has been proposed to have a "loop-fastener" role in the organization of the chromatin loop domains (Gasser et al. 1986; Adachi et al. 1991). Accordingly, specific and non-specific inhibitors of TopoII enzymatic activity block chromosome condensation *in vitro* and *in vivo* (Newport 1987; Newport and Spann 1987; Wright and Schatten 1990; Hirano and Mitchison 1991; Sumner 1992; Buchenau et al. 1993; Gorbsky 1994). Moreover, several condensation defects were reported for both TopoII yeast defective mutants (Uemura et al. 1987) and Topo-II-depleted *Drosophila* tissue culture cells (Chang et al. 2003; Savvidou et al. 2005). A further argument for the role of TopoII in chromosome structure arises from its localization. Several studies reveal that TopoII is widely dispersed on chromatin throughout interphase, but during mitosis, TopoII localizes to a central axis within the chromosome (Gasser et al. 1986; Boy de la Tour and Laemmli 1988; Hock et al. 1996; Tavormina et al. 2002; Maeshima and Laemmli 2003; Swedlow and Hirano 2003), further suggesting a structural role within the chromosome.

However, the structural role of TopoII in mitotic chromosome architecture has been challenged when it was reported that, TopoII activity is indeed required for chromosome assembly of sperm chromatin incubated *Xenopus* mitotic egg extracts, however, once condensation was completed, blocking of TopoII had little effect on chromosome morphology (Hirano and Mitchison 1993). Moreover, TopoII mutants in *S. cerevisiae* show no defects in chromosome condensation (Lavoie et al. 2002). *In vivo* analysis of TopoII dynamics during mitosis in *Drosophila* embryos reveals that its localization is not restricted to a central chromosomal axis and that the TopoII present in early prophase is dynamically leaving the chromatin towards the cytoplasm during mitosis (Swedlow et al. 1993). Thus, it has been proposed that TopoII decatenating activity is indeed required to eliminate steric problems during condensation, and therefore required for the condensation process, but it does not serve as a structural backbone within the chromosomes and therefore its activity is not required once chromosome assembly has been completed. Recent dynamic studies of mammalian cells stably expressing a GFP-tagged version of TopoII α reveal that this protein is highly dynamic, continuously exchanging between chromosomal bound and cytoplasmic pools (Christensen et

al. 2002; Tavormina et al. 2002) which further support an enzymatic rather than a structural role of TopoII in mitotic chromosome establishment.

3.3.3 Condensin

The isolation of condensin subunits as a major non-histone protein present in mitotic chromosomes (Hirano and Mitchison 1994; Saitoh et al. 1994; Hirano et al. 1997) immediately raised the hypothesis that this complex would be one of the main players in mitotic chromosome assembly. Indeed, the initial functional characterization of condensin in the *Xenopus* cell-free system together with genetic studies in yeast strongly argued for a role of this protein complex in mitotic chromosome condensation (Saka et al. 1994; Strunnikov et al. 1995; Hirano et al. 1997; Freeman et al. 2000; Lavoie et al. 2000; Ouspenski et al. 2000). However, subsequent genetic studies in metazoan reveal that condensin is not absolutely required for chromatin compaction, as in its absence, individual chromosomes can be visualized which have an apparently normal longitudinal compaction (discussed in Gassmann et al. 2004). Nevertheless, it is consensual that condensin is required for proper mitotic chromosome organization as in its absence chromosomes display abnormal physical properties. Condensin-depleted chromosomes are less resistant to hypotonic shock treatment suggesting a loss of structural integrity (Hudson et al. 2003; Hirota et al. 2004) and show severe problems in the resolution of the sister chromatids (Steffensen et al. 2001; Bhalla et al. 2002; Coelho et al. 2003). Besides abnormal mitotic chromosome morphology, and possibly an intrinsic consequence of that, the most prominent phenotype observed in condensin mutants is defective chromosome segregation with masses of lagging chromatin interfering with cytokinesis (‘cut’ phenotype in yeast).

While for the related cohesin complex it is well established that it function as a ring structure that embraces DNA molecules, thereby promoting sister chromatid cohesin, the mode of action of condensin is less well understood. Some hypotheses arise from a number of enzymatic activities on the DNA molecule (e.g. supercoiling, knotting and renaturation reactions) displayed by condensin complex *in vitro* (Kimura and Hirano 1997; Sutani and Yanagida 1997; Kimura et al. 1999). It remains to be determined whether condensin displays these activities *in vivo,* and if so, it is possible that condensin might function directly on the DNA molecule and in that way induce chromatin reorganization. However, some arguments still favor a structural rather enzymatic role of condensin. The condensin subunit SMC2 (scII)

was one of the most abundant proteins isolated from mitotic chromosomal scaffold (Lewis and Laemmli 1982; Earnshaw and Laemmli 1983; Saitoh et al. 1994) and immunofluorescence analysis revealed that condensin is found to localize at a central axis of mitotic chromosomes together with Topoisomerase II (Coelho et al. 2003; Maeshima and Laemmli 2003). Interestingly, depletion of condensin causes delocalization of Topoisomerase II, which no longer appears confined to the chromosome axis, suggesting that condensin might provide a structural backbone within the chromosome (Coelho et al. 2003).

As the work presented in this thesis has its main focus on this multiprotein complex, an extensive description of condensin complex architecture and its role and possible modes of function in chromosome structure is presented in more detail in a separate section (see section 4).

3.3.4 Other protein factors

Titin, a giant filamentous protein (~3MDa), known for its function as a component of the thick filament in the sarcomere of muscle cells, has been identified as a component of mitotic chromosomes in *Drosophila* embryos (Machado et al. 1998). By analogy with its function in the muscle, it has been hypothesized that chromosomal titin could account for the elastic properties of the mitotic chromosomes. Interestingly, the elastic properties of mitotic chromosomes were found to be similar to those of purified titin (Houchmandzadeh and Dimitrov 1999). Genetic analysis in *Drosophila* further supports a role of titin in mitotic chromosome structure as titin mutations, besides the expected muscle organization defects, lead to severe chromosomal defects, namely, chromosome undercondensation, chromosome breakage, loss of diploidy and premature sister chromatid separation (Machado and Andrew 2000).

The human chromokinesin hKIF2A was shown to localize along the entire arms of condensed chromosomes, during mitosis, as a punctuate structure similar to known scaffold components like TopoII and condensin subunits (Mazumdar et al. 2004). In fact KIF4A was reported to physically interact with condensin subunits and condensin localization is altered in the absence of KIF2A. Importantly, depletion of KIF2A gives rise to hypercondensed chromosomes, even before nuclear envelope breakdown. These data suggest that KIF2A might serve as a molecular linker and/or spacer between chromosome condensation proteins

and its depletion might result in the collapse of the chromosome fiber giving rise to hypercondensed chromosomes. Indeed, the *Xenopus* homologue of hKIF2A, xKLP1, was found to be a major component of mitotic chromosomes assembled *in vitro* (Vernos et al. 1995) and studies in *Drosophila* reveal that KLP3A, the KIF2A homologue in this organism, also associates with mitotic chromosomes (Kwon et al. 2004). However, depletion studies in *Drosophila* failed to reveal any evident chromosome condensation defects (Goshima and Vale 2003; Kwon et al. 2004). Nonetheless, a recent report has revealed that the semi-sterile meiotic mutant mei-352 is in fact an allele of *klp3a* (Yu et al. 2004). KLP3A has been proposed to regulate the distribution of exchanges during meiosis since mei-352 females have an altered distribution of meiotic exchanges without greatly affecting their total frequency. As meiotic exchange is very likely to be dependent on the condensed state of meiotic chromatin this recent data further links the chromokinesin KLP3A with the chromosome condensation process.

The A-Kinase Anchoring protein AKAP95 was also reported to be involved in chromosome condensation dynamics (Collas et al. 1999). Intranuclear immunoblocking of AKAP95 inhibits chromosome condensation and pre-assembled chromosomes undergo premature decondensation when incubated with AKAP95-immunodepleted extracts or cells are AKAP95-immunoblocked during mitosis. These results reveal that AKAP95 is not only involved in the process of chromosome condensation but it is also required for the maintenance of the condensed state of mitotic chromatin. In contrast to the requirement of AKAP95 to the chromosome condensation process, which was found to be PKA independent, the role of AKAP95 in maintenance of the condensed state of mitotic chromosomes appears to be related with the chromosomal targeting of PKA. Moreover, AKAP95 was shown to be required for the targeting of condensin subunits to mitotic chromatin (Collas et al. 1999; Steen et al. 2000; Eide et al. 2002). Interestingly, motif analysis of the AKAP95 protein reveals that distinct but overlapping domains are involved in chromosome condensation and condensin targeting and that truncated versions of the protein are able to restore condensin chromatin targeting but not the chromosome condensation impair (Eide et al. 2002). This demonstrates that AKAP95 is involved in chromosome condensation through processes other than condensin targeting.

Recently, a new serine/threonine kinase, named Greatwall kinase, was identified and shown to be required for proper chromosome condensation in *Drosophila*. Greatwall kinase mutants and Greatwall kinase-depleted tissue culture cells exhibit undercondensed

chromosomes where the two sister chromatids could still be identified. Greatwall kinase might be involved in chromosome condensation through a mechanism independent of condensin or histone H3 phosphorylation as these undercondensed chromosomes were able to efficiently target condensin subunits and to phosphorylate histone H3. The Greatwall kinase does not localize at mitotic chromosomes which suggest that yet unidentified substrate(s) rather than the kinase itself might be required for chromosome condensation. Therefore, further analysis aiming the identification of Greatwall substrates might identify new players in mitotic chromosome structure.

Several proteins, known for their function in the replication process, have been hypothesized be required for proper mitotic chromosome assembly based on the fact that several replication mutants show condensation defects. As an example, *Orc2* mutants display irregularly condensed chromosomes, with the abnormally late replicating regions of euchromatin exhibiting the greatest problems in mitotic condensation (Loupart et al. 2000). Additionally, homozygous *Orc5* mutants have abnormally condensed metaphase chromosomes, with shorter and thicker chromosomes (Pflumm and Botchan 2001). Similarly, overcondensed chromosomes were found in other replication mutants like *Mcm4*, *Pcna* and *Dup* (Whittaker et al. 2000; Pflumm and Botchan 2001). It has been proposed that the density of functional replication centers might determine the degree of lengthwise chromosome condensation. Thus, in replication mutants the frequency of replication origins is reduced and therefore a larger amount of DNA would be pulled through much fewer fixed DNA replication centers (Pflumm 2002). However, these mutants also show a significant metaphase arrest and therefore, it remains to be determined whether the overcondensation phenotype results directly from the reduced number of replication origins in the substrate for condensation or simply results from the arrested state.

4 – Condensins

4.1 Identification of the condensin complexes

Initial identification of condensin subunits stemmed from both genetic and biochemical approaches. Two independent approaches have biochemically identified condensin subunits, as one of the most abundant proteins present in mitotic chromosomes. In one study, the

condensin subunit SMC2/ScII was shown to be one of the major scaffold components, the chromosome-shaped protein structure that remains after nuclease digestion and histone removal of metaphase chromosomes (Saitoh et al. 1994). ScII was shown to localize, together with topoisomerase II, throughout the axial region of mitotic chromosome arms both in chicken and human tissue culture cells. Sequence analysis revealed that ScII belonged to a family of putative ATPases, the SMC family, whose protein member were at the time being identified in both prokaryotes and eukaryotes (Strunnikov et al. 1993). In parallel, other studies aimed the dissection of the biochemical processes of mitotic chromosome assembly and major progress was made after the development of the *in vitro* chromatin assembly using *Xenopus* egg extracts (Lohka and Masui 1983). In this system, unreplicated sperm chromatin is incubated with unfertilized egg extracts which are arrested in a mitosis-like state (meiotic metaphase II). As a result, sperm chromatin forms entangled prophase-like chromosome fibers that gradually resolve into individual rod-shaped chromatids. The subsequent development of sucrose-gradients sedimentation methods started to isolate and characterize the major structural components of these *in vitro* assembled chromatids (Hirano and Mitchison 1994). This study revealed, in addition to histones, three high-molecular-weight proteins XCAP-B (TopoII), XCAP-C and XCAP-E (XCAP stands for *Xenopus* chromosome-associated polypeptides). XCAP-C and X-CAP-E were found to associate with each other in mitotic extracts and to be targeted to chromatin forming a discrete internal structure within assembled chromatids. Functional studies using antibody blocking assays revealed that XCAP-C is required for both the assembly and the structural maintenance of these assembled chromatids. Sequence analyses have further revealed that both these polypeptides belonged to the emerging protein family of SMC proteins (Strunnikov et al. 1993; Hirano and Mitchison 1994). A subsequent biochemical study revealed that XCAP-E and XCAP-C function as core subunits of a five-subunit protein complex with a sedimentation coefficient of 13S (termed 13S condensin), containing three additional non-SMC subunits (XCAP-D2, XCAP-G, and XCAP-H) (Hirano et al. 1997). XCAP-H was found to be the ortholog of barren, a *Drosophila* protein previously shown to be required during mitosis to resolve anaphase bridges (Bhat et al. 1996). Immunodepletion and add-back experiments reveal that the entire condensin complex is required for rod-shaped chromatin assembly *in vitro*. In an independent study, XCAP-D2 subunit (pEg7) was also identified and shown to be required for condensation *in vitro* (Cubizolles et al. 1998).

In parallel with these biochemical approaches, genetic studies in yeast have identified condensin subunits as proteins required for chromosome condensation and segregation (Strunnikov et al. 1993; Saka et al. 1994; Strunnikov et al. 1995). Subsequent studies showed that condensin complex subunits are highly conserved among higher eukaryotes such as *C. elegans* (Lieb et al. 1998), *Drosophila* (Bhat et al. 1996; Steffensen et al. 2001) and chicken (Saitoh et al. 1994; Hudson et al. 2003).

More recently, two independent studies have simultaneously identified a second condensin complex in HeLa cells (Ono et al. 2003; Yeong et al. 2003). This complex, named condensin II, was shown to share the same core subunits (SMC2 and SMC4) with condensin I, but to associate with different condensin II-specific non-SMC subunits (CAP-D3, CAP-H2 and CAP-G2). Sequence homology reveals that other higher eukaryotes process two condensin complexes. The role of condensin II in mitotic chromosome structure was functionally assayed in HeLa cells and in *Xenopus* egg extracts but remains to be determined in other organisms. No homologues for condensin II subunits were found in yeast whereas the *C. elegans* sole condensin complex appears to be closer to condensin II than to the canonical condensin complex (see table 1).

Even thought the exact contribution of this complex to the mitotic chromosome condensation process remains quite controversial, most of these studies confirm that condensin is essential for cell viability and is required for proper mitotic chromosome architecture and segregation of the genome during mitosis.

Table 1 Components of eukaryotic condensin complexes

		S. cerevisiae	*S. pombe*	*C. elegans*		*D. melanogaster*	*A. thaliana*	*X. laevis*	*H. sapiens*
	Condensin				DCC*				
core	**SMC2**	**Smc2**	**Cut14**	**MIX-1**	**MIX-1**	**DmSMC2**	**AtCAP-E1,E2**	**XCAP-E**	**hCAP-E/hSMC2**
core	**SMC4**	**Smc4**	**Cut3**	**SMC-4**	**DPY-27**	**DmSMC4/gluon**	**AtCAP-C**	**XCAP-C**	**hCAP-C/hSMC4**
Condensin I	**HEAT**	**Ycs4**	**Cnd1**	**-**	**DPY-28**	**DmCAP-D2**	**CAB72176**	**XCAP-D2**	**hCAP-D2/CNAP1**
Condensin I	**HEAT**	**Ycs5/Ycg1**	**Cnd3**	**-**	**-**	**DmCAP-G**	**BAB08309**	**XCAP-G**	**hCAP-G**
Condensin I	**Kleisin γ**	**Brn1**	**Cnd2**	**-**	**DPY-26**	**Barren**	**AAC25941**	**XCAP-H**	**hCAP-H**
Condensin II	**HEAT**	**-**		**HCP-6**		**CG31989**	**At4g15890**	**XCAP-D3**	**hCAP-D3**
Condensin II	**HEAT**	**-**		**F55C5,4**		**-**	**At1g64960**	**XCAP-G2**	**hCAP-G2**
Condensin II	**Kleisin β**	**-**		**C29E42**		**CG14685**	**Atg16730**	**XCAP-H2**	**hCAP-H2**

* The Dosage Compensation Complex is unique to *C. elegans*

4.2 Condensins and mitotic chromosome structure

The initial functional characterization of condensin was made using the *Xenopus* egg extracts system, in which demembraned sperm chromatin is incubated with mitotic extracts derived from *Xenopus* eggs and is progressively converted into rod-shaped chromosomes. This chromatin assembly system is a powerful technique to test the requirement of specific components in the chromosome assembly process by specific removal of those from the extract. Accordingly, immunodepletion of XCAP-C revealed that *in vitro* assembly of chromosomes failed in the absence of this polypeptide (Hirano and Mitchison 1994). Moreover, once chromosomes are already assembled and condensed, depletion of XCAP-C induces partial decondensation. These results have strongly suggested that this SMC protein is not only involved in the chromosome assembly process, but it is also required for the maintenance of the condensed state. After the identification of the other components of the condensin complex, similar results were obtained in response to removal of other subunits, revealing that the entire 13S condensin is absolutely required for chromosome assembly *in vitro* (Hirano et al. 1997).

Genetic studies in *S. cerevisiae* show that condensin subunits are essential for cell viability and further reveal that condensin is required for condensation at both unique and repetitive (rDNA) regions of the mitotic chromosomes and for chromatin segregation (Strunnikov et al. 1995; Freeman et al. 2000; Lavoie et al. 2000; Ouspenski et al. 2000; Bhalla et al. 2002; Lavoie et al. 2002). Similarly, mutants for condensin subunits in *S. pombe* were also shown to be required for viability and show defects in chromosome compaction and segregation during mitosis (Saka et al. 1994; Sutani et al. 1999).

However, genetic analyses in multicellular organisms such as *Drosophila* revealed that loss of condensin subunits leads to strong defects in segregation but had only partial effects on chromosome condensation. Mutations on *Drosophila SMC4/gluon* were shown to severely compromise sister chromatid resolution but not longitudinal axis shortening (Steffensen et al. 2001). In this study, measurements of chromosomal longitudinal length have revealed that end-to-end distance is the same in *gluon* mutants and wild type chromosomes and that the kinetics of chromosome compaction in response to colchicine is also maintained. Previous studies have also shown that in *barren* mutants, the *Drosophila* CAP-H orthologue, sister chromatid segregation is impaired but no chromosome condensation defects were reported. More recently, genetic analyses of *DmCAP-G* mutants show that chromosome condensation is

perturbed in prometaphase but normal condensation levels can be achieved at metaphase (Dej et al. 2004; Jäger et al. 2005). Consistently, depletion of scII/SMC2 in DT40 chicken cells showed that chromosome condensation is delayed, but normal levels are eventually reached (Hudson et al. 2003). Similar results were obtained after depletion of SMC4 and MIX-1 in *C. elegans* where chromosomes exhibit a high degree of condensation during metaphase, despite an altered morphology (Hagstrom et al. 2002).

In HeLa cells, where two distinct condensin complexes have been identified, condensin I and condensin II complexes have different contributions for the mitotic chromosome morphology. Specific depletion of condensin I gives rise to "swollen" whereas depletion of condensin II originates "curly" shaped chromosomes (Ono et al. 2003). Interestingly, in chromosomes depleted for either condensin I or condensin II, subunits from the remaining condensin complex and TopoII are still able to able to localize as a fairly well organized axial structure (Ono et al. 2003; Hirota et al. 2004; Watrin and Legagneux 2005). In contrast, simultaneous depletion of both condensin complexes gives rise to "fuzzy" type chromosome with no apparent axial organization of the chromatid cores (Ono et al. 2003). Interestingly, in vertebrate cells, condensin II, but not condensin I depletion, has a strong effect on chromosome condensation during prophase. On the other hand, condensin I-depleted chromosomes show problems in sister chromatid resolution and longitudinal shortening in response to spindle damage, in contrast to condensin II-depleted ones, which behave similar to controls (Hirota et al. 2004). Nevertheless, cells depleted of either condensin I or condensin II show defects in chromosome segregation, namely, DNA bridges and lagging chromosomes (Watrin and Legagneux 2005; Gerlich et al. 2006a).

All together these studies reveal a striking difference in the requirement of condensin for the mitotic chromosome condensation. In the *in vitro* chromatin assembly assay using *Xenopus* egg extracts condensin is found to be absolutely required for the assembly of unreplicated chromosomes. *In vivo* studies using mutations, RNAi depletion or conditional knock-outs for condensin subunits reveal that condensin is dispensable for the formation of individualized chromosomes which are eventually able to condense despite their abnormal morphology. These differences in condensin requirement rise interesting questions regarding the chromosome condensation process. It can not be ruled out that immunodepletion assays lead to co-depletion of non stoechiometrically associated factors that would be important to

couple condensin activity with other condensation pathways. Far more interesting is the possibility that these differences might arise from the use of different chromatin substrates in the condensation process. One possibility might be that somatic chromosome condensation is intrinsically less demanding since somatic nuclei are organized in chromosome territories with less chromatin tangles, in comparison to sperm chromatin. Alternatively, it might be that progression through S phase turns condensin 'less essential' to chromosome condensation (note that in the *Xenopus* egg chromatin assay, unreplicated chromatids are used). Supporting this last observation, *Drosophila* mutants for *dCAP-G* are able to condense replicated but not unreplicated chromosomes (present in *double parked* mutants) (Dej et al. 2004). If so, this implies that replication-associated mechanism might be involved in the chromosome condensation process. Accordingly, studies in yeast reveal that cohesin and cohesin-associated factor play a role in compacting chromosomes longitudinally, probably by linking adjacent cohesion sites (Guacci et al. 1994; Hartman et al. 2000). However, in higher eukaryotes cohesin appears to have no effect on chromosome condensation (Losada et al. 1998; Sonoda et al. 2001; Mito et al. 2003; Vass et al. 2003). Moreover, simultaneous depletion of both condensin and cohesin subunits in *Drosophila* tissue culture cells does not lead to more dramatic chromosome morphological defects than those observed in condensin-depleted chromosomes (Coelho et al. 2003).

Despite some controversy in the exact requirement of condensin for the chromosome condensation process it is widely accepted that condensins are absolutely required for proper segregation. The most preeminent phenotype reported in all studies of condensin depletion is the appearance of massive chromatin bridges during anaphase movements ('cut' phenotype in yeast). This phenotype leads to the hypothesis that condensin would be absolutely required for the resolution of the interwines between sister-chromatids. The first hints that condensin might be involved in chromosome DNA topology arise from the observation that ectopic expression of Topoisomerase I can partially suppress the cut3/smc4 phenotype (Saka et al. 1994). Several *in vitro* studies on condensin further reveal that condensin is able to modulate DNA topology in the presence of topoisomerases (see below). Indeed, accumulating evidence supports that condensin might act cooperatively with topoisomerase II (TopoII) with regard to the resolution of the sister chromatids. Barren/CAP-H was shown to interact with TopoII (Bhat et al. 1996) and YCS4 (CAP-D2 fission yeast ortologue) function is required to localize DNA topoisomerase I and II to chromosomes (Bhalla et al. 2002). In higher eukaryotes, it has been shown that condensin does not inhibit TopoII chromosomal targeting but it is required to

allow a proper localization of TopoII as an axial structure at the chromosomal core (Coelho et al. 2003; Hudson et al. 2003; Savvidou et al. 2005). This suggests that either condensin function is directly required for proper TopoII localization or alternatively, that condensin is the major organizer of chromosomal axis and its depletion causes loss of axial organization of a central core to which TopoII would be associated. A direct link between condensin and TopoII activity arises from the fact that *in vitro* decatenating activity of TopoII is substantially reduced in condensin-depleted extracts (Coelho et al. 2003). Moreover, simultaneous depletion of cohesin and condensin does not rescue the DNA bridging phenotype, revealing that chromatin linkages observed in the abnormal anaphases characteristic of condensin depletion are cohesin-independent, which further supports that they might results from TopoII malfunction. However, other results suggest that condensin and TopoII function independently in chromosome organization as Brn1 mutants are able to decatenate circular plasmids and the production of broken chromosomes, typical features of top2 inactivation could not be detected (Lavoie et al. 2000).

Regardless of the apparently high degree of chromosome condensation eventually reached by metaphase in the absence of condensin, several studies report that chromosome condensation is delayed and chromosome condensation defects are evident in prophase condensin-depleted chromosomes. Studies in *Drosophila* report that prophase chromosomes from gluon/SMC4 mutants are hypocondensed (Steffensen et al. 2001) and prophase chromosomes from CAP-G mutants show an non-uniform condensation pattern (Dej et al. 2004). In agreement, conditional SMC2 mutant chicken cells show that prophases in $SMC2^{OFF}$ cells (judged by PH3 staining) show a diffuse chromatin organization indistinguishable from that in interphase cells (Hudson et al. 2003). Studies in *C. elegans* show that condensin depletion prevents chromosome individualization during prophase but chromosome condensation occurs after NEBD (Kaitna et al. 2002). Recently, quantitative analysis of chromosome condensation kinetics in *C. elegans* reveals that prophase condensation is biphasic and that condensin depletion specifically affects primary condensation events (Maddox et al. 2006). Taken together, these results strongly suggest that condensin might alone mediate chromosome condensation during prophase and that condensin-independent pathways might contribute to chromosome condensation during metaphase allowing normal levels of chromatin compaction to be reached at metaphase in the absence of condensin. Thus, condensin complex might not be the major factor involved in the

compaction of the mitotic chromosome at later mitotic stages even though it is absolutely required for the resolution of the sister chromatids and proper segregation.

Condensin was also shown to be required for the structural integrity of mitotic chromosomes as condensin-depleted chromosomes are less resistant to hypotonic shock treatment (Hudson et al. 2003; Hirota et al. 2004). Additionally, condensin was also proposed to be required for some kind of "structural memory" of mitotic chromosomes (Hudson et al. 2003). Normal chromosomes can be induced to unfold, through changes in the medium composition, but are able to fold back to their original morphology when the adequate composition of medium is restored. In contrast, condensin-depleted chromosomes once unfolded cannot refold and chromosomes remain vaguely recognizable with many regions of decondensed or disorganized chromatin. Recently, condensin was proposed to be additionally involved in the cohesion of sister chromatids at chromosomal arms, but not at either centromere or telomere-proximal loci (Lam et al. 2006). This condensin-mediated cohesion was shown to be established during mitosis and to be reversible within one cycle. Importantly, condensin-mediated chromatin linkages do not affect cohesin dynamics and function suggesting that they act as two independent cohesion mechanisms.

4.3 Architecture of the SMC complexes

There are not many studies that directly assay the architecture of the condensin complex but several structural aspects might be predicted from what has been reported for structurally related SMC-containing complexes. Bacterial genomes contain a single smc gene (MukB in E. Coli) that forms homodimers. In eukaryotes, there are at least six different SMC proteins that form heterodimers. The SMC1–SMC3 pair constitutes the core of the cohesin complex that mediates sister-chromatid cohesion, whereas SMC2–SMC4 is a component of condensin complexes that are essential for chromosome assembly and segregation. The remaining two SMC proteins, SMC5 and SMC6, form a third complex that has been implicated in DNA-repair and checkpoint responses (reviewed by Lehmann 2005).

SMC proteins are large polypeptides (1,000–1,300 a.a.) that have related globular N- and C-terminal domains which contain two canonical nucleotide-binding motifs, Walker A and Walker B respectively. These two globular domains are separated by two long coiled-coil motifs connected by a non-helical sequence (hinge). An unusual antiparallel arrangement of

the coiled-coils was firstly suggested based on the prediction that only through an antiparallel folding of the long coiled-coil motifs, Walker A and B motifs would be brought together to form an ABC-like ATP-binding pocket at their ends (Saitoh et al. 1994). Further insights on the MukB/SMC proteins geometry arose from electron microscopy studies on the SMC protein from *Bacillus subtilis* (BsSMC) and MukB from *Escherichia coli*. This study reveals that both BsSMC and MukB are folded into a V-shaped structure showing two thin rods with globular domains at the ends emerging from a hinge (Melby et al. 1998). This hinge appeared to be quite flexible as the arms could be seen in open conformations, with the terminal domains separated, or in a closed conformation which brings the terminal globular domains together. Moreover, the symmetry of the folded molecules strongly argued for an antiparallel arrangement of the coils which was further confirmed by elegant experiments in which the MukB's N-terminal globular domain was replaced by a rod shaped segment of fibronectin and the C-terminal domain was removed. These FN-MukB molecules produced V-shaped dimmers with a single rod at the end of each arm and never molecules with two rod shapes at the end of one arm and no fibronectin rods at the other. This antiparallel arrangement could be either intramolecular, with the N-terminal half of SMC proteins folding back on their C-terminal half, or intermolecular, with and N-terminal domain of one subunit associating with the C-terminal domain of another.

Subsequent studies have clarified that the antiparallel arrangement occurs intramolecularly and that dimerization occurs via the hinge region. Studies on cohesin complex structure showed that a version of Smc1 lacking the hinge domain is unable to associate with Smc3 and a chimeric version of Smc3, in which Smc3 hinge domain was replaced by the smc1 hinge domain, is able to associate with other smc3 molecule but not with smc1 (Haering et al. 2002). Several mutation studies further confirm this model as mutations in specific residues within the hinge region disrupt dimerization (Hirano et al. 2001; Hirano and Hirano 2002; Sergeant et al. 2005). Thus, each SMC subunit self-folds by antiparallel coiled-coil interactions, creating a 50 nm-long "arms" with "head" globular domain at one end and a "hinge" domain at the other, which mediates dimerization (Fig. 7).

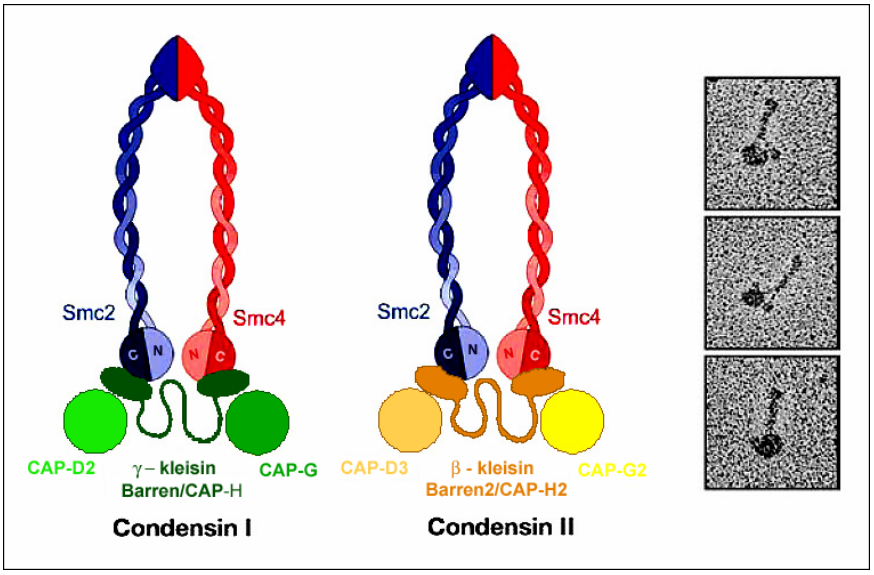

Figure 7. Architecture of the condensin complexes. This predicted structure is based on the assumption that the architecture of the SMC complexes is conserved among different complexes. SMC2 and SMC4 form the core of the condensin complexes. Each SMC subunit folds intramolecularly by antiparallel coiled-coil interactions, and forms an ATP-binding head domain composed of its amino- and carboxy-terminal sequences. Dimerization is achieved by a hinge–hinge interaction between SMC2 and SMC4. The kleisin subunit (kleisinγ/Barren/Cap-H in condensin I and kleisinβ/Barren2/Cap-H2 in condensin II) connects SMC2/SMC4 heads and additional, two Heat-repeats subunits (CAP-D2 and CAP-G, in condensin I and CAP-D3 and CAP-G2 in condensin II) associate with the complexes. Right Electron micrographs show soluble condensin complexes (Adapted from Nasmyth and Haering 2005).

The "head" domain contains an ATP-binding cassette (ABC)-like domain commonly present in other ABC-ATPases such as ABC transporters and the double-strand break (DSB)-repair protein Rad50. Crystal structure of Rad50's ATPase domain provides the first clues on the structure of the "head" domain revealing the dimerization of two ABC domains in a nucleotide-sandwich manner (Hopfner et al. 2000). Identical results were later obtained for ABC transporters (Locher et al. 2002; Smith et al. 2002) and more recently for SMC-complexes (Haering et al. 2004; Lammens et al. 2004). These structural studies predict that ATP binds each head to a pocket formed by Walker A and Walker B motifs and induces their intimate interaction via contacts between the ATP molecule and the C motif, the ABC signature motif found in all ABC-ATPases, from the adjacent head. This model is further confirmed by mutation analysis of these key residues in the *Bacillus subtilis* SMC protein where mutations in the Walker A motif abolish ATP binding while mutations within the C motif allow ATP binding but impair head to head engagement and ATP hydrolysis (Hirano et al. 2001). Moreover, a Glu to Gln substitution within the Walter B motif was shown to stabilize head-head engagement by slowing down ATP hydrolysis (Hirano and Hirano 2004). Furthermore, equivalent mutations in yeast cohesin complex subunits were shown to abolish cohesin function, revealing that ATP binding and hydrolysis is required for the *in vivo*

function of cohesin (Arumugam et al. 2003; Weitzer et al. 2003). In addition, binding of ATP to Smc1 head (but not to Smc3) was shown to be required for scc1 association indicating that ATP binding is involved in the process of assembly of the tripartite ring. This does not depend on ATP hydrolysis but ATP hydrolysis is required for chromatin binding of the cohesin ring. Interestingly, this predicted structure suggests a possible mechanism by which ATP binding and hydrolysis could induce conformational changes in the complex. ATP binding can promote association of the two ATPase heads whereas its hydrolysis might drive them apart.

Crystal structures of the hinge domain from *Thermotoga maritima* has also been resolved giving insights on how the dimerization might be established (Haering et al. 2002). The hinge domain monomer is composed of two domains that are related by a pseudo-2-fold symmetry. The N-terminal region of one monomer associates with the C-terminal region of the same monomer forming an antiparallel coiled coil. Dimerization is achieved primarily by β-sheet interactions between the monomers, producing a doughnut-shaped structure that protrudes two coiled-coil arms in opposite directions.

Although both cohesin and condensin display the two-armed structure that is characteristic of SMC proteins, electron microscopy analysis reveal that their conformations are remarkably different. The hinge of condensin is closed and the coiled-coil arms are placed close together. Three non-SMC subunits of condensin form a subcomplex and bind to one (or both) of the head domains, forming a 'lollipop-like' structure (Anderson et al. 2002; Yoshimura et al. 2002). In contrast, the hinge of cohesin is wide open and the coiled-coils are spread apart from each other (Anderson et al. 2002). A detailed molecular architecture of the whole complex is well understood for cohesin complex. Subunit-subunit interaction assays revealed a ring-shaped configuration of cohesin and further demonstrate that scc1 is directly in association with the head domains of both smc1 and smc3, with scc1's N-terminus bound to smc3 whereas scc1's C-terminus is associated with smc1 head domain (Haering et al. 2002). Similarly, bacterial SMC dimmers associate with non-SMC subunits through their head domains (Yamazoe et al. 1999; Dervyn et al. 2004; Hirano and Hirano 2004).

More recently, a new protein superfamily of SMC-interacting proteins was described, termed kleisins, which includes ScpA, Scc1, Rec8, and Barren among others (Schleiffer et al. 2003). These proteins display reduced overall homology but alignment of the N- and C-terminal domains of the kleisin superfamily shows almost complete identity of the hydrophobic pattern and some conservation of functional residues. There are four classes of

eukaryotic kleisins, α, β, γ and δ. While α-kleisins (e.g. scc1) associate with cohesin's Smc1/Smc3, δ-kleisins (e.g. Qri2) associated with Smc5/Smc6 heterodimer. The two condensin complexes contain a particular class of kleisin. In condensin I, smc2/Smc4 is found in association with γ-kleisin (e.g. CAP-H/barren) whereas in condensin II Smc2/Smc4 binds β-kleisins. In addition to SMCs and kleisins, SMC complexes often include other non-SMC proteins (e.g CAP-D2 and CAP-D3) composed of HEAT repeats, tandemly arranged curlicue-like structures that appear to serve as flexible scaffolding on which other components can assemble (for review see Neuwald and Hirano 2000).

Even thought the molecular architecture of condensin has not been directly assayed it is very likely that the overall structure of the SMC complexes is conserved. Thus, based on the molecular architecture of cohesin complex (Haering et al. 2002), one possible general mechanism is that in SMC complexes the kleisin member directly associates with head domains of SMC proteins while other non-SMC proteins are recruited to the complex via the kleisin moiety. If such assumption is correct, the structure of condensin I and II complexes would be similar to the one depicted in figure 7.

4.4 Enzymology of the SMC proteins

While some progress has been made in defining the role of condensin in mitotic chromosome structure, the exact mechanism by which condensin drives mitotic chromosome organization remains unknown. One approach into the understanding of condensin's mode of action is through the evaluation of its *in vitro* activities in the presence of DNA.

Studies using purified *S. pombe* smc2/4 heterodimer have revealed that this complex is able to efficiently promote DNA renaturation reaction, winding up single-strand DNA into double helical DNA (Sutani and Yanagida 1997). Peculiarly, this activity was shown to be much higher for the smc2/4 heterodimer alone than to the condensin holo-complex (Sakai et al. 2003).

Probably the most promising activity of condensin that could account for chromosome condensation is that purified condensin displays DNA-dependent ATPase activity and catalyzes the formation of positive supercoils of closed circular DNA in the presence of Topoisomerase I (Kimura and Hirano 1997). Interestingly, this activity was stimulated by the presence of ATP and it was found to be much greater for condensin complexes purified from

mitotic extracts when compared to complexes purified from interphase extracts. Structurally, this supercoiling reaction could be explained by three different models. Condensin might overwind the DNA molecule which increases double helical twist (Fig. 8a) or instead it might wrap the DNA around itself creating a local positive supercoil (Fig 8b). Alternatively, condensin might introduce a global writhe by forming a positively supercoiled loop (Fig 8c). To address this issue Bazett-Jones and co-workers (2002) performed a direct visualization of the condensin-mediated DNA supercoiling reaction using electron spectroscopic imaging. This study revealed that the structure of the supercoiling reaction product shows ~190 bp of DNA organized into a compact structure with two distinct domains, indicative of the formation of two oriented gyres (Fig 8b). Moreover, this analysis also showed that a single condensin complex is able to introduce two or more compensatory supercoils into a closed circular DNA, a strong indication that condensin complexes might act individually, rather than cooperatively.

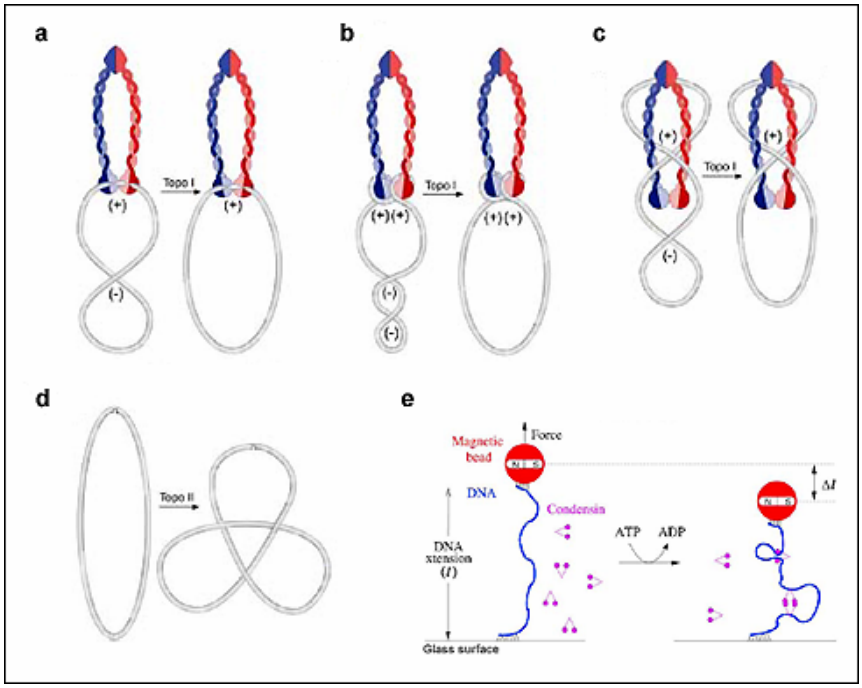

Figure 8. ***In vitro*** **activities of condensin.** Condensin introduces positive supercoils into closed circular DNAs which could be by (a) overwinding of DNA, (b) introduction of gyres into DNA by wrapping around its head domains, or (c) trapping DNA in a global positive writhe. Compensatory negative supercoils could be removed by the action of topo I in all cases. (d) Condensin stimulates the introduction of knots into nicked circular DNA when treated with topo II. (e) Condensin is able to contract linear DNA (adapted from Nasmyth and Haering 2005 and Strick et al. 2004).

In addition to its supercoiling activity, condensin I was also shown to be able to convert nicked circular DNA into a positive knotted form of DNA (trefoil, Fig. 8d) in the presence of Topoisomerase II (Kimura et al. 1999). A similar activity was reported for yeast smc2/4 dimer (Stray and Lindsley 2003).

Recently, single-molecule DNA manipulation experiments reveal that condensin I is able to compact linear DNA (Strick et al. 2004). In these experiments, one end of the linear DNA molecule is attached to a glass slide while the other end is attached to a magnetic bead and linear compaction can be detected by the reduction of the end-to-end extension of the linear DNA. Using this experimental set up, addition of condensin and ATP to the system was shown to promote physical DNA linear compaction; i.e., a reduction in DNA end-to-end extension (Fig. 8e).

Theoretically, all these enzymatic activities could account for chromatin compaction as the end-product of the reaction is more compacted that the initial substrate. It remains to be determined however, whether condensin displays such enzymatic activities *in vivo* and in which extent they contribute to mitotic chromosome condensation process.

4.5 Regulation of condensin activity and chromosomal localization

Spatial and temporal distribution of condensin subunits during cell cycle appears to vary among different species. In *S. cerevisiae*, condensin subunits are nuclear throughout cell cycle (Freeman et al. 2000; Bhalla et al. 2002) whereas in the fission yeast most condensin subunits are found to be mainly cytoplasmic during interphase and transported into the nucleus during mitosis (Sutani et al. 1999). Studies in *Drosophila* reveal a differential localization among condensin subunits. SMC4 and Barren/CAP-H were shown to be mostly cytoplasmic during interphase, although low level nuclear staining is also detected (Steffensen et al. 2001). These subunits were found to be loaded onto chromosomes in early prophase and to dissociate from chromosomes late in anaphase/telophase when decondensation begins. In contrast, CAP-D2 was shown to be predominantly nuclear throughout the cell cycle (Savvidou et al. 2005). In vertebrate cells, where two condensin complexes have been described, condensin II is nuclear during interphase whereas condensin I is sequestered in the cytoplasm until throughout interphase and prophase (Hirota et al. 2004; Ono et al. 2004; Gerlich et al. 2006). Similar dynamics was reported for plant cells (Fujimoto et al. 2005). All together, these studies reveal

a highly dynamic localization of condensin which strongly indicates that there might be molecular mechanisms that regulate condensin chromosomal targeting and activity.

Indeed, *in vitro* studies revealed that CAP-D2 and CAP-H are hyper-phosphorylated by Cdk1 in a mitosis-specific manner (Kimura et al. 1998). Importantly, this phosphorylation was found to be required for *in vitro* supercoiling activity displayed by the condensin complex (Kimura et al. 1998; Kimura et al. 2001). These *in vitro* studies strongly suggest that Cdk1-dependent phosphorylation might be a key factor in condensin regulation *in vivo*. As already mentioned, two independent studies have identified a second condensin complex in HeLa cells, named condensin II (Ono et al. 2003; Yeong et al. 2003). One of these studies has isolated hCAP-D3 (called hHCP-6 in this study) in a two-hybrid screen with the regulatory subunit of PP2A aiming the identification of novel PP2A substrates (Yeong et al. 2003). Indeed, hCAP-D3 was shown to be phosphorylated specifically during mitosis and to be dephosphorylated by PP2A *in vitro*. Thus, PP2A might regulate condensin II through the regulation of the phosphorylated state of CAP-D3. In addition, condensin I supercoiling activity was found to be negatively regulated during interphase through inhibitory phosphorylation by CK2 (Takemoto et al. 2006). All together, these studies suggest that at the G2/M transition, the high activity of mitotic-Cdks activates condensin which in turn mediates chromosome condensation. By the end of mitosis, the drop in Cdk activity would promote condensin inactivation (possibly via PP2A-mediated dephosphorylation and/or CK2 inhibitory phosphorylation) which could contribute to chromatin decondensation. Condensin modifications might not only influence its enzymatic active state but can also contribute to its ability to be targeted to chromatin. Accordingly, nuclear localization of condensin in *S. pombe* was shown to be Cdk1-dependent (Sutani et al. 1999).

Not much is known about how condensin interacts with DNA *in vivo*. CAP-D2 (also known as CNAP1) has been proposed to play a direct role in the targeting of the entire complex (Ball et al. 2002). Transfection experiments with truncated versions of CAP-D2 reveal that its carboxyl terminus, which contains a functional bipartite nuclear localization signal, has a chromosome-targeting domain that does not require other condensin components to localize at mitotic chromosomes. A truncated version of CAP-D2 lacking this C-terminal domain is able to form an entire condensin complex but fails to associate with mitotic chromosomes. Interestingly, the chromosomal targeting of the CAP-D2 C-terminal appears to be mediated by interactions with histones H1 and H3.

In addition to modifications directly on the condensin complex, other chromatin-associated factors have been proposed to play a role in condensin chromosomal targeting. In both *Drosophila* and *C. elegans*, aurora B depletion reduces histone H3 phosphorylation and restrains condensin chromosomal targeting during mitosis (Giet and Glover 2001; Hagstrom et al. 2002; Kaitna et al. 2002). Also, *S. pombe* mutants for Bir1/cut17, homologue of the human survivin which is required for aurora B activity (Lens et al. 2006), fail to recruit condensin to mitotic chromosomes (Morishita et al. 2001). This indicates that either H3 phosphorylation or other aurora B-dependent phosphorylation event might be required for condensin localization on mitotic chromosomes. However, this might not to be a conserved mechanism among different species as depletion or inactivation of Aurora B in budding yeast and vertebrate cells do not abolish condensin chromosomal localization (Losada et al. 2002; MacCallum et al. 2002; Hauf et al. 2003; Lavoie et al. 2004; Ono et al. 2004). Other histone modification has been proposed to play a role in condensin localization. Studies in *Drosophila* reveal that female-sterile mutants for NHK1, a kinase responsible for phosphorylation of histone H2A on Thr 119, show defects in the formation of the meiotic chromosomal structures and fail to recruit condensin onto the oocyte chromosomes (Ivanovska et al. 2005). These mutants also fail to disassemble the synaptonemal complex (SC) and therefore it remains to be determined whether failure in condensin chromosomal targeting results from the absence of phosphorylated H2AThr119 or alternatively, it is due to the maintenance of the SC on meiotic chromosomes.

Factors other than histone modifications have been also implicated in condensin chromosomal targeting. The cAMP-dependent kinase (PKA or A-kinase) anchoring protein AKAP95, was also reported to be required for the targeting of condensin subunits to mitotic chromatin possibly through a direct interaction with CAP-H (Collas et al. 1999; Steen et al. 2000; Eide et al. 2002). Specific motifs within AKAP95 protein were tested for their requirement in condensin targeting, revealing that mutation in the PKA-binding domain and removal of the zinc-finger 1 domain does not affect condensin chromosomal localization (Eide et al. 2002).

A screen in *Saccharomyces cerevisiae* designed to identify potential condensin regulators identified the SUMO protease Ulp2/Smt4 as a multicopy suppressor of the smc2-6 allele (Strunnikov et al. 2001). Suppression by Ulp2/Smt4 is specific for smc2-6 allele as it does not rescue Smc2-8 or Smc4-1 alleles. Interestingly, mutation in SMT4 abolishes mitosis specific targeting of condensin to rDNA locus. This strongly suggests a sumoylation pathways

might be involved in condensin regulation. In agreement, recent studies in *S. cerevisiae* reveal that Ycs4 (CAP-D2 homologue) is monosumoylated prior to mitosis entry and becomes disumoylated specifically during anaphase (D'Amours et al. 2004). This anaphase-specific sumoylation is CDC14-dependent and is required for enrichment of Ycs4 at the nucleolus and proper rDNA segregation.

The studies mentioned above point some evidence for how condensin activity and chromosomal targeting might be regulated. However, the mechanisms that regulate condensin chromatin association *in vivo* are far from being understood. Additionally, little is known about the mechanisms that regulate condensin release from chromatin at the end of mitosis.

4.6 Condensins and meiotic chromosome structure

In the process of meiotic division a haploid gamete is produced from a diploid cell and therefore this is a reductional division. Thus, during first meiotic division homologous chromosomes are disjoined whereas in the second meiotic division sister chromatids are separated. While meiosis II is a “mitosis-like event”, meiosis I is a significant different process which comprises several meiosis-specific chromosomal structural changes. During meiosis I, homologous chromosomes became physically connected along their entire length before they line up at the metaphase I plate. This pairing (also known as synapsis) also allows genetic recombination (crossing-over), whereby a fragment of maternal chromatid may be exchanged for a corresponding fragment of a homologous paternal chromatid. Thus, meiotic prophase I can be divided into five sequential stages: during leptotene, chromosomes start to condense into long strands within the nucleus.; at zygotene, homologous chromosomes start to pair and during pachytene, the synaptonemal complex (SC), a long ladder-like protein core that mediates chromosome synapsis and recombination (crossing-over), extends along the entire length of paired chromosomes and genetic recombination takes place; during diplotene, chromosomes separate through the disassemble of the SC but are held together by the chiasmata, the points where two non sister chromatids had exchanged their genetic material during crossing-over. Finally, during diakinesis, chromosomes condense further and the chromatids are resolved in a way that the four chromatids and the chiasma points became visible.

Several studies have already reported an important role of condensin complexes in the organization of meiotic chromosomes. Initial studies in *C. elegans* reveal that depletion of SMC-4 and MIX-1 by RNAi caused chromosome segregation defects only during meiosis II, while segregation during meiosis I was unaffected (Hagstrom et al. 2002). Subsequent studies in which analysis of HCP-6 RNAi depletion in a hcp-6 genetic mutant background was carried out, revealed that meiosis I was also affected and cohesin-independent linkages lead to prominent chromatin bridges observed between segregating chromosomes during both anaphase I and anaphase II (Chan et al. 2004). Additionally, detailed localization analysis of condensin during wild-type meiosis in *C. elegans* revealed that condensin is not present in pachytene chromosomes, in which cross-over events occur, and becomes enriched in diplotene chromosomes, after synaptonemal complex (SC) disassemble. After chromosome condensation at diakenesis, condensin is found as four discrete foci, at each sister chromatid from the tetrad (Chan et al. 2004). A significant different localization was reported to occur in *S. cerevisiae* where condensin was found to localize to the axial core of pachytene chromosomes (Yu and Koshland 2003). Moreover, condensin mutants display defects in pachytene specific events, namely in synaptonemal complex assembly, leading to defects in homolog pairing and processing of double strand breaks. Studies in Arabidopsis have also reveal that condensation and segregation defects are evident during meiosis I in SMC2 mutant lines (Siddiqui et al. 2003).

All together, these studies strongly indicate that condensin is important for proper chromatin segregation in both meiotic divisions. It remains to be determined whether condensins in multicellular organisms are involved in the meiotic specific events underlying the genetic recombination process similar to what has been described in *S. cerevisiae*.

4.7 – Other functions of condensins

Multiple lines of evidence suggest that in addition to its better studied function during mitosis, condensins have important functions during interphase. Several studies have already shown that condensin is required for transcription regulation and gene expression. For example, *S. cerevisiae* mutants for ysc4 (CAP-D2 homologue) are defective in silencing of silent mating type locus (Bhalla et al. 2002). Additionally, condensin was proposed regulate nucleolar silencing by organizing a specialized topology of rDNA chromatin, which is required for a proper balance of telomeric/nucleolar Sirp2, a protein that has been implicated

in the transcriptional silencing and suppression of recombination (Machin et al. 2004). smc2 mutants were shown to relocalize telomeric Sirp2 to rDNA which consequently leads to an increased repression in rDNA foci and a weaker repression at the telomeres. Studies in *Drosophila* have shown that condensin subunit Barren co-localizes with polycomb group (PcG) target sequences, responsible for the maintenance of embryonic, early determined transcription repression of developmentally regulated genes (Lupo et al. 2001). Barren was shown to interact with the PcG protein Polyhomeotic and *barren* mutants are unable to silence a reporter mini-white gene under the control of Fab-7 PRE (Polycomb Response Element).

Two independent studies have analyzed the role of condensin in Position Effect Variegation (PEV) in *Drosophila*. PEV is the effect on gene expression mediated by the chromatin structure associated with heterochromatic regions (for further reading see Reuter and Spierer 1992). Embryonic lethal alleles of *barren* and *dcap-g* were shown to exhibit a dominant suppression of PEV (Dej et al. 2004). Flies caring the reporter whitem4hgene, which is normally repressed due to its proximity to heterochromatic regions, show red-eyed phenotype as a result of improper gene repression. Contradicting results were recently published where it was shown that several condensin mutants display a strong enhancement (higher repression) of PEV (Cobbe et al. 2006). Exception was found for the glu88-82 allele which showed a strong suppression of PEV, consistent with its classification as a potential neomorphic mutant (suggested by its sequence). Even though the role of condensin in transcription regulation might be only related with the establishment of a proper chromatin structure, the direct involvement of condensin in this process cannot be ruled out. Indeed, a recent study reported that a subfraction of condensin interacts with the DNA methyltrasferase DNMT3B, a key enzyme of the epigenetic machinery, in mammalian cells (Geiman et al. 2004).

Another non-mitotic role of condensin has been well documented in *C. elegans* where a condensin-like complex forms the Dosage Compensation Complex (DCC) (Hagstrom and Meyer 2003). Dosage compensation in hermaphrodite nematodes is achieved by partial downregulation of both X chromosomes. In the DCC complex the SMC2 homologue (MIX-1) associates with a SMC4 variant (DPY-27) and with DPY-26 and DPY-28 which have limited homology to the non-SMC subunits CAP-H and CAP-D2, respectively (see Table 1) (Chuang et al. 1996; Lieb et al. 1998). The DCC is directed onto the X chromosomes of hermafrodites by specific targeting proteins (SDC-2 and SDC-3) which are required for both sex

determination and dosage compensation. Interestingly, SDC-2 also recruits the same complex to the autosomal gene her-1 to repress its transcription > 20 fold (Chu et al. 2002).

Accumulating evidence also support a role of condensin in DNA repair and checkpoint activation. In *S. pombe*, *Cnd2* mutants (Cap-H homologue) do not repair DNA damage leading to a higher sensitivity to ultraviolet radiation and hydroxyurea and fail to activate the checkpoint kinase Cds1/Chk2 (Aono et al. 2002). Further supporting the role of condensin in DNA repair, condensin SMC hinge was found to interact with Cti1, a member of the highly conserved C1D protein family implicated in DNA-repair function (Chen et al. 2004). Moreover, overexpression of Cti1 is able to complement the hypersensitivity of the condensin subunit mutant cnd2-1 for DNA damage drugs. Additionally, hCap-E/SMC4 was found to interact *in vivo* and *in vitro* with DNA ligase IV, an enzyme implicated in the DNA double-strand breaks (DSB) repair via nonhomologous end-joining (Przewloka et al. 2003). Recently, condensin I was also sown to interact with the poly(ADP-ribose) polymerase 1 (PARP-1) protein, a DNA nick sensor that plays a role in DNA repair and maintenance of genome integrity (Heale et al. 2006). This interaction was shown to be significantly enhanced after induction of single-strand breaks (SSB) damage and to be required for stable complex formation between condensin I and the base excision repair factor XRCC1. Moreover, condensin I also binds to other factors involved in base excision repair (FEN-1 and DNA polymerase δ/ε) in a damage-specific manner. Importantly, condensin depletion leads to a decreased rate of SSB repair.

PART II

EXPERIMENTAL WORK

Chapter 1

Role of Condensin I in mitotic chromosome architecture and structural integrity of the centromere

1. Introduction

The genome of eukaryotic proliferating cells undergoes programmed structural changes in order to ensure the integrity of genetic material and cell viability during cell division. First, during S phase when DNA is duplicated, sister chromatid cohesion is established along the entire length of DNA molecules and it is maintained until entry into mitosis. Subsequently, during early stages of mitosis, chromosomes condense into higher order levels of chromatin organization, leading to the resolution of chromosome arms, a prerequisite for genome stability. Although, mitotic chromosomes were one of the first subcellular structures observed (re-edited in Flemming, 1965), the mechanisms underlying their establishment only recently have begun to be unveiled.

A major contribution was the identification of the multiprotein condensin complex, initially purified and characterized from *Xenopus* extracts (Hirano et al., 1997) and later shown to be highly conserved (reviewed in Losada and Hirano 2005). Immunodepletion and add-back experiments in *Xenopus* egg extracts revealed that the condensin complex is required for rod-shaped chromatin assembly *in vitro* (Hirano et al., 1997). Mutation analysis of condensin subunits in both fission and budding yeast showed defects in chromosome condensation and segregation (Saka et al. 1994; Strunnikov et al. 1995; Freeman et al. 2000; Lavoie et al. 2000; Ouspenski et al. 2000).

However, genetic studies in multicellular organisms like *Drosophila* revealed that loss of condensin subunits leads to strong defects in segregation but had only partial effects on chromosome condensation (Bhat et al. 1996; Steffensen et al. 2001; Dej et al. 2004; Jäger et al. 2005). Studies in DT40 chicken cells showed that in the absence of condensins, chromosome condensation is delayed although near normal levels are eventually reached at metaphase (Hudson et al. 2003). More recent studies reveal that in this system condensin depletion results in ~40% less compacted chromosomes, compared to controls, but distinct condensed chromosomes could still be visualized (Vagnarelli et al. 2006). Studies in *C. elegans* have also reported that in the absence of condensin, chromosome condensation is delayed and chromosomes display severe condensation defects during prophase, although normal levels of chromosome condensation can be detected in metaphase (Hagstrom et al. 2002; Kaitna et al. 2002; Maddox et al. 2006). Overall these data suggests that the condensin complex is important for chromosome architecture but might not be the only factor responsible for chromatin compaction.

Recent studies have revealed the identification of a new condensin complex in HeLa cell extracts named Condensin II (Ono et al. 2003; Yeong et al. 2003). Condensin II shares the core SMC proteins with Condensin I but has different regulatory subunits. Not all organisms appear to have the two types of complexes and different condensin complexes might be required for different tissues or at different developmental stages (Ono et al. 2003). Bioinformatic analyses revealed that *Drosophila* genome has homologues for two condensin II specific non-SMC proteins (CAP-D3 and CAP-H2). However, no proteins with close homology with CAP-G2 were found across the genome of this model organism (Ono et al. 2003). Of particular importance in the context of chromosome structure, these two distinct complexes were shown to contribute differently to mitotic chromosome architecture in vertebrate cells. Whereas depletion of condensin I-specific proteins gives rise to chromosomes with a swollen morphology, depletion of condensin II results in curly shaped chromosomes (Ono et al. 2003). Moreover, in these chromosomes depleted of a single condensin complex, the localization of condensin subunits from the remaining complex shows an axial distribution within the chromosome core (Ono et al. 2003; Hirota et al. 2004). Only the simultaneous depletion of both condensin complexes resulted in fuzzy type morphology of mitotic chromosomes with complete misresolution of the sister-chromatids and apparently no axial organization of the chromatin cores.

Up to the date this study was initiated, the only studies that have addressed the role of condensin in *Drosophila melanogaster* were concentrated on the analysis of DmSMC4 (Steffensen et al. 2001, Coelho et al. 2003), a core subunit shared by two condensin complexes. It remained to be addressed whether the canonical condensin I and the putative condensin II complexes have distinct roles in mitotic chromosome structure. Therefore, the study presented in this chapter reports a detailed functional analysis of the role of condensin I upon the organization and segregation of mitotic chromosomes. This was addressed by depletion of Barren/CAP-H, a condensin I specific subunit, from *Drosophila* S2 cells using dsRNA interference technique. This study revealed that depletion of Barren/CAP-H compromises the binding of the other condensin I regulatory subunits, DmCAP-D2 and DmCAP-G, to mitotic chromatin. However, in the absence of Barren/CAP-H, chromatin binding of the DmSMC4/2 core heterodimer is still observed, demonstrating the ability of the heterodimer to associate with chromatin independently of the regulatory condensin I sub-complex. However, no defined axial distribution of these core subunits could be observed. We also show that S2 cells depleted of Barren/CAP-H display abnormal sister chromatid

resolution and segregation. Chromosome architecture defects are very similar to the ones observed after DmSMC4 depletion (Coelho et al. 2003).

Additionally, the study has focused particular attention to the role of condensin I in the in the organization of centromeric chromatin. The centromere plays an essential role in chromosome segregation. First, it underlies the organization of the kinetochore and thereby the attachment and movement of chromosomes along spindle microtubules. Secondly, it ensures sister chromatid cohesion from S-phase until the metaphase-anaphase transition. In this way centromeres contribute to bipolar attachment of chromosomes, essential for the proper partition of the genome during cell division. In the holocentric chromosome of *C. elegans*, several studies indicate that condensin subunits colocalize with CENP-A along the entire chromosome length and play a role in centromere organization. It has been shown that SMC-4 and MIX-1 are required for proper centromere bi-orientation and segregation (Hagstrom et al. 2002).

These results could be attributed to the particular features of *C. elegans* holocentric chromosomes. However, several results suggest that condensin might also have a role at the centromeres of monocentric chromosomes. Studies in *Drosophila* have revealed a strong localization of condensin I at the centromere (Steffensen et al. 2001). Also in *S. pombe*, chromatin immunoprecipitation assays showed that condensin localizes to CEN DNA (Aono et al. 2002). Moreover, in metaphase chromosomes from HeLa cells, condensin II is enriched at the primary constriction (Ono et al. 2004) and in *Drosophila* cells the putative condensin II subunit CAP-D3 localizes exclusively at the centromeres (Savvidou et al. 2005). Finally, it has been recently reported a genetic and physical interaction between *Drosophila* CAP-G and the centromere-specific CID/CENP-A (Jäger et al. 2005). However little is known about the molecular role of condensins in the centromere structure.

Accordingly, the phenotypic analysis of condensin I depletion reported here focused particularly on the structure of centromeric chromatin. Indeed, *in vivo* analysis of Barren/CAP-H depleted cells expressing GFP-Histone H2B together with immunofluorescence analysis of metaphase-arrested cells have revealed that chromosomes are unable to align at the metaphase plate. Immunofluorescence analysis also indicates that although chromosomes show bipolar attachment, intercentromere distances are unusually large. Moreover, centromeric markers appear distorted and the cohesin protein DRAD21 shows an abnormally broad localization. Furthermore, the heterochromatic specific K9 di-

methylated histone H3 is also abnormally distributed in Barren/CAP-H-depleted chromosomes. Taken together, this analysis has revealed that condensin I plays a major role in the organization of centromeric heterochromatin in order to maintain its elastic properties which are essential to withstand the forces exerted by the mitotic spindle.

2. Results

2.1 Analysis of cell cycle progression after depletion of Barren/CAP-H from Schneider 2 (S2) *Drosophila* tissue culture cells

In order to deplete the regulatory subunit Barren/CAP-H, specific of condensin I, double-stranded RNA interference (dsRNAi) was performed in S2 *Drosophila* cells. The depletion levels were monitored by western blot analysis of protein extracts prepared every 24h during the time course of the experiment (Fig.1.1a). Titration of the Barren antibody reveals that this is a very sensitive antibody (detection limit ~$2x10^4$cells; Fig. 1.1b) which ensures that western blot analysis can be used to monitor protein depletion at the cell density used ($5x10^5$ cells per lane). Accordingly, quantification analysis reveals that 24 hours after dsRNA addition the levels of the protein were already significantly reduced to about 20% of control cells levels (Fig 1.1a). At 96 hours the Barren/CAP-H levels were barely detectable (99% reduction). Immunofluorescence analyses of Barren/CAP-H in S2 *Drosophil*a cells further confirmed that this protein is depleted to hardly detectable levels (Fig 1.1c). Metaphase chromosomes from dsRNA treated cells show no accumulation of Barren/CAP-H, in contrast to control cells, where Barren/CAP-H is localized at the axis of mitotic chromosomes.

To evaluate the effect of Barren/CAP-H depletion on the doubling time of the culture, the number of viable cells was counted at every 24 hours (Fig 1.2). The growth curves reveal that Barren/CAP-H depletion causes a significant reduction in cell proliferation which strongly suggests that Barren/CAP-H is essential for cell viability. Despite the clear effect on the cell culture growth, Barren/CAP-H-depleted cells show a mitotic index even slightly higher than control cells (Fig. 1.3).

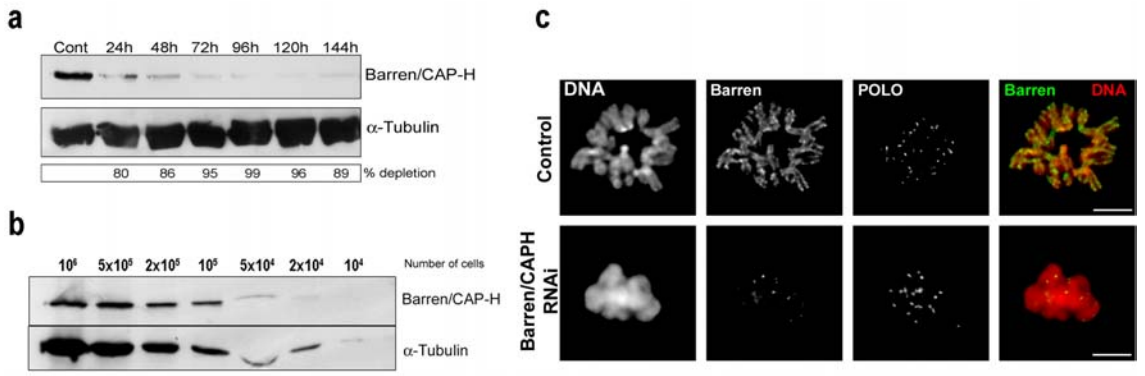

Figure 1.1. Analysis of Barren/Cap-H depletion after dsRNAi. a) Barren/CAP-H depletion monitored at different times of the dsRNAi experiment by western blot. Each lane corresponds to $5x10^5$ cells. α-tubulin was used as loading control. **b)** Titration of the Barren antibody using protein extracts from control cells at different concentrations, to determine detection limit. **c)** Barren/CAP-H depletion revealed by immunofluorescence analysis. Polo staining was used as mitotic marker. Scale bars are 5 μm.

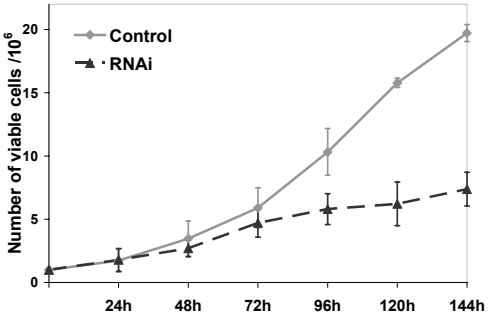

Figure 1.2 – Proliferation profiles of control and Barren/CAP-H depleted cells. The graph shows the average of three independent experiments (Error bars represent standard deviation (SD)). Barren/CAP-H depletion has a strong effect on cell culture doubling time.

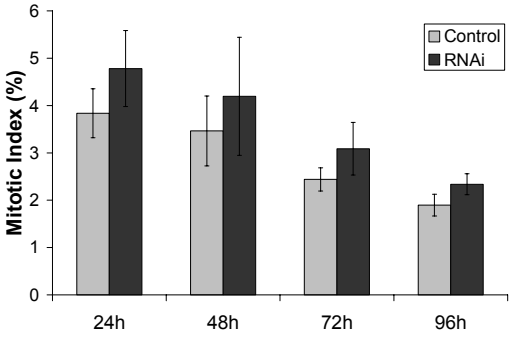

Figure 1.3 – Mitotic index at different time points of the experiment. Quantifications were performed using either POLO/PH3 or α-tubulin/PH3 double straining. Approximately 6.500 cells were counted for each experimental condition. Graphic shows average of quantifications from four different slides out of two independent experiments. Error bars are SD.

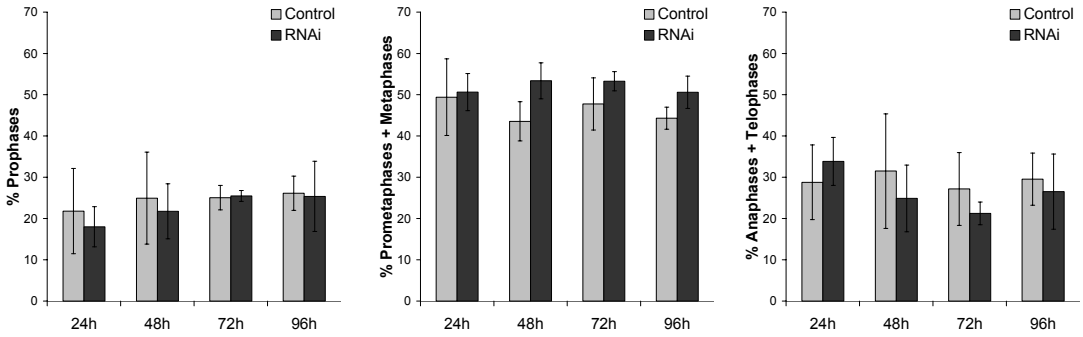

Figure 1.4. Analysis of mitotic progression after Barren/CAP-H depletion. Quantifications were performed using either POLO/PH3 or α-tubulin/PH3 double straining. Approximately 200 mitotic cells were counted for each experimental condition. Graphics show average of quantifications from four different slides out of two independent experiments. Error bars are SD.

To further analyze the effect of Barren/CAP-H depletion in the progression through mitosis, the percentage of cells at each mitotic phase amongst the mitotic population was calculated (Fig 1.4). This quantification indicates that there are no major differences in the frequencies of cells at each stage when compared to control cells, even though there is a consistent slight increase in prometaphase and metaphase figures.

It is well accepted that the frequency of cells in a particular phase can be usually correlated with the time cells spend at this stage. Following this logic, the results obtained by quantifications of fixed material strongly suggest that Barren/CAP-H-depleted cells progress through mitosis with a normal timing. However, a more accurate result can be obtained by *in vivo* analysis of cells while they undergo nuclear division in the absence of Barren/CAP-H. GFP-α-tubulin was previously shown to be a good marker for timing different phases of mitosis (Lopes et al. 2005). The visualization of tubulin asters can be used to detect early mitotic cells and the entry of soluble GFP-tubulin within the nuclear space clearly marks the time of nuclear envelope breakdown (NEBD). Moreover, anaphase onset can be determined by the retraction of the kinetochore bundles. Therefore, time-lapse microscopy analysis of both control and dsRNA treated GFP-tubulin-expressing cells was performed and the time cells spend in prometaphase/metaphase was evaluated by measuring the time between NEBD and anaphase onset (Fig. 1.5 and Movies 1.1 and 1.2).

From the different Barren/CAP-H cells analyzed (n=14 cells), half of them entered mitosis normally, but remained arrested at metaphase for more than 1 hour. This was only observed once in control cells (n=10). Moreover, while control cells spend on average 31 ± 5 minutes (average ± SD) in prometaphase/metaphase, Barren/CAP-H-depleted cells that were

recorded until mitotic exit spend 52 ± 19 minutes in that stage. The NEBD-to-anaphase timing was very divergent amongst RNAi cells varying from 36 min to 86 min.

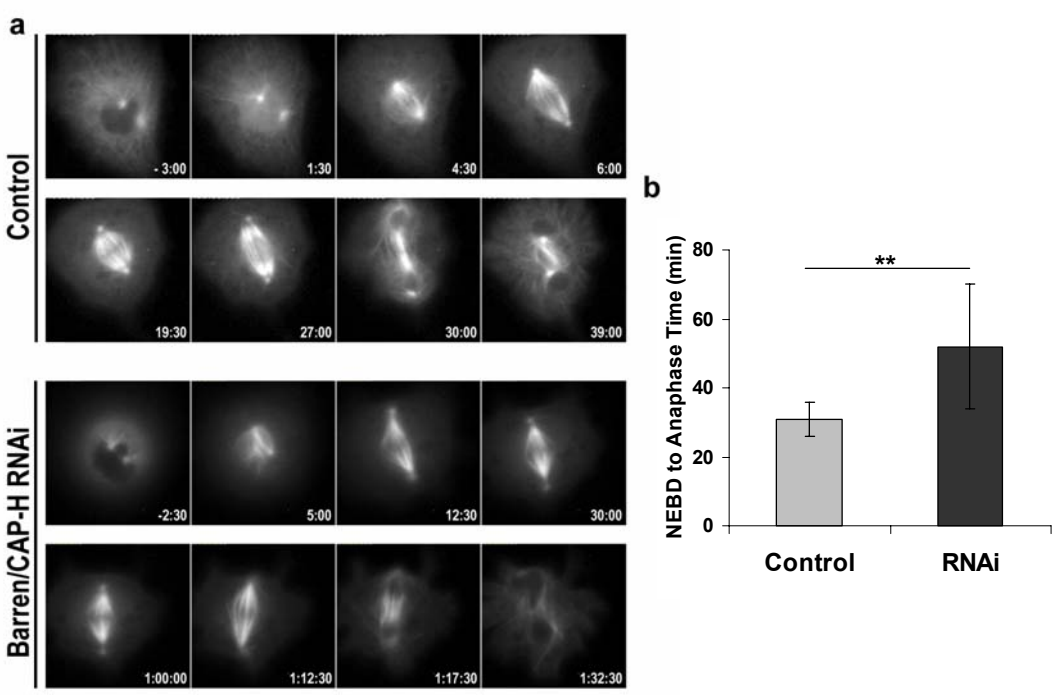

Figure 1.5. ***In vivo*** **analysis of mitotic progression after depletion of Barren/CAP-H. a)** Selected images from time-lapse movies of control (upper panel) and Barren/CAP-H-depleted cells (lower panel). Nuclear envelope breakdown (NEBD) was set as time zero. **b)** Quantification of NEBD-to-anaphase timing in both control (n=9) and RNAi cells (n=7). Error bars are SD; Barren/CAP-H-depleted cells spend significantly more time in prometaphase/metaphase when compared to control cells (**$p<0.01$ by Mann-Whitney test)

These results show that Barren/CAP-H depletion has indeed a strong effect on progression through mitosis, which is in contrast to the results obtained in fixed material quantifications. There are at least two possible explanations that could account for this discrepancy.

First, the mitotic arrest/delay might be an artifact of the fluorescence microscopy analysis. It is known that light can induce DNA damage and DNA damage checkpoint has been shown to be active throughout mitosis and to prevent mitotic exit in case of improperly repaired DNA (Smits et al. 2000; Su and Jaklevic 2001; Mikhailov et al. 2002; Chow et al. 2003; Minemoto et al. 2003). Moreover, condensin has been implicated in DNA damage repair (Aono et al. 2002; Przewloka et al. 2003; Chen et al. 2004; Heale et al. 2006). Therefore, it is possible that the delay observed in this time-lapse microscopy analysis is a

consequence of the accumulation of improperly repaired DNA damage and would not be detected in unperturbed mitosis.

Second, it is also possible that frequency in this case does not correlate with timing. The similar (although slightly higher) mitotic index quantified for Barren-CAP-H depleted cells could result from a less number of cells entering mitosis while the ones that do so, spend more time at mitotic stages. In fact, this would be totally consistent with the slower proliferation displayed by RNAi treated cells (Fig. 1.2). Taking this into consideration, the similarity between the frequency of cells at each mitotic phase between control and Barren/CAP-H-depleted cells suggest that cells spend more time in all phases of mitosis.

Although the first explanation can not be ruled out, the second one is strongly supported by the results presented in this study, which are fully consistent with a prometaphase/metaphase delay (see section 2.4 in this chapter).

2.2 Stability and chromosomal localization of other condensin subunits and Topoisomerase II in the absence of Barren/CAP-H

In order to determine whether Barren/CAP-H is necessary for the localization of other condensin I components, immunolocalization of both core and regulatory subunits of this complex was carried out (Fig. 1.6). In control cells, condensin I subunits DmSMC2, DmSMC4, DmCAP-D2, and DmCAP-G localize at the axis of metaphase chromosomes (Fig. 1.6a-d). In Barren/CAP-H-depleted cells, the two core proteins, DmSMC2 and DmSMC4, are able to localize on chromatin but the staining is no longer confined to a central axis (Fig. 1.6a,b). In contrast, the other non-SMC proteins, DmCAP-D2 and DmCAP-G, could not be detected in Barren/CAP-H-depleted chromosomes (Fig. 1.6c,d). Additionally, quantifications of the mean pixel intensity of fluorescence signal from cells immunostained against all the condensin subunits reveal that while chromatin-associated protein levels of all condensin I non-SMC proteins are severely reduced (<20%), approximately 50% of the core subunits DmSMC4 and DmSMC2 are associated with mitotic chromosomes (Fig 1.7).

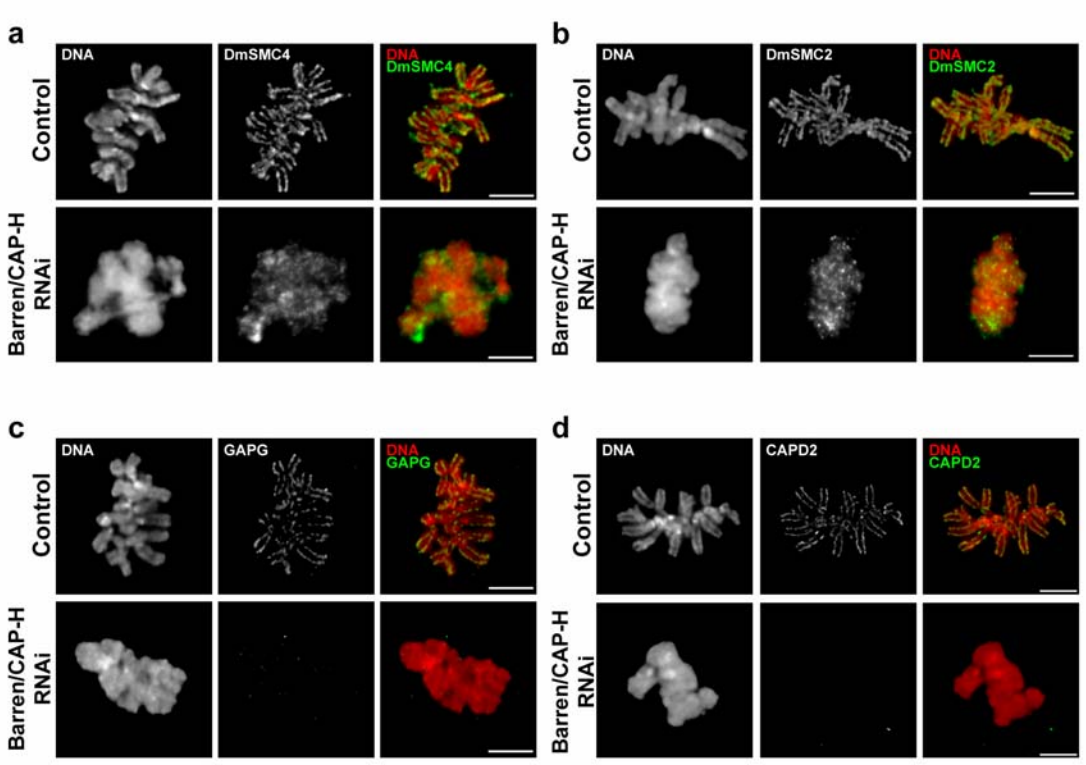

Figure 1.6. Chromosomal localization of condensin subunits in control and Barren/CAP-H-depleted cells. In control cells condensin I subunits, including DmSMC4 **(a)**, DmSMC2 **(b)**, DmCAP-D2 **(c)** Dm-CAP-G **(d)** localize at the central axis of sister chromatids. After depletion of Barren/CAP-H, the core subunits, DmSMC4 and DmSMC2, still localize to chromatin but appear diffuse and no longer confined to an axial structure. The non-SMC proteins of the condensin I complex, DmCAP-D2 and DmCAP-G, could not be detected on mitotic chromosomes after Barren/CAP-H depletion. Scale bars are 5 μm

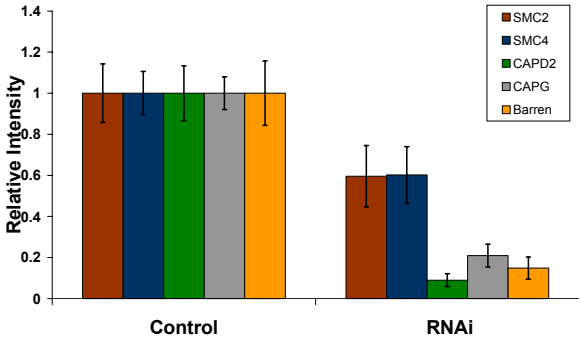

Figure 1.7 – Quantification of chromatin-associated levels of condensin I subunits. For these quantification analyses, chromosomal area was automatically selected based on the DAPI stained DNA and the mean pixel intensity of condensin subunits' signals within this area was measured. Values were normalized for mean pixel intensity of control cells (n=8 cells, error bars are SD)

These results show that in the absence of Barren/CAP-H, the other non-SMC subunits do not associate significantly with mitotic chromosomes. In contrast, the core DmSMC2 and DmSMC4 proteins have the ability to bind mitotic chromatin, even though at decreased levels. Importantly, the associated SMCs are unable to localize to a defined axis at the chromosomal core, which strongly suggests that the axial organization of Barren/CAP-H-

depleted mitotic chromosomes is severely compromised. To address this further, the localization of Topoisomerase II (TopoII) was analyzed. TopoII is also known to localize at a central core within sister-chromatids (Coelho et al. 2003; Maeshima and Laemmli 2003). Accordingly, TopoII was found to localize to a defined inner axis in control cells (Fig. 1.8a). However, in Barren/CAP-H depleted chromosomes, TopoII was detected at normal levels but the staining was no longer restricted to a defined region at the chromosomal core (Fig 1.8a,b).

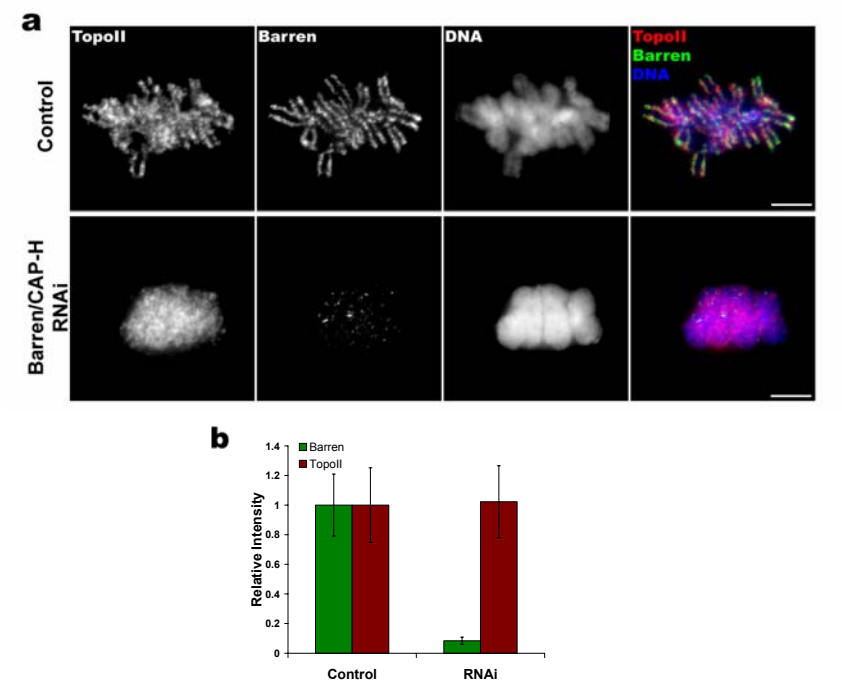

Figure 1.8 – Chromosomal localization of topoisomerase II in control and Barren/CAP-H depleted cells. a) Immunofluorescence analysis of TopoII (red) and Barren/CAP-H (green) localization in metaphase chromosomes from control and RNAi cells. In the merged figure, DNA is shown in blue. Note that TopoII is able to localize to Barren/CAP-H depleted chromosomes but does not appear confined to a central axis. Scale bars are 5 μm. **b)** Quantification of chromatin-associated levels of Topoisomerase II. Chromosomal area was automatically selected based on the DAPI stained DNA and the mean pixel intensity of TopoII signals within this area was measured. Barren/CAP-H levels were also evaluated to confirm protein depletion. Values were normalized for mean pixel intensity of control cells (n=8 cells, error bars are SD).

Additionally, the stability of the remaining condensin subunits in Barren/CAP-H-depleted cells was assayed (Fig. 1.9). Western blot analysis of total protein extracts shows that the levels of DmSMC4 do not change significantly after Barren/CAP-H depletion while those of DmCAP-D2 are reduced by half relative to control levels (Fig. 2E). This suggests that the stability and the chromosomal localization of the other non-SMC regulatory subunits of condensin I is dependent of Barren/CAP-H.

To sum up, in Barren/CAP-H-depleted cells, the other non-SMC proteins of condensin I complex are apparently unstable and do not associate with mitotic chromosomes while core SMC proteins of the complex as well as TopoII are able to localize to chromatin although unable to accumulate at a central axis within the chromatids.

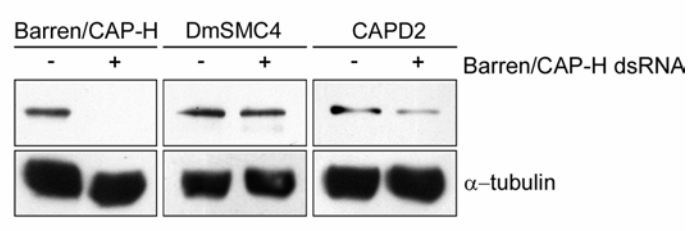

Figure 1.9 – Analysis of total protein levels of condensin subunits. Total proteins extracts from 10^6 cells were assayed by western blot to determine the levels of DmSMC4 and CAP-D2 in control (-) and Barren/CAP-H depleted (+) cells. DmSMC4 levels do not change significantly whereas those of CAP-D2 are significantly reduced (~45%) compared to controls. α-tubulin was used as loading control.

2.3 Depletion of Barren/CAP-H affects sister-chromatids resolution and segregation

In order to define the specific contribution of condensin I to chromosome structure, the phenotype of Barren/CAP-H depleted chromosomes was analyzed (Fig. 1.10). Mitotic chromosomes from depleted cells are unable to resolve their sister chromatids but normally condense along their longitudinal axis. The frequency of cells at metaphase with unresolved sister chromatids increased substantially during the dsRNAi experiment and virtually all metaphase cells show chromosomes with unresolved sister chromatids (Fig. 1.11). Colchicine treatment, used to depolymerize microtubules and extend the period in prometaphase, did not allow better resolution of sister-chromatids in Barren/CAP-H-depleted chromosomes (Fig. 1.10). Moreover, Barren/CAP-H depleted chromosomes were unable to sustain stress induced by hypotonic shock (Fig. 1.10).

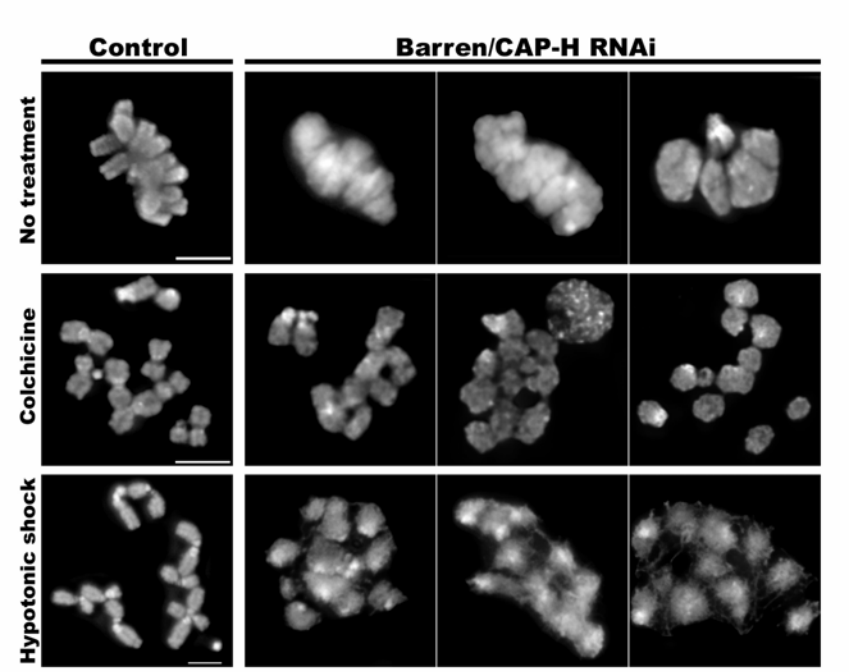

Figure 1.10 – Analysis of mitotic chromosomes structure in Barren/CAP-H-depleted cells. Control and Barren/CAP-H depleted cells (96h) were either directly fixed or incubated with either 30 μM of colchicine for 2 hours or 0.1% sodium citrate hypotonic solution for 10 seconds prior to fixation. In all these experimental conditions no resolution between the sister-chromatids could be observed. Scale bars are 5 μm.

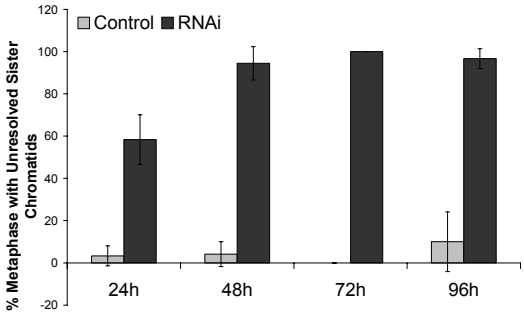

Figure 1.11 – Quantification of metaphases with unresolved sister-chromatids.
These quantifications were performed using either tubulin/PH3 or POLO/PH3 double staining. Percentages were calculated over the total number of metaphase cells (~200 mitotic cells were counted). Graphic shows average of quantifications from four different slides out of two independent experiments. Error bars are SD.

Despite the lack of resolution between sister-chromatids in Barren/CAP-H depleted chromosomes, cells are able to enter anaphase displaying extensive DNA bridges even during very late telophase (Fig. 1.12). Again, quantification analysis reveals that this is a highly penetrant phenotype in which nearly all mitotic RNAi cells analyzed display chromatin bridges during the later stages of nuclear division (Fig 1.13).

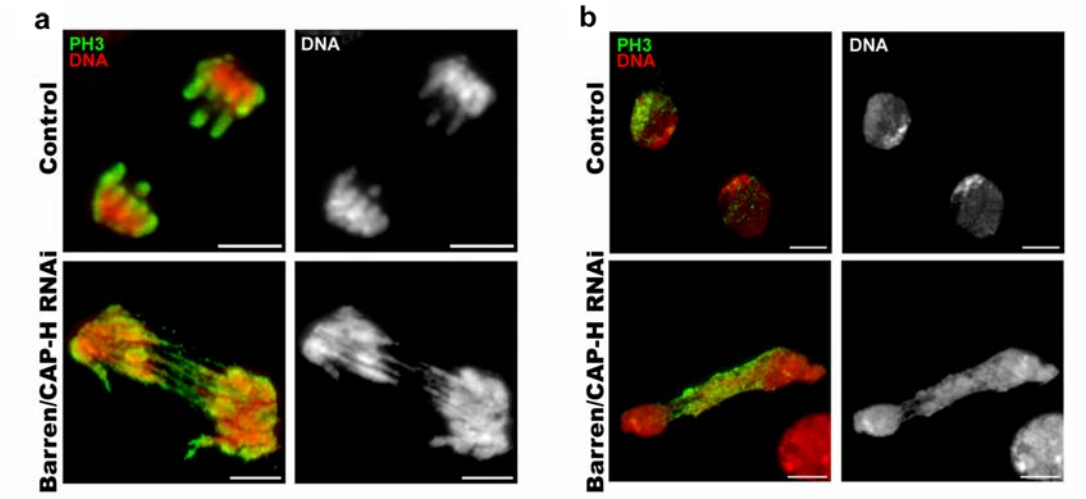

Figure 1.12 – Analysis of anaphase and telophase figure in Barren/CAP-H-depleted cells. Barren/CAP-H depleted cells (96h) show extensive DNA bridges in **(a)** anaphase and **(b)** telophase. Cells were immunostained for phospho-histone H3 (PH3, green) and counterstained for DNA (red). Grey panels show DNA alone. Scale bars are 5 µm.

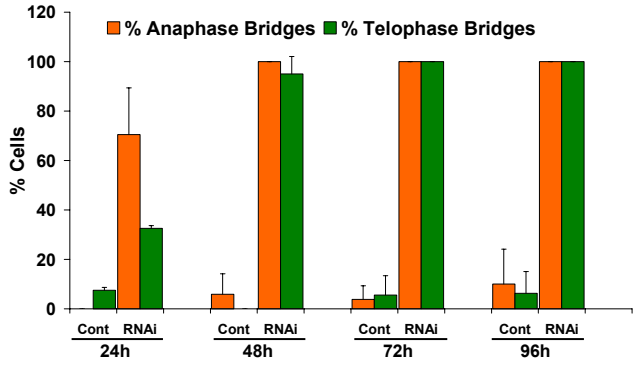

Figure 1.13 – Quantification of chromatin bridges during mitosis.
These quantifications were performed using either tubulin/PH3 or POLO/PH3 double staining. Percentages were calculated over the total number of anaphase or telophase cells (~200 mitotic cells were counted). Graphic shows average of quantifications from four different slides out of two independent experiments. Error bars are SD.

Chromatin bridges were also detected between Barren/CAP-H-depleted interphase cells. Two distinct types of bridges were observed (Fig. 1.14). Some cells were apparently separated at the cytoplasmic level, as judged by the phase contrast image and tubulin staining, but remained connected by a thin chromatin bridge (red arrow in fig 1.14). Other cells appear as "giant binucleated cells", where a thicker DNA bridge is visualized between two nuclei that share a common cytoplasm (white arrow in Fig. 1.14). These later phenotype strongly indicates that Barren/CAP-H depletion can result in cytokinesis failure. The frequency of these two types of interphase chromatin bridges increases in the initial stages of the experiment but it is not cumulative at later time points, i.e. there is no substantial increase between 72h and 96h (Fig. 1.15). This suggests that either cells are ultimately able to resolve the bridge or, alternatively, cells with this phenotype eventually die.

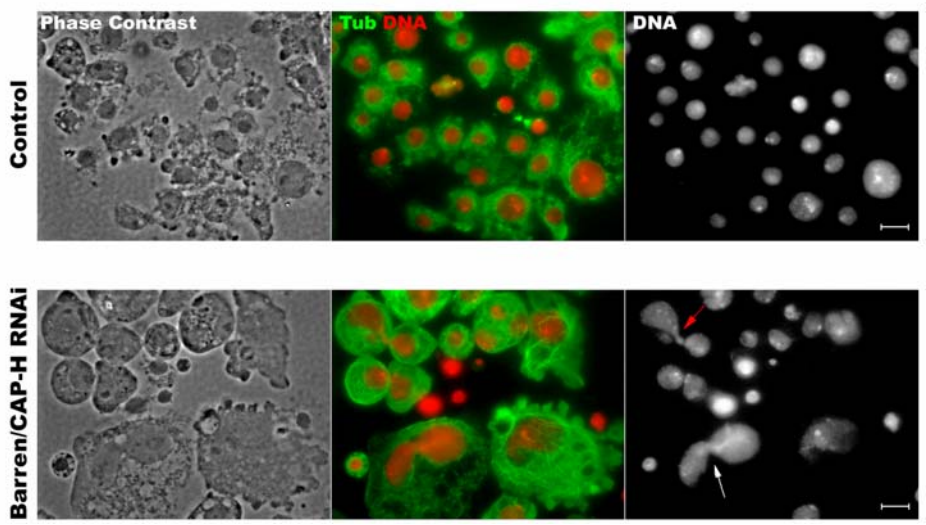

Figure 1.14 – Analysis of interphase cells after Barren/CAP-H depletion. Representative images from control and Barren/CAP-H depleted cells (96h) analyzed by phase-contrast, immunostained against tubulin and counterstained for DNA. Barren/CAP-H-depleted cells often show two individual cells that remain connected by thin interphase bridges (red arrow) and "giant cells" that contain two nuclei connected by a thick DNA bridge (white arrow). Scale bars are 10 μm.

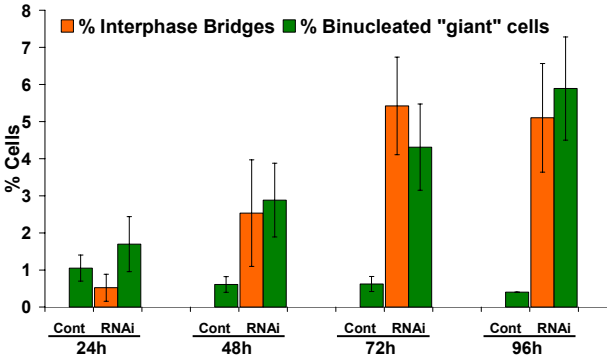

Figure 1.15 – Quantification of interphase bridges and binucleated cells. These quantifications were performed using tubulin and DNA double staining. Percentages were calculated over the total number of cells (~6500 cells were counted). Graphic shows average of four different quantifications out of two independent experiments. Error bars are SD.

FACS analyses of both control and Barren/CAP-H depleted cells revealed that depletion of Barren/CAP-H causes increased aneuploidy and the formation of highly polyploid cells (Fig. 1.16). Whereas in control cells we observe that most cells maintain a normal ploidy over the time course of the experiment, after depletion of Barren/CAP-H we observe a lower frequency of cells with a 2C DNA content and increased frequency of cells with a DNA content lower that 2C and 2-4C intermediate, suggesting defects in segregation and aneuploidy. Aneuploidy was further confirmed by the quantification of the number of kinetochores observed in each mitotic cell (Fig. 1.17). Approximately 90% of control cells have 20 to 24 kinetochores, corresponding to 10-12 chromosomes. In contrast, ~35% of Barren/CAP-H-depleted cells show abnormally higher of lower number of kinetochores per

cell, which strongly indicates abnormal chromosome segregation on previous nuclear divisions. This method uniquely addresses aneuploidy at the level of kinetochore segregation. Previous studies on *DmSMC4* mutants have shown that more than 70% of the cells segregate normally their centromeres even though chromatin bridges (mostly euchromatic and telomeric regions) were still observed (Steffensen et al. 2001). Thus, the 35% aneuploidy revealed by the kinetochore number per cell is very likely to be an underestimation of the real value.

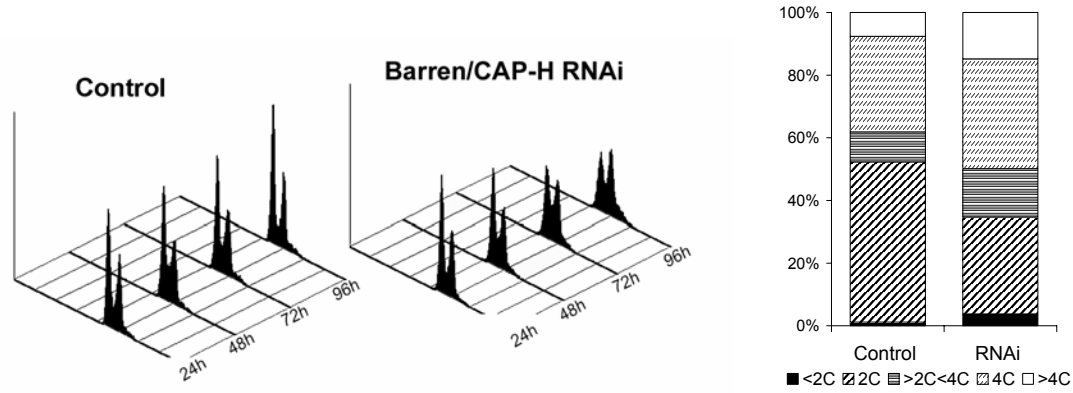

Figure 1.16 – FACS analysis of cells cultures over the time course of the experiment. a) FACS profiles of control and Barren/CAP-H-depleted cells, showing DNA content and cell number. **b)** Graphic representation of the frequency of cells with different DNA content obtained from FACS analysis at 96h after dsRNA addition.

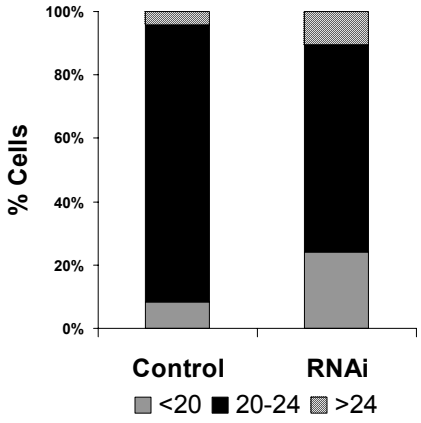

Figure 1.17 – Quantification of the percentage of cells with different centromere numbers. For these quantifications, the number of centromeres in control (n=48) and Barren/CAP-H-depleted (n=58) prometaphase and metaphase cells was counted based on the signal of the centromere marker CID. Most control cells have 20-24 CID-stained centromeres while Barren/CAP-H-depleted cells show a higher frequency of cells with either lower of higher number of centromeres.

Moreover, FACS analysis has also revealed an increased frequency of cells with 4C and higher DNA content in Barren/CAP-H-depleted cells, further suggesting that condensin I depletion can lead to cytokinesis failure resulting in polyploid cells (Fig. 1.16). The observed cytokinesis failure, however, does not appear to be due to mislocalization of essential factors to the cytoplasmic division process, as INCENP and POLO, two proteins already reported to be required for cytokinesis (Carmena et al. 1998; Adams et al. 2001), localize normally to the spindle midzone during telophase in Barren/CAP-H depleted cells (Fig. 1.18). Thus, cytokinesis failure is more likely to be related with a physical constrain to cell division caused by the presence of chromatin bridges at the cleavage furrow.

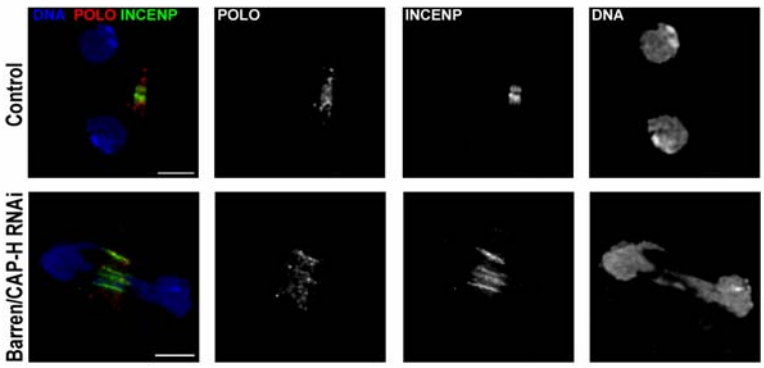

Figure 1.18 – Immunofluorescence analysis of INCENP and POLO localization during telophase /cytokinesis. Telophase figures from both control and Barren-CAP-H-depleted cells show INCENP (green) and POLO (red) normally localized at the midbody. Scale bars are 5 μm.

2.4 *In vivo* analysis of chromosome dynamics in Barren/CAP-H depleted cells.

To highlight Barren/CAP-H depleted chromosome dynamics during mitosis we performed time lapse fluorescence imaging in S2 cells stably expressing GFP-Histone H2B (Fig. 1.19). In control cells we can clearly observe chromosome congression to the metaphase plate, sister chromatid separation and segregation to opposite poles (Fig. 1.19a and Movie 1.3). However, in Barren/CAP-H depleted cells we consistently observed persistent oscillation of chromosomes during an extended prometaphase. Indeed, a well defined metaphase plate was rarely observed before anaphase onset, suggesting that chromosomes fail to align properly (Fig. 1.19b upper panel and Movie 1.4). Furthermore, in Barren/CAP-H depleted cells, DNA bridges are detected since anaphase onset. DNA bridges were found in 92,3% (n=13) of Barren/CAP-H depleted cells whereas in control cells only one cell showed DNA

bridging in anaphase (n=11). In 15,4% (n=13) of Barren/CAP-H depleted cells we observed the formation of massive DNA bridges that after the initial separation at anaphase onset fused back into a single large nucleus (Fig. 1.19b lower panel; and Movie 1.5). These results further support a cytokinesis failure as inferred by both FACS and immunofluorescence analyses.

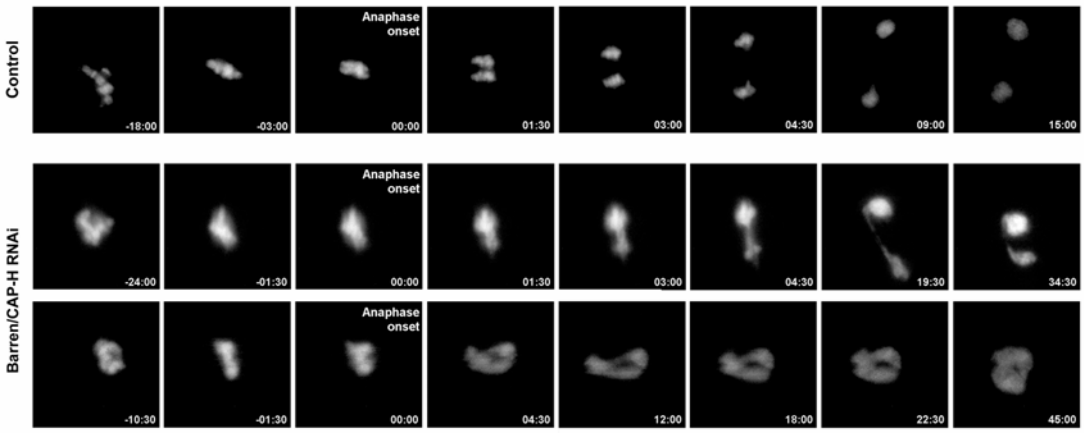

Figure 1.19. ***In vivo*** **analysis of nuclear division after depletion of Barren/CAP-H.** Selected images from time-lapse movies of control and Barren/CAP-H-depleted S2 cells stably expressing GFP-HisH2B acquired every 2 minutes from the time mitotic chromosomes could be visualized. To align the movies, anaphase onset was defined as time zero. In control cells, prometaphase is followed by a tight organization of the chromosomes at the metaphase plate, which after a few minutes, initiate sister chromatid separation. In Barren/CAP-H depleted cells a well defined metaphase plate is rarely observed and chromatin bridges are observed as soon as anaphase is initiated. In some cases, cells depleted of Barren/CAP-H undergo anaphase onset but extensive chromatin bridges are formed, and after an initial attempt to segregate, the chromatin collapses back into a single large nucleus (lower panel).

2.5 Chromosomes depleted of Barren/CAP-H have functional kinetochores but fail to congress normally

Time lapse fluorescence imaging of Barren/CAP-H depleted cells in mitosis shows that chromosome alignment at the metaphase plate is not achieved, which suggests a failure in chromosome congression. To address this further, analysis of chromosome congression was performed in cells arrested at metaphase, giving further time for alignment at the metaphase plate. Anaphase onset is a proteasome-dependent event since sister chromatid separation is ultimately achieved after activation of the protease separase, which is kept inactive by an inhibitory protein securin before metaphase/anaphase transition. At anaphase onset, securin degradation by the proteasome is triggered, releasing active separase which then cleaves the cohesin subunit Scc1 and thereby removes the cohesion between sister chromatids (for review see Yanagida 2005). Therefore, anaphase onset can be prevented by the use of proteasome

inhibitors, such as MG132 (Genschik et al. 1998). Accordingly, control and Barren/CAP-H-depleted cells were incubated with the proteasome inhibitor MG123 for 2 hours to induce metaphase arrest. Cells were then fixed and immunostained for POLO, used as a kinetochore marker (Llamazares et al. 1991), and ZW10 which migrates to spindle microtubules when chromosomes reach bipolar attachment (Williams et al. 1992) (Fig. 1.20a) and quantifications of kinetochore alignment were carried out. A box perpendicular to the spindle, that included approximately 85% of the kinetochores from control cells (10x3µm area) was used to quantify congression (Fig. 1.20a,b). In Barren/CAP-H-depleted cells 45±13 % of kinetochores localize outside the box suggesting that Barren/CAP-H-depleted chromosomes are unable to congress properly even if arrested in mitosis.

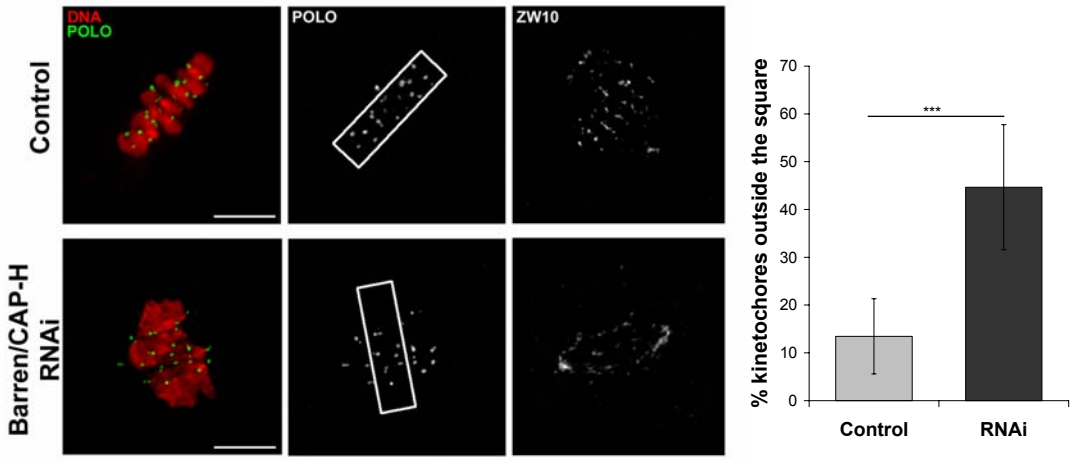

Figure 1.20. Analysis of chromosome congression after depletion of Barren/CAP-H. Both control and Barren/CAP-H-depleted cells were arrested in metaphase by incubation with the proteasome inhibitor MG132 for 2 hours. Cells were immunostained for POLO (green) used as kinetochore marker and ZW10 (left grey panel), to reveal spindle orientation of cells under attachment. In order to evaluate kinetochore congression, a box comprising 85% of aligned kinetochores in a control metaphase was defined. The same box was placed over Barren/CAP-H-depleted metaphases, perpendicularly to the spindle (indicated by ZW10 spindle staining). The percentage of kinetochores placed outside the defined box in both control and Barren/CAP-H depleted metaphase cells was calculated (n=14 cells; ~ 300 kinetochores; graphic shows average and error bars are SD; ***$p<0.001$ by Mann-Whitney test). Note that Barren/CAP-H depletion causes a severe increase in the frequency of misaligned kinetochores.

Several studies have already shown that chromosome misalignment is usually associated with defective microtubule-kinetochore interaction (Wood et al. 1997; Adams et al. 2001; Kline-Smith et al. 2004). Therefore, the state of microtubule/kinetochore attachments was investigated in order to address whether Barren/CAP-H depleted chromosomes are able

to establish stable microtubule attachments. To detect only kinetochore microtubules, control and Barren/CAP-H depleted cells were treated with calcium (Fig. 1.21), which specifically destabilizes non-kinetochore microtubules (Mitchison et al. 1986; Kapoor et al. 2000). Similarly to controls, Barren/CAP-H depleted chromosomes were found to be mostly under bipolar attachment with kinetochores located at the end of well defined microtubule bundles. Also, ZW10 was observed along kinetochore fibers suggesting a normal kinetochore microtubule interaction (Fig. 1.20). Finally, immunofluorescence analysis failed to detect Mad2 (data not shown), a checkpoint protein known to leave kinetochores only after spindle attachment (Logarinho et al. 2004). These results strongly suggest that Barren/CAP-H depleted chromosomes, although unable to resolve their sister chromatids, organize well defined kinetochores that can bind spindle microtubules. Therefore, the inability of Barren/CAPH depleted chromosomes to congress to the metaphase plate is not due to abnormal kinetochore-microtubule attachment.

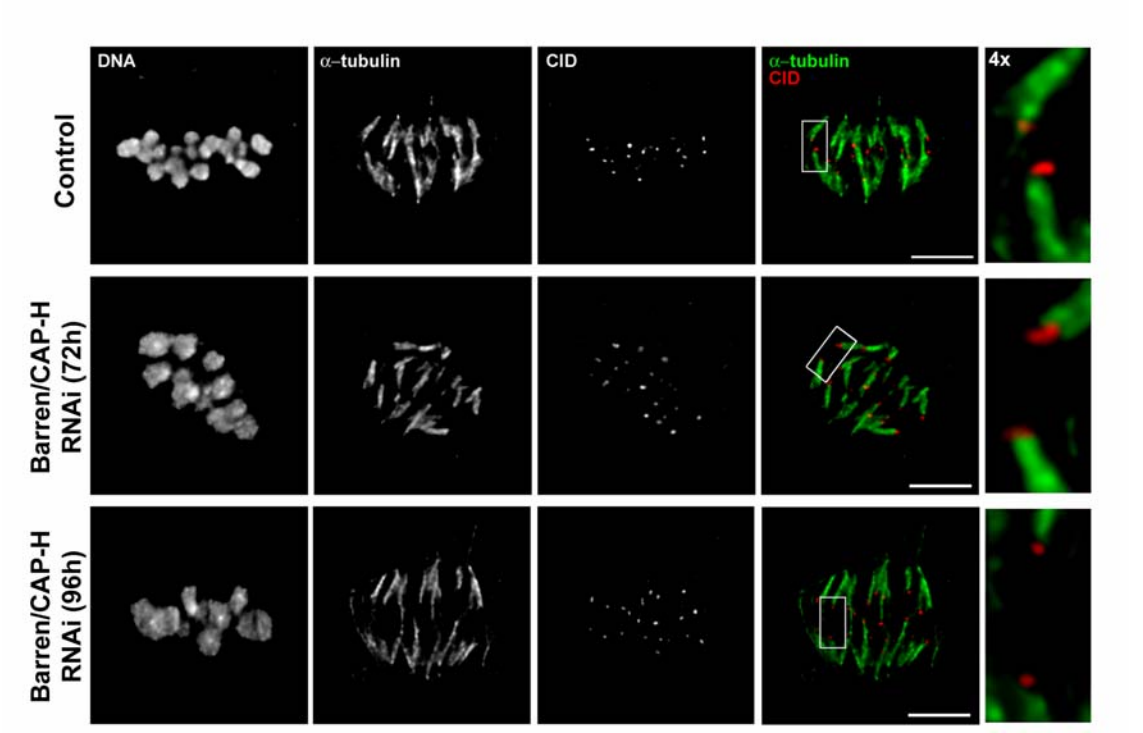

Figure 1.21. Analysis of kinetochore-microtubule interactions after depletion of Barren/CAP-H. Control and Barren/CAP-H-depleted cells were arrested in metaphase by incubation with the proteasome inhibitor MG132 for 2 hours. In order to evaluate kinetochore microtubule attachment, cells were incubated with calcium prior to fixation, to remove all the microtubules except the more stable kinetochore fibers. Cells were immunostained for α-tubulin (green) and CID (red). Higher magnification images (4x) show that in both control and Barren/CAP-H depleted cells, metaphase chromosomes are under bipolar attachment. Scale bars are 5 μm.

2.6 Barren/CAP-H-depleted chromosomes show unusually large distances between sister-centromeres after bipolar attachment

The result presented above show that the congression defect observed in Barren/CAP-H depleted cells could not be explained by an incorrect microtubule-kinetochore interaction. Additionally, closer inspection of the distances between the centromeres marker dots in metaphase-arrested Barren/CAP-H-depleted cells reveals that in fact these are unusually large when compared to control cells (Fig 1.21). To quantify this, the distances between CID labeled centromeres of each chromosome in metaphase-arrested cells was measured (Fig 1.22). In control cells, sister centromeres are 1.07±0.21 µm apart (mean±SD; n=85 measurements). Barren/CAP-H-depleted chromosomes showed intercentromere distances of 1.88±0.34 µm (n=44) and 2.26±0.40 µm (n=51) for 72h- and 96h-depleted cells, respectively. Thus, the distance across the centromeres in Barren/CAP-H depleted chromosomes is approximately two-fold the one observed in controls. Moreover, the severity of this phenotype appears to correlate with the depletion level as the distances observed in 96h-depleted chromosomes are significantly higher ($p<0.001$ by *t*-test) than the ones observed 72h after dsRNA addition.

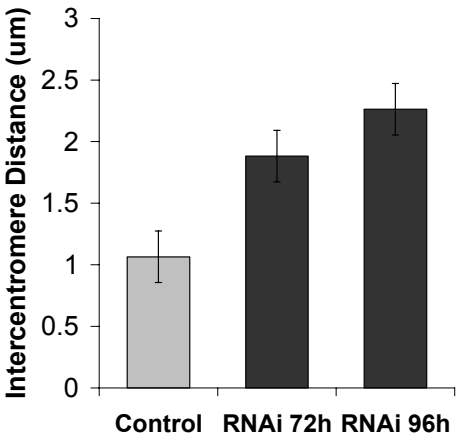

Figure 1.22 – Quantification of the distance across centromeres from metaphase-arrested chromosomes. Intercentromere distances were calculated by measuring the distance between the two CID dots of each chromosome. Graphic shows average of different measurements and error bars represent SD.

These results reveal that the structural properties of the centromere-proximal chromatin are severely affected and strongly suggest condensin I is required for centromeres to maintain a rather rigid structure capable of withstanding the extreme pulling forces exerted by the spindle without being abnormally elongated. To test this hypothesis an "*in vivo* elasticity

assay" aiming to evaluate the effects of the spindle forces on the centromeric region of Barren/CAP-H-depleted chromosomes was performed (Fig. 1.23). Since more severely depleted chromosomes (96h) often show a stretch of the centromeric marker CID, the analysis presented below was performed at 72h, where CID staining more often remains as a dot like staining.

First, the intercentromere distance after colchicine incubation was measured. Under these conditions no microtubules are present and therefore the spindle pulling forces exerted upon kinetochores is avoided. The intercentromere distance was 0.93±0.17 μm (n=62) for control and 1.20±0.24 μm (n=62) for Barren/CAP-H depleted cells (Fig. 1.23a,e). This indicates that already in the absence of pulling forces, the centromeres appear slightly further apart than in control cells. However, this distance was considerably increased in chromosomes subjected to the opposite pulling forces exerted by the spindle (measured in MG132 metaphase arrested cells). Under spindle attachment conditions, the centromeres from control chromosomes show a distance of 1.02±0.13 μm (n=33) whereas in Barren/CAP-H depleted chromosomes sister centromeres are 1.88±0.34 μm (n=44) apart (Fig. 1.23b,e). This distance is significantly different from the distance observed in control cells under the same experimental conditions and also significantly different from Barren/CAP-H depleted chromosomes not subjected to spindle attachment ($p<0.001$ by *t*-test). Thus, stretching of the centromeric region is by far more pronounced in chromosomes attached to the mitotic spindle. This suggests that indeed in Barren/CAP-H depleted cells, spindle attachment causes a strong elongation of the centromeric chromatin.

If the deformation of the centromeric region is within its elastic limit, it is expected that the centromeres return to their original position once the force applied by the spindle is released. To address this, cells were first incubated with MG132 to arrest them in metaphase, under bipolar attachment, and then colchicine was used to induce microtubule depolymerization (Fig. 1.23c,e). Under these conditions, in Barren/CAP-H depleted chromosomes the distance across sister centromeres remains significantly higher ($p<0.001$ by *t*-test) than that of controls (1.57±0.27 μm, n=40 versus 0.99±0.13 μm n=51). Similar results were obtained after inhibition of microtubule dynamics by treatment with low doses of taxol (1.66±0.35 μm, n=37 versus 1.00±0.18 μm, n=47) (Fig. 1.23d,e). Notably, the intercentromere distance observed in these "force released" situations is significantly higher ($p<0.001$ by *t*-test) than the one observed in the absence of microtubule attachment (1.57±0.27 μm and 1.66±0.35 μm versus 1.20±0.24 μm). These results show that the removal

of the pulling forces exerted by the spindle did not allow sister centromeres to recover their original organization, indicating that the elastic properties of the centromere proximal chromatin are irreversibly compromised in the absence of Barren/CAPH.

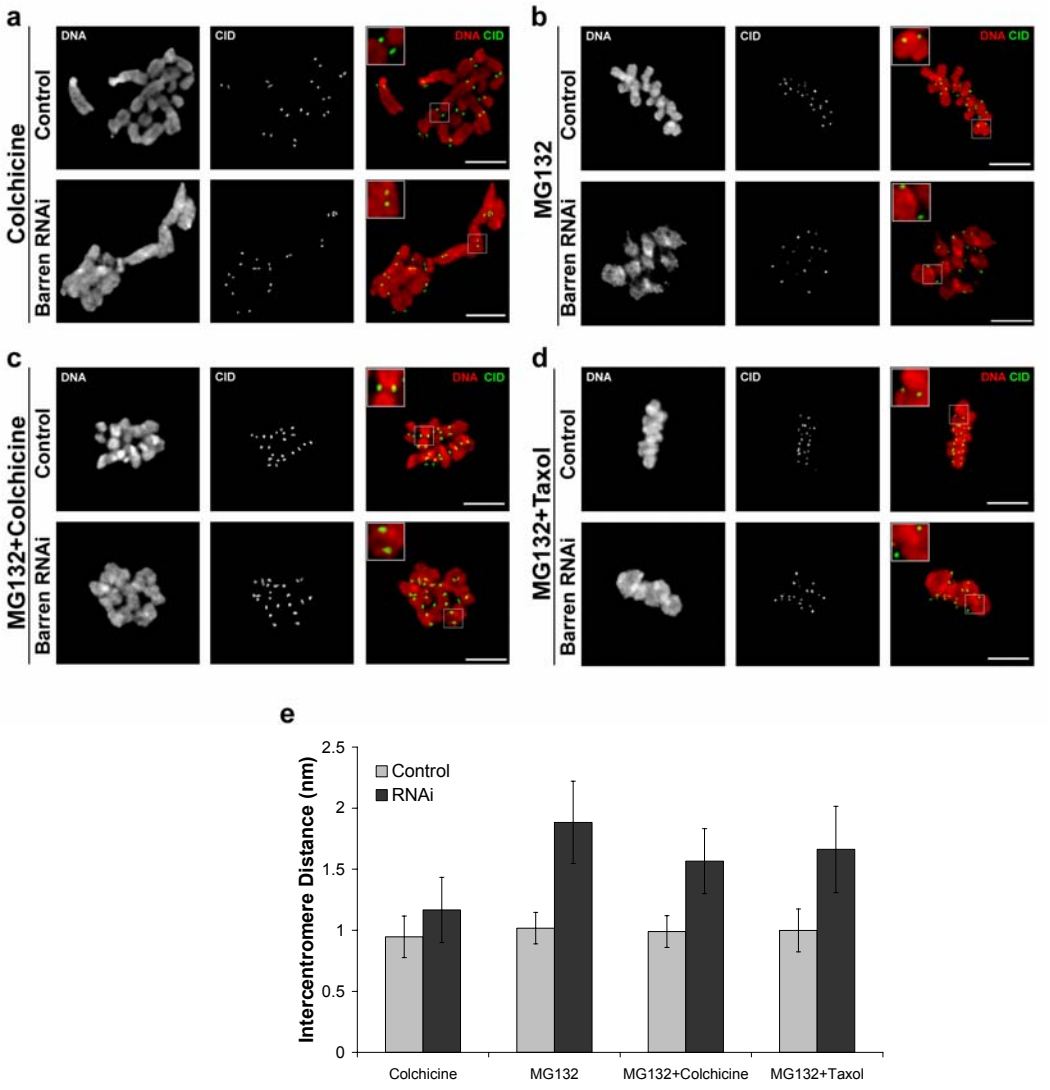

Figure 1.23. Analysis of intercentromere distances after depletion of Barren/CAP-H in response to spindle attachment. a) to **d)** Both control and Barren/CAP-H-depleted cells (72h) were immunostained for CID (green) and counterstained for DNA (red). Cultures were **a)** incubated with 30 µM colchicine for 2h to depolymerise all microtubules before entering mitosis; **b)** incubated for 2h with 20 µM MG132 to arrest cell in metaphase; **c)** incubated with 20 µM MG132 to arrest cells in metaphase followed by a 30-min incubation with 30 µM colchicine to depolymerise all microtubules that were previously attached to the kinetochores; **d)** incubated with 20 µM MG132 to arrest cells in metaphase followed by a 30-min incubation with 10 nM taxol to inhibit microtubule dynamics. Scale bars are 5 µm. Inserts show 2x higher magnifications. **e)** Quantification of the intercentromere distances of control and Barren/CAP-H-depleted cells after the indicated experimental conditions; Columns show average of different measurements and error bars are SD.

2.7 Barren/CAP-H-depleted have a structurally compromised pericentromeric heterochromatin which undergoes considerable distortion after bipolar attachment.

The results presented above show that the centromeric region from Barren/CAP-H depleted chromosomes is unable to maintain a normal distance across their centromeres once bipolar attachment is achieved. An abnormal separation of sister centromeres could result from two distinct scenarios. In one hand Barren/CAP-H depletion could interfere with sister chromatid cohesion through the loss of cohesin, the complex responsible for chromatid cohesion from S-phase until anaphase onset. One the other hand, condensin I depletion could cause a loss of centromeric chromatin rigidity, which once subjected to spindle pulling forces undergoes irreversible distortion.

Previous studies have reported a normal kinetics of cohesin localization after condensin depletion (Coelho et al. 2003) which could argue against the first possibility. However, none of these studies have evaluated cohesin localization in a metaphase-arrest state, the experimental condition used in this study. Therefore, localization of cohesin in control and Barren/CAP-H-depleted metaphase-arrested cells was evaluated. Immunofluorescence analyses of the cohesin subunit SCC1/DRAD21 show that it localizes between the abnormally apart sister-centromeres as cells reach a metaphase-like configuration (Fig. 1.24). However, in contrast to control cells in which SCC1/DRAD21 localizes as a thin line between sister-centromeres, in Barren/CAP-H depleted chromosomes, SCC1/DRAD21 distribution is very broad occupying a large area between the two separated centromeres (Fig. 1.24a). To clarify if the broad SCC1/DRAD21 staining results from chromatin stretch induced by bipolar attachment, control and Barren/CAP-H depleted cells that were treated with colchicine for a long period were also analyzed, so that kinetochore-microtubule interactions were never established. Under these conditions the localization of SCC1/DRAD21 in Barren/CAP-H depleted chromosomes appears now confined to the centromeric and pericentromeric regions resembling the staining obtained in control cells (Fig. 1.24b). These results indicate that the abnormal broad distribution of SCC1/DRAD21 in Barren/CAP-H depleted chromosome is only observed after spindle bipolar attachment. Importantly, these observations demonstrate that cohesin is still present in Barren/CAP-H depleted chromosomes despite the distortion of centromeric region and therefore loss of sister chromatid cohesion is not the cause of centromeric region abnormal elongation.

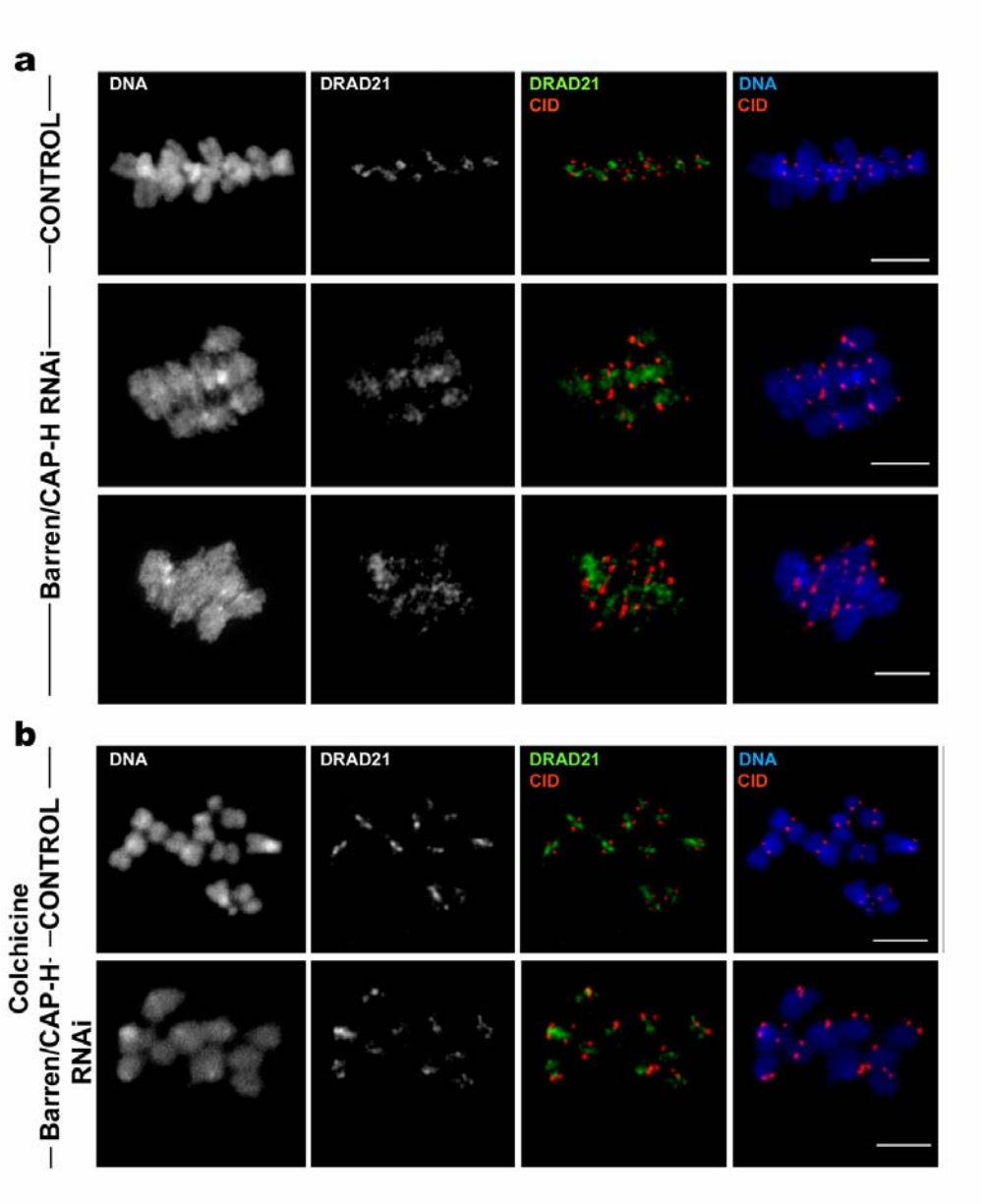

Figure 1.24. Analysis of SCC1/DRAD21 localization on metaphase chromosomes after depletion of Barren/CAP-H. Both control and Barren/CAP-H-depleted cells (96h) were immunostained for CID (red) and DRAD21. **a)** Cell arrested at metaphase by 2h incubation with 20 μM MG132. In control cells, SCC1/DRAD21 localizes between sister chromatids as a tight line between sister centromeres. However, after depletion of Barren/CAP-H, SCC1/DRAD21 is distributed over a broad area between sister centromeres. **b)** Cells were incubated with 30 μM for 2 h to arrest them at prometaphase before microtubules could bind kinetochores. In these cells, SCC1/DRAD21 localizes to a thin line between sister-centromeres in both control and Barren/CAP-H-depleted chromosomes. Scale bars are 5 μM.

The broad distribution pattern displayed by SCC1/DRAD21 in metaphase Barren/CAP-H-depleted chromosomes not only excludes the first possible explanation for centromeric stretch (loss of local cohesion) but additionally supports the second one (loss of chromatin structural integrity). Previous studies in higher eukaryotes, including *Drosophila*, have reported that the bulk of cohesin is released during prophase and cohesin remains at the pericentromeric region until anaphase onset. Thus, the broad distribution of cohesin strongly suggests that the underlying pericentromeric heterochromatin is distorted. To address this directly, the structure of the pericentromeric heterochromatin was evaluated. Metaphase-arrested control and Barren/CAP-H depleted cells were immunostained with an antibody that specifically detects the di-methylated lysine 9 of histone H3 (diMeK9) and the centromere marker CID (Fig. 1.24). Di-methylation on lysine 9 of histone H3 is known to localize specifically to heterochromatin (Schotta et al. 2002). Accordingly, in control cells, diMeK9 staining was mainly observed at the centromeric and pericentromeric region, as shown by the localization of the centromere marker CID (Fig. 1.25a). However, after depletion of Barren/CAP-H, diMeK9 staining appears to occupy a much broader area extending significantly beyond the stretched centromere as defined by CID. The altered pattern of diMeK9 chromatin staining strongly suggests that pericentromeric heterochromatin is structurally compromised. However, an alternative interpretation of this result could be that abnormal methylation of Histone H3 occurs in the absence of Barren/CAP-H.

To test this, cells treated with colchicine for 3 hours were analyzed so that bipolar attachment does not take place and therefore no structural alterations are induced. As mentioned above, a pronounced elongation of the centromeric region occurs after spindle attachment. When microtubules are depolymerized and no-attachment occurs the staining of diMeK9 is almost identical in control and Barren/CAP-H depleted chromosomes (Fig. 1.25b) which reveals that dimethylation of histone H3 occurs normally in the absence of Barren/CAP-H. Therefore, the distinct diMeK9 staining reported for control and Barren/CAP-H depleted cells after metaphase-arrest can only reflect a difference in the organization of the centromeric and pericentromeric heterochromatin which after bipolar attachment undergoes irreversible distortion.

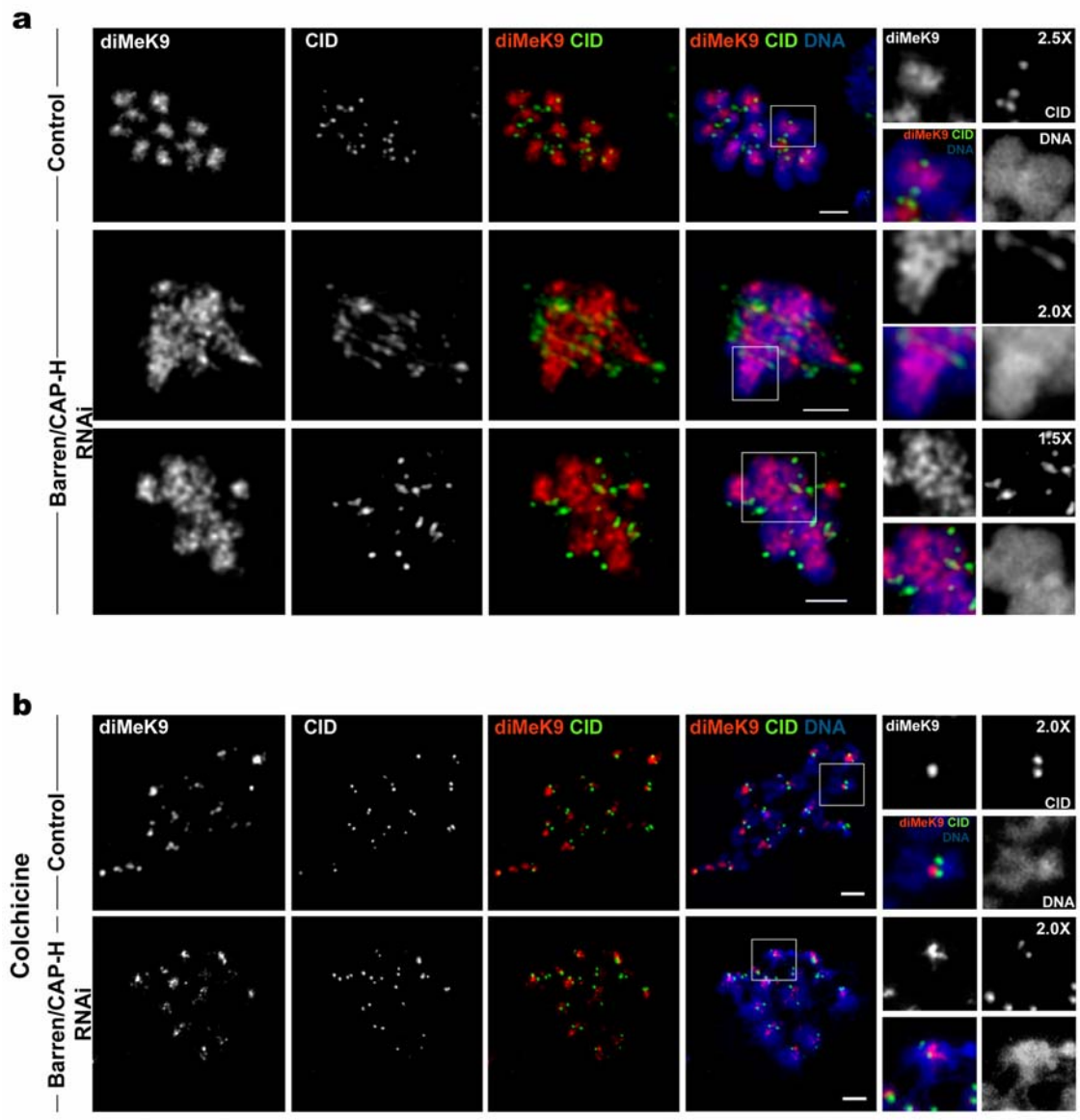

Figure 1.25. Analysis of heterochromatin structure in Barren/CAP-H-depleted cells. Control and Barren/CAP-H-depleted cells (96h) were immunostained for the centromere marker CID (green) and for the dimethylated lysine 9 of histone H3 (diMeK9), used as a marker for heterochromatic regions. a) In metaphase-arrested control cells, diMeK9 is confined to a defined heterochromatic region close to the centromeres. However, after depletion Barren/CAP-H, the pattern of diMeK9 appears to be significantly altered in chromosomes under bipolar attachment. diMeK9 is now detected over a broad area of chromatin localized between the two CID-labeled centromeres. b) Cells were incubated with 30 μM for 2 h to depolymerize microtubules and the diMeK9 was analyzed. Note that in the absence of microtubules, diMeK9 is confined to a tight region between sister centromeres in both control and Barren/CAP-H-depleted cells. Scale bars are 5 μM.

Additionally, a comparative analysis between control and Barren/CAP-H-depleted euchromatic chromosome arms was performed. Euchromatin was specifically visualized with an antibody that recognizes the dimethylated form of lysine 4 from histone H3 (diMeK4), specific of euchromatic regions (Byrd and Shearn 2003) (Fig. 1.26). Despite a broader staining observed in Barren/CAP-H depleted chromosomes, as a result of an overall altered chromosome structure, the diMeK4 pattern remains confined to the chromosome arms and chromatin distortion is not as severe as found at the centromeric and pericentromeric regions. These data further support that severe structural alterations occur specifically at the centromeric and pericentromeric heterochromatin as a result of the opposite pulling forces exerted by the spindle.

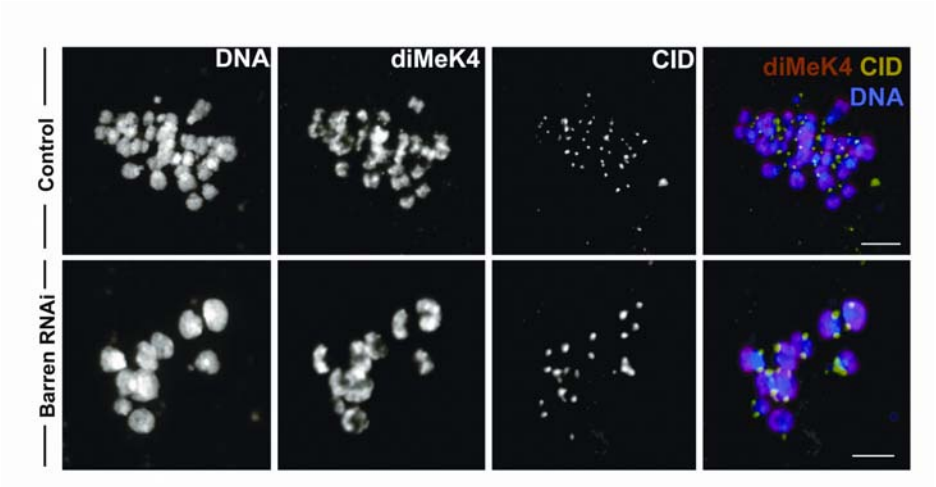

Figure 1.26. Analysis of euchromatic regions in Barren/CAP-H-depleted mitotic chromosomes. Both control and Barren-CAP-H depleted cells (96h) were arrested at metaphase by incubation with MG132 for 2 hours and hypotonic shocked to induce chromosomal spread. Cells were immunostained for the centromere marker CID (green) and for the dimethylated lysine 4 of histone H3 (diMeK4), used as a marker for euchromatic regions. In control cells at metaphase, diMeK4 localizes to the chromosome arms, excluding the heterochromatic chromatin proximal to the centromere region. After depletion of Barren/CAP-H the pattern of diMeK4 appears to be unaltered although is detected as a broader area. However, no significant distortion of euchromatin is observed. Scale bar are 5μm.

3. Discussion

The present study provides evidence that condensin I is absolutely required for proper mitotic chromosome architecture and cell viability. In the absence of condensin I DNA bridges are observed during anaphase and telophase. Importantly, this study revealed for the first time that condensin I depletion results in congression defects associated with alterations in the structural integrity of the centromere-proximal chromatin.

Depletion of Barren/CAP-H, a condensin I specific subunit in *Drosophila* S2 cells, leads to the formation of chromosomes that cannot resolve their sister-chromatids and are unable to sustain an axial distribution of core condensin proteins and TopoII. Approximately half of DmSMC2/4 normal levels were found in association with chromatin but appear diffused over the chromatin and are not confined to a well-defined central axis. In fully concordance with these findings, analysis of CAP-D2 depletion in *Drosophila* tissue culture cells has recently shown that DmSMC4 is diffusively associated with CAP-D2-depleted mitotic chromosomes (Savvidou et al. 2005). Moreover, the present study additionally shows that TopoII binds mitotic chromatin at normal levels but its axial distribution is also lost in Barren/CAP-H-depleted chromosomes, similar to what has been described in previous studies on DmSMC4 depletion (Coelho et al. 2003). All together, these results strongly suggest that specific depletion of condensin I results in mitotic chromosomes with a poorly defined axial organization. In contrast, studies in vertebrate cells have reported that depletion of condensin I-specific subunits does not alter the axial localization of the remaining core and condensin-II specific subunits and a complete disruption of chromatid axial organization was only observed when both condensin I and condensin II were absent (Ono et al. 2003; Hirota et al. 2004). All these studies were performed using RNAi knockdown technique and therefore it cannot be excluded that these divergences result from different levels of depletion. Alternatively, this discrepancy might point towards a different requirement for condensin I in the maintenance chromosomal axis between *Drosophila* and vertebrate systems. Thus, in *Drosophila* tissue culture cells, condensin I might be absolutely required for an axial organization of the chromatid core whereas in vertebrate cells some axial assembly is still preserved in the absence of condensin I, possibly mediated by the condensin II complex.

Whilst the contribution of condensin II to mitotic chromosome structure in *Drosophila* still remains undetermined, previous studies in S2 cells have shown that if both condensin complexes are removed by depleting one core subunit (DmSMC4), sister chromatid resolution is specifically affected (Coelho et al. 2003). Accordingly, the present study shows that depletion of Barren/CAP-H results in a chromosome structure phenotype similar to that previously described for depletion of DmSMC4. These observations suggest that in S2 tissue culture cells, if a condensin II complex does exist, it does not play a significant role in mitotic chromosome organization.

Nevertheless, DmSMC2 and DmSMC4, the two core proteins shared by both condensin I and II are able to localize to Barren/CAP-H depleted chromosomes. It cannot be ruled out

that the chromatin associated core proteins are from the putative condensin II complex. However, for the reasons mentioned above (and others that will be presented in the following chapters), condensin II appears to have a minor role in mitotic chromosome structure in *Drosophila*. If so, the partial localization of DmSMC2/4 to mitotic chromosomes suggests that this heterodimer binds DNA independently of the regulatory subunits. In agreement, *in vitro* studies have shown that the core SMCs heterodimer alone has DNA binding properties (Kimura and Hirano 2000; Stray and Lindsley 2003). Furthermore, siRNAi depletion of hCAP-D2 from HeLa cells does not alter the levels of hCAP-E/SMC2 on mitotic chromosomes (Watrin and Legagneux 2005). In contrast, studies in budding yeast revealed that only the entire condensin complex is able to associate with DNA (Lavoie et al. 2002). This diversity probably results from species differences in the mechanism responsible for loading condensin to mitotic chromosomes. While these studies strongly suggest that in higher eukaryotes the chromosomal targeting of the 8S core heterodimer can occur independently of the regulatory complex, several studies show that the regulatory complex never shows chromatin localization on its own. In the absence of core proteins, the non-SMC proteins are unable to localize to mitotic chromatin (Coelho et al. 2003; Hirota et al. 2004; Vagnarelli et al. 2006) and the 11S regulatory sub-complex alone does not show DNA binding activity *in vitro* (Kimura and Hirano 2000).

Additionally, we also showed here that the condensin I regulatory subunits, DmCAP-D2 and DmCAP-G, do not localize to Barren/CAP-H depleted mitotic chromosomes. Moreover, a recent study has revealed that Barren/CAP-H is unable to associate to chromosomes depleted of DmCAP-D2 (Savvidou et al. 2005). Taking together, these data indicates that loading of the regulatory sub-complex to mitotic chromosomes requires all non-SMC subunits to be present. Interestingly, a homologue for CAP-G2 was not found in *Drosophila* (Ono et al. 2003) and it has been suggested that the DmCAP-G subunit could be shared by both condensin I and II in this organism. If this were the case then the absence of absence of DmCAP-G in Barren/CAP-H depleted chromosomes suggests that condensin II complex is totally absent from mitotic chromosomes in S2 cells. However, it is still possible that *Drosophila* contains a “true” CAP-G2 homologue but it has not yet been identified.

In addition, the total protein levels of the remaining non-SMC proteins from the condensin I complex are substantially reduced when either Barren/CAP-H or CAP-D2 proteins are depleted (this study and Savvidou et al. 2005). These findings suggest that either

the proteins are unstable if the 11S regulatory complex is not formed or, alternatively, that the expression of these proteins is regulated by the levels of the sub-complex partners.

The present study shows that specific depletion of condensin I results in severe defects in chromosome morphology. Even thought Barren/CAP-H-depleted chromosomes appear to compact normally along their longitudinal length, no resolution between the sister-chromatids was observed in prometaphase/metaphase chromosomes. Moreover, these chromosomes appear to be less resistant to stress induced by hypotonic shock. Whereas wild type chromosomes retain their X-shape morphology and remain compacted after this stress, Barren/CAP-H-depleted chromosomes appear undercondensed in the same experimental conditions. This finding is fully consistent with previous studies on condensin depletion and strongly argues for a major role of condensin I complex in the structural integrity of the mitotic chromosomes (Hudson et al. 2003; Hirota et al. 2004).

One of the consequences of depleting condensins from mitotic chromosomes is the consistent presence of DNA bridges formed during anaphase that remain unresolved until telophase or even further. Analysis in fixed material confirmed that Barren/CAP-H-depleted cells display this phenotype. Moreover, the study shows for the first time by *in vivo* visualization of chromosome dynamics in the absence of condensin I that the chromatin bridges are observed as soon as anaphase onset is initiated. This strongly suggests that intertwines between sister chromatids are already present at the metaphase-anaphase transition and that chromatin bridges are most likely a consequence of the misresolution of the sister chromatids detected in prometaphase/metaphase. Previous studies have also suggested that these interchromatid links should be present during metaphase since depletion of condensin was shown to be able to recover the prometaphase arrest caused by depletion of cohesin (Coelho et al. 2003). Thus, depletion of condensin depletion appears to restore sister chromatids cohesion which is required to overcome the spindle assembly checkpoint, a clear indication that condensin depletion results in DNA linkages between sister-chromatids at metaphase.

Previous studies have already suggested that the DNA intertwines observed in condensin-depleted cells are most likely to be due to the inability to resolve catenated sister chromatids. The *in vitro* activity of topoisomerase II, the enzyme responsible for DNA decatenation, is significantly reduced in DmSMC4 depleted extracts and chromatin bridges are still present in cohesin/condensin double depletion clearly showing that the linkages

observed between sister-chromatids during chromosome segregation are cohesin independent (Coelho et al. 2003). Results in chicken cells have very recently proposed that condensin depletion does not impair topoisomerase II activity (Vagnarelli et al. 2006). In this study the resolution of a 2.3 Mb centromeric DXZ1 human mini X chromosome was used to probe topoisomerase activity and shown to have normal cleavage pattern in condensin depleted cells. Moreover, chromosomal insertions containing tandemly repeated *lac* operator regions (GFP-labeled *lac* repressor) reveal that these foci segregate normally during anaphase further suggesting a normal activity of topoisomerase II. Thus, these recent studies suggest that in vertebrate cells condensin depletion does not impair topoisomerase II. However, these assays only probe topoisomerase II at specific chromosomal regions and therefore do not exclude that a condensin-dependent topoisomerase II activity at other chromosomal foci might indeed be the cause of the chromatin bridges observed in condensin-depleted cells.

The formation of thicker chromatin bridges in Barren/CAP-H depleted-cells was also shown to disrupt cytokinesis. Cytokinesis failure has already been correlated with condensin depletion in other studies (Bhat et al. 1996; Hudson et al. 2003). This correlation is more likely related to a physical incapacity in completing cell division due to DNA bridges at the cleavage furrow than to a direct role of condensin in cytokinesis.

In vivo analysis of condensin I depleted cells in mitosis also revealed that chromosome congression is abnormal. Accordingly, analysis in fixed material has shown that Barren/CAP-H depleted chromosomes are unable to align at the metaphase plate even when extra time is provided by preventing anaphase onset with the proteasome inhibitor MG132. Studies in HeLa cells have also pointed out abnormal chromosome alignment after depletion of condensin I (Ono et al. 2004; Watrin and Legagneux 2005) and it has been suggested that condensin is required for normal centromere/kinetochore function. Condensin-depleted chromosomes in HeLa cells are unable to maintain a regular distance to the poles after induction of monopolar spindle formation by monastrol treatment (Ono et al. 2004). Whereas in control cells, after monastrol treatment, chromosomes appear uniformly radiated from a single pole, in condensin-depleted cells, the pole-to-kinetochore distance became extremely variable and chromosomes were irregularly placed around the pole. These results certainly argue for a role of condensin complexes in the maintenance of a stable kinetochore–microtubule interaction. In contrast, the results reported in this present study show that in *Drosophila* cells, in the absence of condensin I, the centromere supports the formation of a functional kinetochore as revealed by the normal localization of POLO and the correct

kinetochore-microtubule bipolar attachment. Previous experiments where DmSMC4 was depleted in S2 cells also reported a normal kinetochore organization and function (Coelho et al. 2003). These findings show that in *Drosophila*, the organization of the kinetochore does not require the underlying chromatin to contain condensins. Nevertheless, chromosome congression is defective which most likely results in a prometaphase/metaphase arrest/delay as inferred in this study by the NEBD-to-anaphase timing revealed by time-lapse microscopy of Barren/CAP-H-depleted cells expressing tubulin-GFP. Live analysis in vertebrate cells has also revealed that condensin I-depleted cells progress through mitosis slower, while condensin II depletion does not strongly affect mitotic progression (Hirota et al. 2004).

The results reported here demonstrate that the abnormal chromosome congression observed in Barren/CAP-H depleted cells is likely to be related to the loss of centromere elasticity rather than to kinetochore malfunction. In the absence of Barren/CAP-H, after bipolar attachment is established, the centromeric region elongates nearly twice the distance observed in control chromosomes. In agreement, abnormal centromere separation has also been recently reported when CAP-G is mutated in *Drosophila* (Dej et al. 2004). Also, several studies in *C. elegans* have suggested a role for condensin II (the sole condensin complex in this organism) in centromere resolution and integrity (Hagstrom et al. 2002; Stear and Roth 2002; Moore et al. 2005). More recently, the same effect of centromeric region elongation after bipolar attachment has been described in vertebrate cells depleted of condensin I (Gerlich et al. 2006a). Notably, this effect was specifically associated with condensin I depletion and chromosomes depleted of condensin II were shown to retain a normal distance across their centromeres once bipolar attachment is achieved.

A possible explanation for the abnormal separation of sister centromeres could be due to an altered cohesion between sister-chromatids in the absence of Barren/CAP-H. However, this hypothesis has been ruled out since immunofluorescence analysis clearly show that despite its broad distribution pattern SCC1/DRAD21 is still present between the abnormally apart sister-centromeres in metaphase arrested cells. Additionally, it was previously described that cohesin follows a normal dynamics during mitosis in DmSMC4 depleted cells (Coelho et al. 2003). Thus, the structural alterations we observed after depletion of Barren/CAP-H, are unlikely to result from abnormal cohesin distribution.

This study has also shown that not only the pairing domain of sister chromatid is altered, but also that the pericentric heterochromatin-associated dimethylated K9 histone H3

is irregularly distributed and centromere marker CID appears distorted. It has been demonstrated that centric and pericentric heterochromatin show stronger attachment to a central proteinaceous scaffold or matrix (Bickmore and Oghene 1996; Sumer et al. 2003). Reciprocally, chromatin-immunoprecipitation experiments in *S. pombe* revealed a preferential association of condensin subunits with central centromeric sequences (Aono et al. 2002). Recently, a genetic and direct interaction between Drosophila CAP-G and the centromere specific histone H3 variant CID was reported (Jäger et al. 2005). These observations taken together with our data strongly support that the association between the centromere/pericentromere chromatin and the chromosome axis is required for the establishment of an elastic but rigid structure able to resist the forces exerted by the spindle upon sister centromeres during congression.

The elasticity assay reported in the present study reveals that the normal organization of pericentric heterochromatin is not restored after removal of microtubules or microtubules dynamics, since a normal intercentromere distance could not be observed under these experimental conditions. This suggests that Barren/CAP-H is essential to prevent irreversible loss of centromere integrity after bipolar attachment. In contrast to this, studies in vertebrate cells revealed that the elongation observed in condensin-depleted centromeres is reversible (Gerlich et al. 2006a). After taxol incubation, the abnormally large intercentromere distance can be restore to values similar to control ones, revealing that the centromeric region has still recompacting activity after the induced stretch. With that regard, chromatin in S2 cells appears to be less elastic. It cannot be ruled out that the irreversibly of the stretch is related to the experimental setup used. The studies in vertebrate cells have analyzed unperturbed live mitosis and the period the centromeres were subjected to the spindle opposite pulling forces was restricted to the prometaphase/metaphase timing (~ 40 min). In our study the analysis was performed in fixed material after a 2 hours metaphase arrest. Thus, it is possible that a prolonged incubation period in prometaphase/metaphase could be the cause for the irreversible elongation.

Several studies regarding the longitudinal elastic properties of mitotic chromosomes have shown that these behavior strongly depends on the continuity of the DNA chain (Poirier and Marko 2002; Almagro et al. 2004). However, the contribution of the protein scaffold for elastic response of chromatin is controversial. It has been shown that the elastic and bending properties of mitotic chromosomes are inconsistent with the existence of a well-defined central chromosome 'scaffold' and alternatively, it has been suggested that the mitotic

chromosome is essentially a chromatin network (Poirier and Marko 2002). Other studies revealed that the elastic properties depend on a mitotic chromosome protein scaffold, in particular on SMC proteins, as chromatin domains containing SMC proteins were shown to exhibit a higher elastic response (Almagro et al. 2004). Whilst most studies have concentrated on the elastic properties of the arms, much less is known about the centromeric region. However, several studies have pointed out the elastic properties of the centromere-proximal chromatin (Shelby et al. 1996; He et al. 2000). Indeed the present study shows that the absence of condensin I compromises the elastic properties of centromeric chromatin and favors the hypothesis that at least in the centromeric region, the elastic properties of chromosomes are indeed dependent on a proteinaceous structure.

In summary, the present study shows that Barren-CAP-H is essential to allow the organization of a defined chromosome axis and to resolve sister chromatids. Furthermore, condensin I is not required for the organization of functional kinetochores but is essential to maintain the structural integrity of the centromeric region during mitosis.

Chapter 2

Dynamics of condensin I association with mitotic chromatin in *Drosophila*

1. Introduction

The assembly of mitotic chromosomes is a highly dynamic process in which entangled chromatin fibers are resolved and packed into individualized structures, the mitotic chromosomes. Significant data indicates that key factors for the establishment of correct chromosome architecture are the condensin complexes (reviewed in Hirano 2005). A second condensin complex (condensin II) was recently identified in HeLa cells (Ono et al., 2003; Yeong et al., 2003) and in vertebrate cells, condensin I and II complexes were shown to contribute distinctly to mitotic chromosome architecture and depletion of a single condensin complex gives rise to distinct chromosome morphology defects. Specific depletion of condensin I originates "swollen" chromosomes whereas in the absence of condensin II the chromosomes acquire a "curly" configuration. Chromosomes depleted of both condensin I and II complexes show a more severe morphological defects appearing "fuzzy". The results shown in chapter 1, indirectly suggest that in *Drosophila*, condensin I is the major condensin complex involved in mitotic chromosome organization since the morphological defects associated with depletion of condensin I resemble those observed after depletion of both condensin I and II complexes in vertebrate cells.

In addition to the different contribution for mitotic chromosome morphology, condensin I and II complex were shown to exhibit a differential association with mitotic chromatin in HeLa cells (Gerlich et al., 2006a; Hirota et al., 2004; Ono et al., 2004; Ono et al., 2003). Condensin II was shown to be nuclear throughout interphase and to stably associate with chromosomes during prophase. In contrast, the canonical condensin I was mainly cytoplasmic during interphase and prophase and was shown to gain access to chromatin only after nuclear envelope breakdown. Thus, condensin II in vertebrate cells is the only condensin complex involved in the initial stages of chromosome condensation during prophase. The results reported in this chapter aimed to characterize in detail the association of condensin I with chromatin during mitosis. This study revealed that the condensin I-specific subunit Barren localizes to chromatin already in prophase, accumulating first at the centromeric regions. Subsequently, as the chromosome condenses Barren-EGFP spreads distally throughout the chromosome arms.

While some progress has been made in defining the role of condensin in mitotic chromosome structure, the exact mechanism by which condensin drives mitotic chromosome organization remains unknown. Whether condensin has an enzymatic or structural role (or

both) in mitotic chromosome architecture remains controversial. Several *in vitro* studies have shown that purified condensin complex displays a number of enzymatic activities on the DNA molecule (e.g. supercoiling, knotting and renaturation reactions) that could account for chromatin compaction (Kimura and Hirano, 1997; Kimura et al., 1999; Sutani and Yanagida, 1997). However, some arguments still favor a structural rather than enzymatic role of condensin. The condensin subunit SMC2 (scII) was one of the most abundant proteins isolated from mitotic chromosomal scaffold (Earnshaw and Laemmli, 1983; Lewis and Laemmli, 1982; Saitoh et al., 1994) and immunofluorescence analysis revealed that condensin is found to localize at a central axis of mitotic chromosomes together with Topoisomerase II (Coelho et al., 2003; Maeshima and Laemmli, 2003). Interestingly, depletion of condensin causes delocalization of Topoisomerase II, which no longer appears confined to the chromosome axis, suggesting that condensin might provide a structural backbone within the chromosome (Coelho et al., 2003).

To gain further insight into the molecular mechanism underlying condensin function, the stability of chromatin-associated Barren subunit was evaluated. Fluorescence Recovery After Photobleaching (FRAP) analysis showed that Barren-EGFP undergoes a continuous and rapid exchange between chromatin-bound and free-cytoplasmic forms. The highly dynamic behavior of this condensin I subunit fails to support a model for the organization of a static axial structure to which DNA loops could attach and suggest that if a chromosome axis does exit it must be highly dynamic.

2. Results

2.1 Construction of fluorescent-tagged Barren fusion proteins

Several studies have already shown that the condensin complex associates with mitotic chromosomes during mitosis. However, most of this data comes from immunofluorescence studies in fixed material, mainly in tissue culture cells, and consequently the results vary considerably according not only to the cell type analyzed but also to the fixation protocols and antibodies that were used. Therefore, live imaging was chosen to allow a more accurate and detailed *in vivo* analysis of condensin I association with chromatin during mitosis.

Accordingly, several fluorescent-tagged versions of Barren, a condensin I-specific subunit, were produced. Enhanced Green Fluorescent Protein (EGFP) and monomeric form of Red Fluorescence Protein (mRFP1) were fused with Barren at either C- or N-termini. The expression and localization of these fusion proteins was initially assessed by transient transfection in Schneider 2 *Drosophila* tissue culture cells, using an inducible system (pRmHa-3/pMTV vector, containing the metallothionein promoter induced by Cu^{2+}). Transient transfection of Barren-EGFP (Barren with a C-terminal EGFP fusion) reveals that this protein is expressed throughout the cell cycle, accumulating as a thin central axis of prometaphase/metaphase sister chromatids (Fig. 2.1). The levels of protein expression vary considerably amongst transfected cells and cells with a high expression levels do not show a chromosomal accumulation of Barren-EGFP (Fig. 2.1b).

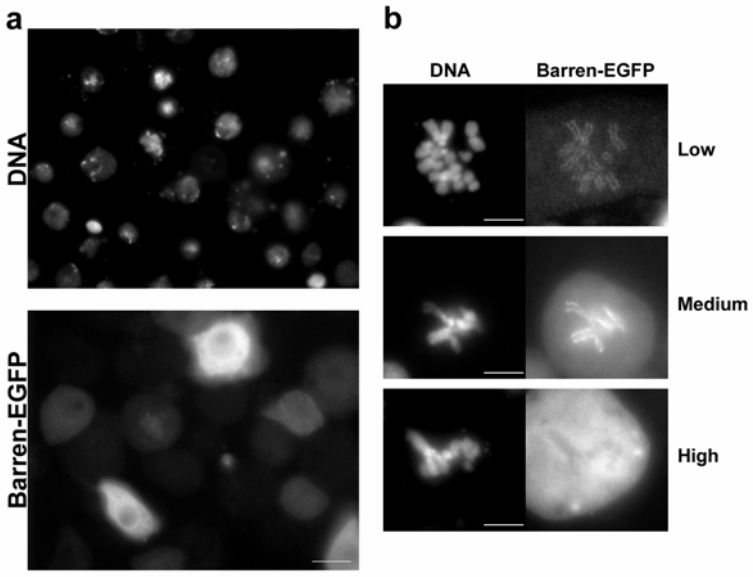

Figure 2.1. Transient transfection of S2 cells with Barren-EGFP. a) Analysis of Barren-EGFP expression ~16h after protein expression induction ($CuSO_4$ addition). Scale bar is 10 µm **b)** Detailed analysis of prometaphase/metaphase cells with different levels of expression of Barren-EGFP. Barren-EGFP localizes at a central axis within chromatids of prometaphase/metaphase chromosomes in cells that express low to medium levels of Barren-EGFP. In contrast, cells that express high levels of the fusion protein, chromosomal localization could not be observed. Scale bars are 5 µm.

In interphase cells, Barren-EGFP was found dispersed between the cytoplasm and the nucleus (Fig. 2.1a and 2.2). To avoid possible artifacts on protein distribution associated with fixation procedures, transfected cells were analyzed live under a fluorescence microscope (Fig. 2.2). Interestingly, cells with apparently similar levels of expression can display a different accumulation of Barren-EGFP during interphase. While some cells show a higher

accumulation of the protein within the nuclear area (left side cell in Fig. 2.2), some others present higher levels of the protein dispersed at the cytoplasm, with reduced amounts within the nucleus (right side cell in Fig 2.2). This suggests that nuclear localization of Barren-EGFP might depend on the cell state, possibly on the cell cycle stage. Nevertheless, in all the cells analyzed, Barren-EGFP appeared to be excluded fromthe nucleoli.

EGFP-Barren (Barren with a N-terminal EGFP fusion) and Barren-mRFP1 (Barren with a C-terminal mRFP1 fusion) constructs were also analyzed by inducible transient transfection and the results were very similar to the ones described for Barren-EGFP. Accordingly, these fusion proteins were observed at the chromosomal axis of mitotic chromosomes (Fig. 2.3).

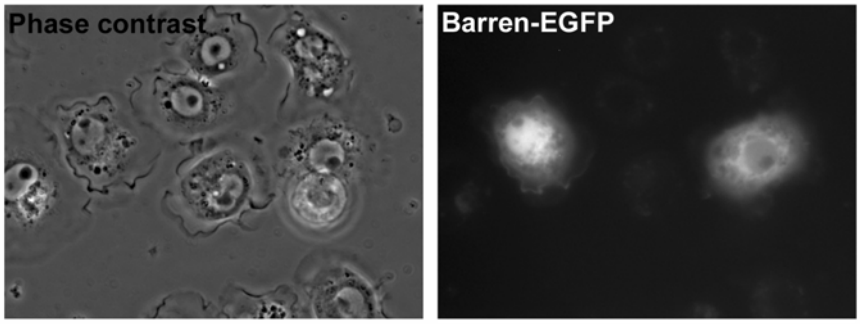

Figure 2.2. Live analysis of interphase S2 cells after transient transfection with Barren-EGFP. Transfected cells (~16h of induction) were transferred to a concanavalin A-coated coverslip and flatten cells visualized under a fluorescence microscope.

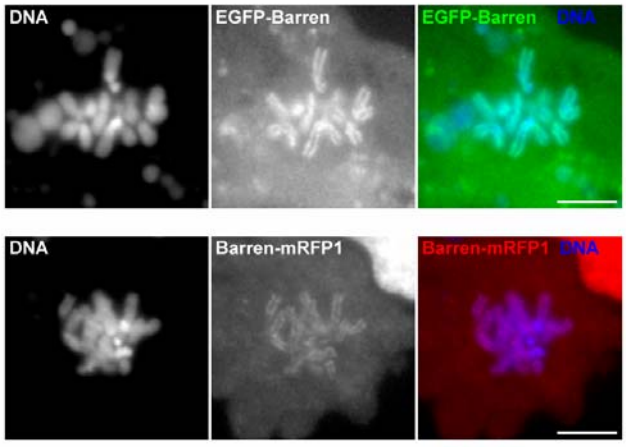

Figure 2.3. Transient transfection of S2 cells with EGFP-Barren and Barren-mRFP1. Analysis of EGFP-Barren (upper panel) and Barren-mRFP1 (lowed panel) chromosomal localization in mitotic cells. Expression was induced for ~ 16h ($CuSO_4$ addition) before fixation. Scale bar is 10 µm

2.2 Production of Barren-EGFP expressing flies

In order to fully characterize the condensin I association with mitotic chromatin in a living organism, transgenic flies that express the EGFP-tagged Barren (Barren-EGFP) under the control of the UAS/GAL4 system (Brand and Perrimon 1993) were constructed. *Barren-EGFP* fusion gene was cloned in the pUASP vector used for germline P-element-mediated transformation. Several transformed lines were established and insertions were mapped either on the second (lines II.1, II.2 and II.3) or on the third (lines III.1, III.2 and III.3) chromosomes. All the lines established are viable as homozygous revealing that insertion did not disrupt any essential gene.

To test Barren-EGFP protein expression, the different *UASP-Barren-EGFP* strains were crossed with the *α-4tub-GAL4-VP16* driver and ovaries from the resulting females were dissected and probed for Barren-EGFP by western blot (Fig. 2.4). The six different established lines were shown to express Barren-EGFP.

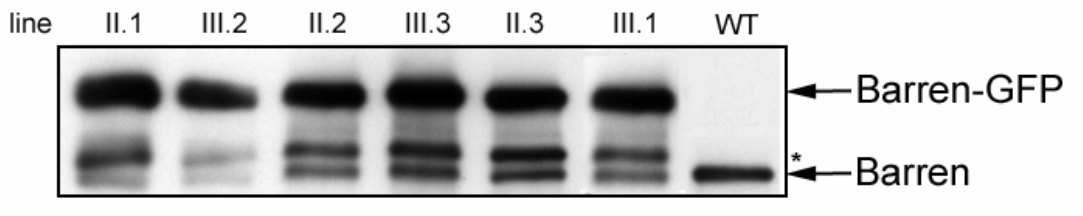

Figure 2.4. Western blot analysis of different *UASP-Barren-EGFP* transgene insertions. Five ovaries from 5 days old females were loaded on SDS-PAGE, transferred to a nitrocellulose membrane and probed by western blot using a Barren antibody. The six different *UASP-Barren-EGFP* transgenes were shown to express Barren-EGFP and endogenous Barren. A possible degradation product (*) is also detected.

In order to address whether overexpression of Barren-EGFP produces any phenotype, *UASP-Barren-EGFP III.1* and *III.2* expression was induced in the eye imaginal discs using both *eyeless-GAL4* (Hazelett et al. 1998) and *GMR-GAL4* (Freeman 1996) drivers (Fig. 2.5). *Eyeless-GAL4* drives expression of GAL4 in early eye imaginal discs and anterior to the furrow in the third instar discs whereas *GMR-GAL4* induces protein expression in all cells posterior to the differentiation furrow. As positive control, *UAST-Pannier* (*Pnr*) was used (Haenlin et al. 1997). Accordingly, overexpression of *Pnr* abolishes head development and leads to a very strong rough eye phenotype when GAL4 is induced by *eyeless-GAL4* and

GMR-GAL4 drivers, respectively. In contrast, two different *UASP-Barren-EGFP* transgenes showed no phenotype when expression is induced by these same drivers which strongly indicates that there is no phenotype associated with Barren-EGFP overexpression.

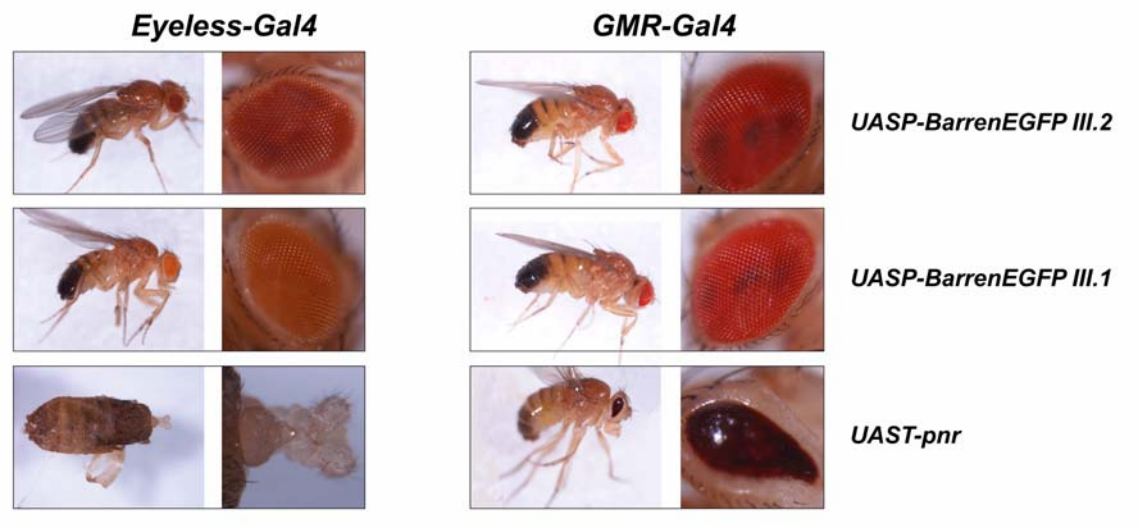

Figure 2.5. Analysis of Barren-EGFP overexpression phenotype. *Eyeless-GAL4/CyO* or *GMR-Gal4* virgin females were crossed with either *UASP-Barren-EGFP III.2* or *UASP-Barren-EGFP III.1* males. Non balanced progeny was observed for phenotypes associated with Barren-EGFP overexpression during eye development. No evident phenotypes could be identified. *UAST-Pnr* was used as positive control.

2.3 Barren-EGFP is a fully functional protein

EGFP-fusion can interfere with protein function and therefore it is essential to test whether fusion protein is fully functional. Only then one can ensure that the dynamic behavior observed can be correlated with that of the endogenous protein. Accordingly, rescue experiments were performed in order to address whether ectopic expression of Barren-EGFP is able to complement the lethality associated with a *Barren* null allele, $Barr^{L305}$. $Barr^{L305}$ allele has been previously shown to be a recessive embryonic lethal allele, with homozygous embryos arresting in mitosis 16 as a consequence of chromatin segregation failures associated with extensive chromatin bridges (Bhat et al. 1996). Rescue experiments reveal that Barren-EGFP expression can rescue this embryonic lethality when GAL4 is expressed ubiquitously (Table 2.1).

Table 2.1 – Relative viability out of the rescue of *Barr*^{L305} allele with Barren-EGFP ectopic expression.

	UASP-Barr-EGFP III.1				***UASP-Barr-EGFP III.2***			
	pupae		**adult**		**pupae**		**adult**	
Driver	n[a]	R.V.[b]	n[a]	R.V.[b]	n[a]	R.V.[b]	n[a]	R.V.[b]
daGAL4	n.d.[c]	n.d.[c]	541	35.1	n.d.[c]	n.d.[c]	956	88.5
TubGAL4	1044	69.3	1432	16.0	1247	70.4	972	93.0

a) n – number of observations
b) R.V. – Relative Viability: percentage of rescued pupae/adults, normalized to the expected mendelian ratio in case of a full complementation
c) n.d. – not determined

Two independent lines were tested and both were able to give rise to viable adults. While both insertions rescue very efficiently up to the pupal stage, insertion *UASP-Barren-EGFP III.1* appears to rescue less well to the adult stage. Moreover, the percentage of flies *UASP-Barren-EGFP III.1/daGAL4* is considerably reduced even in a wild type background (relative viability = 7.2%). These results could indicate that high levels of Barren-EGFP might be toxic. However, insertions *UASP-Barren-EGFP III.1* and *UASP-Barren-EGFP III.2* were shown to express Barren-EGFP at similar levels (Fig 2.4 and data not shown) and both insertions do not lead to any phenotype when overexpression is induced during eye development (Fig. 2.5).

Alternatively, the reduced relative viability of *UASP-Barren-EGFP III.1* compared to *UASP-Barren-EGFP III.2* might be related with a possible genetic interaction between Barren-EGFP overexpression and the gene disrupted by insertion *UASP-Barren-EGFP III.1*. Notably, no differences in the rescue efficiency between the two tested lines were found until the pupal stage indicating that if a genetic interaction between *Barren* and the gene disrupted by insertion *III.1* does exist, it must be at later developmental stages. Despite the differences in the rescue efficiency, both lines were shown to effectively complement the lethality associated with *Barr*^{L305} null allele. In agreement, brain squashes from third instar larvae expressing only Barren-EGFP show no defects in chromosome morphology and chromatin segregation at later mitotic stages (Fig. 2.6). Additionally, females expressing Barren-EGFP in a *Barren* mutant background are fertile and syncytial embryos derived from these females show no mitotic defects (Fig. 2.7). This further reveals that Barren-EGFP is functional in early *Drosophila* embryos.

All together, these results indicate that Barren-EGFP is a fully functional fusion protein and therefore its dynamic behavior is very likely to faithfully reflect the dynamic properties of endogenous protein.

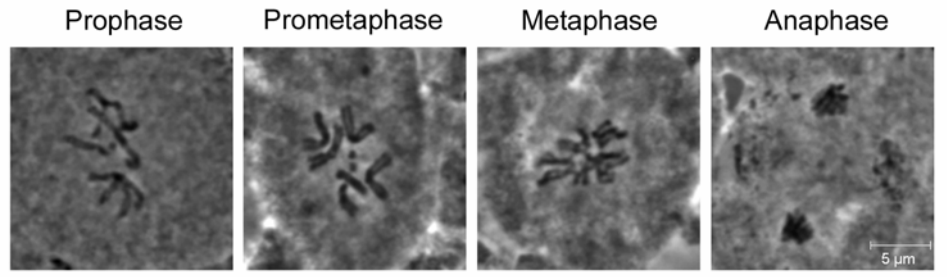

Figure 2.6. Analysis of mitotic figures in rescued third instar larval brains. Orcein-stained brain squashes from third instar larvae expressing Barren-EGFP in a *Barren* mutant background (*Barr^{L305}/Df(2L)Exel7077*; *UAS-Barr-EGFP III.2/daGAL4*). Rescued larvae show no mitotic defects. Scale bar is 5µm

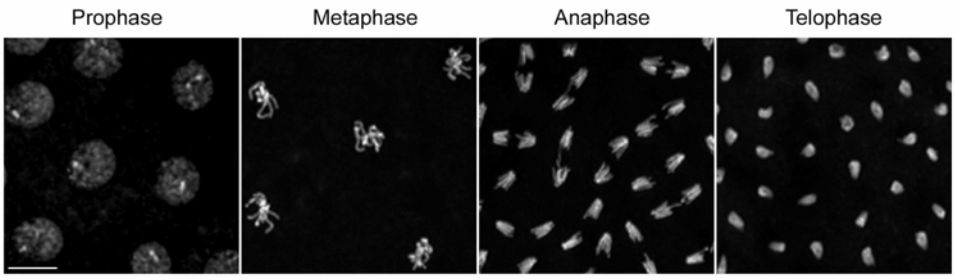

Figure 2.7. Analysis of syncytial embryos derived from females that express Barren-EGFP in a mutant background. Confocal images from syncytial embryos derived from *Barr^{L305}/ Df(2L)Exel7077*; *UAS-Barren-EGFP III.2, daGAL4* females. Images show Hoechst stained DNA. Scale bar is 10 µm. Note that these embryos show no mitotic defects.

2.4 Analysis of Barren-EGFP chromatin association during *Drosophila* syncytial nuclear divisions

To evaluate the dynamic association of Barren-EGFP with chromatin during mitosis, quantitative fluorescence analysis in *Drosophila* embryos undergoing syncytial blastoderm cycles was carried out. Early embryonic cycles have several advantages for quantitative fluorescence analysis. First, syncytial blastoderm cycles occur very rapidly (each cycle takes on average ~ 10 min) allowing the observer to follow several mitosis in a short period of time.

Secondly, these cycles occur in a meta-synchronous manner which enables the use of a large number of nuclei for the quantitative evaluation. Accordingly, embryos expressing maternally supplied Barren-EGFP and also HisH2Av-mRFP1, used to correct for fluctuations in chromatin organization during mitosis, were recorded during blastoderm syncytial nuclear divisions using a confocal laser microscope (Movie 2.1). In these embryos, Barren-EGFP was found to be expressed approximately 1.5 fold above endogenous levels (Fig. 2.8).

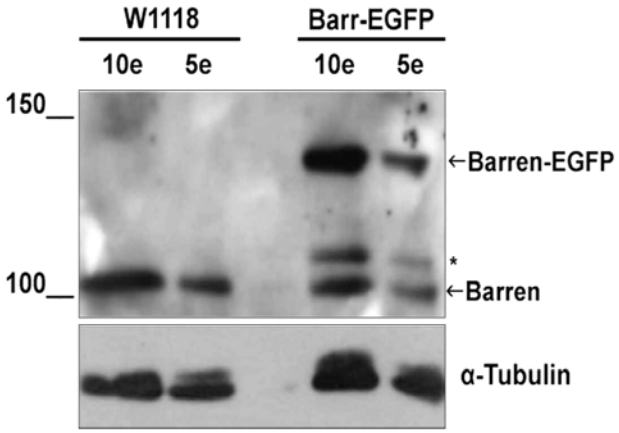

Figure 2.8. Western Blot analysis of barren-EGFP protein levels in early embryos. A 1h-2h embryo collection of both control and Barren-EGFP expressing embryos was obtained from *W1118* and *UASP-Barren-EGFP III.1, α-4tub-GAL4-VP16/MKRS* females respectively. Different amounts of extract were loaded to facilitate quantification (corresponding to 10 and 5 embryos). Western blot using a Barren specific antibody detects endogenous Barren in both extracts and ectopically expressed Barren-EGFP in Barren-EGFP embryos. A possible degradation product (*) is also detected. Tubulin was used as loading control. Quantification analyses reveal that Barren-EGFP is expressed ~ 1.5 fold above the endogenous levels.

To align different time-lapse recordings (n=10) from embryos undergoing mitosis 12, anaphase onset was defined as time zero (see materials and methods for quantification details). In syncytial nuclear divisions, Barren-EGFP was found to start to associate with chromatin during prophase, several minutes before nuclear envelope breakdown (NEBD) (Fig. 2.9). NEBD timing was defined by the time soluble Barren-EGFP was observed to enter the nuclear space (Fig. 2.10; between the two last frames). Using this method, NEBD in mitosis 12 was determined to occur 159.1 ± 13.2 sec (mean ± standard deviation (SD); n=10) before anaphase onset. This value is in agreement with determination of NEBD timing using the entry of soluble GFP-tubulin within the nuclear area as a marker (determined to be 166.8 ± 10.3 sec in GFP-Tubulin expressing embryos; n=5). The quantitative fluorescence analysis also indicates that more than 50% of the total chromosome associated Barren-EGFP protein is already loaded to chromatin during prophase (Fig. 2.9). These observations strongly suggest that in *Drosophila* syncytial divisions, condensin I might be involved in the initial stages of chromosome compaction during prophase unlike in human tissue culture cells where

condensin II is the only condensin complex associated with chromatin before NEBD (Gerlich et al., 2006a; Hirota et al., 2004; Ono et al., 2004).

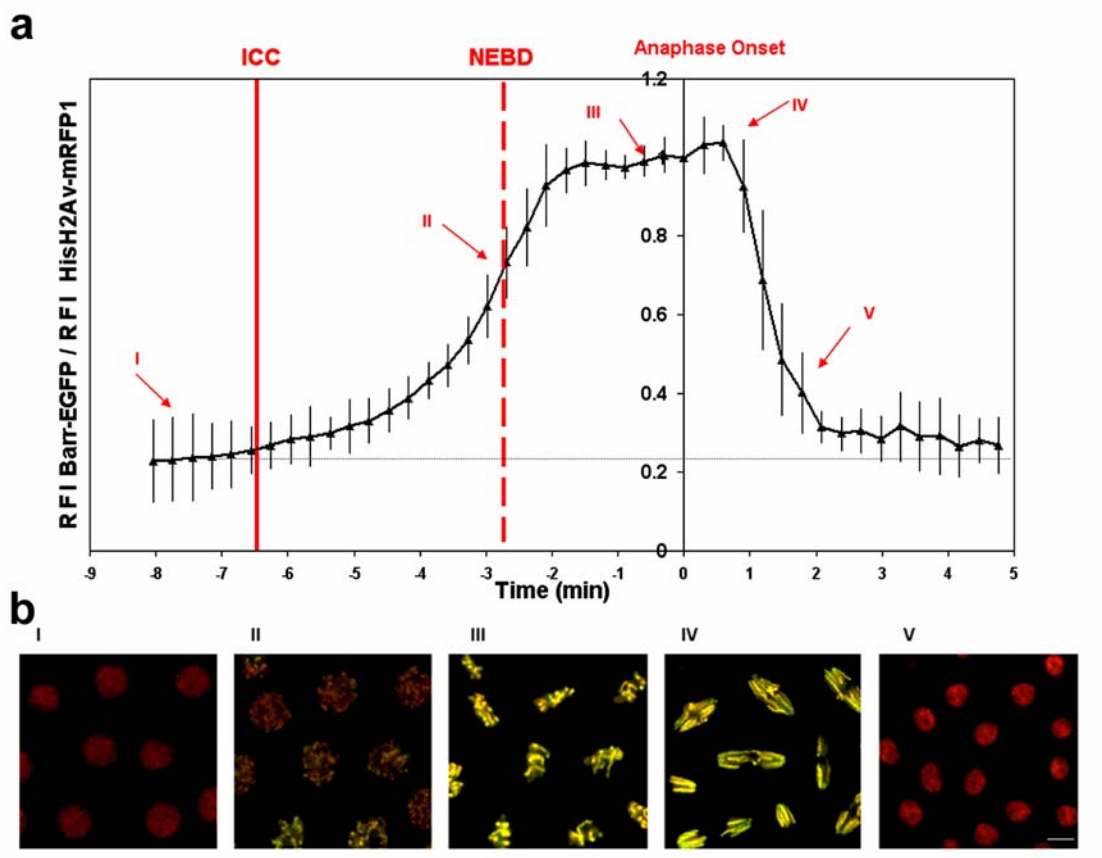

Figure 2.9. Real-time analysis of Barren-EGFP association with chromatin during mitosis. Quantification of fluorescence intensities during mitosis 12 in live embryos in which Barren-EGFP and HisH2Av-mRFP1 were maternally deposited. **a)** Graphic representation of relative fluorescence intensity of Barren-EGFP on chromosomes over time. Different movies (n=10) were aligned accordingly to anaphase onset timing (t_0 = last metaphase). The times of Initiation of Chromosome Condensation (ICC) and Nuclear Envelope Breakdown (NEBD) are also indicated by the continuous and dashed red lines, respectively. **b)** Representative images at different time points of the cycle (corresponding to the roman numbered arrows in the graph in a.) Scale bar is 5 μm.

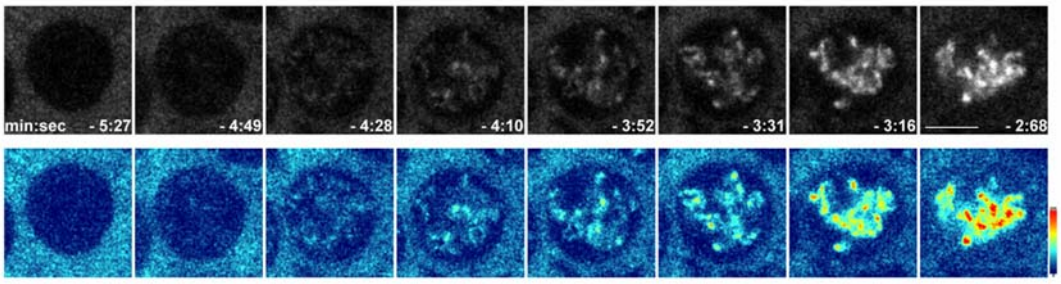

Figure 2.10. Detailed analysis of Barren-EGFP chromatin association during prophase. Representative images from single stack time-lapse microscopy visualization of Barren-EGFP entry in the nuclear space during prophase. Upper panel shows gray scale images of Barren-EGFP signal over time (relative times are indicated, t_0 = last metaphase) which were converted to a gradient LUT images (lower panel) for better visualization. Note that Barren-EGFP is already associated with mitotic chromosomes during prophase, before NEBD. Scale bar is 5 μm.

In order to determine whether chromatin association of Barren-EGFP occurs simultaneously with the Initiation of Chromosome Condensation (ICC), the ICC timing was defined as the first time that strong dots of HisH2Av-mRFP can be detected (Fig. 2.11). In mitosis 12 ICC was found to occur 6.3 ± 1.2 min (mean ± SD; n=10) before anaphase onset (~3.7 min before NEBD). Aligning this data with the accumulation of Barren-EGFP (Fig. 2a) indicates that Barren-EGFP signal starts to increase at the time of ICC. Therefore, these results strongly suggest that the start of condensin I loading on mitotic chromosomes during *Drosophila* syncytial embryonic divisions is concomitant with the initiation of chromosome condensation. Chromatin association of Barren-EGFP occurs gradually in a slow single step so that Barren-EGFP levels reach a steady state by the time chromosomes have congressed to the metaphase plate, approximately 2 min before anaphase onset (Fig. 2.9). While in metaphase, there appears to be no overall increase of Barren-EGFP levels on mitotic chromosomes and its levels remain high as chromosomes begin poleward movement during anaphase. However, Barren-EGFP must be rapidly released since it is no longer observed in chromatin during the beginning of telophase (Fig. 2.9). The kinetics of disassociation appears to be much faster than the association step which occurs during chromosome condensation. The loading phase takes ~4.5 min whereas dissociation of Barren-EGFP from chromatin at the end of mitosis occurs within less than 2 min. Subsequently, during syncytial divisions, Barren-EGFP is excluded from the nucleus during interphase. It is important to refer that *Drosophila* embryonic syncytial divisions are characterized by the absence of G (gap) phases. Thus, the nuclear exclusion observed in these nuclear divisions does not exclude that condensin I might be nuclear during interphase of complete cycles.

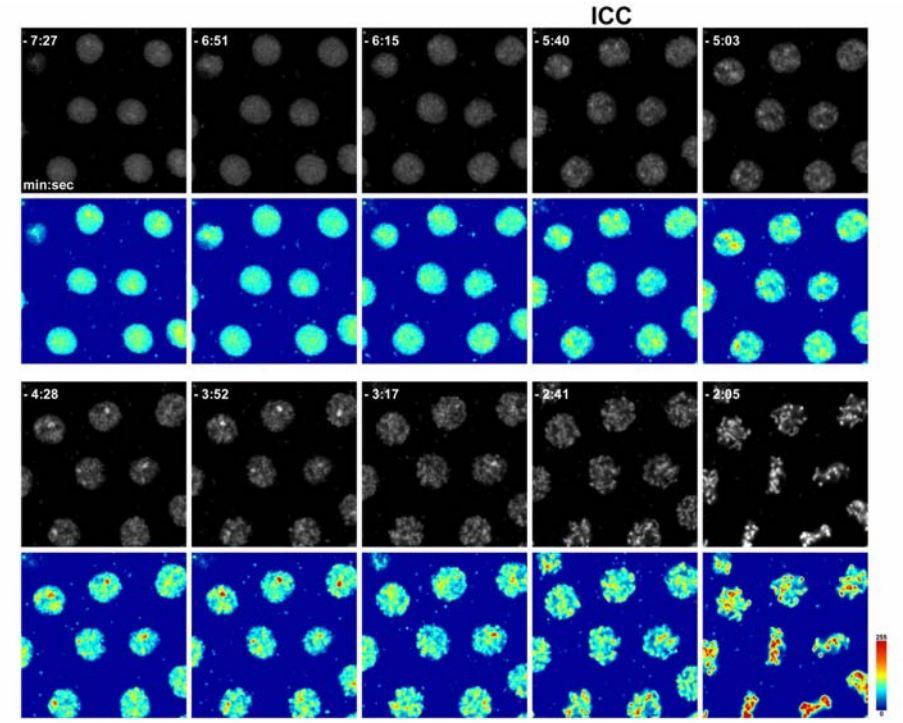

Figure 2.11. Initiation of Chromosome Condensation (ICC) Timing. ICC was determined by the time strong dots of HisH2Av-mRFP1 start to be observed (at -5:40 in this example). Raw data images of the HisH2Av-mRFP1 channel (upper panel) were converted to a gradient LUT panel (lower panel) to facilitate the visualization of differences in fluorescence intensity. ICC timing was defined by the time dark-orange/red pixels start to be visualized in the LUT converted image. Analysis of different movies (n=10) reveals that ICC occurs 6.3 ± 1.2 min (mean ± SD) before anaphase onset.

The fast release of Barren-EGFP from chromatin suggests the presence of regulatory mechanisms activated after anaphase onset. To evaluate if the chromatin dissociation event is dependent on total protein amount, Barren levels at different stages of mitosis were analyzed. Cellularized embryos were forced to progress through mitosis 14 in a synchronous manner, as previously described (Sauer et al., 1995), and embryos at different phases were sorted. Protein extracts of embryos at each mitotic phase were analyzed by western blot (Fig. 2.12). This analysis reveals that Barren protein levels do not change considerably from G2 until metaphase. However, after anaphase onset, there is a strong decrease in Barren total protein levels to about 50% of the levels found at early mitotic stages. This strongly suggests that Barren might be undergoing specific degradation which might explain its rapid release from chromatin.

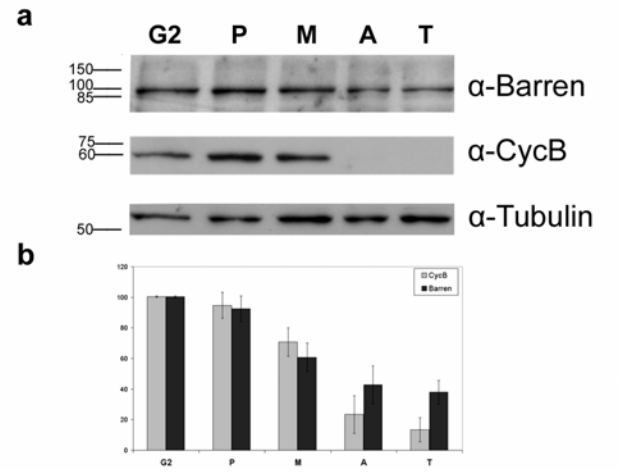

Figure 2.12. Analysis of Barren levels at different mitotic stages. a) Protein extracts from synchronous sorted embryos were probed for Barren levels by western blot. Cyclin B was used as sorting control and tubulin as loading control. **b)** Quantifications of Barren and Cyclin B levels at each mitotic stage. Intensity levels were normalized for tubulin intensity and further normalized for the highest level phase value (set as 100%). Graphic represents average of two independent experiments and error bars are SD.

2.5 Analysis of Barren-EGFP chromatin association in cellularized embryos and larval neuroblasts

The analysis of Barren-EGFP association with chromatin suggests that it takes place already during prophase, which is considerably different from what has been previously described in human cells (Gerlich et al., 2006a; Hirota et al., 2004; Ono et al., 2004). It is possible that this discrepancy is due to the very special type of embryonic syncytial divisions that characterize *Drosophila* early embryogenesis. These nuclei are known to undergo a modified cell cycle where all the nuclei share a common cytoplasm, without cytokinesis, and gap phases are absent. Therefore, to address this further, Barren-EGFP association to chromatin was analyzed in postblastoderm embryonic divisions. Accordingly, the dynamic behavior of Barren-EGFP was characterized in "mitotic domains". These domains are clusters of post-blastodermal cells that undergo synchronized mitosis (Foe, 1989). The results show that in these cells, Barren-EGFP was found to localize inside the nuclear space at the brighter HisH2Av-mRFP foci, already during late G2, where it continues to accumulate with chromatin as condensation proceeds during prophase (Fig. 2.13 and movie 2.2). During prometaphase, metaphase and anaphase Barren-EGFP levels remain high and at late anaphase and early telophase it rapidly disappears.

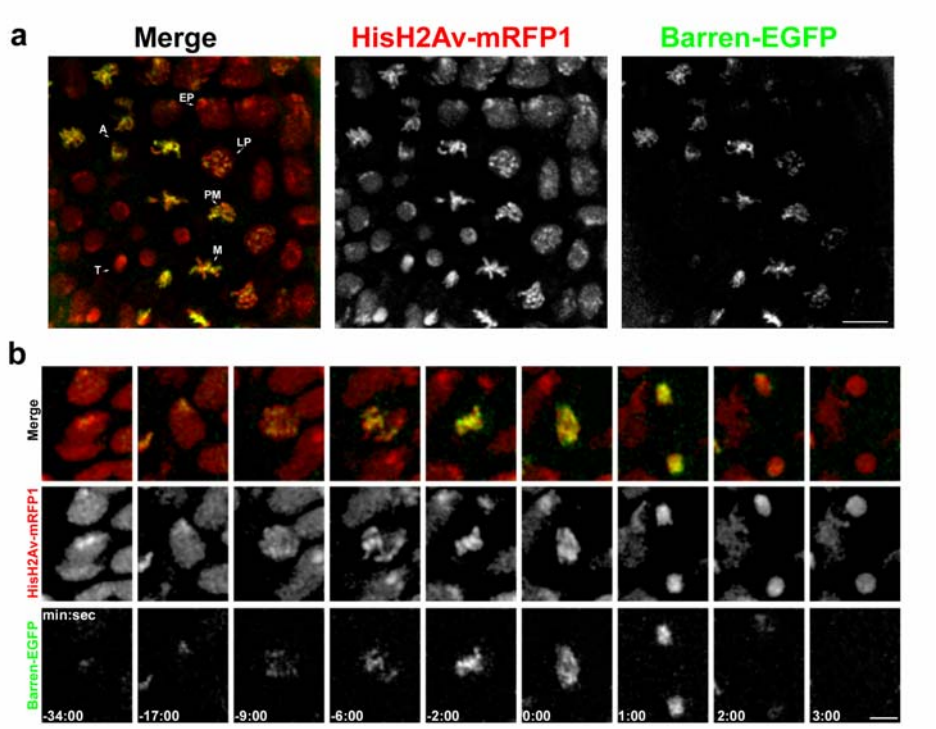

Figure 2.13. Analysis of Barren-EGFP accumulation to mitotic chromatin in cellularized embryos. a) Live embryos expressing Barren-EGFP (green) and HisH2Av-mRFP1 (red) were observed while progressing through mitosis 14, after cellularization of the blastoderm. A mitotic domain is shown in which several mitotic figures can be observed. Barren-EGFP can be detected already in G2/early prophase (EP) at the sites of higher degree of condensation. Later in prophase (LP) Barren-EGFP is detected all over chromatin. Levels remain high during prometaphase (PM), metaphase (M), and in anaphase (A) figures. In telophase (T) Barren-EGFP is nearly undetectable. Scale bar is 10 μm **b)** Time lapse analysis of a single cell undergoing a post-blastodermal division. Barren-EGFP is already found associated with chromatin in late G2/early prophase, well before NEBD. The levels of Barren-EGFP associated with mitotic chromosomes progressively increase and remain high until anaphase but they are significantly reduced during telophase. By the end of telophase Barren-EGFP is no longer detected. Scale bar is 5 μm

Barren-EGFP chromatin association was also studied in post-embryonic cells. Brains from third instar larvae expressing Barren-EGFP in a *Barren* mutant background were visualized by time lapse confocal microscopy in order to follow asymmetric cell divisions of the neuroblasts (Fig. 2.14). Barren-EGFP in these brains was found to be expressed ~2-fold above the endogenous levels in wild type brains (Fig.2.15). For live imaging purposes, neuroblasts can be easily distinguished within the brain by their bulk size when compared to the other cell types. In agreement with what was observed in both syncytial early nuclear divisions and post-blastoderm cell divisions, Barren-EGFP chromatin association in neuroblasts was also found to initiate during prophase, well before nuclear envelope breakdown (Fig. 2.14). During prometaphase and metaphase protein levels remain high. High levels of Barren-EGFP are also detectable in anaphase, while the neuroblast divides asymmetrically, but the levels start to decrease as soon as chromatids complete anaphase.

Accordingly, during early telophase the levels of Barren-EGFP associated with chromatin decrease significantly.

Overall, these results show that Barren-EGFP has a highly reproducible chromatin association dynamics in very different dividing tissues clearly demonstrating that in *Drosophila*, condensin I appears to gain access to chromatin before nuclear envelope breakdown.

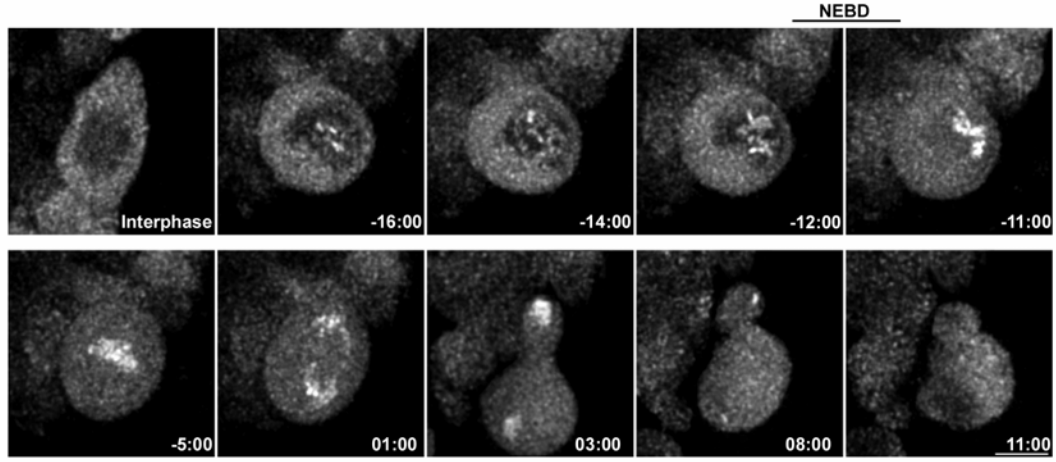

Figure 2.14. Analysis of Barren-EGFP accumulation to mitotic chromatin in third instar larval neuroblasts. Time lapse analysis of an asymmetric cell division in a *Drosophila* neuroblast expressing Barren-EGFP. Barren-EGFP is found to be nuclear excluded in the majority of the interphase neuroblasts but its association starts during early stages of prophase. Overall, the association profile is similar to the one observed in embryonic divisions. Scale bar is 5 μm.

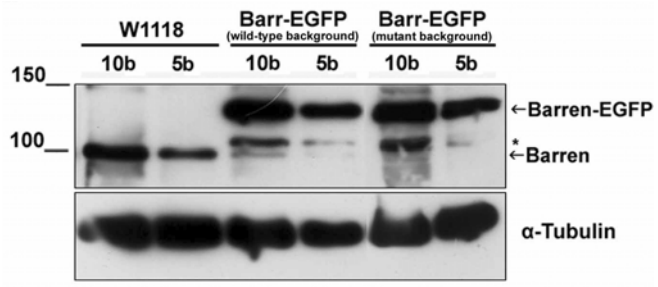

Figure 2.15. Western Blot analysis of Barren-EGFP protein levels in third instar larval brains. Brains from wild-type larvae, from larvae that express Barren-EGFP in a wild-type background (*W;;UAS-Barr-GFP III.2, daGAL4*) and from larvae that express Barren-EGFP in a *Barren* mutant background (*W*;*Barr*^{L305}*/Df(2L)Exel7077;UAS-Barr-GFP III.2, daGAL4*) were dissected in PBS and resuspended in SDS-sample buffer. Different amounts of extract were loaded to facilitate quantification (corresponding to 10 and 5 brains). Western blot using a Barren specific antibody detects ectopically expressed Barren-EGFP and endogenous Barren, which is considerably down-regulated in brains that overexpress Barren-EGFP. A possible degradation product (*) is also detected. Tubulin was used as loading control. Quantification analysis reveal that Barren-EGFP is expressed ~ 2 fold above the levels detected in wild type brains.

2.6 Initial localization pattern of Barren-EGFP to mitotic chromatin

The analysis of both syncytial and cellularized embryos suggested that loading of Barren-EGFP to chromatin might be initiated at specific foci, as Barren-EGFP starts to accumulate in the nuclear space during G2/prophase as well defined dots. To assess whether the initial accumulation of Barren-EGFP corresponds to centromeric regions, transgenic flies that co-express Barren-EGFP and a red fluorescent version of Cid were produced. Cid is the *Drosophila* Histone-H3-like homologue of the human centromeric protein CENP-A which localizes to the centromeres throughout the cell cycle (Henikoff et al., 2000). Embryos co-expressing Barren-EGFP and Cid-mRFP were analyzed while progressing through post-blastodermal cycles (Fig. 2.16). As expected, Cid-mRFP shows discrete dot-like localization throughout the nuclear divisions. In cells progressing through G2 and early prophase, the stronger Barren-EGFP signals were found to co-localize with the centromere marker Cid-mRFP, revealing that the initial sites of Barren-EGFP association correspond to the centromeres. Later in prophase, Barren-EGFP appears to be distributed also along chromosome arms.

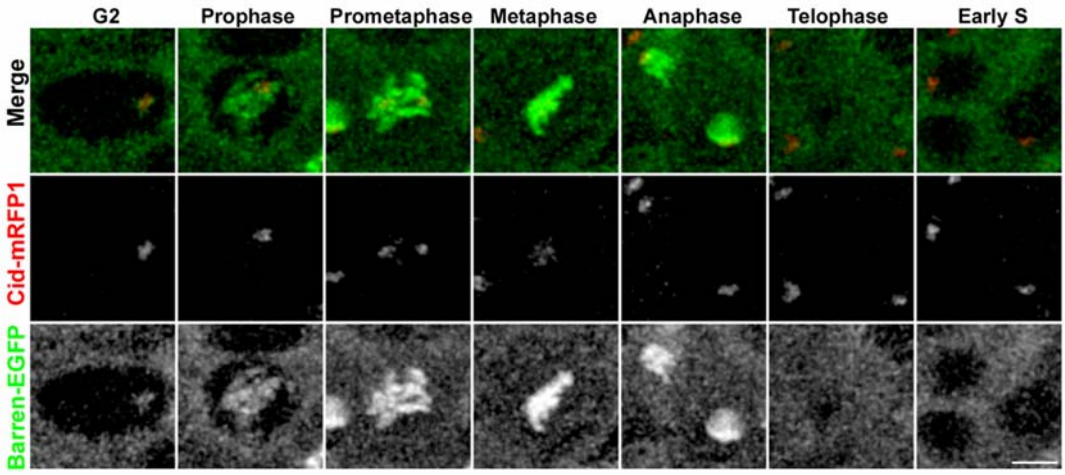

Figure 2.16. Analysis of initial sites of Barren-EGFP chromatin association in post-blastodermal embryos. 4D confocal microscopy analysis of live embryos simultaneously expressing Cid-mRFP1 and Barren-EGFP. Image shows selected frames of post-blastodermal embryonic cells at different cell cycle stages. Note that Cid-mRFP (red) is always present at the centromeres. Barren-EGFP (green) is found to localize inside the nuclear space already in G2 specifically at the centromeric region. Scale bar is 5 μm.

To confirm these observations, early syncytial embryos that express simultaneously maternally supplied Cid-mRFP1 and Barren-EGFP were also analyzed by 4D confocal image analysis (Fig. 2.17 and Movie 2.3). The data revealed that a strong accumulation of Barren-EGFP is first visible at the centromeric regions, when the nuclei enter prophase. The first brighter spots of Barren-EGFP were found very close to or overlapping with Cid-mRFP1 signals, with only very small amounts detected at other sites within the nuclear space (Fig. 2.17). Subsequently, at later stages of prophase (t=-2.30 min; t_0=NEBD) the stronger Barren-EGFP signals appear to extend into the chromosome arms. To quantify this sequential association of Barren-EGFP to chromatin a method that evaluates Barren-EGFP association at different chromosomal sites was developed (Fig. 2.18). Based on the Cid-mRFP channel, the centromere-proximal region was defined (about ¼ of nuclear area, red circle in Fig. 2.18a) and the mean fluorescence intensity of Barren-EGFP inside this region was measured (MFI cen-proximal). A second region placed inside the nuclear space but further away of the centromeres, the centromere-distant region, was also defined (between red and green circles in Fig. 2.18a), and the mean fluorescence intensity of Barren-EGFP at this site measured (MFI cen-distant). As expected, when MFI cen-proximal/MFI cen-distant ratio is plotted over time, the ratio is 1 during interphase. However, as chromosome condensation begins (ICC), the MFI cen-proximal/MFI cen-distant ratio increases, indicating a preferential association of condensin I at the centromeric region. By the end of prophase, the MFI cen-proximal/MFI cen-distant ratio for Barren-EGFP returns to 1 which reveals that Barren-EGFP is now equally distributed between centromeric and chromosome arms regions. This stronger accumulation of Barren-EGFP observed specifically at the centromeres during early mitosis results directly from Barren-EGFP chromatin accumulation and is not an artifact of chromosome compaction particularly in this chromosomal region. Similar analysis of HisH2Av-mRFP1 reveals that even though chromosome condensation is occasionally detected specifically at the centromeric region, this does not result in a preferential increase of fluorescence intensity in this area. Accordingly, the MFI cen-proximal/MFI cen-distant ratio for HisH2Av-mRFP1 remains close to 1 (Fig. 2.18b). This analysis strongly suggests that condensin I association follows a spatial order along the chromosome, with the centromeric region being the initial region of significant association.

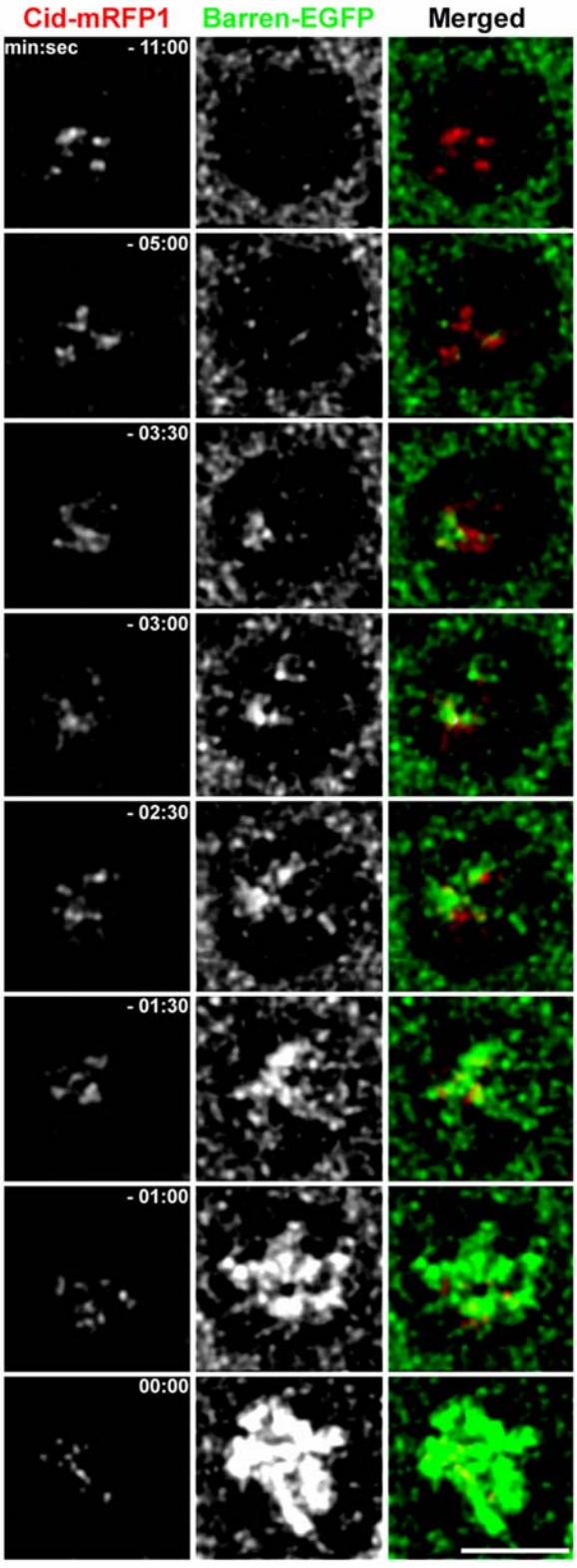

Figure 1.17. Analysis of initial sites of Barren-EGFP chromatin association in syncytial embryos. Projection from 4D confocal microscopy analysis of a live embryo while progressing through syncytial mitosis 12. Barren-EGFP is shown in green and Cid-mRFP in red. Image contrast was adjusted in order to clear the nuclear space during interphase (top figure) for better visualization of initial sites of major Barren-EGFP association. Cid-mRFP is always observed at the centromeres and Barren-EGFP first accumulates at Cid-mRFP positive sites. Strong association of Barren-EGFP to chromosome arms only appears later. Scale bar is 5 µm.

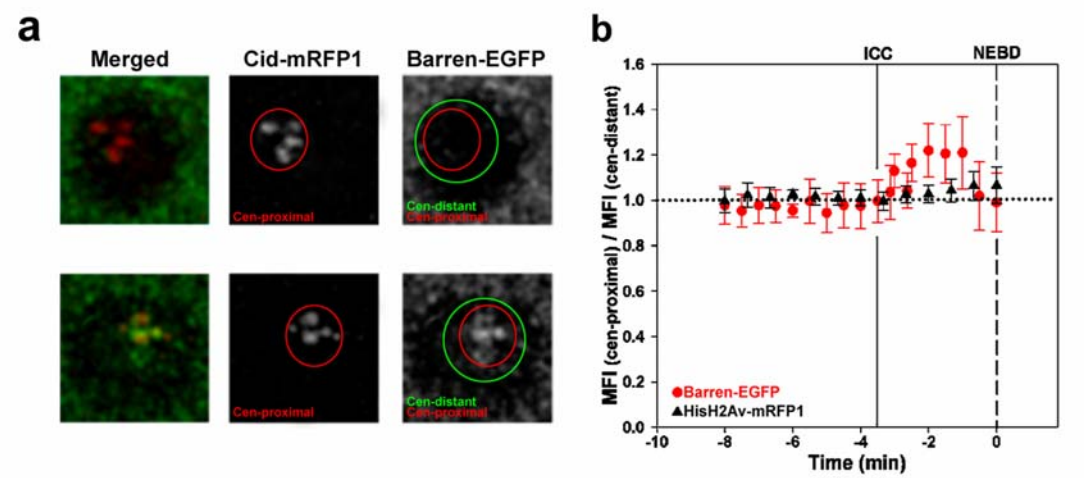

Figure 1.18. Quantification of the preferential initial association of Barren-EGFP to the centromere-proximal chromatin. a) Example of the definition of centromere-proximal region (red circle) and the centromere-distant region (between red and green circles) used for the quantification of Barren-EGFP fluorescent signal represented in b). **b)** Graphic representation of the ratio between the mean fluorescence intensity in the centromere-proximal region (MFI cen-proximal) and the mean fluorescence intensity in the centromere-distant region (MFI cen-distant), plotted over time, for both Barren-EGFP (red circles, n=8) and HisH2Av-mRFP (black triangles, n=5). Times are relative to Nuclear Envelope Breakdown. The time of ICC is also indicated by the continuous line; error bars = SD.

2.7 FRAP analysis of Barren-EGFP in mitotic chromosomes

The analysis of Barren-EGFP association to mitotic chromatin showed that at metaphase there appears to be no net increase of chromosome-associated protein levels, even though mitotic chromosomes are still condensing. Therefore, we set out to investigate if Barren-EGFP associated with mitotic chromatin becomes stably bound or, alternatively, its association is dynamic. To address this question, Fluorescence Recovery After Photobleaching (FRAP) analysis in syncytial embryos undergoing mitosis 12 and 13 was performed. The use of syncytial embryos for FRAP analysis has several advantages. First, all the dividing nuclei share the same cytoplasm and the bleached molecules are not a significant part of the total molecules in the embryo and are rapidly diffused away so that photobleaching does not affect total fluorescence intensity of the embryo. Second, the nuclear divisions occur in a synchronous manner allowing one to use the neighboring nuclei as control for photobleaching and recovery events. Therefore, we photobleached an entire metaphase plate, so that the recovery observed is not affected by rearrangements of the chromatin but reflects only incorporation of molecules from the cytoplasmic pool. The fluorescence recovery was

monitored over time and Relative Fluorescence Intensity (RFI) was calculated as the ratio between the mean fluorescence intensity of the bleached metaphase and the mean fluorescence intensity of a non-bleached metaphase used as control (Fig. 2.19). This type of analysis corrects for any extra loading and the increase in RFI is only a reflection of exchange between chromosomal bound and cytoplasmic pools.

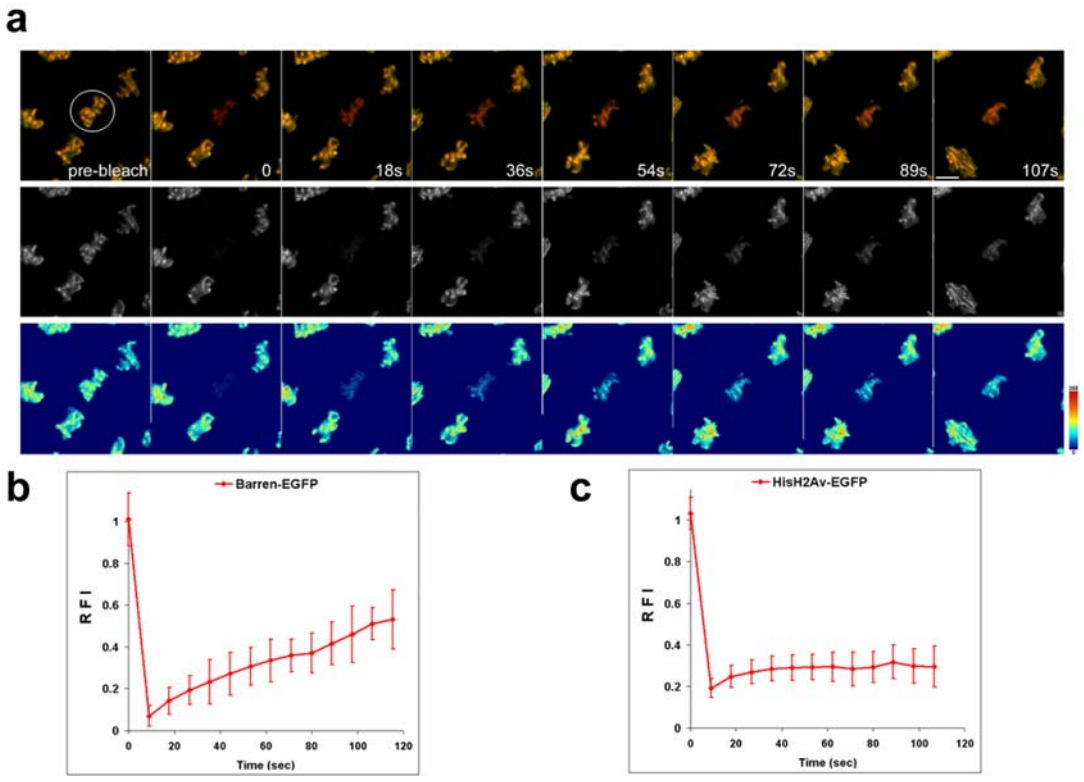

Figure 2.19. FRAP analysis of Barren-EGFP in syncytial *Drosophila* embryos. FRAP analysis was performed in living embryos derived from females expressing both Barren-EGFP and HisH2Av-mRFP1. A Region of Interest (ROI) was selected in order to bleach an entire metaphase plate (white circle) and subsequently images were collected every 9 sec. **a)** Selected images from an individual FRAP experiment are shown. Upper panel shows a merged image of Barren-EGFP (green) and HisH2Av-mRFP1 (red). Middle panels shows gray scale Barren-EGFP channel alone. These images were converted to a gradient LUT image to facilitate visualization of differences in fluorescence intensity (bottom panel). Scale bar is 5 µm. **b)** Relative Fluorescence Intensity (RFI) of Barren-EGFP plotted over time. RFI was calculated as the ratio between the mean fluorescence intensity of the bleached metaphase and the mean fluorescence intensity of a non-bleached metaphase used as control; n = 10; error bars = SD; Quantitative analysis showed that Barren-EGFP is mobile and recovers with an initial recovery rate of 28 ± 4 % per minute. **c)** FRAP analysis of HisH2Av-EGFP was also performed as control; n = 11; error bars = SD; HisH2Av-EGFP fluorescence did not recover significantly after photobleaching.

FRAP analysis of HisH2Av-EGFP was performed for comparative analysis. As expected, it did not recover significantly after photobleaching (Fig. 2.19c). On the other hand, chromosome-associated Barren-EGFP shows significant recovery after photobleaching with an initial recovery rate of 28 ± 4 % per minute (mean ± SD, n=10) (Fig. 1.19a, b). However, as the embryonic syncytial divisions are very fast, this type of analysis can only be performed for about 2 minutes which only allowed the evaluation of initial rates of recovery but fluorescence recovery could not reach saturation. Thus, several dynamic parameters as half time of recovery and mobile and immobile fractions could not be determined using this experimental set up.

In order to perform FRAP analysis for longer periods, embryonic nuclei were arrested in prometaphase by injection with 1mM Colcemid and FRAP analysis was performed 15-30 min after colcemid injection (Fig. 2.20). The initial recovery rate in colcemid arrested embryos was not significantly different from non-arrested embryos (22 ± 6 % per minute vs. 28 ± 4 % per minute, respectively). This indicates that the recovery rate is independent of the arrested state as well as the presence or absence of microtubules. Using this set up we could observe recovery to reach saturation levels and data points were shown to fit to a single exponential curve (Fig. 2.20c). Analysis of the exponential equations reveals that 84±11% of Barren-EGFP is mobile and turns over with a half time of 121±38 sec. A detailed analysis of a single chromosome from a colcemid arrested embryo is also shown demonstrating that the recovery is evenly distributed along the chromosome arms (Fig. 2.20b). As a negative control we also analyzed the behavior of HisH2Av-EGFP which was shown to be virtually immobile (Fig. 2.20d). These results show very clearly that in *Drosophila* Barren-EGFP is highly mobile and is rapidly exchanging between the chromatin and the cytoplasmic pool.

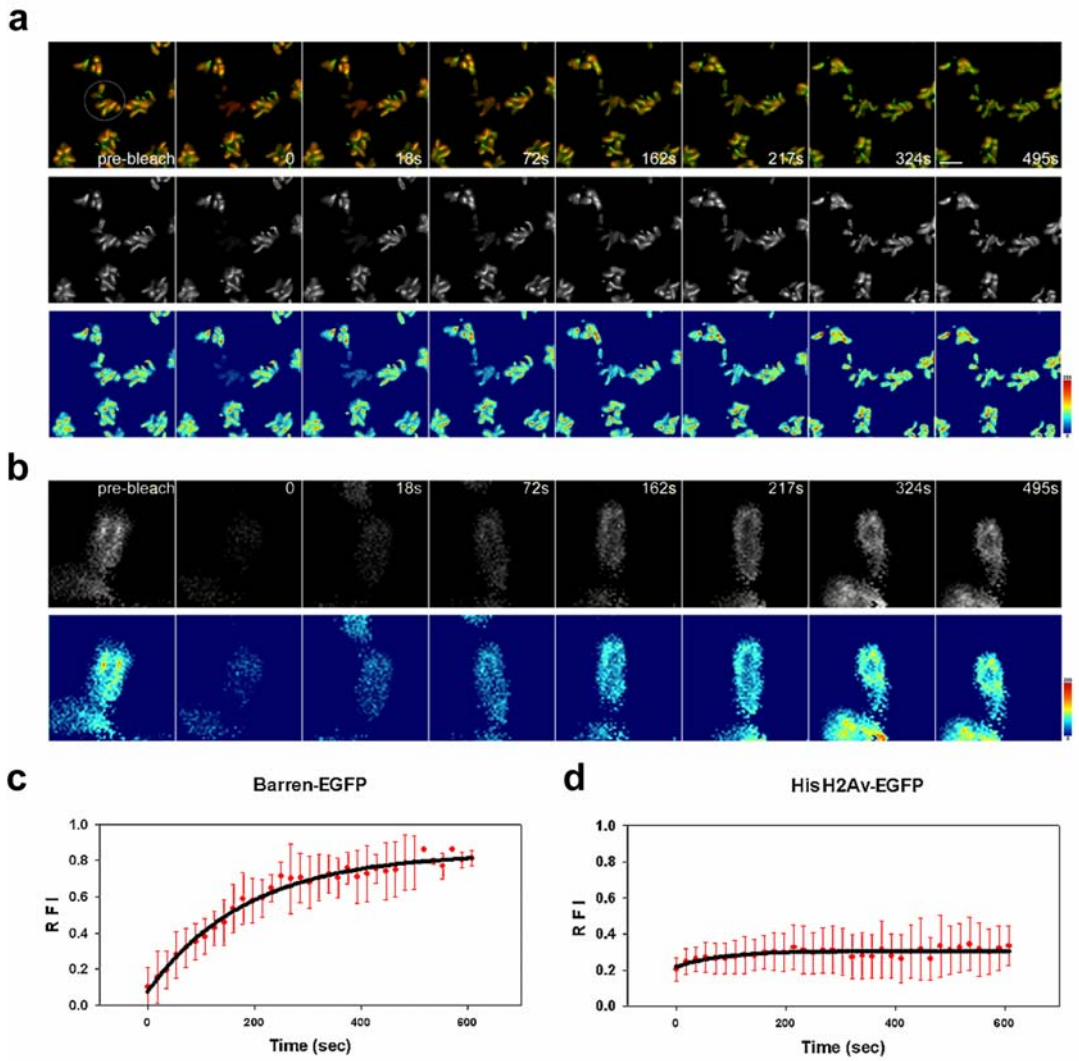

Figure 2.20. FRAP analysis of Barren-EGFP in syncytial *Drosophila* embryos arrested with colcemid. FRAP analysis was performed in live embryos derived from females expressing both Barren-EGFP and HisH2Av-mRFP1 at mitosis 12 or 13, after being injected with 1 mM colcemid to prevent anaphase onset. A ROI was selected in order to bleach an entire metaphase plate (white circle) and subsequently images were collected every 18 sec. **a)** Selected images from an individual FRAP experiment are shown. Upper panel shows a merged image of Barren-EGFP (green) and HisH2Av-mRFP1 (red). Middle panels shows gray scale Barren-EGFP channel alone. These images were converted to a gradient LUT image to facilitate visualization of differences in fluorescence intensity (bottom panel). Scale bar is 5 µm. **b)** Higher magnification (8x) of a single chromosome is also shown for more detailed visualization. **c)** Relative Fluorescence Intensity (RFI) of Barren-EGFP plotted over time. Data points are in red; n = 7 error bars=SD; Fitting curve is shown in black; Data fit analysis reveals that 84+112% of Barren-EGFP is mobile and turns over with a t1/2= 128 121±38 sec. **d)** FRAP analysis of HisH2Av-EGFP was also performed as a control; n = 7 error bars=SD. HisH2Av-EGFP fluorescence did not recover significantly after photobleaching.

2.8 Construction of DmSMC4-EGFP fusion protein and DmSMC4-EGFP expressing flies.

The analysis of Barren-EGFP dynamic behavior is very likely to reflect the dynamics of the entire condensin I complex. However, it would be of particular interest to analyze whether all condensin complex subunits share a similar dynamic behavior or if different subunits associate to mitotic chromatin with a particular dynamic profile. Additionally, it would be interesting to address whether a condensin I-specific subunit (Barren) and a subunit shared by condensin I and the putative condensin II complexes display any differences in chromatin association dynamics. To address these questions, SMC4-EGFP fusion proteins were produced (unpublished work by Søren Steffensen). EGFP was inserted in frame within SMC4 genomic coding region after a.a. 587. This corresponds to a region before the hinge/heterodimerization domain. Transient transfection of this construct in S2 *Drosophila* tissue culture cells indicates that this fusion protein is indeed able to localize to the chromatin central axis in metaphase chromosomes, similarly to the localization of SMC4 revealed by immunofluorescence analysis (Fig. 2.21).

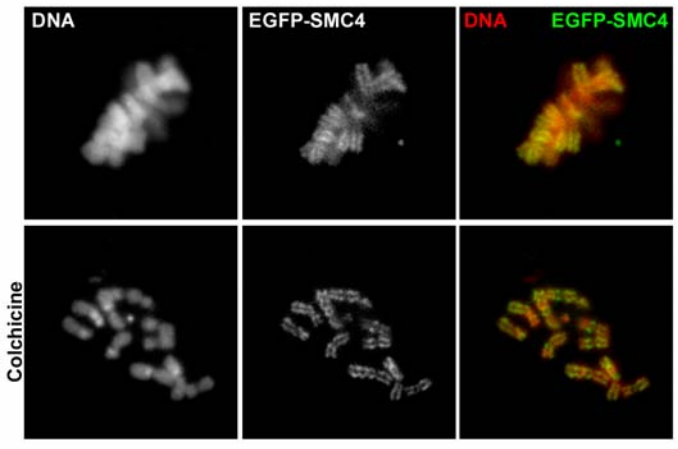

Figure 1.21. Transient transfection of S2 cells with EGFP-SMC4. Analysis of EGFP-SMC4 chromosomal localization in **a)** a metaphase cell from asynchronous culture and in **b)** a colchicine arrested cell (30µm colchicine). In both situations, EGFP-SMC4 localizes at a central axis within chromatids of prometaphase/metaphase chromosomes. (Kindly provided by Søren Steffensen).

In order to perform a dynamic analysis of EGFP-SMC4 similar the one carried out for Barren-EGFP, transgenic flies that express EGFP-SMC4 under the control of the UAS/GAL4 system (Brand and Perrimon 1993) were produced. EGFP-SMC4 fusion gene was cloned in the pUASP vector used for germline P-element-mediated transformation. Several transformed lines were established and insertions were mapped to either the II (lines II.1, II.2 and II.3) or the III (lines III.1, III.2, III.3 and III.4) chromosomes. The lines whose insertion was mapped to the second chromosome are viable as homozygous whereas the four different lines with insertion on the third chromosome are homozygous lethal.

To address protein localization, the different *UASP-EGFP-SMC4* lines were crossed with *α-4tub-GAL4-VP16* driver and embryos derived from the resulting non-balanced females were collected and fixed in order to evaluate EGFP-SMC4 chromosomal localization (Fig. 2.22). All lines tested showed EGFP-SMC4 expression and localization to mitotic chromosomes during mitosis in syncytial embryos. Moreover, overexpression of EGFP-SMC4 during eye development does not produce any evident eye phenotype (Fig.2.23)

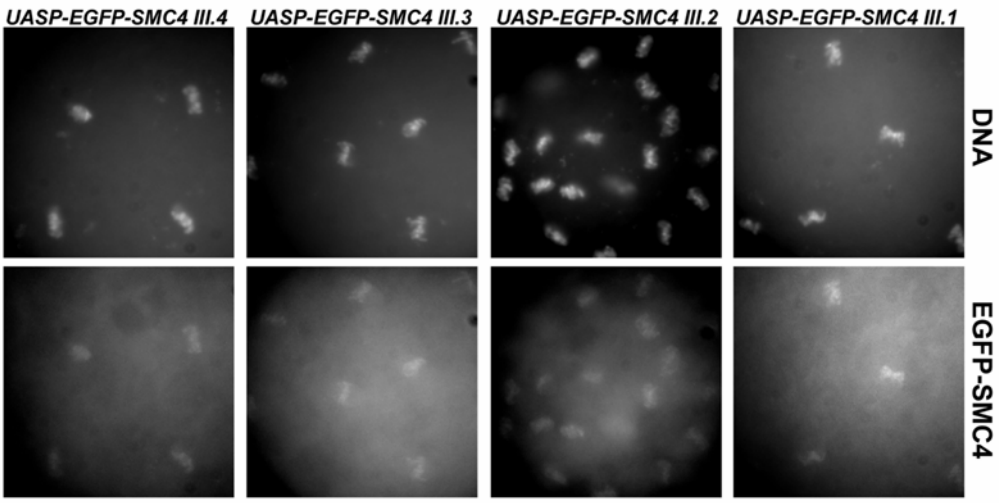

Figure 1.22. Chromosomal localization of EGFP-SMC4 during *Drosophila* embryonic syncytial divisions. A 0-2h embryos collection was obtained from females that carry each *UASP-SMC4* insertion and which expression in the germline was driven by the *α-4tub-GAL4-VP16* driver. The four different lines evaluated were shown to express SMC4-EGFP and this fusion protein was shown to localize at the mitotic chromosomes during syncytial embryonic cycles.

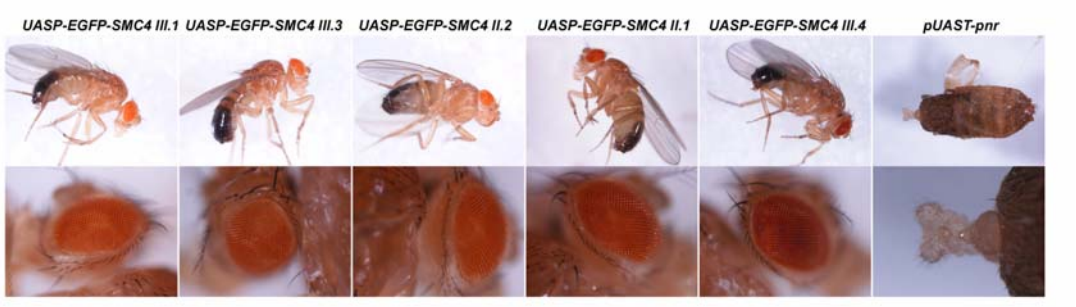

Figure 1.23. Analysis of SMC4-EGFP overexpression phenotype. *Eyeless-GAL4/CyO* virgin females were crossed with males caring the different *UASP-SMC4-EGFP* insertions. Non balanced progeny was observed for phenotypes associated with SMC4-EGFP overexpression during eye development. No evident phenotypes could be identified. *UAST-Pnr* was used as positive control.

To characterize EGFP-SMC4 association with chromatin during mitosis, syncytial embryos that express maternally deposited EGFP-SMC4 and HisH2Av-mRFP1 were analyzed by confocal microscopy. Surprisingly, embryonic divisions in those embryos often showed chromatin segregation defects and do not developed normally. Chromatin bridges were observed in virtually all embryos visualized, and often strong chromatin defects were observed (Fig. 2.24). Notably, these defects could not be observed in embryos expressing EGFP-SMC4 alone. Thus, the defects observed when EGFP-SMC4 is co-expressed with HisH2Av-mRFP1 might reflect an interaction constrained by the bulk tags present simultaneously on both proteins.

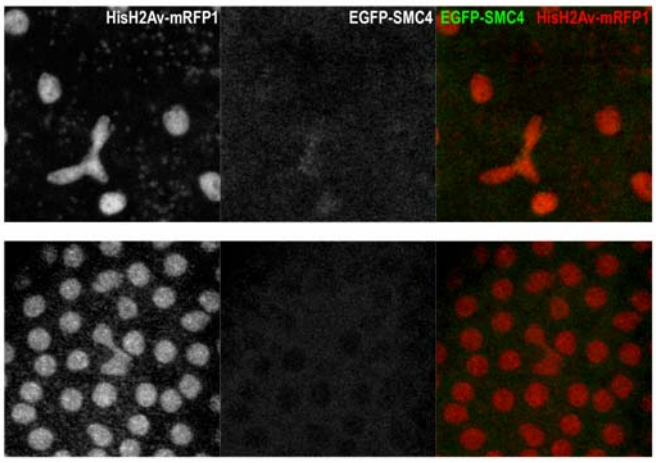

Figure 1.24. Live analysis of SMC4-EGFP/HisH2Av-mRFP1 co-expressing embryos. Selected images from live analysis of embryos simultaneously expressing EGFP-SMC4 and HisH2Av-mRFP1 showing chromatin bridges at the later mitotic stages.

Furthermore, several attempts to rescue the lethality associated with *gluon1* and *gluon2* DmSMC4 alleles (Steffensen et al., 2001) with ectopic expression of EGFP-SMC4 failed. This could be related with the fact that the levels of DmSMC4 need to be strictly regulated to achieve full complementation (rescue was attempted with *daGAL4* driver). Moreover, this very likely indicates that the fusion protein, although able to localize at mitotic chromosomes, is not fully functional. In fact, recent studies have described that specific residues at the hinge region of SMCs mediate DNA-SMCs interaction (Hirano and Hirano 2006) and other studies have strongly suggested cohesin loading onto chromatin involves the opening of the tripartite at the hinge/dimerization region (Gruber et al. 2006). Thus, if a similar loading mechanism is used by condensins, regions close to the hinge region might not be the most favorable region for fusion of the EGFP tag as the bulk size of EGFP (27 KDa) might interfere with chromatin loading. As this EGFP-SMC4 construct could not be proven to be functional and could not be co-expressed with HisH2Av-mRFP1, no further quantitative analysis was performed.

Nevertheless, qualitative analysis of embryos that divided with less severe defects showed that EGFP-SMC4 chromatin-association profile is very similar to the one reported for Barren-EGFP (Fig. 2.25 and Movie 2.4). EGFP-SMC4 is found to be nuclear excluded during interphase and to associate with mitotic chromosomes during prophase. The initial association appears at discrete sites at the apical part of the nucleus which very likely corresponds to the centromeres, as shown for Barren-EGFP (Fig. 2.25 t=-5:40). A significant amount of EGFP-SMC4 is already loaded before nuclear envelope breakdown (Fig. 2.25 t=-2:40, nuclei in the right-down corner of the image). Protein levels remain high during metaphase and anaphase and are substantially reduced by the end of mitosis.

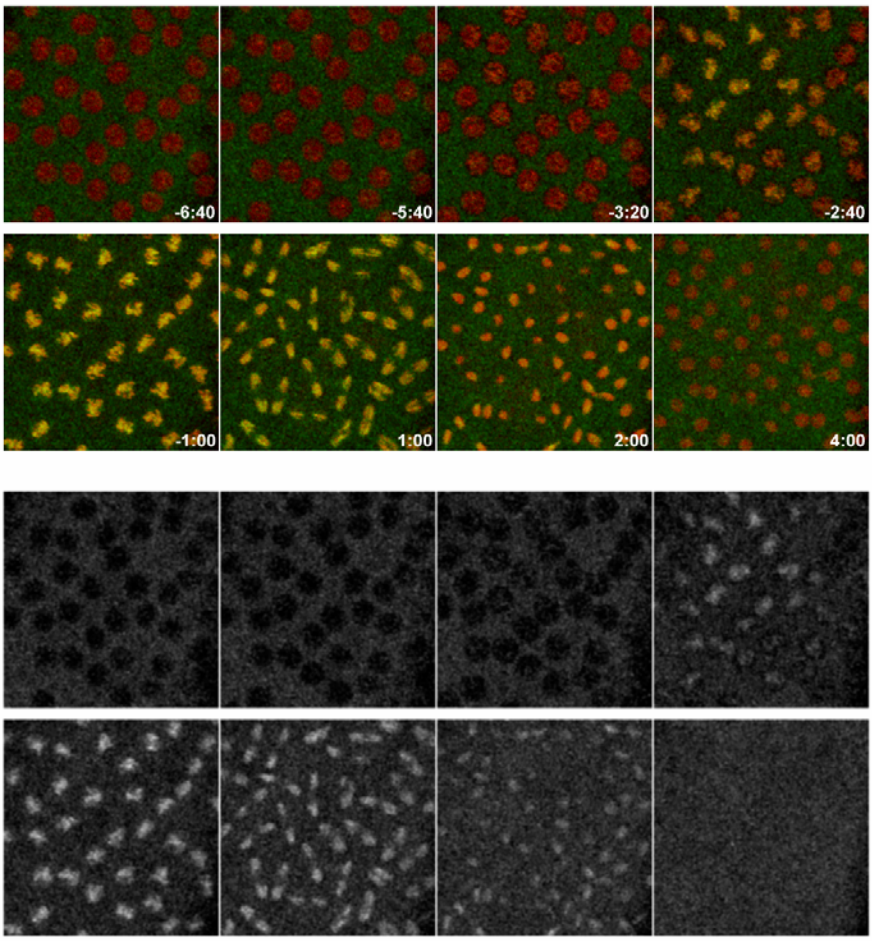

Figure 1.25. Time-lapse analysis of EGFP-SMC4 chromatin association during mitosis. 4D analysis of a syncytial embryo expressing simultaneously EGFP-SMC4 (green) and HisH2Av-mRFP1 (red). Lower panel shows EGFP-SMC4 alone. EGFP-SMC4 associates with chromatin during prophase, before NEBD and is released at the end of mitosis.

3. Discussion

The main aim of this study was to gain further insights into the function of condensin I in mitotic chromosome structure through the characterization of its dynamic behavior during mitosis. To address this, an extensive dynamic analysis of a functional EGFP-tagged version of the non-SMC subunit Barren was performed.

Previous studies have indicated that many organisms contain two condensin complexes that might contribute to chromosome condensation (Ono et al., 2003; Yeong et al., 2003). In HeLa cells, condensin I and II complexes have been described to contribute distinctly to the

process of mitotic chromosome organization (Hirota et al., 2004; Ono et al., 2003). Condensin II was shown to drive the initial stages of chromosome compaction, during prophase, whereas the canonical condensin I complex was shown to gain access to the chromosomes only after nuclear envelope breakdown (NEBD) both in HeLa cells (Hirota et al., 2004; Ono et al., 2004) and more recently in plant cells (Fujimoto et al., 2005). The *in vivo* analysis reported here clearly shows that in *Drosophila* nuclear divisions Barren-EGFP, and most likely the entire condensin I complex, starts to be loaded already in prophase, before nuclear envelope breakdown, at the same time that the first signs of chromosome condensation appear. These observations strongly suggest that in *Drosophila* condensin I is already involved in the early chromosome morphological changes observed during prophase. Even though homologues for two condensin II-specific subunits (CAP-D3 and CAP-H2) were found in *Drosophila* (Ono et al., 2003), the contribution to mitotic chromosome condensation of the putative condensin II complex in this organism remains to be determined. In contrast, emerging evidence suggests that condensin II might only have a minor role for mitotic chromosome architecture in *Drosophila*. Firstly, it was previously described that depletion of the condensin I specific non-SMC subunit Barren in S2 cells (chapter 1) gives rise to mitotic chromosome morphology defects that are indistinguishable from those observed after depletion of the core SMC4 subunit, which is required by both condensin complexes (Coelho et al., 2003). Secondly, a condensin II specific non-SMC subunit, CAP-D3, was not found to localize along chromosomal arms (Savvidou et al., 2005). Instead, this protein was only detected at the centromeres and therefore it is unlikely that condensin II plays any role in mitotic chromosome arms organization. Moreover, mutants for a condensin II specific subunit (CAP-D3) were reported to be viable but sterile (Savvidou et al., 2005) which might suggest a specific role of condensin II in meiotic chromosome organization. Also, we have analyzed a CAP-H2 mutant line and observed that it is viable but male sterile (described in chapter 3) fully supporting previous observation on mutant lines for CAP-D3. Finally, extensive bioinformatics analysis of the *Drosophila* genome has failed to reveal any protein resembling CAP-G2 (Ono et al., 2003) suggesting that either condensin II in *Drosophila* differs from condensin II of other organisms, lacking CAP-G2 equivalent or with a distinct yet unidentified CAP-G2 protein, or, alternatively, that a fully autonomous condensin II complex might not exist in this organism. All these observations together with the dynamic behavior of condensin I reported in this chapter suggest that in *Drosophila* condensin I is the major complex required for mitotic chromosome organization. However, future analysis on the

putative condensin II non-SMC subunits will clarify what is the exact role, if any, of this second condensin complex in mitotic chromosome structure in *Drosophila*.

The *in vivo* analysis of Barren-EGFP association with mitotic chromosomes together with simultaneous visualization of the centromere marker Cid-mRFP, allowed for the first time the analysis of the early stages of accumulation of this condensin I-specific subunit relative to a particular chromosomal region, the centromeres. This analysis revealed that during prophase, Barren-EGFP accumulated preferentially at the centromeric region and only later is detected at significant levels at chromosome arms. Supporting this observation is the fact that in hypomorphic mutants of *DmSMC4*, endogenous Barren only appears associated with the centromere of mitotic chromosomes (Steffensen et al., 2001). Furthermore, targeting of condensin I to the centromeres might be augmented by the reported interaction of the non-SMC condensin CAP-G with Cid (Jäger et al., 2005). This spatially ordered pattern of Barren-EGFP chromatin association, from the centromeres towards the arms, strongly suggests that the establishment of higher order levels of chromatin organization, involving condensin I, occurs as a sequential process. Since the chromosomal "scaffold" has been shown to be helical shaped (Boy de la Tour and Laemmli, 1988) and immunofluorescence studies directly on condensin further revealed an axial helical localization (Kireeva et al., 2004; Steffensen et al., 2001), the establishment of a regular helical coil would be facilitated if its folding occurs in an ordered sequential manner. This ordered accumulation of condensin I from the centromere towards chromosomal arms resembles the sequential phosphorylation previously reported for Histone H3 (Hendzel et al., 1997). Even though the exact role of Histone H3 phosphorylation in chromosome condensation is highly controversial, it has been proposed that this post-translational modification might act on the recruitment of condensation factors. Interestingly, it has been reported that depletion of Aurora B leads to a decrease in Histone H3 phosphorylation levels and a decrease in condensin loading in both *Drosophila* (Giet and Glover, 2001) and *C. elegans* (Hagstrom et al., 2002; Kaitna et al., 2002). Taken together, these observations suggest that loading of condensin I and Histone H3 phosphorylation might be mechanistically coordinated.

Early studies on the organization of mitotic chromosomes suggested that sister chromatids might be organized around a protein-based structure that was called the "scaffold" (Earnshaw and Laemmli, 1983). Subsequent studies identified Topoisomerase II (Earnshaw et al., 1985; Gasser et al., 1986) and the condensin complexes (Saitoh et al., 1994) as integral components of this axial structure. These studies suggest that the scaffold could be a network

of binding sites to which chromatin loops are attached underlying some of the peculiar properties of mitotic chromosomes. To gain more insight into the nature of this axial structure, detailed dynamic analysis must be performed. Dynamic studies on Topoisomerase II surprisingly revealed that this enzyme could exchange dynamically between chromatin-bound and free cytoplasmic pools (Christensen et al., 2002; Tavormina et al., 2002). Accordingly, the dynamic properties of condensin I in *Drosophila* were evaluated. FRAP analysis revealed that Barren-EGFP turns over rapidly after it associates with mitotic chromosomes. The majority (~84%) of Barren-EGFP molecules that are bound to mitotic chromosomes can exchange dynamically with the cytoplasmic pool. This findings are in agreement with what has been very recently reported for condensin I in HeLa cells, where 83% of condensin I was shown to be mobile (Gerlich et al., 2006a). This study as also demonstrated that in contrast to condensin I, condensin II complex displays a rather stable association with chromatin during mitosis. However, unlike in HeLa cells where condensin I was shown to exchange with a half-life of approximately 3.5 minutes, in *Drosophila* syncytial mitotic chromatin condensin I exchanges faster with a half-life of about 2.0 minutes. The faster recovery rates obtained for *Drosophila* syncytial divisions might arise from a need for faster changes in chromosome architecture, due to the rapid embryonic syncytial divisions. In mitosis 12 prometaphase takes on average 2.65 ± 0.22 min (n=10), an incredibly short time to complete chromosome congression when compared with HeLa cells which spend 25 min in prometaphase (Meraldi et al., 2004).

Current models for condensin function propose that condensin acts on mitotic chromosomes through the imposition of superhelical tension and/or the formation of chiral loops directly on the DNA molecule where the loops might then be trapped within condensin complex. Higher levels of organization would be achieved by protein-protein interactions of condensin complexes trapped at distinct chromosomal sites (reviewed by Hirano, 2006). The dynamic behavior observed in *Drosophila* (reported here) and in human cells (Gerlich et al., 2006a) is inconsistent with a model in which condensin I associates through static topological embracement of DNA. In this respect, condensin is clearly different from the cohesin complex which, although it has a comparable overall structure, is thought to hold sister chromatids within a rather stable protein ring (Gerlich et al., 2006b; Haering et al., 2002). These results support that condensin I helps to form and maintain a highly dynamic structural axis of mitotic chromosomes in which subunits are constantly being exchanged between the chromatin bound and the free cytoplasmic pool. A highly regulated process, in which

exchange of condensin subunits at one site would prevent exchange at adjacent sites, together with the existence of a immobile fraction (~16% in the experimental conditions used, but that might change during condensation process) could cooperate in the establishment and maintenance of a stable chromosomal structure.

The dynamic behavior of condensin I (Gerlich et al., 2006a and this study), together with the dynamic properties previously reported for topoisomerase II (Christensen et al., 2002; Tavormina et al., 2002), reveal that the chromosomal scaffold is very dynamic in nature. Interestingly, both the bending and elastic properties of mitotic chromosomes have been reported to be inconsistent with a rigid proteinaceous scaffold (Poirier and Marko, 2002). A highly dynamic rather than a static scaffold could in principle act as a structural backbone that reduces resistance by allowing continuous changes in shape as the chromosome binds microtubules and is moved within the cytoplasm during the complex events that take place during mitosis.

Previous observations have suggested that the condensin complex is pre-assembled before chromatin association, since the entire 13S particle is the major form of condensin when immunopurified from mitotic soluble extracts (Hirano et al., 1997). Additionally, immunoprecipitation experiments using extracts from early *Drosophila* embryos have also demonstrated that all condensin I can be co-immunoprecipitated as a complex (Savvidou et al., 2005). Thus, the dynamic behavior reported in this study using a functional Barren-EGFP protein very likely reflects the dynamics of the entire condensin I complex. However, it would be interesting to compare data from different subunits using the same methodology to verify whether the dynamic behavior reported for Barren-EGFP is observed for the entire complex or, alternatively, different condensin subunits display distinct dynamical properties once bound to mitotic chromosomes.

Chapter 3

Preliminary studies on the Condensin II Complex of *Drosophila melanogaster*

1. Introduction

The canonical condensin I complex was thought for many years to be the central player known in mitotic chromosome structure. However, recently a second condensin complex, named condensin II, was identified in vertebrate cells (Ono et al., 2003; Yeong et al., 2003). In vertebrate cells, the two condensin complexes were reported to have distinct contributions to mitotic chromosome architecture. Accordingly, specific depletion of condensin I was shown to originate "swollen" chromosomes, with some resolution of the sister chromatids and axial distribution of the condensin II specific subunits at the chromatid core. In the absence of condensin II the chromosomes acquire a "curly" configuration and condensin I specific subunits are found to be distributed along the chromosome axis. Chromosomes depleted of both condensin complexes show a very severe morphological defect appearing "fuzzy" with no apparent resolution of chromosome arms. The results presented in chapter 1 of this thesis, indirectly suggested that in *Drosophila*, condensin I is the major condensin complex involved in mitotic chromosome organization since the morphological defects associated with depletion of condensin I resemble those observed after depletion of both condensin I and II complexes in vertebrate cells. In addition, the dynamic localization of condensin I presented in chapter 2 suggests that condensin I participates in the initial steps of chromosome condensation during prophase, a feature attributed to condensin II complex in vertebrate cells. All together, these results strongly support the possibility that condensin I is the major condensin complex involved in mitotic chromosome structure in *Drosophila*. To directly test this, analysis of the role of the putative condensin II complex specific subunits in mitotic chromosome structure in *Drosophila* must be performed.

The results presented in this chapter report a preliminary characterization of the condensin II specific subunit, DmCAP-H2. Even though not fully conclusive, the results strongly support that DmCAP-H2 is not required for mitotic chromosome organization and appears to be involved in other aspects of chromatin organization, namely in meiotic chromosome segregation and interphase chromatin structure in polyploid cells.

2. Results

2.1 The *DmCAP-H2* gene

In order to address whether condensin II complex exits in *Drosophila* and which is the distinct contribution of the two condensin complexes for mitotic chromosome organization, the role of the protein encoded by the gene CG14685 was characterized. This gene was previously reported to code for the *Drosophila* kleisin-β homologue of human hCAP-H2 (Ono et al., 2003; Schleiffer et al., 2003). Therefore it will be called *DmCAP-H2* hereafter.

This gene is located in the third chromosome (3R) at cytological region 86C5-86C6. The flybase map of this chromosomal region is depicted in Fig. 3.1. Four possible transcripts and their correspondent proteins have been predicted. The four putative isoforms are very similar with a significant difference at the N-terminus. Isoforms A and B start at the initiation codon located within the first exon whereas isoforms C and D start at an alternative initiation codon (fourth exon), giving rise to an approximately 180 a.a. shorter protein. Isoform D diverges at the C-terminus. Since a cDNA with the longer transcripts is not available, all the following experiments were performed using a cDNA that encodes a smaller predicted protein (DGC:SD09295; codes for isoform C).

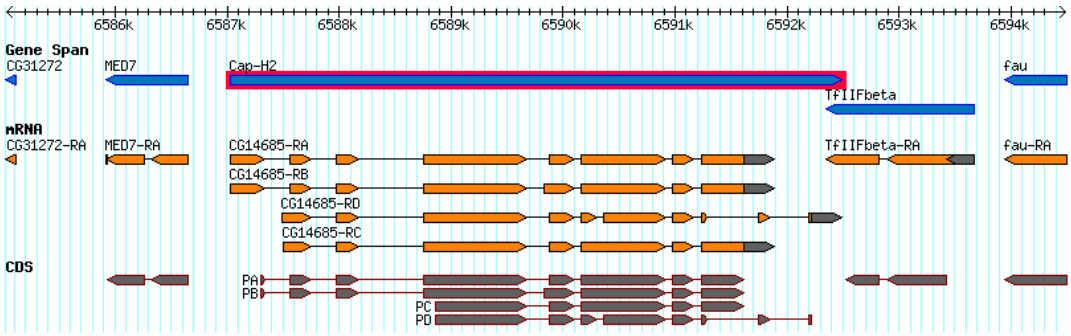

Figure 3.1. Map of genomic region that contains the *DmCAP-H2*/CG14685 gene. Graphic represents the gene (in blue) and four predicted transcripts (middle panel, depicted in orange). The four distinct transcripts give rise to four putative protein isoforms (lower panel, depicted in grey). Adapted from FlyBase (http://flybase.bio.indiana.edu/)

2.2 Production of EGFP-tagged DmCAP-H2 fusion proteins

In order to investigate whether DmCAP-H2 is able to localize at mitotic chromosomes, DmCAP-H2(PC) constructs fused to EGFP at both C- and N- termini were produced and its localization was evaluated using transient transfection of S2 *Drosophila* tissue culture cells (Fig. 3.2). Both fusion proteins were shown to localize within the nucleus during interphase, however, neither showed any accumulation to mitotic chromosomes.

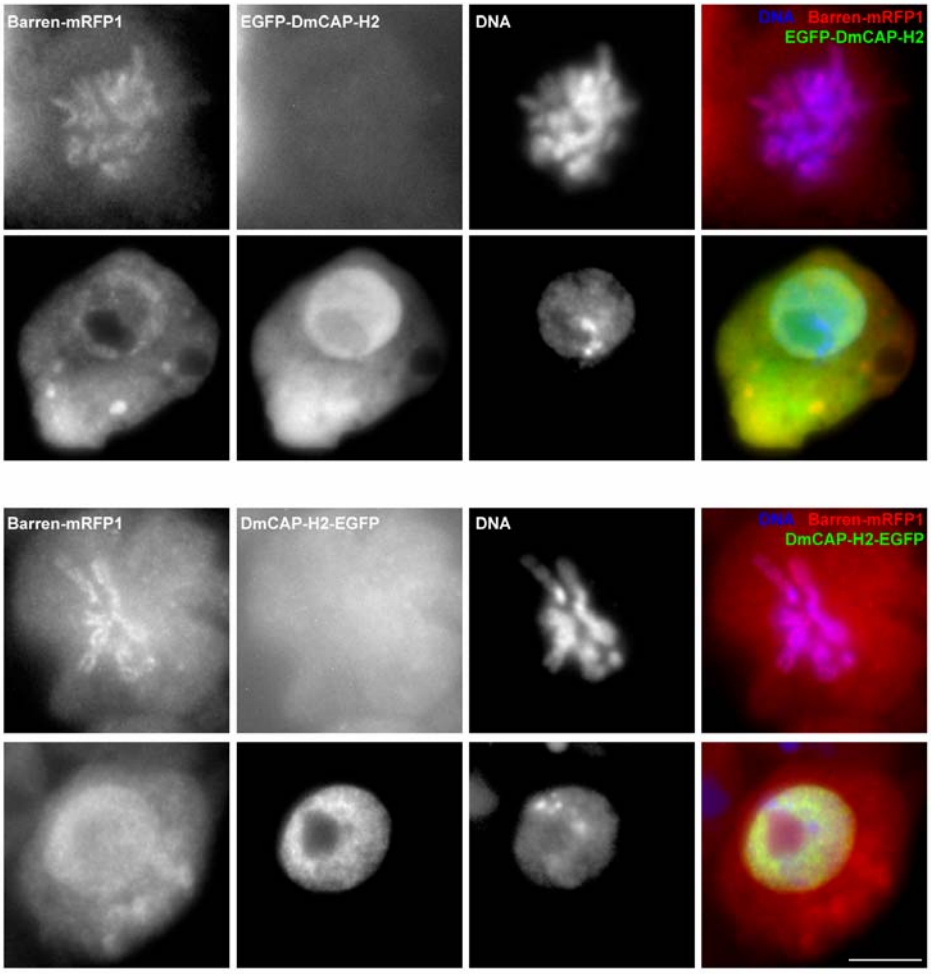

Figure 3.2. Transient transfection of Barren-mRFP1 together with either EGFP-DmCAP-H2 or DmCAP-H2-EGFP. In contrast to Barren-mRFP1, none of the DmCAP-H2 constructs shows any particular localization to mitotic chromosomes. During interphase, DmCAP-H2 is predominantly nuclear whereas Barren-mRFP1 appears distributed between the nucleus and the cytoplasm. Scale bar is 5 μm and applies to all images.

Condensin II has been proposed to have a minor role during early development and be more important in somatic cell divisions (Ono et al., 2003). Taking into account that S2

Drosophila cells are embryonic derived, transgenic flies expressing *DmCAPH2(PC)-EGFP* were produced, aiming to study the protein localization at later developmental stages. *DmCAPH2(PC)-GFP* construct was subcloned into a pUASP vector that was used for P-element germline transformation. Five different lines were obtained and the insertions were mapped to either the second or the third chromosomes. When the expression was driven in neuroblasts (*MZ1061-GAL4* driver, a neuroblast specific driver, kindly provided by J. Urban), no accumulation in mitotic chromosomes was observed (data not shown).

Taken together, these results suggest that the protein encoded by the CG14685 gene does not accumulate at condensed chromosomes during mitosis. However, the ~180 a.a. at the N-terminus absent in this shorter isoform could be crucial for protein function or even fusion with EGFP could give rise to a non-functional protein. Therefore, these results are not fully conclusive.

2.3 Production of DmCAP-H3 antibody

Since the results obtained with the EGFP tagged versions of DmCAP-H2 were unable to unequivocally determine the localization of the protein during mitosis, the subsequent approach was the production of a specific antibody. In order to do so, a histidine-tag was fused to the first half of the protein (a.a.1-419). When expressed in *E. coli*, this fusion protein is found in the insoluble fraction of the total bacterial protein extract (Fig. 3.3a). The inclusion bodies were solubilized and recombinant protein was purified over a Ni^{2+} column (Fig. 3.3b). Even though the predicted size of the DmCAP-$H2_{1-149}$-$(His)_6$ is 52 KDa, this protein was observed to run at higher molecular weight (~65KDa), possibly due its low isoelectric point (pI=4.99).

The purified protein was then used to immunize four different rats. The four serums obtained were found to efficiently detect the purified His-tagged protein (example of serum #4 in Fig. 3.4a). This antibody was shown to be quite sensitive allowing the detection of as little as 0.5 ng of protein. Moreover, the serum is also able to detect the EGFP-tagged protein when ectopically expressed in *Drosophila* ovaries (Fig. 3.4b, last lane). This DmCAP-H2-EGFP fusion protein should run at ~ 110 KDa but displays reduced electrophoretic mobility.

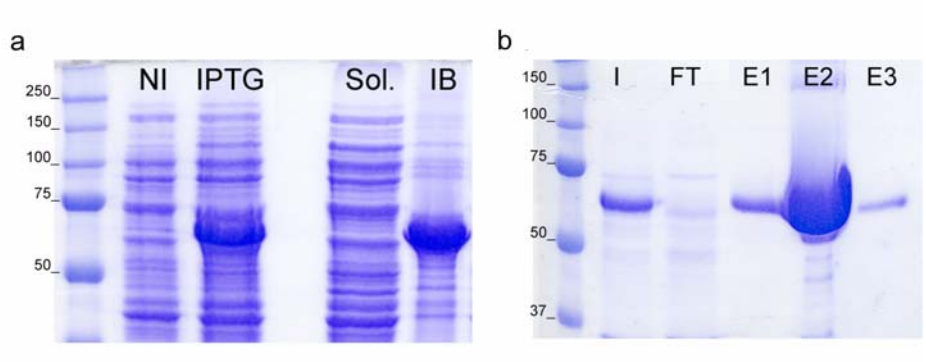

Figure 3.3. DmCAP-H2 $_{1\text{-}149}$-(His)$_6$ protein expression and purification. a) Coomassie staining showing *E. coli* extracts before protein expression induction (NI); after protein induction (IPTG); soluble proteins of the induced extract (Sol.) and proteins found in inclusion bodies (IB) **b)** Protein purification using a HiTrap Quelating Column. 10 µl of each sample were loaded on the gel from a total 30 ml input (I) and corresponding flow through (FT). Purified protein was collected in 1 ml sequential elutions (E).

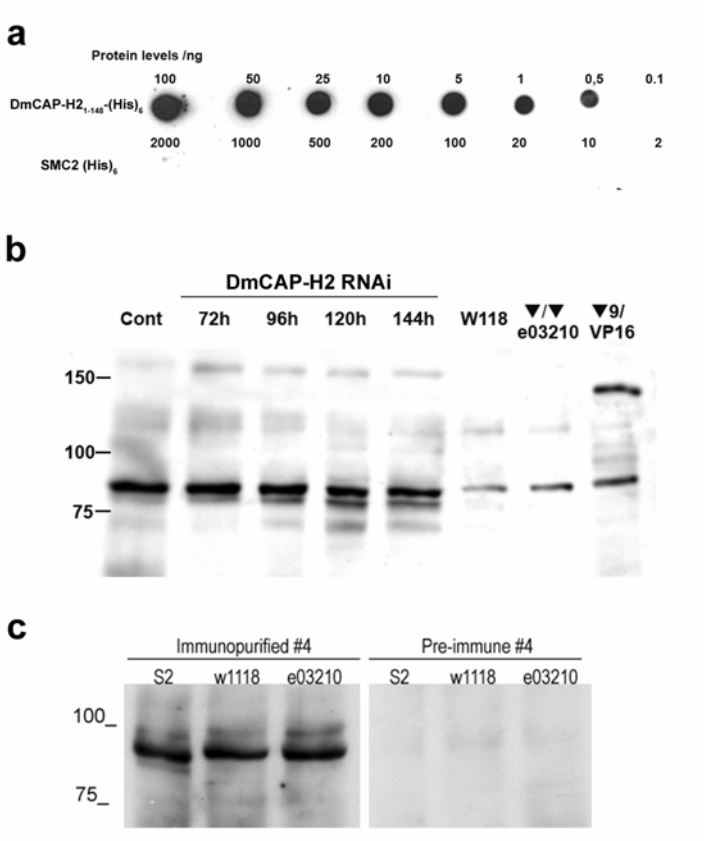

Figure 3.4. Analysis of the anti-DmCapH2 antibody. a) Spot-blot analysis with serial dilutions of purified DmCAP-H2$_{1\text{-}149}$-(His)$_6$ protein used for rats immunization (upper lane) and serial dilutions of SMC2-(His)$_6$ used as negative control (lower lane). The protein was detected using anti-DmCapH2 serum from rat #4 at 1:500 dilution. **b)** Western blot analysis of S2 cells (Lanes 1-5) and flies ovaries (lanes 6-8). Lanes 2-5 correspond to S2 cells treated with dsRNA specific of DmCapH2 at different time points after dsRNA addition; lane 7 is a sample of ovaries from adult females homozygous for a piggyBac insertion on CG14685 gene (*e03210*); lane 8 is a sample from *α-4tub-GAL4-VP16* driven expression of a UASP-EGFP-DmCapH2 construct (line 9). **c)** Western blot analysis of S2 cells and flies ovaries (from *w1118* and *e03210* homozygous females), using immunopurified and pre-immune serums from rat #4.

The serum #4 was also shown to recognize a protein band of about 80 KDa, not detected by the other three serums (Fig. 3.4b). However, this band is unlikely to be the endogenous DmCAP-H2 protein since it is still observed at the same quantitative levels on a putative mutant for this protein (see details in the next section) and also on S2 cells treated with dsRNA for this protein (Fig. 3.4b). Moreover, the predicted sizes of the isoforms A and B are 108 KDa and 110 KDa respectively, whereas the shorter isoforms should have 88 KDa (PC) and 78 KDa (PD) in weight. Thus, keeping in mind the reproducible reduced electrophoretic mobility observed in tagged versions of this protein, a band at ~80 KDa does not correspond to any of the isoforms of the endogenous protein. Nevertheless, this band is still preserved after immunopurification of the serum against the fusion protein and is not observed in the preimmune serum (Fig. 3.4c) which suggests that most likely this ~80 KDa protein shares some epitopes with DmCAP-H2. No specific staining was obtained using this or any of the other serums in immunofluorescence on S2 cells (data not shown) and no other specific band was recognized by these serums, suggesting that the endogenous protein levels are probably very low.

Analysis of several databases available on the web also point towards a very low expression of *DmCAP-H2* gene. Microarray expression profiles reveal that DmCAP-H2 and also the putative DmCAP-D3 condensin II specific subunit, are not expressed in S2 cells (nor in other *Drosophila* cell types analyzed) in contrast to all other condensin I subunits (http://flight.licr.org/). Nevertheless, these proteins must be transcribed in S2 cells, since several ESTs corresponding to the respective genes were obtained from S2 cDNA libraries (http://flybase.bio.indiana.edu/). Most likely, the expression levels are very low which could account for the failure to be detected by the microarray assays.

Additionally, RT-PCR analysis in the adult fly reveals that the corresponding transcripts of the putative DmCAP-H2 and DmCAP-D3 are not greatly detected in adult tissues (table 3.1) (http://flyatlas.org/). In contrast, all the condensin I subunits are highly transcribed, and are considerably up-regulated in the ovaries. As the first embryonic nuclear divisions depend upon maternally deposited material, virtually all proteins involved in the mitotic machinery are consistently highly enriched in ovaries at mRNA or protein levels.

Moreover, *in situ* analysis of the *DmCAP-D3* gene expression reports a very week/no signal throughout embryogenesis (http://fruitfly.org/cg1-bin/ex/insitu.pl). No *in situ* data for *DmCAP-H2* is yet available.

Table 3.1 – RT-PCR results from whole flies and specific adult tissues assays (from Fly Atlas: http://flyatlas.org/)

Tissue	mRNA signal[a]	Present Call[b]	Enrichment[c]	Affy Call
***DmCAP-H2* (condensin II)**				
Brain	82 ± 3	4 of 4	2.66	Up
Head	36 ± 5	4 of 4	1.16	None
Midgut	31 ± 2	4 of 4	1.01	None
Tubule	22 ± 1	4 of 4	0.73	Down
Hindgut	39 ± 1	4 of 4	1.27	Up
Ovary	41 ± 1	4 of 4	1.33	Up
Testis	30 ± 0	4 of 4	0.99	None
Whole fly	30 ± 1	4 of 4	-	
***DmCAP-D3* (condensin II)**				
Brain	9 ± 0	4 of 4	2.17	Up
Head	6 ± 1	3 of 4	1.55	None
Midgut	2 ± 1	0 of 4	0.66	None
Tubule	2 ± 0	0 of 4	0.50	Down
Hindgut	3 ± 0	1 of 4	0.77	None
Ovary	2 ± 0	0 of 4	0.49	None
Testis	7 ± 1	2 of 4	1.71	None
Whole fly	4 ± 0	1 of 4	-	
***Gluon/DmSMC4* (condensin I and II)**				
Ovary	338±8	4 of 4	3.11	Up
Whole fly	108±11	4 of 4	-	
***DmSMC2* (condensin I and II)**				
Ovary	233 ± 5	4 of 4	3.03	Up
Whole fly	77 ± 9	4 of 4	-	
***Barren/CAP-H* (condensin I)**				
Ovary	545 ± 9	4 of 4	2.13	Up
Whole fly	256 ± 6	4 of 4	-	
***CAP-D2* (condensin I)**				
Ovary	150 ± 8	4 of 4	2.81	Up
Whole fly	53 ± 8	3 of 4	-	
***CAP-G* (condensin I)**				
Ovary	223 ± 9	4 of 4	2.09	Up
Whole fly	106 ± 7	4 of 4	-	

a – mRNA signal values are expressed as mean ± SEM
b – Present call indicates how many of the four arrays for each sample gave a detectable expression
c – Enrichment represents the level of expression on a particular tissue normalized to the levels detected in the whole fly

2.4 Analysis of a putative *DmCAP-H2* mutant

To further analyze the function of this putative condensin II specific subunit, a stock from the Exelixis *Drosophila* stock collection containing a piggyBac insertion within the CG14685 gene was obtained. The insertion site is located within the third intron of the *DmCAP-H2*/CG14685 gene (Fig. 3.5).

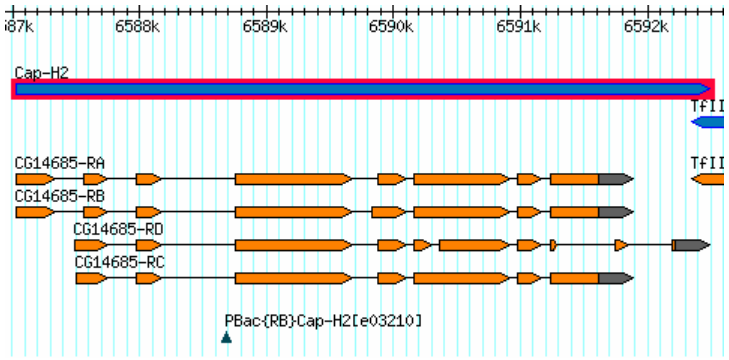

Figure 3.5. Cytological map of *DmCAP-H2*/CG14685 gene showing the insertion site of the PiggyBac element in the *e03210* allele. Graphic represents the gene (in blue) and four predicted transcripts (in orange). Green triangle depicts insertion site determined by sequencing analysis. Adapted from FlyBase (http://flybase.bio.indiana.edu/)

This mutant is mostly (90%) homozygous viable but *e03210/e03210* homozygous males are sterile and females exhibit reduced fertility. Male sterility is most likely correlated with meiotic defects detected in *DmCAP-H2* mutants (T. Hartl and G. Bosco, personal communication). On the other hand, the reduced fertility observed in homozygous females is probably related with the phenotype observed in the nuclear morphology of nurse cells. Whilst in control cells the DNA from nurse cells at advanced stages (e.g. stage 10) appears highly dispersed, in mutant cells the chromatin remains polytene with a well defined banding pattern (Fig. 3.6). During oogenesis in *Drosophila melanogaster*, 15 nurse cells, the mitotic sisters of the developing oocyte, synthesize most of the egg contents and transport them to the oocyte (reviewed by Spradling 1993). This massive transcriptional activity is achieved by a continuous growth accompanied by 10-12 endocycles. In contrast to most of *Drosophila* polyploid cells (e.g. polytene chromosomes in the salivary glands), which retain a constant chromosome morphology throughout the endocycles, the chromatin of nurse cells undergoes a programmed structural alteration. They retain polytene structure in stage 2-4 egg chambers but usually dissociate during stage 4 and 5, after which polytene structure is no longer visible

(Painter and Reindorp 1939; Hsu and Hansen 1953; Brun and Chevassu 1958). The phenotype observed in *e03210/e03210* mutants clearly suggests that the dispersal process does not take place, and polytene chromosome structure is still preserved at later developmental stages of egg chamber development. Up to date, the mechanisms that mediate chromosome dispersion of nurse cells nuclei during oogenesis is still not understood but this result indicates that this might be a DmCAP-H2-, and possibly condensin II- dependent process.

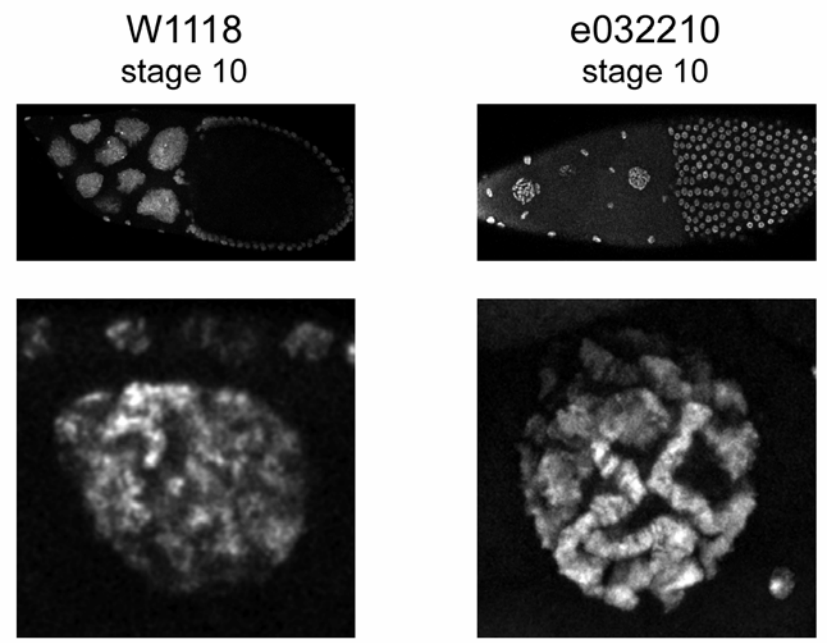

Figure 3.6. Analysis of the nuclear morphology in nurse cells from *DmCAP-H2*/CG14685 mutant females. Top images show Hoechst-stained stage 10 egg chambers from wild-type (left) and *e03210/e03210* homozygous females (right). Lower images show the nuclear morphology of single nuclei revealing a well defined polytene structure in the mutant cells.

Detailed observation of mitotic cells showed that the mutation did not cause any mitotic abnormality in third instar larvae (Fig. 3.7). Orcein-stained brain squashes reveal that chromosome condensation occurs normally in neuroblasts from the putative *DmCAP-H2* mutant. Therefore, contrary to studies in vertebrate cells, which revealed that prophase chromosome condensation was severely affected in the absence of condensin II subunits (Hirota et al. 2004; Ono et al. 2004), prophase chromosomes in neuroblasts from *e03210/e03210* larvae appear well condensed and two sister chromatids can be clearly observed.

.

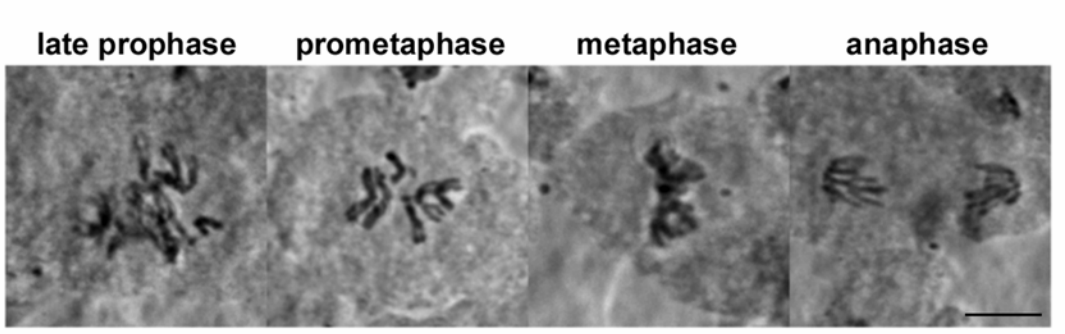

Figure 3.7. Analysis of mitotic figures in *DmCAP-H2* mutant third instar larval brains. Orcein-stained brain squashes from third instar larvae (*w;; e03210/e03210*) No mitotic defects could be observed and chromosome condensation appears normal. Scale bar is 5 µm.

2.5 DsRNA interference of DmCAP-H2 in S2 cells

To further analyze the role of DmCAP-H2, the protein was depleted from S2 cells using dsRNA interference. In order to validate protein depletion in the RNAi experiment, an indirect approach was used since the polyclonal antibody raised against DmCAP-H2 was unable to recognize endogenous protein in S2 extracts. Accordingly, S2 cells were co-transfected with pUASP-DmCAP-H2-EGFP and pW8-GAL4, to achieve a constitutive transient transfection. Five days after transfection the culture was diluted and dsRNA was added. 96h after dsRNA addition, depletion of ectopically expressed DmCAP-H2-EGFP was monitored by western blot using an antibody that specifically recognizes EGFP (Fig. 3.8).

Indeed, whereas control cells (no dsRNA added) show expression of DmCAP-H2-EGFP, this protein is virtually undetectable in dsRNA-treated cells. Cells transfected with pUAST-EGFP and pW8-GAL4 were also analyzed to ensure that protein depletion does not result from knock down specific of the EGFP tag. These results clearly indicate that DmCAP-H2-EGFP is efficiently depleted during the RNAi experiment which strongly suggests that the endogenous protein is also down-regulated.

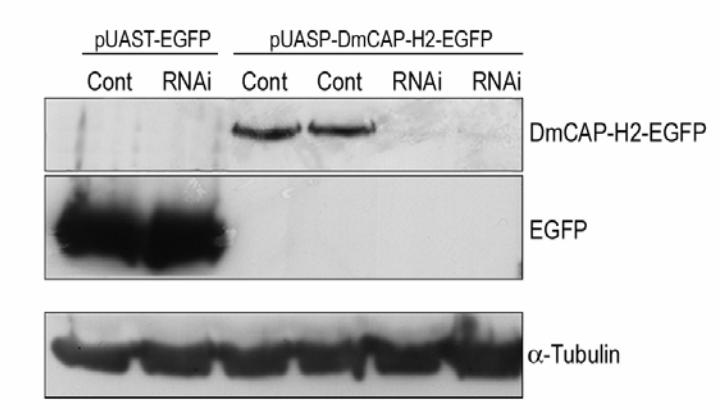

Figure 3.8. Analysis of DmCAP-H2-EGFP depletion after dsRNAi. Control (C) and CAP-H2 dsRNA-treated (R) cells from cultures previously transfected with either pUAST-EGFP (lanes 1 and 2) or pUASP-DmCAP-H2-EGFP (lanes 3 to 6). Levels of EGFP and DmCAP-H2-EGFP were monitored using an anti-GFP antibody. α-tubulin was used as loading control. Each lane corresponds to $5x10^5$ cells.

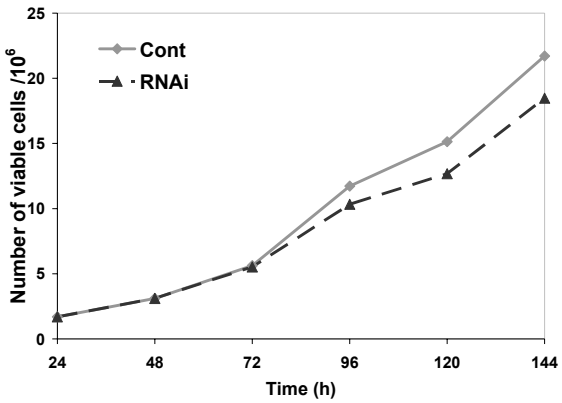

Figure 3.9. Proliferation profiles of control and DmCAP-H2 depleted cells. Growth curves of control and DmCAP-H2-RNAi- treated cells throughout the time course of the experiment. DmCAP-H2-RNAi treated cells grow less than control cells.

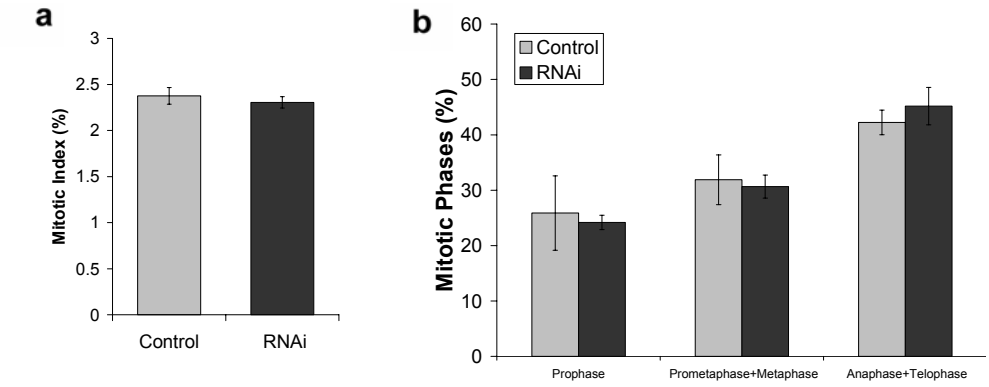

Figure 3.10 – Mitotic progression of control and DmCAP-H2 depleted cells (96h). Quantifications were performed using α-tubulin/PH3 double straining. Approximately 9.000 cells were counted for each experimental condition. Graphic shows average of quantifications from three different slides and error bars are SD. **a)** Mitotic index was calculated over the total number of cells; **b)** Percentage of cells at each mitotic phase was calculated over the total of mitotic phases.

DsRNA treated cells grew slightly slower than controls (Fig. 3.9) suggesting that DmCAP-H2 might be required for normal cell proliferation. However, there are no differences in the mitotic index or in the percentage of cells at each mitotic phase between control and DmCAP-H2-RNAi cells (Fig. 3.10). Moreover, no significant mitotic defects could be observed. In particular, chromosome morphology in DmCAP-H2 depleted cells appeared as normal as in the control situation (Fig. 3.11) and only a small percentage of cells showed chromatin bridges in the later stages of mitosis (16 ± 5%, compared to 12 ± 8% observed in control cells). These results suggest that condensin II plays a minor, if any role in mitotic chromosome structure in *Drosophila* tissue culture cells.

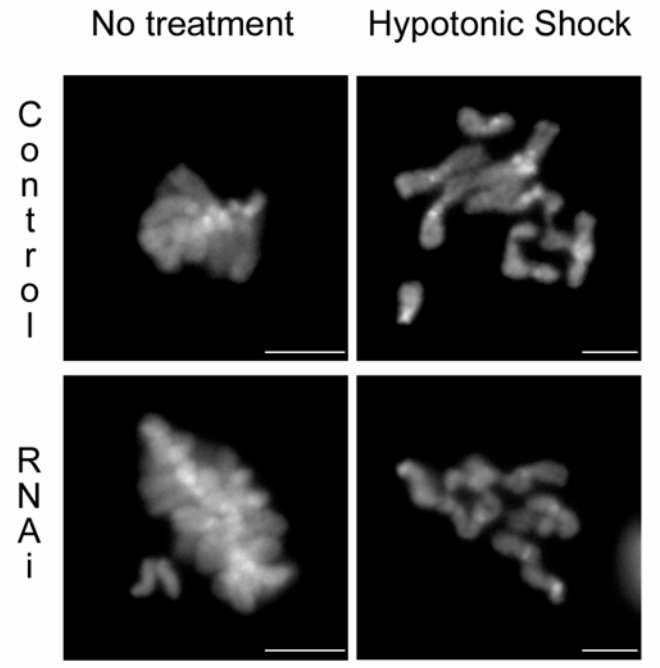

Figure 3.11 – Analysis of chromosome morphology in control and DmCAP-H2-RNAi cells. Cells were either directly fixed (no treatment) or incubated with 0.1% sodium citrate hypotonic solution for 10 seconds prior to fixation (hypotonic shock). No chromosome structure defects could be detected in both situations. Scale bars are 5 μm.

3. Discussion

Previous studies have indicated that vertebrate cells contain two condensin complexes (condensin I and condensin II) that contribute distinctly to chromosome condensation (Ono et al., 2003; Yeong et al., 2003). The specific role of the canonical condensin I complex in *Drosophila* chromosome structure has been already expensively studied (Dej et al. 2004;

Savvidou et al. 2005; results presented in chapter 1) but the contribution of the putative condensin II complex in this model organism remains to be determined. Homologues for two condensin II-specific subunits (CAP-D3 and CAP-H2) were found in *Drosophila* but not for CAP-G2 (Ono et al., 2003). Accordingly, in order to analyze the role of the putative condensin II complex in mitotic chromosome structure, the function of DmCAP-H2 was studied.

The results reported in this chapter, although yet preliminary, strongly suggest that the putative condensin II subunit DmCAP-D2 does not have a major role in the assembly or maintenance of mitotic chromosomes. EGFP-tagged versions of one of the predicted isoforms (PC) are unable to accumulate at chromosomes during mitosis. Moreover, antibodies raised against DmCAP-H2 are able to recognize purified protein and ectopically expressed versions of the protein but fail to detect endogenous DmCAP-H2 both in immunofluorescence and western blot analysis. This later result strongly supports that expression levels of DmCAP-H2 might be extremely low, which is further confirmed by expression analysis revealed by public data bases. Thus, if condensin II does exist in *Drosophila*, it must have a minor role in mitotic chromosome structure when compared to condensin I since in contrast to condensin II subunits, all the condensin I proteins are very abundant in highly proliferative tissues and in the adult ovary, a common feature of the major components of the mitotic machinery.

Importantly, no mitotic alterations or chromosome morphology phenotypes were detected in either the putative *DmCAP-H2* mutant or S2 cells depleted of DmCAP-H2. In addition, we found no alteration in chromosome segregation when compared to control cells. These results are in contrast to what has been reported in vertebrate cells where condensin II depletions results in abnormally “curly” shaped chromosomes and anaphase and telophase chromatin bridges are often observed (Ono et al. 2003; Hirota et al. 2004; Gerlich et al. 2006a).

All together, these results raise reasonable doubts regarding a possible role of DmCAP-H2 in mitosis. Thus, condensin I appears to be the only condensin complex involved in mitotic chromosome organization during mitosis in *Drosophila melanogaster*.

Indeed, analysis of the line carrying an insertion in the gene encoding the DmCAP-H2 protein suggests that if condensin II really exists in flies it is likely to be involved in other types of chromatin organization namely in the structure of meiotic chromosomes and the structure of chromatin in polyploid cells.

Homozygous *DmCAP-H2* mutants are viable but male sterile. Chromatin bridges are observed during anaphase I in male meiosis which might be explained by failures in the separation of homologous pairing (T. Hartl and G. Bosco, personal communication). This would be consistent with polytene chromosomes found in ovarian nurse cells. Moreover, chromatin organization defects were also found in this mutant during pre-meiotic G2 phase. In wild type, three "chromosome territories" are usually formed (two of these correspond to the second and the third chromosomes whereas the third territory is composed of the fourth and sex chromosomes) (Hawley 2002). In contrast, in male sterile *DmCAP-H2* mutants, these territories are never observed during G2 and prophase I but chromatin appears normally condensed at metaphase I (T. Hartl and G. Bosco, personal communication).

The second most striking phenotype of *DmCAP-H2* mutants is the morphology of ovarian nurse cells chromatin. Instead of dispersing their polytene structure at stage 4-5, chromosomes retain the polytene configuration up to later stages in oogenesis. This strongly suggests that *DmCAP-H2,* and possibly condensin II, is involved in the process that triggers the disassembly of the pairing of the sister chromatids. It remains to be determined what are the mechanisms involved in the establishment of polytene structure and the programmed disassembly of this pairing in ovarian nurse cells. It has been recently suggested that these changes in the structure of chromatin occur under cell cycle control and that the state of chromatin organization (polytene, blob-like or dispersed) is correlated with particular phases of nurse cell endocycle (Dej and Spradling 1999). However, the molecular mechanisms underlying this structural chromatin change are far from being understood. Other mutants have been previously shown to display this persistent polytene chromatin structure in ovarian nurse cells. The most well studied examples are the *ovarian tumor (Otu)* differentiating mutants (King et al. 1981). *Fs(2)B* mutants are also a classical example of persistent polytene organization of nurse cells chromatin (Koch and King 1964). More recently, *fs(2)cup* has also been implicated in the polytene dispersal and proposed to act together with *otu* and *fs(2)B* in a common cytoplasmic pathway with multiple functions during oogenesis, including nurse cells chromatin reorganization (Keyes and Spradling 1997).

Other genes like *Hrb27C*, *Squid (Sqd)* and *half pint (hfp)* are also required for normal polytene chromosomes dispersal in ovarian nurse cells (Goodrich et al. 2004). However, their involvement might be indirect since they have been shown to be required for the accumulation of the isoform Otu104 (e.g. through involvement in the alternative splicing process) and this Otu isoform has been shown to be the one involved in polytene dispersal

(Steinhauer and Kalfayan 1992). So far, the characterization of these mutants has been mainly descriptive and it remains to be determined the molecular mechanisms that trigger this particular rearrangement of chromatin organization.

In contrast to all these mutants, which are usually female sterile (unless in interallelic combinations), homozygous *DmCAP-H2* mutant females are fertile. This difference might be related with the fact that some of these genes have multiple functions throughout oogenesis such as cyst development, trafficking of microtubule-associated vesicles, transfer of the contents of the nurse cells into the oocyte and localization of *gurken (grk)* mRNA. Analysis of the *DmCAP-H2* mutant reveals that polytene structure of the nurse cells *per se* does not lead to female sterility. Nevertheless, these females have a reduced fertility which suggests that proper polytene dispersal, even though not absolutely required, might facilitate egg development. In fact, it has been described that polytene chromosomes show normal gene activity but some mRNAs are abnormally accumulated in the pseudonurse cell nuclei of *otu* mutants (Heino et al. 1995). If the same is true for *DmCAP-H2* mutants, this might account for the reduced fertility observed in homozygous females.

In summary, these results point towards a role of DmCAP-H2, and possibly condensin II, in the dispersal of chromosome pairing rather than in mitotic chromosome condensation.

PART III

GENERAL DISCUSSION

1. General Discussion

The ultimate goal of cell division is to segregate the genome equally between the resulting daughter cells. An essential step for accurate chromatid segregation is the proper assembly of interphase chromatin into well defined structures known as mitotic chromosomes. Every time cells enter mitosis, chromatin undergoes remarkable physical and topological changes as a result of a highly dynamic, yet poorly understood, process of chromatin condensation. Chromosome condensation serves distinct purposes essential for efficient mitosis. Firstly, it physically compacts interphase chromatin making cell division feasible within the cell space. Secondly, it removes topological links between different chromosomes (individualization) and between sister chromatids (resolution) that naturally arise during interphase. Finally it ensures that chromosomes acquire proper rigidity/flexibility balance that enables them to sustain all the movements that take place during their segregation.

How the organization of metaphase chromosomes is achieved and maintained remains a major puzzle in Cell Biology. Several models for chromosome assembly have been proposed but the folding path of the chromatid fibers within a chromosome remains still to be unveiled. Additionally, several proteins and protein modifications have been implicated in chromosome assembly but the molecular mechanisms underlying their involvement is also far from being understood.

The work presented in this thesis aimed to characterize the role of condensin I complex in the process of mitotic chromosome condensation using *Drosophila melanogaster* as a model system. In addition to a functional analysis based on the phenotype associated with condensin I depletion, further insights into the molecular mechanisms in which condensin might be involved were obtained from the live analysis of the association of condensin I during the cell cycle.

It is consensual that condensins are central players in the proper organization and segregation of mitotic chromosomes. However, it is still a matter of debate whether condensins *per se* drive mitotic chromosome compaction or are uniquely involved in the resolution (untangling) of the sister chromatids. The first functional analysis using immunodepletion studies in *Xenopus* egg extracts led to the proposal that condensins are required for chromosome assembly, since unreplicated sperm chromatin is unable to be

converted into rod shaped chromosome-like structures in the absence of the condensin complex (Hirano et al. 1997). However, subsequent studies in several organisms have shown that the recurring phenotype for condensin-depleted cells is compromised lateral structural integrity with tangled sisters but not longitudinally extended mitotic chromosomes (Steffensen et al. 2001; Hagstrom et al. 2002; Hudson et al. 2003). The results presented in this thesis (chapter 1) further support these observations. In the absence of condensin I subunit Barren/CAP-H, chromosomes are able to shorten along their longitudinal axis but fail to resolve sister chromatids which leads to severe segregation defects. Thus, condensins are unlikely to be involved in the longitudinal compaction of mitotic chromosomes, as initially proposed, which suggests the existence of a yet undiscovered molecular mechanism driving chromosome condensation.

The recent identification of a condensin II complex in vertebrate cells and *Xenopus* eggs (Ono et al. 2003; Yeong et al. 2003) adds a new player in the mitotic chromosome assembly process. In vertebrate cells, condensin I and II complexes were shown to distinctly contribute to the structure of the metaphase chromosome (Ono et al. 2003; Hirota et al. 2004). In contrast, the results presented in this thesis provide compelling evidence that condensin II is not involved in mitotic chromosome structure in *Drosophila melanogaster*. Chromosome morphological defects associated with condensin I depletion from *Drosophila* S2 cells (chapter 1) resemble those associated with depletion of both condensin complexes in vertebrate cells (Ono et al. 2003; Hirota et al. 2004) and are indistinguishable from those reported after depletion of DmSMC4 in *Drosophila* (Coelho et al. 2003), a subunit shared by both complexes. In particular, in the absence of condensin I the two sister chromatids fail to resolve and the heterodimer SMC4/2, although still associates with chromatin, is unable to localize to a well-defined central axis. Moreover, the results presented in chapter 2 of this thesis clearly demonstrate that condensin I starts to associate with chromatin during prophase at the same time as chromosome condensation is initiated. This finding is in contradiction to what has been reported in vertebrate cells, where condensin II is the only condensin complex involved in chromatin organization during prophase and condensin I only associates with chromatin after nuclear envelope breakdown (Hirota et al. 2004; Ono et al. 2004; Gerlich et al. 2006a). More direct evidence comes from preliminary studies on the function of the putative *DmCAP-H2*, a condensin II-specific subunit (chapter 3). This low abundant protein does not localize at mitotic chromosomes and analysis of a *DmCAP-H2* putative mutant and S2 cells depleted of DmCAP-H2 reveal that mitotic chromosome morphology is not affected.

Instead, DmCAP-H2 appears to be involved in the polytene structure disassembly in ovarian nurse cells and also in meiotic chromosome segregation. All together, these results support that condensin I is the major condensin complex in *Drosophila* involved in mitotic chromosome structure and the putative condensin II complex is very likely to be participate in other types of chromatin organization. Therefore, *Drosophila* might be seen as a unique system among higher eukaryotes that appears to rely solely on condensin I for mitotic chromosome organization. An important question follows this minimal requirement: why would higher eukaryotes evolve to have two condensin complexes? To address this issue, first the differential role of condensin II must be elucidated. It should be noticed that while condensin I depletion leads to severe defects in the lateral compaction and resolution of the sister chromatids, condensin II-depleted chromosomes have well resolved sister chromatids with an increased distance between sister chromatid arms (Ono et al. 2003). Thus, the function of condensin II in chromosome structure is clearly not additive to the one condensin I and therefore, its involvement might dictate species-specific differences in the process of mitotic chromosome assembly. It remains to be determined if condensin II displays the same enzymatic activities observed for condensin I and what is the exact contribution of condensin II for mitotic chromosome structure. Therefore, possible justifications for the different requirement for condensin I and II complexes in the process of chromosome assembly are so far merely speculative.

Nevertheless, there might be specific requirements for condensin II during different stages of embryonic development. Based on the different ratios between condensin I and condensin II in vertebrate tissue culture cells (1:1) and *Xenopus* egg extracts (5:1), it has been proposed that condensin I plays a major role during early embryonic divisions while the contribution of condensin II is more prominent in somatic cells (Ono et al. 2003). These different contributions might relate with differences in chromosome structure at different developmental stages. Indeed, chromosomes from early embryonic cells are known to be longer and thinner than those in somatic cells (Belmont et al. 1987) and to have different mechanical properties (Marshall et al. 2001; Poirier et al. 2002; Almagro et al. 2004).

An alternative simple explanation for the evolution of condensin II might be related with different genome sizes amongst different organisms. Species with reduced genome sizes like yeast, *Drosophila* and *C. elegans* use only one condensin complex (typically the canonical condensin I with exception of *C. elegans* that uses uniquely condensin II). In species with larger genomes, the DNA untangling process might be more demanding due to a

higher probability for chromatin entanglements. Therefore, condensin II might have evolved in these organisms to facilitate the assembly of mitotic chromosomes. Together with its identification, it has been proposed that condensin II evolved to provide chromosomes with an additional level of organization and rigidity (Ono et al. 2003). However, it was recently shown that condensin I, but not condensin II is required for chromosome stiffness at the centromeric region both in *Drosophila* and HeLa cells (chapter 1 and Gerlich et al. 2006a). Indeed, the results presented in chapter 1 showed for the first time that condensin I is required to maintain the structural rigidity of pericentromeric heterochromatin. The assay developed to study the stiffness of mitotic chromatin uses the natural force of the mitotic spindle which acts particularly on the centromeric region. Whether the stiffness of the arms of mitotic chromosomes lacking condensin I complex are also affected remains to be elucidated. Nevertheless, the pericentromeric chromatin rigidity is in this regard the more physiologically relevant chromosomal region in the sense that this region is subjected to both pulling and pushing forces exerted by the spindle during mitosis.

Studies in vertebrate cells have shown that condensins depletion affects kinetochore-spindle attachments (Ono et al. 2004). In contrast, our results show that in the absence of condensin I, centromeres are able to support the formation of functional kinetochores that attach normally to the mitotic spindle. However, chromosome congression is severely impaired. A plausible explanation relates with the excessive flexibility of the centromeric chromatin observed in condensin-I depleted chromosomes that might compromise bi-orientation on the mitotic spindle delaying metaphase alignment. In this way, condensin I depletion severely affects progression through mitosis.

Thus, the structural integrity of the pericentromeric region appears to be a pre-requisite for efficient mitosis. However, the molecular mechanism by which condensin I confers stiffness at the centromere remains to be unveiled. It is possible that condensin I has a particularly important role at the centromere since stronger attachments of the scaffold to centromeric chromatin are thought to take place (Bickmore and Oghene 1996; Aono et al. 2002; Sumer et al. 2003). Alternatively, a higher concentration of condensin might directly increase the rigidity of this region. In fact, it has been previously shown that condensins are enriched at the primary constriction (Steffensen et al. 2001). It is slightly counterintuitive that the highly dynamic condensin I (as revealed by FRAP analysis, chapter 2), would be involved in maintaining the rigidity of chromosomes. Interestingly, condensin II, which is not required for chromatin stiffness, is very stably associated with mitotic chromatin (Gerlich et al. 2006a),

implying that regardless of the mechanism used by condensin I to confer chromatin rigidity, it must be compatible with a highly dynamic process of exchange.

In contrast to its role in centromere rigidity, the dynamic exchange of condensin I subunits along chromosomal length might also confer flexibility to the chromosome allowing changes in shape throughout mitosis. If condensin I was not able to exchange dynamically the chromosome would be too stiff imposing severe resistance to the cytoplasm and limiting its mobility. By constantly making and remaking the structure of the mitotic chromosome through its high dynamicity, chromosomes might be continually remodeling their form to achieve the most favorable conformation that minimizes resistance during the movements of congression and segregation. Thus, these results point towards a new role of condensin I as a key regulator of the balance between rigidity/flexibility of the chromosome essential for efficient chromosome movement during mitosis.

A major problem in the understanding of the mechanistical aspects of condensin function in mitotic chromosome structure relates to the fact that the real nature of chromatin compaction is not yet well understood. It is not known whether the end-products of the enzymatic reactions carried out by condensins (e.g. supercoils, trefoils) are in fact intermediates of the chromosome condensation process. Moreover, up to date, no studies have yet clarified if condensin displays these activities *in vivo* and whether these activities are required for the chromosome condensation process. In addition, even though several models can be found in the literature, it is still unclear how sister chromatid fibers are folded and organized to assemble a metaphase chromosome. Thus, a more detailed description on both the chromatin assembly process and on the activity of condensin towards its natural subtract might in the future help to elucidate the assembly of mitotic chromosomes and how exactly condensins contribute to this process. Nevertheless, the analysis of the stability of condensin I-DNA association *in vivo* reported here brings new insights into the role of condensin I in chromosome condensation and raises reasonable doubts regarding many of the proposed molecular mechanisms for condensins function and chromosome assembly.

Most textbook models of mitotic chromosome structure present the scaffold/radial-loop model in which loops of 30 nm chromatin fibers are attached to an axial scaffolding structure. This model emerged when EM visualization of nuclease-digested and histone-depleted metaphase chromosomes, revealed that the insoluble residue retains the characteristic metaphase chromosome shape (Paulson and Laemmli 1977). Subsequent studies have

identified the condensin subunit SMC2 and topoisomerase II as the major components of the chromosomal scaffold (Earnshaw et al., 1985; Gasser et al., 1986; Saitoh et al., 1994). It has been proposed that this scaffold could organize the higher-order structure of mitotic chromosomes and would be the basis of chromosome assembly. Although these experiments brought invaluable contributions into the filed of chromosome biology, the exact contribution of the scaffold into the process of chromosome assembly has been subject to particular controversy (discussed in Belmont 2002). The dynamic behavior of condensin I (Gerlich et al., 2006a and chapter 2), together with the dynamic properties previously reported for topoisomerase II (Christensen et al., 2002; Tavormina et al., 2002), which was also shown to display a very dynamic association with mitotic chromatin, revealed that these major chromosomal scaffold components do not serve as an immobilized static structural backbone within chromatin cores. Possibly, the chromosome scaffold is the end-product of a highly dynamic process of chromosome condensation process and not a preassembled structure to which chromatin loops eventually attach. In support of this idea axial localization of condensin subunits is only observed at the end of prophase, when well condensed chromosomes can already be observed (Kireeva et al. 2004). Additionally, after mild protease treatment metaphase chromosomes still exhibit elastic response which suggests that the scaffold is not the structure responsible for the continuity of the chromosome (Pope et al. 2006).

More recent models for condensin function propose that condensin-chromatin interaction occurs in an ATP-independent manner and this interaction triggers hydrolysis of ATP promoting the opening of the arms. Intermolecular head-head engagements could assemble a nucleoprotein filament in which positive superhelical tension is trapped or, alternatively, intramolecular head–head engagement might impose chiral loop formation, trapped within condensin ring. Higher levels of organization would be achieved by protein-protein interactions of condensin complexes trapped at distinct chromosomal sites through helical coiling of the prometaphase fiber (reviewed by Hirano, 2006). Although very attractive, this model also implies a very stable association of condensin with chromatin, being its major function to trap chromatin loops within chromatid core. The dynamic behavior observed for condensin I reveals that this is certainly not the case. Condensin I must have a much more dynamic role during chromosome condensation than statically holding chromatin loops. This result does not rule out the structural role of condensin in the assembly of the chromosomes. Indeed, accumulating evidence support that condensin I is in fact required for

the structural integrity of chromatin (chapter 1; Hudson et al. 2003; Hirota et al. 2004; Gerlich et al. 2006a). However, the dynamic association of condensin I to mitotic chromatin suggest that both the assembly and maintenance of the metaphase chromosome is clearly a much more dynamic process that previously thought.

Important aspects yet to be resolved are the mechanistical implications of the dynamic exchange of condensin subunits observed in mitotic chromosomes. Is a continuous exchange of condensin I required to maintain chromosomal shape? Is condensin I also exchanging during the initial steps of chromosome condensation in prophase? Is condensin II in *C. elegans* stably associated with mitotic chromatin, as condensin II in vertebrate cells or does it show a highly dynamic behavior as condensin I in *Drosophila* and vertebrate cells? Does condensin become less dynamic as chromosome condensation is being completed? Can chromosomes be established without any static non-histone protein component?

Answers to some of these questions will certainly help to bring further understanding into one of the oldest problems in Cell Biology: how does chromatin folds into compact mitotic chromosomes?

PART IV

MATERIALS AND METHODS

1. Materials and methods

1.1 Generation of recombinant plasmid constructs

Standard molecular biology techniques were performed according to Sambrook et al (1989). Digestion of plasmid DNA or PCR product, with appropriate restriction enzymes, was performed according to manufacturer's instructions. After digestion, linearized vector was dephosphorylated by adding 1 µl (20 units) of alkaline phosphatase (Boehringer) to the restriction reaction and incubated at 37 ºC for 30 min. Restriction products were separated in a preparative standard agarose gel and purified using QIAquick Gel Extraction Kit (Quiagen). Ligations were performed by T4 DNA ligase (Gibco BRL), mixing a 1:3 vector:insert molar ratio, incubated at 16 ºC overnight. Ligation products were used for transformation of competent DH5α or XL1blue cells grown in LB medium containing the appropriate selective antibiotic. The presence and orientation of the desired insert was assayed by restriction analysis after a small scale plasmid DNA isolation using the 1,2,3 method (Sambrook et al 1989). Accurate ligation was further confirmed by DNA sequencing of positive recombinant plasmids. Recombinant plasmid DNA used for sequencing, microinjection, transfection or ssRNA synthesis was purified using the QIAGEN Plasmid Midi Kit (Qiagen).

1.2 Protein electrophoresis and western blotting

Protein extract were run on a polyacrilamide gel until the running front has reached the end of the gel. Proteins were transferred to a nitrocellulose membrane (Schleicher & Shuel) using a semi dry system at a 20-25V for 1:30h. The membrane was incubated overnight in blocking solution [5% powder milk (PD), 0.5% fish skin gelatin-FSG (Sigma) in PBST]. All primary and secondary antibodies were diluted in PBST containing 3% BSA, 1% FSG and membrane was incubated for 1-2h with primary antibody solution. Secondary antibodies conjugated to HRP (Amersham) were used according to the manufacturer's instructions. Blots were developed by Enhanced Chemiluminescent (ECL) method (see appendix 2 for recipes). The membrane was then used to impress an X-ray film (Fuji Medical X-Ray Film) and the results were obtained by manual or automatic development of the film.

1.3 Double stranded RNA interference in *Drosophila* S2 cells

To deplete Barren/CAP-H from *Drosophila* S2 tissue culture cells, a 1445-bp EcoRI-AccI fragment spanning the 5' untranslated region and including the ATG initiation codon obtained from a full length Barren/CAP-H cDNA clone (RE48802, Berkeley *Drosophila* Genome

Project, BDGP) was cloned into pSPT18 and pSPT19 vectors (Roche). For DmCAP-H2 depletion, a 846-bp EcoRI-XbaI fragment spanning the 5' untranslated region and including the ATG initiation codon obtained from a DmCAP-H2 cDNA clone (SD09295, BDGP) was cloned into pSPT18 and pSPT19 vectors (Roche). In both cases, single stranded RNA (ssRNA) synthesis was performed using the T7 Megascript kit (Ambion) using the recombinant vectors as templates. Equimolar amounts of sense and anti-sense ssRNA were heated for 1 hour at 65 ºC, to denaturate secondary structures. Annealing was achieved by cooling down the mixture at room temperature, in a pre-heated (65 ºC) beaker containing 200 mL of water. In all RNA interference (RNAi) experiments, 15 µg of double-stranded RNA (dsRNA) was added to 10^6 *Drosophila* S2 cells in 1 ml Schneider's medium (Gibco BRL) and incubated for 1 h at 25°C, in six-well plates. Cells were then supplemented with 2 ml medium with 10% fetal bovine serum (FBS) (Gibco BRL). For Barren/CAP-H RNAi three independent experiments were performed each of them with duplicates for every time point. When required, cells were incubated with 20 µM MG132 (Calbiochem) or/and with 30 µM colchicine (Sigma). Hypotonic shock was performed by resuspending cells in a 0.1% sodium citrate solution for 10 seconds. Growth curves were plotted by quantification of viable cells, which do not stain with Trypan blue (Sigma), at each time point of the experiment. To monitor protein depletion, cells were processed for immunoblotting. $5x10^5$ cells were collected by centrifugation at 10,000 rpm for 10 min, washed with PBS supplemented with protease inhibitors (Roche) and resuspended in 20 µl of sodium dodecyl sulfate (SDS) sample buffer (see appendix 2 for recipe). Samples were boiled for 5 min before loading on a 7.5% polyacrylamide-SDS gel electrophoresis.

1.4 Immunofluorescence in *Drosophila* S2 cells

Cells were centrifuged onto slides, fixed in 3.7% methanol free formaldehyde, 0.5% Triton X-100 in 1 x PBS for 10 min followed by three washes in PBS-T (1x PBS, 0.05% Tween 20) for 5 min. For visualization of α-tubulin, cells were firstly fixed in 4 % formaldehyde in 1 x PHEM (see appendix 2 for recipe) and subsequently extracted with 0.5% Triton X-100 in 1 x PBS for 10 min Blocking was performed in PBS-TF (PBS-T, 10% FBS) for 30 min at room temperature. Primary antibody incubations were performed in PBS-TF for 1 h at room temperature followed by PBS-T wash (three times for 5 min). Incubation with fluorescent labeled secondary antibodies was according to manufacturer's instructions (Molecular Probes, The Netherlands). Slides were washed again three times with PBS-T for 5 min and mounted in Vectashield with 1 µg/ml of 4',6'- diamidino-2-phenylindole (DAPI) (Vector, United

Kingdom). Calcium treatment was performed as previously described (Kapoor et al. 2000). Briefly, cells were permeabilized for 90 s in a calcium containing buffer (see appendix 2 for recipe) and then fixed for 10 min in the same buffer supplemented with 4% formaldehyde. Immunofluorescence was performed as described above using Tris-buffered saline instead of phosphate-buffered saline.

Images were collected either in the Zeiss Axiovert 200 M microscope (Carl Zeiss, Germany) using an Axiocam (Carl Zeiss, Germany) or the Leica Confocal SP2 (Leica Microsystems, Germany). Data stacks were deconvolved, using the Huygens Essential version 3.0.2p1 (Scientific Volume Imaging B.V., The Netherlands). Intercentromere distances measurements were performed analyzing each image stack by stack. CID-labeled centromeres found in the same stack flanking a brighter DAPI-stained region (heterochromatin) of a chromosome were considered as sister centromeres and the distance was measured using AxioVision4.3 software (Carl Zeiss, Germany).

1.5. Antibodies

The primary antibodies were anti-α-tubulin mouse B512 (Sigma- Aldrich) used at 1:4000 for immunofluorescence (IF) and 1:10000 for immunoblotting (IB); anti-phospho-histone H3 rabbit polyclonal (Upstate Biotechnology) used at 1:1000; anti-POLO mouse monoclonal MA294 (Llamazares et al. 1991) used at 1:30; anti-Barren/ CAP-H rabbit polyclonal (Bhat et al., 1996) used at 1:1500 (IF) and 1:3000 (IB); anti-DmSMC4 rabbit polyclonal (Steffensen et al., 2001) used at 1:500 (IB) and sheep polyclonal used at 1:500 (IF); anti- SMC2 rabbit polyclonal used at 1:1000; anti-CAP-D2 rabbit polyclonal (Savvidou et al., 2005) used at 1:10000 (IB) and 1:2000 (IF); immunopurified anti-CAP-G rabbit polyclonal used at 1:5; anti-CID chicken polyclonal (Blower and Karpen, 2001) used at 1:100; anti-CID rabbit polyclonal (Henikoff et al., 2000) used at 1:1500; anti-dimethylated K9 histone H3 rabbit polyclonal (Upstate Biotechnology) used according to the manufacturer's instructions; anti-dimethylated K4 histone H3 rabbit polyclonal (Upstate Biotechnology) used according to the manufacturer's instructions; anti-DRAD21 rabbit polyclonal (Warren et al., 2000) used at 1:1000; anti-INCENP rabbit polyclonal used at 1:1500 (Adams et al., 2001); anti-ZW10 rabbit polyclonal (Williams et al., 1992) used at 1:500; anti-topoisomerase II mouse monoclonal used at 1:30 (IF) (Swedlow et al. 1993); anti-Cyclin B mouse monoclonal used at 1:40 (IB) (Knoblich and Lehner 1993) and anti-GFP antibody used at 1:1000 (IB) (gift from Stefan Heidmann).

1.6. Time-Lapse Fluorescence Imaging of *Drosophila* S2 cells

Live analysis of mitosis was performed on S2 cells stably expressing green fluorescent protein (GFP)-Histone H2B (kindly provided by P. O'Farrell) and on S2 cells stably expressing GFP-Tubulin (kindly provided by R. Vale). Control or Barren/CAP-H RNAi-treated cells were incubated for 72 h and plated on glass coverslips treated with 100 µg/ml concanavalin A (Sigma). For GFP-Histone H2B cells, time-lapse images were collected at 1.5-min intervals, starting from the time mitotic chromosomes could be visualized. For GFP-Tubulin cells, time-lapse images were collected at 1.5-min intervals, starting from the time asters of microtubules could be visualized. Both time-lapse analyses were performed using a Cell Observer System (Carl Zeiss, Germany) and image processing and movie assembly was processed using AxioVision4.3 software (Carl Zeiss, Germany).

1.7. Fluorescence-Activated Cell Sorting (FACS) analysis

For FACS analysis 10^6 cells were spun at 3000 rpm for 5 min and resuspended in 200 µl PBS. Cells were fixed with 2 ml 70% ice-cold ethanol in PBS added drop by drop with continuous vortexing. Samples were kept on ice for 30 min before being spun at 3,000 rpm for 5 min and resuspended in 200 µl PBS with 100 µg/ml RNase and 100 µg/ml propidium iodide. Samples were incubated at 37°C for 30 min. To analyze DNA content we used a FACS Calibur (Becton Dickinson) flow cytometer and data from 25,000 cells were obtained. Results were analyzed using CellQuest data acquisition software.

1.8. Construction of fluorescent-tagged version of Barren

For Barren-EGFP fusion gene construction, a sequence which contains a full-length Barren cDNA insert (excluding stop codon) was amplified from the clone RE48802 (Berkeley *Drosophila* Genome Project, BDGP), by PCR, using primers that introduce a KpnI site at 5' and an ApaI site at 3'. The digested PCR product was cloned in the KpnI/ApaI cut pEGFP-N1 vector (Clontech) for C-terminal EGFP fusion. The Barren-EGFP insert (KpnI/HincII) was cloned in pRmHa-3 (Bunch et al. 1988), suitable for transient transfection in *Drosophila* S2 cells. Barren-EGFP insert (KpnI-SpeI) was cloned in pUASP (Rorth, 1998) vector using KpnI/XbaI sites, suitable for germline transformation. For Barren-mRFP fusion gene construction, Barren cDNA flanked by KpnI/ApaI sites was obtained as described above and cloned in the KpnI/ApaI cut pmRFPN1 vector (see appendix 2) for C-terminal mRFP1 fusion. The Barren-mRFP insert (KpnI/HincII) was cloned in pRmHa-3. For EGFP-Barren fusion

gene construction, Barren cDNA flanked by KpnI/ApaI sites was obtained as described above and cloned in pMTV-EGFP vector (invitrogen). For primers and vector maps see appendix 3.

1.9. Construction of EGFP-tagged versions of DmCAP-H2

For DmCAP-H2-EGFP fusion gene construction, a sequence coding for one predicted isoforms (PC) (excluding stop codon) was amplified from the clone SD09295 (Berkeley *Drosophila* Genome Project), by PCR, using primers that introduce a KpnI site at 5' and an ApaI site at 3'. The digested PCR product was cloned in the KpnI/ApaI cut pRmHa-3 vector for C-terminal EGFP fusion. The DmCAP-H2-EGFP insert (KpnI-SpeI) was cloned in pUASP (Rorth, 1998) vector using KpnI/XbaI sites, suitable for germline transformation. For EGFP-DmCAP-H2 fusion gene construction, DmCAP-H2 (PC) cDNA flanked by KpnI/ApaI sites was obtained as described above and cloned in pMTV-EGFP vector (invitrogen). For primers and vector maps see appendix 3.

1.10. Transient Transfection

Transfections were performed using the calcium-phosphate method (Invitrogen). *Drosophila* S2 cells (3 ml at 106 cells/ml) were incubated at 25 ºC in Schneider's medium (Sigma) supplemented with 10% fetal bovine serum (FBS). After a 24 hours growing period, cells were incubated for 16 h with a transfection mix [19 µg of plasmid, 36 µl of CaCl2 2 M and 245 µl of sterile water and 300µl of 2 x Hepes-Buffered Saline (see appendix 2 for recipe)]. In case of co-transfections, 9.5 µg of each plasmid were used. The calcium phosphate solution was removed by cell centrifugation (800 rpm for 3 minutes) and cells were then washed and re-suspended with complete Schneider's medium. Foe inducible transfection experiments, after 12 hours of incubation, expression of transfected constructs was induced by addition of 1.0 mM $CuSO_4$, which activates the metallothionein promoter. Cells were cytospun onto slides and fixed as described above after a 16 hours induction period.

1.11. *Drosophila* stocks

W1118 was obtained from the Bloomington Stock Center (IN) and was used as control strain.
For dynamic analysis of Barren, Barren-EGFP transgenic flies were produced. Barren-EGFP was cloned into pUASP vector and the resulting pUASP-Barren-EGFP plasmid was injected together with the helper plasmid pa25.lwc in w1118 embryos for germline P-element mediated transformation. Several transformed lines were established and insertions were mapped to be either on the II or on the III chromosome. For all the dynamic analysis

experiments, two independent lines whose insertion was mapped to be on the third chromosome were used: *UASP-Barren-EGFP III.1* or *UASP-Barren-EGFP III.2*. These two transgene insertions were shown to efficiently rescue the lethality associated with a *Barren* null allele ($Barr^{L305}$ (Bhat et al. 1996)) as follows. *UASP-Barren-EGFP III.1* and *UASP-Barren-EGFP III.2* were expressed using two different GAL4 drivers (*daughterless (da) GAL4* (Wodarz et al. 1995) and *Tubulin (Tub) GAL4* (Bloomington Stock Centre)) in a hemizygous *Barren* mutant background, $Barr^{L305}$*/Df(2L)Exel7077*. *Df(2L)Exel7077* deletes *Barren* and 16 adjacent genes (Bloomington Stock Centre). To determine pupal relative viability, virgin females *Df(2L)Exel7077; UASP-Barren-EGFP III.1/Ts;Tl* or *Df(2L)Exel7077; UASP-Barren-EGFP III.2/Ts;Tl* were crossed with males $Barr^{L305}$*; TubGAL4 / Ts; Tl* and the percentage of rescued pupae was scored based on the absence of the marker *Tubby* (Tb). To determine adult relative viability, virgin females *Df(2L)Exel7077/CyO; UASP-Barren-EGFP III.1/MKRS* or *Df(2L)Exel7077*/CyO; UASP-Barren-EGFP III.2 were crossed with males $Barr^{L305}$*/CyO, TubGAL4/MKRS* or *BarrL305/CyO; daGAL4* and the percentage of rescued flies was scored based on the absence of the marker *Curly* (Cy).

To drive maternal expression of *UASP-Barren-EGFP*, we have generated recombinant chromosomes containing either *UASP-Barren-EGFP III.1* and *maternal-α-tubulin VP16 GAL4 driver (α-4tub-GAL4-VP16)*, obtained from the Bloomington Stock Centre, or *UASP-Barren-EGFP III.2* and the *daughterless GAL4 driver (daGAL4)* (Wodarz et al. 1995). For quantitative live imaging of syncytial nuclei and Fluorescence Recovery After Photobleaching (FRAP) analysis, *UASP-Barren-EGFP III.1, α-4tub-GAL4-VP16/ HisH2Av-mRFP1 III.1* (Schuh et al. 2007) females were generated. For FRAP analysis of Histone H2Av, a *HisH2Av-EGFP* transgene was used (Clarkson and Saint 1999). For visualization of Barren-EGFP and HisH2Av-mRFP1 in post-cellularization embryos, *UASP-Barren-EGFP III.2, daGAL4 / HisH2Av-mRFP1 III.1* females were produced. For the construction of a red fluorescent CID variant, the mRFP1 coding sequence was PCR-amplified using pRSET-mRFP1 (generously provided by R. Tsien, UCSD) as template and inserted into an internal position between the codons specifying amino acids 118 and 119 of CID. This insertion position was chosen based on the previous construction of a fully functional *EGFP-CID* variant, in which the EGFP sequence was inserted at the same position (Schuh et al. 2007). Transgenic strains expressing *mRFP1-cid* under control of the *cid* genomic regulatory region were obtained after P-element-mediated germline transformation of the final DNA fragment cloned in pCaSpeR4.

For visualization of Barren-EGFP and Cid-mRFP1 in both post-cellularization and syncytial embryos *Cid-mRFP1 II.1, Cid-mRFP1 II.2; UASP-Barren-EGFP III.1/α-4tub-GAL4-VP16* females were generated. For analysis of third instar larval brains, $Barr^{L305}$*/Df(2L)Exel7077; daGAL4, UASP-Barren III.2* larvae were used.

For overexpression during eye development analysis, *UASP-Pnr* (Haenlin et al. 1997), *eyeless-GAL4* (Hazelett et al. 1998) and *GMR-GAL4* (Freeman 1996) stocks were obtained from Bloomington Stock Center (IN).

In order to prepare protein extracts from embryos at defined stages of mitosis 14, the stock *w; string7B, P[w+, Hs-string]/TM3* (Sauer et al., 1995) was used, which contains the *string* mutant allele previously described (Edgar and O'Farrell, 1989).

For analysis of SMC4 localization, *DmSMC4-EGFP* transgenic flies were produced. DmSMC4-EGFP (EGFP internally fused after a.a. 587, produced by Soren Steffensen) was cloned into pUASP vector and the resulting pUASP-DmSMC4-EGFP plasmid was injected together with the helper plasmid pa25.lwc in w1118 embryos for germline P-element mediated transformation. Several transformed lines were established and insertions were mapped to be either on the II or on the III chromosome.

For analysis of DmCAP-H2, a strain containing a *piggyBac* insertion within *DmCAP-H2/*CG14685 gene (e03210) was obtained from Exelixis *Drosophila* Stock Collection (http://drosophila.med.harvard.edu/).

For analysis of DmCAP-H2 localization, *DmCAP-H2(PC)-EGFP* transgenic flies were produced. DmCAP-H2(PC)-EGFP (see above) was cloned into pUASP vector and the resulting pUASP-DmCAP-H2(PC)-EGFP plasmid was injected together with the helper plasmid pa25.lwc in w1118 embryos for germline P-element mediated transformation. Several transformed lines were established and insertions were mapped to be either on the II or on the III chromosome.

1.12. Cytological analysis of *Drosophila* neuroblasts

Brains from third instar larvae were dissected in 0.7 % NaCl, fixed in 45% acetic acid for 30 seconds and stained with 3% orcein in 45% acetic acid for 3 minuntes. The excess of dye was removed with a quick wash in 60 % acetic acid and the brain squashed between a slide and coverslip containing a drop (5 µl) of 3 % orcein in 60% acetic acid.

1.13. Cytological analysis of early embryos

For cytological analysis of syncytial embryos, a 0.5-2 hours collection was obtained and processed as previously described (Sullivan et al. 2000). Embryos were fixed in 1:1 methanol:n-heptane for 5 minutes followed by three methanol washes. Embryos were then washed with PBST (0.1 % triton X-100 in PBS) and incubated with 5µg/ml of Hoechst in PBS for 5 minutes, for DNA counterstaining. After 3 washes with PBST and a final wash with PBS embryos were mounted in Vectashield (Vector, UK).

1.14. Quantitative analysis of Barren-EGFP loading on mitotic chromosomes

For quantitative analysis of Barren-EGFP association to mitotic chromatin, Barren-EGFP and HisH2Av-mRFP1 co-expressing embryos were collected (0.5-1.5 hours) and processed as previously described (Sullivan et al. 2000). Single stack confocal images were acquired every 18s using a Zeiss LSM510 confocal system (Carl Zeiss, Germany), equipped with a 63x/1.40 oil immersion objective, a 488 nm Ar laser and a 543 nm He/Ne laser for the excitation of EGFP and mRFP1 respectively. Syncytial embryos undergoing mitosis 12 were used for fluorescence quantification and different movies were aligned by the anaphase onset time (the last metaphase frame was set as t=0). Quantitative analysis was performed using ImageJ 1.3v software (http://rsb.info.nih.gov/ij/). In order to select for the chromosomal area, images from both channels were segmented based on an 85% threshold in the HisH2Av-mRFP1 channel. Barren-EGFP mean intensities were normalized and corrected for chromatin compaction changes (by dividing by the normalized mean intensity of HisH2Av-mRFP1 at the same time point), using the formula:

R.F.I = $[I^{Barr}_{t} / I^{Barr}_{t0}] / [I^{His}_{t} / I^{His}_{t0}]$, where $I^{Barr/Hist}$ = mean fluorescence intensity of Barren-EGFP/ HisH2Av-mRFP1 at each time point.

1.15. 4D analysis of post-blastodermal and syncytial embryos

For analysis of post blastodermal embryonic nuclear divisions, embryos expressing simultaneously either Barren-EGFP and HisH2Av-mRFP1 or Barren-EGFP and Cid-mRFP1 were collected and aged in order to obtain a 3 to 5 hours egg collection. For simultaneous visualization of Barren-EGFP and Cid-mRFP in syncytial embryos, a 0.5 -1.5 hours egg collection was obtained from females expressing both proteins in the germline. Embryos were processed as previously described (Sullivan et al. 2000), and z-stack confocal images were acquired either every 1 minute, in the case of post-blastodermal cell division analysis or every 30 sec, in case of syncytial embryos visualization, using the Leica Confocal SP2 system

(Leica Microsystems, Germany). Data stacks were deconvolved, using the Huygens Essential version 3.0.2p1 (Scientific Volume Imaging B.V., The Netherlands) and projected using ImageJ 1.3v software (http://rsb.info.nih.gov/ij/). Fluorescence intensity quantification was performed on undeconvolved raw images after maximal intensity projection using ImageJ 1.3v software.

1.16. Visualization of mitosis in *Drosophila* neuroblasts

Confocal analysis of larval brains was performed as previously described (Buffin et al. 2005) using third instar larval brains that express Barren-EGFP in a *Barren* mutant background. Brains from third instar larvae were dissected in 0.7% NaCl and the attached imaginal discs were removed as much as possible. Individual brains were transferred to a drop of 0.7% NaCl placed on a 24x50 mm coverslip. An 18x18 mm coverslip was placed on top and the excess of liquid was removed with a paper tissue in order to flatten the brain. The preparation was sealed with Halocarbon Oil 700 (Sigma) and z-stack confocal images were acquired every 1 min using the Leica Confocal SP2 system (Leica Microsystems, Germany). Data stacks were processed as described above.

1.17. Fluorescence Recovery After Photobleaching analysis of Barren-EGFP

FRAP analysis was performed using 0.5-1.5 hours collection embryos from females expressing in the germline either Barren-EGFP and HisH2Av-mRFP1 or HisH2Av-EGFP alone. Embryos were collected and processed as previously described (Sullivan et al. 2000). FRAP analysis was performed using the Zeiss LSM510 system with the appropriate FRAP software (Carl Zeiss, Germany). After a pre-bleach image acquisition, photobleaching was achieved by 8 pulses of 100% 488 nm laser intensity within a region of interest (ROI) selected in order to bleach an entire metaphase plate. Post-bleach images were acquired every 9s or 18s, for non-treated and colcemid arrested embryos respectively. When indicated, embryos were arrested in prometaphase by lateral injection with 1mM Colcemid in 10 % DMSO and FRAP analysis was carried out 15-30 min after colcemid injection. Quantitative analysis was performed using ImageJ 1.3v software. Relative Fluorescence Intensity (RFI) was calculated as the ratio between the mean fluorescence intensity of the bleached metaphase (I_B) and the mean fluorescence intensity of a non-bleached metaphase (I_{NB}) used as control, after background correction (Bg), using the formula: $RFI = (I_B\text{-}Bg_B) / (I_{NB}\text{-}Bg_{NB})$. Data points were fit to a single exponential curve using SigmaPlot9.0 (Systat Software, Inc) by regression to: $y = A^* (1–e^{–b.x}) + y0$. Half times of recovery were determined based on the formula: $t_{1/2} =$

ln(0.5)/-b. The mobile fraction (Fm) was calculated using the formula: Fm = ($RFI_{t\infty}$ - RFI_{t0})/(1-RFI_{t0}), where RFIt∞ is the maximal recovery and RFI_{t0} is the RFI at time zero (both calculated based on the regression curve equation).

1.18. Preparation of protein extracts from embryos at defined stages of mitosis 14

Extracts from embryos at defined stages of mitosis 14 were obtained similarly to what has been previously described (Sauer et al., 1995). Eggs were collected from the stock *w; string^{7B}, P[w+, Hs-string]/TM3* on apple agar plates every 30 min and aged for 160 min. In this situation, all embryonic cells from homozygous embryos (*string^{7B}, P[w+, Hs-string] / string^{7B}, P[w+, Hs-string]*) are arrested in G2. To allow the synchronization of the embryos at different mitotic stages, the collections plates were floated for 20 min on a 37ºC water bath in order to express the inducible Hs-string transgene, and allowed to recover for different time periods (5', 8', 12' and 15'). For the collection of G2 arrested embryos, these were aged for additional 20 minutes without heat shock. Embryos were dechoryonated, fixed and Hoechst 33258 stained as described above, using EB buffer (see appendix 2 for recipe) instead of PBS and stored in 60%glycerol/40%EB at -20 ºC. Embryos were visualized under an inverted microscope and s*tring^{7B}, P[w+, Hs-string]/ string^{7B}, P[w+, Hs-string]* embryos at the desired mitotic phase were selected and pooled. Selected embryos were then resuspended in KEB (see appendix 2 for recipe) and different amount were run on a 7.5% polyacrilamide SDS gel.

1.19. Cytological analysis of female ovaries

Mature females (~ 5 days old) were fed with yeast paste for at least 24 hours. Ovaries were dissected in ice cold PBS and fixed in 4 % paraformaldehyde in PBS for 20 minutes. Ovaries were washed 3 times with PBS-Tx (0.1 % triton X-100 in PBS) and ovaries were pipetted up and down to separate individual egg chambers. Membrane permealization was achieved by incubation with 0.5% Triton X-100, 10 % FBS in PBS for 2 hours. For immunofluorescence, egg chambers were incubated with the desired primary antibodies at the respective dilution, for 2 hours at room temperature or overnight at 4 ºC, followed by 3 times wash in PBS-Tx. Fluorescence labelling was accomplished by incubation with the respective secondary antibody for 2 hours at room temperature. For DNA counterstaining egg chambers were incubated with 5µg/ml of Hoechst 33258 in PBS for 10 minutes followed by 3 washes of 10 minutes each with PBS-Tx. A final washing step with PBS was performed and egg chambers were incubated at 4 ºC overnight with 87% glycerol, before mounting on a slide (~ 40 µl per 22x22 mm coverslip).

1.20. Protein expression, purification and antibody production

For generation of a Barren2 recombinant protein, the corresponding cDNA was amplified from the SD09295 clone (BDGP) by PCR and the digested PCR product was subcloned into the expression vector pET-23a (Qiagen) at the EcoRI/HincII sites (see appendix 3 for cloning details), for a C-terminal histidine tag fusion. Constructs were transformed into expression host cells, *E. coli* BL21, and several colonies were tested for protein expression. Single colonies were inoculated in LB medium with 100 μg/mL ampicilin and grown overnight at 37ºC. For a large-scale expression, 5 mL of the overnight culture were transferred into 100 mL of LB with appropriate antibiotics and cultures were grown until OD_{600nm} = 0.6-0.7. Protein expression was induced for 3 hours after addition of 0.4 mM IPTG. The recombinant protein was mainly found in inclusion bodies and to isolate those, cells were collected by centrifuging for 30 min at 5000 rpm at 4 ºC and were resuspended in 10 ml of ice-cold sonication buffer (see appendix 2). Lysis was achieved by 15 min incubation at 37 ºC followed by sonication. Inclusion bodies were collected by centrifuging at 13000 rpm for 30 min and dissolved in 10 mL Purification Buffer (see appendix 2). DmCAP-$H2_{1-419}(His)_6$ protein was purified by affinity chromatography over a Ni^{2+} column (Amersham) following manufacturer's instructions. Purified recombinant protein was run on SDS-PAGE, using standard procedures, and a grinded gel slice was used for rat immunization. Four rats were immunized and the respective anti-sera we designated as #1 to #4. The anti-serum #4 was affinity purified against the fusion protein, immobilized on nitrocellulose membrane. The specific antibodies were eluted by incubating the membrane with 100 mM glycine pH 2.8 and the solution was neutralized with 100 mM Tris-HCl pH 8.0.

1.21. Statistical analyses

All the statistical analyses were performed using the SPSS for windows version 14.0 (SPSS Inc, Chicago, IL, USA). The significance levels of $p<0.05$ (*), $p<0.01$ (**) and $p<0.001$ (***) were used. Independent samples *t*-test (2-tailed) or Mann-Whitney test were used to compare the means.

PART V

REFERENCES

Adachi, Y., Luke, M., and Laemmli, U.K. 1991. Chromosome assembly in vitro: topoisomerase II is required for condensation. Cell 64(1): 137-148.

Adams, R.R., Maiato, H., Earnshaw, W.C., and Carmena, M. 2001. Essential roles of *Drosophila* inner centromere protein (INCENP) and aurora B in histone H3 phosphorylation, metaphase chromosome alignment, kinetochore disjunction, and chromosome segregation. J Cell Biol 153(4): 865-880.

Adolph, K.W. 1980. Isolation and structural organization of human mitotic chromosomes. Chromosoma 76(1): 23-33.

Adolph, K.W., Cheng, S.M., Paulson, J.R., and Laemmli, U.K. 1977. Isolation of a Protein Scaffold from Mitotic HeLa Cell Chromosomes. PNAS 74(11): 4937-4941.

Ajiro, K., Yasuda, H., and Tsuji, H. 1996a. Vanadate triggers the transition from chromosome condensation to decondensation in a mitotic mutant (tsTM13) inactivation of p34cdc2/H1 kinase and dephosphorylation of mitosis-specific histone H3. Eur J Biochem 241(3): 923-930.

Ajiro, K., Yoda, K., Utsumi, K., and Nishikawa, Y. 1996b. Alteration of cell cycle-dependent histone phosphorylations by okadaic acid. Induction of mitosis-specific H3 phosphorylation and chromatin condensation in mammalian interphase cells. J Biol Chem 271(22): 13197-13201.

Alberts, B., Jonhnson, A., Lewis, J., Raff, M., Roberts, K., and Walter, P. 2002. Molecular Biology of the Cell. Garland Publishing, New York.

Almagro, S., Riveline, D., Hirano, T., Houchmandzadeh, B., and Dimitrov, S. 2004. The Mitotic Chromosome Is an Assembly of Rigid Elastic Axes Organized by Structural Maintenance of Chromosomes (SMC) Proteins and Surrounded by a Soft Chromatin Envelope. J Biol Chem 279(7): 5118-5126.

Amor, D.J., Kalitsis, P., Sumer, H., and Choo, K.H. 2004. Building the centromere: from foundation proteins to 3D organization. Trends Cell Biol 14(7): 359-368.

Anderson, D.E., Losada, A., Erickson, H.P., and Hirano, T. 2002. Condensin and cohesin display different arm conformations with characteristic hinge angles. J Cell Biol 156(3): 419-424.

Aono, N., Sutani, T., Tomonaga, T., Mochida, S., and Yanagida, M. 2002. Cnd2 has dual roles in mitotic condensation and interphase. Nature 417(6885): 197-202.

Aparicio, J.G., Viggiani, C.J., Gibson, D.G., and Aparicio, O.M. 2004. The Rpd3-Sin3 histone deacetylase regulates replication timing and enables intra-S origin control in *Saccharomyces cerevisiae*. Mol Cell Biol 24(11): 4769-4780.

Arumugam, P., Gruber, S., Tanaka, K., Haering, C.H., Mechtler, K., and Nasmyth, K. 2003. ATP hydrolysis is required for cohesin's association with chromosomes. Curr Biol 13(22): 1941-1953.

Bak, A.L., Zeuthen, J., and Crick, F.H. 1977. Higher-order structure of human mitotic chromosomes. Proc Natl Acad Sci U S A 74(4): 1595-1599.

Ball, A.R., Jr., Schmiesing, J.A., Zhou, C., Gregson, H.C., Okada, Y., Doi, T., and Yokomori, K. 2002. Identification of a chromosome-targeting domain in the human condensin subunit CNAP1/hCAP-D2/Eg7. Mol Cell Biol 22(16): 5769-5781.

Baumgartner, M., Dutrillaux, B., Lemieux, N., Lilienbaum, A., Paulin, D., and Viegas-Pequignot, E. 1991. Genes occupy a fixed and symmetrical position on sister chromatids. Cell 64(4): 761-766.

Bazett-Jones, D.P., Kimura, K., and Hirano, T. 2002. Efficient supercoiling of DNA by a single condensin complex as revealed by electron spectroscopic imaging. Mol Cell 9(6): 1183-1190.

Belmont, A.S. 2002. Mitotic chromosome scaffold structure: new approaches to an old controversy. Proc Natl Acad Sci U S A 99(25): 15855-15857.

Belmont, A.S., Sedat, J.W., and Agard, D.A. 1987. A three-dimensional approach to mitotic chromosome structure: evidence for a complex hierarchical organization. J Cell Biol 105(1): 77-92.

Bernard, P., Maure, J.F., Partridge, J.F., Genier, S., Javerzat, J.P., and Allshire, R.C. 2001. Requirement of heterochromatin for cohesion at centromeres. Science 294(5551): 2539-2542.

Bhalla, N., Biggins, S., and Murray, A.W. 2002. Mutation of YCS4, a budding yeast condensin subunit, affects mitotic and nonmitotic chromosome behavior. Mol Biol Cell 13(2): 632-645.

Bhat, M.A., Philp, A.V., Glover, D.M., and Bellen, H.J. 1996. Chromatid segregation at anaphase requires the barren product, a novel chromosome-associated protein that interacts with Topoisomerase II. Cell 87(6): 1103-1114.

Bhatt, A.M., Lister, C., Page, T., Fransz, P., Findlay, K., Jones, G.H., Dickinson, H.G., and Dean, C. 1999. The DIF1 gene of *Arabidopsis* is required for meiotic chromosome segregation and belongs to the REC8/RAD21 cohesin gene family. Plant J 19(4): 463-472.

Bickmore, W.A. and Oghene, K. 1996. Visualizing the spatial relationships between defined DNA sequences and the axial region of extracted metaphase chromosomes. Cell 84(1): 95-104.

Blower, M.D. and Karpen, G.H. 2001. The role of *Drosophila* CID in kinetochore formation, cell-cycle progression and heterochromatin interactions. Nat Cell Biol 3(8): 730-739.

Boggs, B.A., Allis, C.D., and Chinault, A.C. 2000. Immunofluorescent studies of human chromosomes with antibodies against phosphorylated H1 histone. Chromosoma 108(8): 485-490.

Boy de la Tour, E. and Laemmli, U.K. 1988. The metaphase scaffold is helically folded: sister chromatids have predominantly opposite helical handedness. Cell 55(6): 937-944.

Branzei, D. and Foiani, M. 2005. The DNA damage response during DNA replication. Curr Opin Cell Biol 17(6): 568-575.

Brinkley, B.R. and Stubblefield, E. 1966. The fine structure of the kinetochore of a mammalian cell in vitro. Chromosoma 19(1): 28-43.

Brun, J. and Chevassu, D. 1958. L'evolution des structures chromatinienes dans les cellules nourricières des ovocytes chez *Drosophila melanogaster*. Chromosoma 9: 537-558.

Buchenau, P., Saumweber, H., and Arndt-Jovin, D.J. 1993. Consequences of topoisomerase II inhibition in early embryogenesis of *Drosophila* revealed by in vivo confocal laser scanning microscopy. J Cell Sci 104 (Pt 4): 1175-1185.

Buffin, E., Lefebvre, C., Huang, J., Gagou, M.E., and Karess, R.E. 2005. Recruitment of Mad2 to the kinetochore requires the Rod/Zw10 complex. Curr Biol 15(9): 856-861.

Bunch, T.A., Grinblat, Y., and Goldstein, L.S. 1988. Characterization and use of the *Drosophila* metallothionein promoter in cultured *Drosophila melanogaster* cells. Nucleic Acids Res 16(3): 1043-1061.

Byrd, K.N. and Shearn, A. 2003. ASH1, a *Drosophila* trithorax group protein, is required for methylation of lysine 4 residues on histone H3. Proc Natl Acad Sci U S A 100(20): 11535-11540.

Cai, S.Y., Babbitt, R.W., and Marchesi, V.T. 1999. A mutant deubiquitinating enzyme (Ubp-M) associates with mitotic chromosomes and blocks cell division. Proc Natl Acad Sci U S A 96(6): 2828-2833.

Carmena, M., Riparbelli, M.G., Minestrini, G., Tavares, A.M., Adams, R., Callaini, G., and Glover, D.M. 1998. *Drosophila* polo kinase is required for cytokinesis. J Cell Biol 143(3): 659-671.

Chakravarthy, S., Park, Y.J., Chodaparambil, J., Edayathumangalam, R.S., and Luger, K. 2005. Structure and dynamic properties of nucleosome core particles. FEBS Lett 579(4): 895-898.

Chan, G.K., Liu, S.T., and Yen, T.J. 2005. Kinetochore structure and function. Trends Cell Biol 15(11): 589-598.

Chan, R.C., Severson, A.F., and Meyer, B.J. 2004. Condensin restructures chromosomes in preparation for meiotic divisions. J Cell Biol 167(4): 613-625.

Chang, C.J., Goulding, S., Earnshaw, W.C., and Carmena, M. 2003. RNAi analysis reveals an unexpected role for topoisomerase II in chromosome arm congression to a metaphase plate. J Cell Sci 116(Pt 23): 4715-4726.

Chen, E.S., Sutani, T., and Yanagida, M. 2004. Cti1/C1D interacts with condensin SMC hinge and supports the DNA repair function of condensin. Proc Natl Acad Sci U S A 101(21): 8078-8083.

Chow, J.P., Siu, W.Y., Fung, T.K., Chan, W.M., Lau, A., Arooz, T., Ng, C.P., Yamashita, K., and Poon, R.Y. 2003. DNA damage during the spindle-assembly checkpoint degrades CDC25A, inhibits cyclin-CDC2 complexes, and reverses cells to interphase. Mol Biol Cell 14(10): 3989-4002.

Christensen, M.O., Larsen, M.K., Barthelmes, H.U., Hock, R., Andersen, C.L., Kjeldsen, E., Knudsen, B.R., Westergaard, O., Boege, F., and Mielke, C. 2002. Dynamics of human DNA topoisomerases IIalpha and IIbeta in living cells. J Cell Biol 157(1): 31-44.

Chu, D.S., Dawes, H.E., Lieb, J.D., Chan, R.C., Kuo, A.F., and Meyer, B.J. 2002. A molecular link between gene-specific and chromosome-wide transcriptional repression. Genes Dev 16(7): 796-805.

Chuang, P.T., Lieb, J.D., and Meyer, B.J. 1996. Sex-specific assembly of a dosage compensation complex on the nematode X chromosome. Science 274(5293): 1736-1739.

Ciosk, R., Zachariae, W., Michaelis, C., Shevchenko, A., Mann, M., and Nasmyth, K. 1998. An ESP1/PDS1 complex regulates loss of sister chromatid cohesion at the metaphase to anaphase transition in yeast. Cell 93(6): 1067-1076.

Clarke, D.J., Johnson, R.T., and Downes, C.S. 1993. Topoisomerase II inhibition prevents anaphase chromatid segregation in mammalian cells independently of the generation of DNA strand breaks. J Cell Sci 105 (Pt 2): 563-569.

Clarkson, M. and Saint, R. 1999. A His2AvDGFP fusion gene complements a lethal His2AvD mutant allele and provides an in vivo marker for *Drosophila* chromosome behavior. DNA Cell Biol 18(6): 457-462.

Cobbe, N., Savvidou, E., and Heck, M.M. 2006. Diverse mitotic and interphase functions of condensins in *Drosophila*. Genetics 172(2): 991-1008.

Coelho, P.A., Queiroz-Machado, J., and Sunkel, C.E. 2003. Condensin-dependent localisation of topoisomerase II to an axial chromosomal structure is required for sister chromatid resolution during mitosis. J Cell Sci 116(Pt 23): 4763-4776.

Collas, P., Le Guellec, K., and Tasken, K. 1999. The A-kinase-anchoring protein AKAP95 is a multivalent protein with a key role in chromatin condensation at mitosis. J Cell Biol 147(6): 1167-1180.

Comings, D.E. 1972. The structure and function of chromatin. Adv Hum Genet 3: 237-431.

Comings, D.E.. 1980. Arrangement of chromatin in the nucleus. Hum Genet 53(2): 131-143.

Cremer, T., Cremer, M., Dietzel, S., Muller, S., Solovei, I., and Fakan, S. 2006. Chromosome territories--a functional nuclear landscape. Curr Opin Cell Biol 18(3): 307-316.

Crosio, C., Fimia, G.M., Loury, R., Kimura, M., Okano, Y., Zhou, H., Sen, S., Allis, C.D., and Sassone-Corsi, P. 2002. Mitotic phosphorylation of histone H3: spatio-temporal regulation by mammalian Aurora kinases. Mol Cell Biol 22(3): 874-885.

Cubizolles, F., Legagneux, V., Le Guellec, R., Chartrain, I., Uzbekov, R., Ford, C., and Le Guellec, K. 1998. pEg7, a new Xenopus protein required for mitotic chromosome condensation in egg extracts. J Cell Biol 143(6): 1437-1446.

Cvetic, C. and Walter, J.C. 2005. Eukaryotic origins of DNA replication: could you please be more specific? Semin Cell Dev Biol 16(3): 343-353.

D'Amours, D., Stegmeier, F., and Amon, A. 2004. Cdc14 and condensin control the dissolution of cohesin-independent chromosome linkages at repeated DNA. Cell 117(4): 455-469.

Davey, C.A., Sargent, D.F., Luger, K., Maeder, A.W., and Richmond, T.J. 2002. Solvent mediated interactions in the structure of the nucleosome core particle at 1.9 a resolution. J Mol Biol 319(5): 1097-1113.

de la Barre, A.E., Angelov, D., Molla, A., and Dimitrov, S. 2001. The N-terminus of histone H2B, but not that of histone H3 or its phosphorylation, is essential for chromosome condensation. Embo J 20(22): 6383-6393.

Dej, K.J. and Spradling, A.C. 1999. The endocycle controls nurse cell polytene chromosome structure during *Drosophila* oogenesis. Development 126(2): 293-303.

Dej, K.J., Ahn, C., and Orr-Weaver, T.L. 2004. Mutations in the *Drosophila* condensin subunit dCAP-G: defining the role of condensin for chromosome condensation in mitosis and gene expression in interphase. Genetics 168(2): 895-906.

DePamphilis, M.L., Blow, J.J., Ghosh, S., Saha, T., Noguchi, K., and Vassilev, A. 2006. Regulating the licensing of DNA replication origins in metazoa. Curr Opin Cell Biol 18(3): 231-239.

Dervyn, E., Noirot-Gros, M.F., Mervelet, P., McGovern, S., Ehrlich, S.D., Polard, P., and Noirot, P. 2004. The bacterial condensin/cohesin-like protein complex acts in DNA repair and regulation of gene expression. Mol Microbiol 51(6): 1629-1640.

Diffley, J.F. 2004. Regulation of early events in chromosome replication. Curr Biol 14(18): R778-786.

DuPraw, E.J. 1965. Macromolecular organization of nuclei and chromosomes: a folded fibre model based on whole-mount electron microscopy. Nature 206(982): 338-343.

DuPraw, E.J. 1966. Evidence for a 'folded-fibre' organization in human chromosomes. Nature 209(23): 577-581.

DuPraw, E.J. 1972. Stages in chromosome evolution: the chromatid twins and how they grew. Brookhaven Symp Biol 23: 230-249.

Earnshaw, W.C. and Laemmli, U.K. 1983. Architecture of metaphase chromosomes and chromosome scaffolds. J Cell Biol 96(1): 84-93.

Earnshaw, W.C., Halligan, B., Cooke, C.A., Heck, M.M., and Liu, L.F. 1985. Topoisomerase II is a structural component of mitotic chromosome scaffolds. J Cell Biol 100(5): 1706-1715.

Edgar, B.A. and O'Farrell, P.H. 1989. Genetic control of cell division patterns in the *Drosophila* embryo. Cell 57(1): 177-187.

Eide, T., Carlson, C., Tasken, K.A., Hirano, T., Tasken, K., and Collas, P. 2002. Distinct but overlapping domains of AKAP95 are implicated in chromosome condensation and condensin targeting. EMBO Rep 3(5): 426-432.

Fan, Y., Nikitina, T., Zhao, J., Fleury, T.J., Bhattacharyya, R., Bouhassira, E.E., Stein, A., Woodcock, C.L., and Skoultchi, A.I. 2005. Histone H1 depletion in mammals alters global chromatin structure but causes specific changes in gene regulation. Cell 123(7): 1199-1212.

Finch, J.T. and Klug, A. 1976. Solenoidal model for superstructure in chromatin. Proc Natl Acad Sci U S A 73(6): 1897-1901.

Fischer, S.G. and Laemmli, U.K. 1980. Cell cycle changes in Physarum polycephalum histone H1 phosphate: relationship to deoxyribonucleic acid binding and chromosome condensation. Biochemistry 19(10): 2240-2246.

Fitzgerald-Hayes, M., Clarke, L., and Carbon, J. 1982. Nucleotide sequence comparisons and functional analysis of yeast centromere DNAs. Cell 29(1): 235-244.

Flemming, W. 1965. Historical paper. Contributions to the knowledge of the cell and its vital processes. Journal of Cell Biology 25(Suppl): 1-69.

Foe, V.E. and Alberts, B.M. 1985. Reversible chromosome condensation induced in *Drosophila* embryos by anoxia: visualization of interphase nuclear organization. J Cell Biol 100(5): 1623-1636.

Foster, H.A. and Bridger, J.M. 2005. The genome and the nucleus: a marriage made by evolution. Genome organisation and nuclear architecture. Chromosoma 114(4): 212-229.

Freeman, L., Aragon-Alcaide, L., and Strunnikov, A. 2000. The condensin complex governs chromosome condensation and mitotic transmission of rDNA. J Cell Biol 149(4): 811-824.

Freeman, M. 1996. Reiterative use of the EGF receptor triggers differentiation of all cell types in the *Drosophila* eye. Cell 87(4): 651-660.

Fujimoto, S., Yonemura, M., Matsunaga, S., Nakagawa, T., Uchiyama, S., and Fukui, K. 2005. Characterization and dynamic analysis of *Arabidopsis* condensin subunits, AtCAP-H and AtCAP-H2. Planta 222(2): 293-300.

Gasser, S.M. and Laemmli, U.K. 1987. A glimpse at chromosomal order. Trends in Genetics 3: 16.

Gasser, S.M., Laroche, T., Falquet, J., Boy de la Tour, E., and Laemmli, U.K. 1986. Metaphase chromosome structure. Involvement of topoisomerase II. J Mol Biol 188(4): 613-629.

Gassmann, R., Vagnarelli, P., Hudson, D., and Earnshaw, W.C. 2004. Mitotic chromosome formation and the condensin paradox. Exp Cell Res 296(1): 35-42.

Geiman, T.M., Sankpal, U.T., Robertson, A.K., Chen, Y., Mazumdar, M., Heale, J.T., Schmiesing, J.A., Kim, W., Yokomori, K., Zhao, Y., and Robertson, K.D. 2004. Isolation and characterization of a novel DNA methyltransferase complex linking DNMT3B with components of the mitotic chromosome condensation machinery. Nucleic Acids Res 32(9): 2716-2729.

Genschik, P., Criqui, M.C., Parmentier, Y., Derevier, A., and Fleck, J. 1998. Cell cycle -dependent proteolysis in plants. Identification Of the destruction box pathway and metaphase arrest produced by the proteasome inhibitor mg132. Plant Cell 10(12): 2063-2076.

Gerlich, D., Hirota, T., Koch, B., Peters, J.M., and Ellenberg, J. 2006. Condensin I Stabilizes Chromosomes Mechanically through a Dynamic Interaction in Live Cells. Curr Biol 16(4): 333-344.

Gerlich, D., Koch, B., Dupeux, F., Peters, J.M., and Ellenberg, J. 2006. Live-Cell Imaging Reveals a Stable Cohesin-Chromatin Interaction after but Not before DNA Replication. Curr Biol 16(15): 1571-1578.

Giet, R. and Glover, D.M. 2001. *Drosophila* aurora B kinase is required for histone H3 phosphorylation and condensin recruitment during chromosome condensation and to organize the central spindle during cytokinesis. J Cell Biol 152(4): 669-682.

Gimenez-Abian, J.F., Clarke, D.J., Mullinger, A.M., Downes, C.S., and Johnson, R.T. 1995. A postprophase topoisomerase II-dependent chromatid core separation step in the formation of metaphase chromosomes. J Cell Biol 131(1): 7-17.

Gimenez-Abian, J.F., Sumara, I., Hirota, T., Hauf, S., Gerlich, D., de la Torre, C., Ellenberg, J., and Peters, J.M. 2004. Regulation of sister chromatid cohesion between chromosome arms. Curr Biol 14(13): 1187-1193.

Goodrich, J.S., Clouse, K.N., and Schupbach, T. 2004. Hrb27C, Sqd and Otu cooperatively regulate gurken RNA localization and mediate nurse cell chromosome dispersion in *Drosophila* oogenesis. Development 131(9): 1949-1958.

Gorbsky, G.J. 1994. Cell cycle progression and chromosome segregation in mammalian cells cultured in the presence of the topoisomerase II inhibitors ICRF-187 [(+)-1,2-bis(3,5-dioxopiperazinyl-1-yl)propane; ADR-529] and ICRF-159 (Razoxane). Cancer Res 54(4): 1042-1048.

Goshima, G. and Vale, R.D. 2003. The roles of microtubule-based motor proteins in mitosis: comprehensive RNAi analysis in the *Drosophila* S2 cell line. J Cell Biol 162(6): 1003-1016.

Goto, H., Tomono, Y., Ajiro, K., Kosako, H., Fujita, M., Sakurai, M., Okawa, K., Iwamatsu, A., Okigaki, T., Takahashi, T., and Inagaki, M. 1999. Identification of a novel phosphorylation site on histone H3 coupled with mitotic chromosome condensation. J Biol Chem 274(36): 25543-25549.

Goto, H., Yasui, Y., Nigg, E.A., and Inagaki, M. 2002. Aurora-B phosphorylates Histone H3 at serine28 with regard to the mitotic chromosome condensation. Genes Cells 7(1): 11-17.

Gruber, S., Arumugam, P., Katou, Y., Kuglitsch, D., Helmhart, W., Shirahige, K., and Nasmyth, K. 2006. Evidence that loading of cohesin onto chromosomes involves opening of its SMC hinge. Cell 127(3): 523-537.

Gruber, S., Haering, C.H., and Nasmyth, K. 2003. Chromosomal cohesin forms a ring. Cell 112(6): 765-777.

Guacci, V., Hogan, E., and Koshland, D. 1994. Chromosome condensation and sister chromatid pairing in budding yeast. J Cell Biol 125(3): 517-530.

Guacci, V., Koshland, D., and Strunnikov, A. 1997. A direct link between sister chromatid cohesion and chromosome condensation revealed through the analysis of MCD1 in *S. cerevisiae*. Cell 91(1): 47-57.

Guenatri, M., Bailly, D., Maison, C., and Almouzni, G. 2004. Mouse centric and pericentric satellite repeats form distinct functional heterochromatin. J Cell Biol 166(4): 493-505.

Guo, X.W., Th'ng, J.P., Swank, R.A., Anderson, H.J., Tudan, C., Bradbury, E.M., and Roberge, M. 1995. Chromosome condensation induced by fostriecin does not require p34cdc2 kinase activity and histone H1 hyperphosphorylation, but is associated with enhanced histone H2A and H3 phosphorylation. Embo J 14(5): 976-985.

Haenlin, M., Cubadda, Y., Blondeau, F., Heitzler, P., Lutz, Y., Simpson, P., and Ramain, P. 1997. Transcriptional activity of pannier is regulated negatively by heterodimerization of the GATA DNA-binding domain with a cofactor encoded by the u-shaped gene of *Drosophila*. Genes Dev 11(22): 3096-3108.

Haering, C.H., Lowe, J., Hochwagen, A., and Nasmyth, K. 2002. Molecular architecture of SMC proteins and the yeast cohesin complex. Mol Cell 9(4): 773-788.

Haering, C.H., Schoffnegger, D., Nishino, T., Helmhart, W., Nasmyth, K., and Lowe, J. 2004. Structure and stability of cohesin's Smc1-kleisin interaction. Mol Cell 15(6): 951-964.

Hagstrom, K.A. and Meyer, B.J. 2003. Condensin and cohesin: more than chromosome compactor and glue. Nat Rev Genet 4(7): 520-534.

Hagstrom, K.A., Holmes, V.F., Cozzarelli, N.R., and Meyer, B.J. 2002. *C. elegans* condensin promotes mitotic chromosome architecture, centromere organization, and sister chromatid segregation during mitosis and meiosis. Genes Dev 16(6): 729-742.

Hanks, S.K., Rodriguez, L.V., and Rao, P.N. 1983. Relationship between histone phosphorylation and premature chromosome condensation. Exp Cell Res 148(2): 293-302.

Hartman, T., Stead, K., Koshland, D., and Guacci, V. 2000. Pds5p is an essential chromosomal protein required for both sister chromatid cohesion and condensation in *Saccharomyces cerevisiae*. J Cell Biol 151(3): 613-626.

Hauf, S., Cole, R.W., LaTerra, S., Zimmer, C., Schnapp, G., Walter, R., Heckel, A., van Meel, J., Rieder, C.L., and Peters, J.M. 2003. The small molecule Hesperadin reveals a role for Aurora B in correcting kinetochore-microtubule attachment and in maintaining the spindle assembly checkpoint. J Cell Biol 161(2): 281-294.

Hawley, R.S. 2002. Meiosis: how male flies do meiosis. Curr Biol 12(19): R660-662.

Hazelett, D.J., Bourouis, M., Walldorf, U., and Treisman, J.E. 1998. decapentaplegic and wingless are regulated by eyes absent and eyegone and interact to direct the pattern of retinal differentiation in the eye disc. Development 125(18): 3741-3751.

He, X., Asthana, S., and Sorger, P.K. 2000. Transient sister chromatid separation and elastic deformation of chromosomes during mitosis in budding yeast. Cell 101(7): 763-775.

Heale, J.T., Ball, A.R., Jr., Schmiesing, J.A., Kim, J.S., Kong, X., Zhou, S., Hudson, D.F., Earnshaw, W.C., and Yokomori, K. 2006. Condensin I interacts with the PARP-1-XRCC1 complex and functions in DNA single-strand break repair. Mol Cell 21(6): 837-848.

Heino, T.I., Lahti, V.P., Tirronen, M., and Roos, C. 1995. Polytene chromosomes show normal gene activity but some mRNAs are abnormally accumulated in the pseudonurse cell nuclei of *Drosophila melanogaster* otu mutants. Chromosoma 104(1): 44-55.

Hendzel, M.J., Wei, Y., Mancini, M.A., Van Hooser, A., Ranalli, T., Brinkley, B.R., Bazett-Jones, D.P., and Allis, C.D. 1997. Mitosis-specific phosphorylation of histone H3 initiates primarily within pericentromeric heterochromatin during G2 and spreads in an ordered fashion coincident with mitotic chromosome condensation. Chromosoma 106(6): 348-360.

Henikoff, S., Ahmad, K., Platero, J.S., and van Steensel, B. 2000. Heterochromatic deposition of centromeric histone H3-like proteins. Proc Natl Acad Sci U S A 97(2): 716-721.

Henneke, G., Koundrioukoff, S., and Hubscher, U. 2003. Multiple roles for kinases in DNA replication. EMBO Rep 4(3): 252-256.

Hirano, M. and Hirano, T. 2002. Hinge-mediated dimerization of SMC protein is essential for its dynamic interaction with DNA. Embo J 21(21): 5733-5744.

Hirano, M. and Hirano, T. 2004. Positive and negative regulation of SMC-DNA interactions by ATP and accessory proteins. Embo J 23(13): 2664-2673.

Hirano, M. and Hirano, T. 2006. Opening closed arms: long-distance activation of SMC ATPase by hinge-DNA interactions. Mol Cell 21(2): 175-186.

Hirano, M., Anderson, D.E., Erickson, H.P., and Hirano, T. 2001. Bimodal activation of SMC ATPase by intra- and inter-molecular interactions. Embo J 20(12): 3238-3250.

Hirano, T. 2005. Condensins: organizing and segregating the genome. Curr Biol 15(7): R265-275.

Hirano, T. and Mitchison, T.J. 1991. Cell cycle control of higher-order chromatin assembly around naked DNA in vitro. J Cell Biol 115(6): 1479-1489.

Hirano, T. and Mitchison, T.J. 1993. Topoisomerase II does not play a scaffolding role in the organization of mitotic chromosomes assembled in Xenopus egg extracts. J Cell Biol 120(3): 601-612.

Hirano, T. and Mitchison, T.J. 1994. A heterodimeric coiled-coil protein required for mitotic chromosome condensation in vitro. Cell 79(3): 449-458.

Hirano, T., Kobayashi, R., and Hirano, M. 1997. Condensins, chromosome condensation protein complexes containing XCAP-C, XCAP-E and a Xenopus homolog of the *Drosophila* Barren protein. Cell 89(4): 511-521.

Hiraoka, Y., Minden, J.S., Swedlow, J.R., Sedat, J.W., and Agard, D.A. 1989. Focal points for chromosome condensation and decondensation revealed by three-dimensional in vivo time-lapse microscopy. Nature 342(6247): 293-296.

Hirota, T., Gerlich, D., Koch, B., Ellenberg, J., and Peters, J.M. 2004. Distinct functions of condensin I and II in mitotic chromosome assembly. J Cell Sci 117(Pt 26): 6435-6445.

Hock, R., Carl, M., Lieb, B., Gebauer, D., and Scheer, U. 1996. A monoclonal antibody against DNA topoisomerase II labels the axial granules of Pleurodeles lampbrush chromosomes. Chromosoma 104(5): 358-366.

Holm, C., Goto, T., Wang, J.C., and Botstein, D. 1985. DNA topoisomerase II is required at the time of mitosis in yeast. Cell 41(2): 553-563.

Hopfner, K.P., Karcher, A., Shin, D.S., Craig, L., Arthur, L.M., Carney, J.P., and Tainer, J.A. 2000. Structural biology of Rad50 ATPase: ATP-driven conformational control in DNA double-strand break repair and the ABC-ATPase superfamily. Cell 101(7): 789-800.

Houchmandzadeh, B. and Dimitrov, S. 1999. Elasticity measurements show the existence of thin rigid cores inside mitotic chromosomes. J Cell Biol 145(2): 215-223.

Houchmandzadeh, B., Marko, J.F., Chatenay, D., and Libchaber, A. 1997. Elasticity and Structure of Eukaryote Chromosomes Studied by Micromanipulation and Micropipette Aspiration. J Cell Biol 139(1): 1-12.

Howell, B.J., Moree, B., Farrar, E.M., Stewart, S., Fang, G., and Salmon, E.D. 2004. Spindle checkpoint protein dynamics at kinetochores in living cells. Curr Biol 14(11): 953-964.

Howman, E.V., Fowler, K.J., Newson, A.J., Redward, S., MacDonald, A.C., Kalitsis, P., and Choo, K.H. 2000. Early disruption of centromeric chromatin organization in centromere protein A (Cenpa) null mice. Proc Natl Acad Sci U S A 97(3): 1148-1153.

Hoyt, M.A., Totis, L., and Roberts, B.T. 1991. *S. cerevisiae* genes required for cell cycle arrest in response to loss of microtubule function. Cell 66(3): 507-517.

Hsu, J.Y., Sun, Z.W., Li, X., Reuben, M., Tatchell, K., Bishop, D.K., Grushcow, J.M., Brame, C.J., Caldwell, J.A., Hunt, D.F., Lin, R., Smith, M.M., and Allis, C.D. 2000. Mitotic phosphorylation of histone H3 is governed by Ipl1/aurora kinase and Glc7/PP1 phosphatase in budding yeast and nematodes. Cell 102(3): 279-291.

Hsu, W.S. and Hansen, R.W. 1953. The chomosomes in the nurse cells of *Drosophila melanogaster*. Cytologia 18: 330-342.

Hudson, D.F., Vagnarelli, P., Gassmann, R., and Earnshaw, W.C. 2003. Condensin is required for nonhistone protein assembly and structural integrity of vertebrate mitotic chromosomes. Dev Cell 5(2): 323-336.

Irniger, S. 2002. Cyclin destruction in mitosis: a crucial task of Cdc20. FEBS Lett 532(1-2): 7-11.

Ivanovska, I., Khandan, T., Ito, T., and Orr-Weaver, T.L. 2005. A histone code in meiosis: the histone kinase, NHK-1, is required for proper chromosomal architecture in *Drosophila* oocytes. Genes Dev 19(21): 2571-2582.

Jäger, H., Rauch, M., and Heidmann, S. 2005. The *Drosophila melanogaster* condensin subunit Cap-G interacts with the centromere-specific histone H3 variant CID. Chromosoma 113(7): 350-361.

Johnson, R.T. and Rao, P.N. 1970. Mammalian cell fusion: induction of premature chromosome condensation in interphase nuclei. Nature 226(5247): 717-722.

Jokelainen, P.T. 1967. The ultrastructure and spatial organization of the metaphase kinetochore in mitotic rat cells. J Ultrastruct Res 19(1): 19-44.

Kaitna, S., Pasierbek, P., Jantsch, M., Loidl, J., and Glotzer, M. 2002. The aurora B kinase AIR-2 regulates kinetochores during mitosis and is required for separation of homologous Chromosomes during meiosis. Curr Biol 12(10): 798-812.

Kapoor, T.M., Mayer, T.U., Coughlin, M.L., and Mitchison, T.J. 2000. Probing Spindle Assembly Mechanisms with Monastrol, a Small Molecule Inhibitor of the Mitotic Kinesin, Eg5. J Cell Biol 150(5): 975-988.

Kaszas, E. and Cande, W.Z. 2000. Phosphorylation of histone H3 is correlated with changes in the maintenance of sister chromatid cohesion during meiosis in maize, rather than the condensation of the chromatin. J Cell Sci 113 (Pt 18): 3217-3226.

Keyes, L.N. and Spradling, A.C. 1997. The *Drosophila* gene fs(2)cup interacts with otu to define a cytoplasmic pathway required for the structure and function of germ-line chromosomes. Development 124(7): 1419-1431.

Kimura, K. and Hirano, T. 1997. ATP-dependent positive supercoiling of DNA by 13S condensin: a biochemical implication for chromosome condensation. Cell 90(4): 625-634.

Kimura, K. and Hirano, T. 2000. Dual roles of the 11S regulatory subcomplex in condensin functions. Proc Natl Acad Sci U S A 97(22): 11972-11977.

Kimura, K., Cuvier, O., and Hirano, T. 2001. Chromosome condensation by a human condensin complex in Xenopus egg extracts. J Biol Chem 276(8): 5417-5420.

Kimura, K., Hirano, M., Kobayashi, R., and Hirano, T. 1998. Phosphorylation and activation of 13S condensin by Cdc2 in vitro. Science 282(5388): 487-490.

Kimura, K., Rybenkov, V.V., Crisona, N.J., Hirano, T., and Cozzarelli, N.R. 1999. 13S condensin actively reconfigures DNA by introducing global positive writhe: implications for chromosome condensation. Cell 98(2): 239-248.

King, R.C., Riley, S.F., Cassidy, J.D., White, P.E., and Paik, Y.K. 1981. Giant polytene chromosomes from the ovaries of a *Drosophila* mutant. Science 212(4493): 441-443.

Kireeva, N., Lakonishok, M., Kireev, I., Hirano, T., and Belmont, A.S. 2004. Visualization of early chromosome condensation: a hierarchical folding, axial glue model of chromosome structure. J Cell Biol 166(6): 775-785.

Kirschner, M. and Mitchison, T. 1986. Beyond self-assembly: from microtubules to morphogenesis. Cell 45(3): 329-342.

Kline-Smith, S.L., Khodjakov, A., Hergert, P., and Walczak, C.E. 2004. Depletion of centromeric MCAK leads to chromosome congression and segregation defects due to improper kinetochore attachments. Mol Biol Cell 15(3): 1146-1159.

Knoblich, J.A. and Lehner, C.F. 1993. Synergistic action of *Drosophila* cyclins A and B during the G2-M transition. Embo J 12(1): 65-74.

Koch, E.A. and King, R.C. 1964. Studies On The Fes Mutant Of *Drosophila Melanogaster*. Growth 28: 325-369.

Kwon, M., Morales-Mulia, S., Brust-Mascher, I., Rogers, G.C., Sharp, D.J., and Scholey, J.M. 2004. The chromokinesin, KLP3A, dives mitotic spindle pole separation during prometaphase and anaphase and facilitates chromatid motility. Mol Biol Cell 15(1): 219-233.

Labib, K. and Diffley, J.F. 2001. Is the MCM2-7 complex the eukaryotic DNA replication fork helicase? Curr Opin Genet Dev 11(1): 64-70.

Laemmli, U.K., Cheng, S.M., Adolph, K.W., Paulson, J.R., Brown, J.A., and Baumbach, W.R. 1978. Metaphase chromosome structure: the role of nonhistone proteins. Cold Spring Harb Symp Quant Biol 42 Pt 1: 351-360.

Lam, W.W., Peterson, E.A., Yeung, M., and Lavoie, B.D. 2006. Condensin is required for chromosome arm cohesion during mitosis. Genes Dev 20(21): 2973-2984.

Lammens, A., Schele, A., and Hopfner, K.P. 2004. Structural Biochemistry of ATP-Driven Dimerization and DNA-Stimulated Activation of SMC ATPases. Curr Biol 14(19): 1778-1782.

Lavoie, B.D., Hogan, E., and Koshland, D. 2002. In vivo dissection of the chromosome condensation machinery: reversibility of condensation distinguishes contributions of condensin and cohesin. J Cell Biol 156(5): 805-815.

Lavoie, B.D., Hogan, E., and Koshland, D. 2004. In vivo requirements for rDNA chromosome condensation reveal two cell-cycle-regulated pathways for mitotic chromosome folding. Genes Dev 18(1): 76-87.

Lavoie, B.D., Tuffo, K.M., Oh, S., Koshland, D., and Holm, C. 2000. Mitotic chromosome condensation requires Brn1p, the yeast homologue of Barren. Mol Biol Cell 11(4): 1293-1304.

Lawrence, J.B., Singer, R.H., and McNeil, J.A. 1990. Interphase and metaphase resolution of different distances within the human dystrophin gene. Science 249(4971): 928-932.

Lehmann, A.R. 2005. The role of SMC proteins in the responses to DNA damage. DNA Repair (Amst) 4(3): 309-314.

Lens, S.M., Vader, G., and Medema, R.H. 2006. The case for Survivin as mitotic regulator. Curr Opin Cell Biol.

Lewis, C.D. and Laemmli, U.K. 1982. Higher order metaphase chromosome structure: evidence for metalloprotein interactions. Cell 29(1): 171-181.

Li, R. and Murray, A.W. 1991. Feedback control of mitosis in budding yeast. Cell 66(3): 519-531.

Lieb, J.D., Albrecht, M.R., Chuang, P.T., and Meyer, B.J. 1998. MIX-1: an essential component of the *C. elegans* mitotic machinery executes X chromosome dosage compensation. Cell 92(2): 265-277.

Llamazares, S., Moreira, A., Tavares, A., Girdham, C., Spruce, B.A., Gonzalez, C., Karess, R.E., Glover, D.M., and Sunkel, C.E. 1991. polo encodes a protein kinase homolog required for mitosis in *Drosophila*. Genes Dev 5(12): 2153-2165.

Locher, K.P., Lee, A.T., and Rees, D.C. 2002. The E. coli BtuCD structure: a framework for ABC transporter architecture and mechanism. Science 296(5570): 1091-1098.

Lodish, H., Berk, A., Zipursky, S.L., Matsudaira, P., Baltimore, D., and Darnell, J.E. 2000. Molecular Cell Biology.

Logarinho, E., Bousbaa, H., Dias, J.M., Lopes, C., Amorim, I., Antunes-Martins, A., and Sunkel, C.E. 2004. Different spindle checkpoint proteins monitor microtubule attachment and tension at kinetochores in *Drosophila* cells. J Cell Sci 117(Pt 9): 1757-1771.

Lohka, M.J. and Masui, Y. 1983. Formation in vitro of sperm pronuclei and mitotic chromosomes induced by amphibian ooplasmic components. Science 220(4598): 719-721.

Lopes, C.S., Sampaio, P., Williams, B., Goldberg, M., and Sunkel, C.E. 2005. The *Drosophila* Bub3 protein is required for the mitotic checkpoint and for normal accumulation of cyclins during G2 and early stages of mitosis. J Cell Sci 118(Pt 1): 187-198.

Losada, A. and Hirano, T. 2005. Dynamic molecular linkers of the genome: the first decade of SMC proteins. Genes Dev 19(11): 1269-1287.

Losada, A., Hirano, M., and Hirano, T. 1998. Identification of Xenopus SMC protein complexes required for sister chromatid cohesion. Genes Dev 12(13): 1986-1997.

Losada, A., Hirano, M., and Hirano, T. 2002. Cohesin release is required for sister chromatid resolution, but not for condensin-mediated compaction, at the onset of mitosis. Genes Dev 16(23): 3004-3016.

Losada, A., Yokochi, T., Kobayashi, R., and Hirano, T. 2000. Identification and characterization of SA/Scc3p subunits in the Xenopus and human cohesin complexes. J Cell Biol 150(3): 405-416.

Loupart, M.L., Krause, S.A., and Heck, M.S. 2000. Aberrant replication timing induces defective chromosome condensation in *Drosophila* ORC2 mutants. Curr Biol 10(24): 1547-1556.

Luger, K. 2006. Dynamic nucleosomes. Chromosome Res 14(1): 5-16.

Luger, K. and Hansen, J.C. 2005. Nucleosome and chromatin fiber dynamics. Curr Opin Struct Biol 15(2): 188-196.

Lupo, R., Breiling, A., Bianchi, M.E., and Orlando, V. 2001. *Drosophila* chromosome condensation proteins Topoisomerase II and Barren colocalize with Polycomb and maintain Fab-7 PRE silencing. Mol Cell 7(1): 127-136.

MacAlpine, D.M. and Bell, S.P. 2005. A genomic view of eukaryotic DNA replication. Chromosome Res 13(3): 309-326.

MacCallum, D.E., Losada, A., Kobayashi, R., and Hirano, T. 2002. ISWI remodeling complexes in Xenopus egg extracts: identification as major chromosomal components that are regulated by INCENP-aurora B. Mol Biol Cell 13(1): 25-39.

Machado, C. and Andrew, D.J. 2000. D-Titin: a giant protein with dual roles in chromosomes and muscles. J Cell Biol 151(3): 639-652.

Machado, C., Sunkel, C.E., and Andrew, D.J. 1998. Human autoantibodies reveal titin as a chromosomal protein. J Cell Biol 141(2): 321-333.

Machin, F., Paschos, K., Jarmuz, A., Torres-Rosell, J., Pade, C., and Aragon, L. 2004. Condensin regulates rDNA silencing by modulating nucleolar Sir2p. Curr Biol 14(2): 125-130.

Maddox, P.S., Portier, N., Desai, A., and Oegema, K. 2006. Molecular analysis of mitotic chromosome condensation using a quantitative time-resolved fluorescence microscopy assay. Proc Natl Acad Sci U S A 103(41): 15097-15102.

Maeshima, K. and Laemmli, U.K. 2003. A two-step scaffolding model for mitotic chromosome assembly. Dev Cell 4(4): 467-480.

Maiato, H. and Sunkel, C.E. 2004. Kinetochore-microtubule interactions during cell division. Chromosome Res 12(6): 585-597.

Maiato, H., Sampaio, P., and Sunkel, C.E. 2004. Microtubule-associated proteins and their essential roles during mitosis. Int Rev Cytol 241: 53-153.

Manders, E.M., Kimura, H., and Cook, P.R. 1999. Direct imaging of DNA in living cells reveals the dynamics of chromosome formation. J Cell Biol 144(5): 813-821.

Maresca, T.J., Freedman, B.S., and Heald, R. 2005. Histone H1 is essential for mitotic chromosome architecture and segregation in Xenopus laevis egg extracts. J Cell Biol 169(6): 859-869.

Marsden, M.P. and Laemmli, U.K. 1979. Metaphase chromosome structure: evidence for a radial loop model. Cell 17(4): 849-858.

Marshall, W.F., Marko, J.F., Agard, D.A., and Sedat, J.W. 2001. Chromosome elasticity and mitotic polar ejection force measured in living *Drosophila* embryos by four-dimensional microscopy-based motion analysis. Curr Biol 11(8): 569-578.

Marshall, W.F., Marko, J.F., Agard, D.A., and Sedat, J.W. 2001. Chromosome elasticity and mitotic polar ejection force measured in living *Drosophila* embryos by four-dimensional microscopy-based motion analysis. Curr Biol 11(8): 569-578.

May, K.M. and Hardwick, K.G. 2006. The spindle checkpoint. J Cell Sci 119(Pt 20): 4139-4142.

Mazumdar, M., Sundareshan, S., and Misteli, T. 2004. Human chromokinesin KIF4A functions in chromosome condensation and segregation. J Cell Biol 166(5): 613-620.

McEwen, B.F., Arena, J.T., Frank, J., and Rieder, C.L. 1993. Structure of the colcemid-treated PtK1 kinetochore outer plate as determined by high voltage electron microscopic tomography. J Cell Biol 120(2): 301-312.

McGuinness, B.E., Hirota, T., Kudo, N.R., Peters, J.M., and Nasmyth, K. 2005. Shugoshin prevents dissociation of cohesin from centromeres during mitosis in vertebrate cells. PLoS Biol 3(3): e86.

Melby, T.E., Ciampaglio, C.N., Briscoe, G., and Erickson, H.P. 1998. The symmetrical structure of structural maintenance of chromosomes (SMC) and MukB proteins: long, antiparallel coiled coils, folded at a flexible hinge. J Cell Biol 142(6): 1595-1604.

Mellone, B.G. and Allshire, R.C. 2003. Stretching it: putting the CEN(P-A) in centromere. Curr Opin Genet Dev 13(2): 191-198.

Meluh, P.B., Yang, P., Glowczewski, L., Koshland, D., and Smith, M.M. 1998. Cse4p is a component of the core centromere of *Saccharomyces cerevisiae*. Cell 94(5): 607-613.

Mersfelder, E.L. and Parthun, M.R. 2006. The tale beyond the tail: histone core domain modifications and the regulation of chromatin structure. Nucleic Acids Res 34(9): 2653-2662.

Michaelis, C., Ciosk, R., and Nasmyth, K. 1997. Cohesins: chromosomal proteins that prevent premature separation of sister chromatids. Cell 91(1): 35-45.

Mikhailov, A., Cole, R.W., and Rieder, C.L. 2002. DNA damage during mitosis in human cells delays the metaphase/anaphase transition via the spindle-assembly checkpoint. Curr Biol 12(21): 1797-1806.

Minemoto, Y., Uchida, S., Ohtsubo, M., Shimura, M., Sasagawa, T., Hirata, M., Nakagama, H., Ishizaka, Y., and Yamashita, K. 2003. Loss of p53 induces M-phase retardation following G2 DNA damage checkpoint abrogation. Arch Biochem Biophys 412(1): 13-19.

Mirkovitch, J., Mirault, M.E., and Laemmli, U.K. 1984. Organization of the higher-order chromatin loop: specific DNA attachment sites on nuclear scaffold. Cell 39(1): 223-232.

Mitchison, T., Evans, L., Schulze, E., and Kirschner, M. 1986. Sites of microtubule assembly and disassembly in the mitotic spindle. Cell 45(4): 515-527.

Mito, Y., Sugimoto, A., and Yamamoto, M. 2003. Distinct developmental function of two Caenorhabditis elegans homologs of the cohesin subunit Scc1/Rad21. Mol Biol Cell 14(6): 2399-2409.

Moore, L.L., Stanvitch, G., Roth, M.B., and Rosen, D. 2005. HCP-4/CENP-C Promotes the Prophase Timing of Centromere Resolution by Enabling the Centromere Association of HCP-6 in Caenorhabditis elegans. Mol Cell Biol 25(7): 2583-2592.

Morgan, D.O. 1997. Cyclin-dependent kinases: engines, clocks, and microprocessors. Annu Rev Cell Dev Biol 13: 261-291.

Morishita, J., Matsusaka, T., Goshima, G., Nakamura, T., Tatebe, H., and Yanagida, M. 2001. Bir1/Cut17 moving from chromosome to spindle upon the loss of cohesion is required for condensation, spindle elongation and repair. Genes Cells 6(9): 743-763.

Mueller, R.D., Yasuda, H., Hatch, C.L., Bonner, W.M., and Bradbury, E.M. 1985. Identification of ubiquitinated histones 2A and 2B in Physarum polycephalum. Disappearance of these proteins at metaphase and reappearance at anaphase. J Biol Chem 260(8): 5147-5153.

Murnion, M.E., Adams, R.R., Callister, D.M., Allis, C.D., Earnshaw, W.C., and Swedlow, J.R. 2001. Chromatin-associated protein phosphatase 1 regulates aurora-B and histone H3 phosphorylation. J Biol Chem 276(28): 26656-26665.

Musacchio, A. and Hardwick, K.G. 2002. The spindle checkpoint: structural insights into dynamic signalling. Nat Rev Mol Cell Biol 3(10): 731-741.

Nasmyth, K. and Haering, C.H. 2005. The structure and function of SMC and kleisin complexes. Annu Rev Biochem 74: 595-648.

Neuwald, A.F. and Hirano, T. 2000. HEAT repeats associated with condensins, cohesins, and other complexes involved in chromosome-related functions. Genome Res 10(10): 1445-1452.

Newport, J. 1987. Nuclear reconstitution in vitro: stages of assembly around protein-free DNA. Cell 48(2): 205-217.

Newport, J. and Spann, T. 1987. Disassembly of the nucleus in mitotic extracts: membrane vesicularization, lamin disassembly, and chromosome condensation are independent processes. Cell 48(2): 219-230.

Nicklas, R.B. 1983. Measurements of the force produced by the mitotic spindle in anaphase. J Cell Biol 97(2): 542-548.

Nigg, E.A. 2001. Mitotic kinases as regulators of cell division and its checkpoints. Nat Rev Mol Cell Biol 2(1): 21-32.

Nonaka, N., Kitajima, T., Yokobayashi, S., Xiao, G., Yamamoto, M., Grewal, S.I., and Watanabe, Y. 2002. Recruitment of cohesin to heterochromatic regions by Swi6/HP1 in fission yeast. Nat Cell Biol 4(1): 89-93.

Nyberg, K.A., Michelson, R.J., Putnam, C.W., and Weinert, T.A. 2002. Toward maintaining the genome: DNA damage and replication checkpoints. Annu Rev Genet 36: 617-656.

Oegema, K., Desai, A., Rybina, S., Kirkham, M., and Hyman, A.A. 2001. Functional analysis of kinetochore assembly in Caenorhabditis elegans. J Cell Biol 153(6): 1209-1226.

Ohnuki, Y. 1968. Structure of chromosomes. I. Morphological studies of the spiral structure of human somatic chromosomes. Chromosoma 25(4): 402-428.

Ohsumi, K., Katagiri, C., and Kishimoto, T. 1993. Chromosome condensation in Xenopus mitotic extracts without histone H1. Science 262(5142): 2033-2035.

Ono, T., Fang, Y., Spector, D.L., and Hirano, T. 2004. Spatial and temporal regulation of Condensins I and II in mitotic chromosome assembly in human cells. Mol Biol Cell 15(7): 3296-3308.

Ono, T., Losada, A., Hirano, M., Myers, M.P., Neuwald, A.F., and Hirano, T. 2003. Differential contributions of condensin I and condensin II to mitotic chromosome architecture in vertebrate cells. Cell 115(1): 109-121.

Oudet, P., Gross-Bellard, M., and Chambon, P. 1975. Electron microscopic and biochemical evidence that chromatin structure is a repeating unit. Cell 4(4): 281-300.

Ouspenski, II, Cabello, O.A., and Brinkley, B.R. 2000. Chromosome condensation factor Brn1p is required for chromatid separation in mitosis. Mol Biol Cell 11(4): 1305-1313.

Painter, T.S. and Reindorp, E.C. 1939. Endomitosis in the nurse cells of the ovary of *Drosophila melanogaster*. Chromosoma 1: 276-283.

Paulson, J.R. and Laemmli, U.K. 1977. The structure of histone-depleted metaphase chromosomes. Cell 12(3): 817-828.

Paulson, J.R. and Taylor, S.S. 1982. Phosphorylation of histones 1 and 3 and nonhistone high mobility group 14 by an endogenous kinase in HeLa metaphase chromosomes. J Biol Chem 257(11): 6064-6072.

Pflumm, M.F. 2002. The role of DNA replication in chromosome condensation. Bioessays 24(5): 411-418.

Pflumm, M.F. and Botchan, M.R. 2001. Orc mutants arrest in metaphase with abnormally condensed chromosomes. Development 128(9): 1697-1707.

Pinsky, B.A. and Biggins, S. 2005. The spindle checkpoint: tension versus attachment. Trends Cell Biol 15(9): 486-493.

Poirier, M.G. and Marko, J.F. 2002. Mitotic chromosomes are chromatin networks without a mechanically contiguous protein scaffold. Proc Natl Acad Sci U S A 99(24): 15393-15397.

Poirier, M.G., Eroglu, S., and Marko, J.F. 2002. The bending rigidity of mitotic chromosomes. Mol Biol Cell 13(6): 2170-2179.

Poirier, M.G., Eroglu, S., and Marko, J.F. 2002. The bending rigidity of mitotic chromosomes. Mol Biol Cell 13(6): 2170-2179.

Pope, L.H., Xiong, C., and Marko, J.F. 2006. Proteolysis of mitotic chromosomes induces gradual and anisotropic decondensation correlated with a reduction of elastic modulus and structural sensitivity to rarely cutting restriction enzymes. Mol Biol Cell 17(1): 104-113.

Preuss, U., Landsberg, G., and Scheidtmann, K.H. 2003. Novel mitosis-specific phosphorylation of histone H3 at Thr11 mediated by Dlk/ZIP kinase. Nucleic Acids Res 31(3): 878-885.

Prigent, C. and Dimitrov, S. 2003. Phosphorylation of serine 10 in histone H3, what for? J Cell Sci 116(Pt 18): 3677-3685.

Przewloka, M.R., Pardington, P.E., Yannone, S.M., Chen, D.J., and Cary, R.B. 2003. In vitro and in vivo interactions of DNA ligase IV with a subunit of the condensin complex. Mol Biol Cell 14(2): 685-697.

Rattner, J.B. and Lin, C.C. 1985. Radial loops and helical coils coexist in metaphase chromosomes. Cell 42(1): 291-296.

Reuter, G. and Spierer, P. 1992. Position effect variegation and chromatin proteins. Bioessays 14(9): 605-612.

Rieder, C.L. 1982. The formation, structure, and composition of the mammalian kinetochore and kinetochore fiber. Int Rev Cytol 79: 1-58.

Ris, H. and Witt, P.L. 1981. Structure of the mammalian kinetochore. Chromosoma 82(2): 153-170.

Robinson, P.J. and Rhodes, D. 2006. Structure of the '30 nm' chromatin fibre: a key role for the linker histone. Curr Opin Struct Biol 16(3): 336-343.

Rorth, P. 1998. Gal4 in the *Drosophila* female germline. Mech Dev 78(1-2): 113-118.

Roth, S.Y. and Allis, C.D. 1992. Chromatin condensation: does histone H1 dephosphorylation play a role? Trends Biochem Sci 17(3): 93-98.

Saitoh, N., Goldberg, I.G., Wood, E.R., and Earnshaw, W.C. 1994. ScII: an abundant chromosome scaffold protein is a member of a family of putative ATPases with an unusual predicted tertiary structure. J Cell Biol 127(2): 303-318.

Saka, Y., Sutani, T., Yamashita, Y., Saitoh, S., Takeuchi, M., Nakaseko, Y., and Yanagida, M. 1994. Fission yeast cut3 and cut14, members of a ubiquitous protein family, are required for chromosome condensation and segregation in mitosis. Embo J 13(20): 4938-4952.

Sakai, A., Hizume, K., Sutani, T., Takeyasu, K., and Yanagida, M. 2003. Condensin but not cohesin SMC heterodimer induces DNA reannealing through protein-protein assembly. Embo J 22(11): 2764-2775.

Sambrook, J., Fritsch, E.F., and Maniatis, T. 1989. Molecular Cloning: A Laboratory Manual. Cold Spring Harbor Laboratory Press; 2nd edition.

Sauer, K., Knoblich, J.A., Richardson, H., and Lehner, C.F. 1995. Distinct modes of cyclin E/cdc2c kinase regulation and S-phase control in mitotic and endoreduplication cycles of *Drosophila* embryogenesis. Genes Dev 9(11): 1327-1339.

Sauve, D.M., Anderson, H.J., Ray, J.M., James, W.M., and Roberge, M. 1999. Phosphorylation-induced rearrangement of the histone H3 NH2-terminal domain during mitotic chromosome condensation. J Cell Biol 145(2): 225-235.

Savvidou, E., Cobbe, N., Steffensen, S., Cotterill, S., and Heck, M.M. 2005. *Drosophila* CAP-D2 is required for condensin complex stability and resolution of sister chromatids. J Cell Sci 118(Pt 11): 2529-2543.

Schalch, T., Duda, S., Sargent, D.F., and Richmond, T.J. 2005. X-ray structure of a tetranucleosome and its implications for the chromatin fibre. Nature 436(7047): 138-141.

Schleiffer, A., Kaitna, S., Maurer-Stroh, S., Glotzer, M., Nasmyth, K., and Eisenhaber, F. 2003. Kleisins: a superfamily of bacterial and eukaryotic SMC protein partners. Mol Cell 11(3): 571-575.

Schotta, G., Ebert, A., Krauss, V., Fischer, A., Hoffmann, J., Rea, S., Jenuwein, T., Dorn, R., and Reuter, G. 2002. Central role of *Drosophila* SU(VAR)3-9 in histone H3-K9 methylation and heterochromatic gene silencing. Embo J 21(5): 1121-1131.

Schuh, M., Lehner, C.F., and Heidmann, S. 2007. Incorporation of *Drosophila* CID/CENP-A and CENP-C into centromeres during early embryonic anaphase. Curr Biol 17: (in press).

Sedat, J. and Manuelidis, L. 1978. A direct approach to the structure of eukaryotic chromosomes. Cold Spring Harb Symp Quant Biol 42 Pt 1: 331-350.

Sergeant, J., Taylor, E., Palecek, J., Fousteri, M., Andrews, E.A., Sweeney, S., Shinagawa, H., Watts, F.Z., and Lehmann, A.R. 2005. Composition and architecture of the *Schizosaccharomyces pombe* Rad18 (Smc5-6) complex. Mol Cell Biol 25(1): 172-184.

Shah, J.V., Botvinick, E., Bonday, Z., Furnari, F., Berns, M., and Cleveland, D.W. 2004. Dynamics of centromere and kinetochore proteins; implications for checkpoint signaling and silencing. Curr Biol 14(11): 942-952.

Shannon, K.B., Canman, J.C., and Salmon, E.D. 2002. Mad2 and BubR1 function in a single checkpoint pathway that responds to a loss of tension. Mol Biol Cell 13(10): 3706-3719.

Shelby, R.D., Hahn, K.M., and Sullivan, K.F. 1996. Dynamic elastic behavior of alpha-satellite DNA domains visualized in situ in living human cells. J Cell Biol 135(3): 545-557.

Shen, X., Yu, L., Weir, J.W., and Gorovsky, M.A. 1995. Linker histones are not essential and affect chromatin condensation in vivo. Cell 82(1): 47-56.

Siddiqui, N.U., Stronghill, P.E., Dengler, R.E., Hasenkampf, C.A., and Riggs, C.D. 2003. Mutations in *Arabidopsis* condensin genes disrupt embryogenesis, meristem organization and segregation of homologous chromosomes during meiosis. Development 130(14): 3283-3295.

Smith, P.C., Karpowich, N., Millen, L., Moody, J.E., Rosen, J., Thomas, P.J., and Hunt, J.F. 2002. ATP binding to the motor domain from an ABC transporter drives formation of a nucleotide sandwich dimer. Mol Cell 10(1): 139-149.

Smits, V.A., Klompmaker, R., Arnaud, L., Rijksen, G., Nigg, E.A., and Medema, R.H. 2000. Polo-like kinase-1 is a target of the DNA damage checkpoint. Nat Cell Biol 2(9): 672-676.

Sonoda, E., Matsusaka, T., Morrison, C., Vagnarelli, P., Hoshi, O., Ushiki, T., Nojima, K., Fukagawa, T., Waizenegger, I.C., Peters, J.M., Earnshaw, W.C., and Takeda, S. 2001. Scc1/Rad21/Mcd1 is required for sister chromatid cohesion and kinetochore function in vertebrate cells. Dev Cell 1(6): 759-770.

Spradling, A.C. 1993. Germline cysts: communes that work. Cell 72(5): 649-651.

Stambrook, P.J. and Flickinger, R.A. 1970. Changes i chromosomal DNA replication tterns in developing frog embryos. J Exp Zool 174(1): 101-113.

Stear, J.H. and Roth, M.B. 2002. Characterization of HCP-6, a *C. elegans* protein required to prevent chromosome twisting and merotelic attachment. Genes Dev 16(12): 1498-1508.

Steen, R.L., Cubizolles, F., Le Guellec, K., and Collas, P. 2000. A kinase-anchoring protein (AKAP)95 recruits human chromosome-associated protein (hCAP)-D2/Eg7 for chromosome condensation in mitotic extract. J Cell Biol 149(3): 531-536.

Steffensen, S., Coelho, P.A., Cobbe, N., Vass, S., Costa, M., Hassan, B., Prokopenko, S.N., Bellen, H., Heck, M.M., and Sunkel, C.E. 2001. A role for *Drosophila* SMC4 in the resolution of sister chromatids in mitosis. Curr Biol 11(5): 295-307.

Steinhauer, W.R. and Kalfayan, L.J. 1992. A specific ovarian tumor protein isoform is required for efficient differentiation of germ cells in *Drosophila* oogenesis. Genes Dev 6(2): 233-243.

Stray, J.E. and Lindsley, J.E. 2003. Biochemical analysis of the yeast condensin Smc2/4 complex: an ATPase that promotes knotting of circular DNA. J Biol Chem 278(28): 26238-26248.

Strick, T.R., Kawaguchi, T., and Hirano, T. 2004. Real-time detection of single-molecule DNA compaction by condensin I. Curr Biol 14(10): 874-880.

Strukov, Y.G., Wang, Y., and Belmont, A.S. 2003. Engineered chromosome regions with altered sequence composition demonstrate hierarchical large-scale folding within metaphase chromosomes. J Cell Biol 162(1): 23-35.

Strunnikov, A.V., Aravind, L., and Koonin, E.V. 2001. *Saccharomyces cerevisiae* SMT4 encodes an evolutionarily conserved protease with a role in chromosome condensation regulation. Genetics 158(1): 95-107.

Strunnikov, A.V., Hogan, E., and Koshland, D. 1995. SMC2, a *Saccharomyces cerevisiae* gene essential for chromosome segregation and condensation, defines a subgroup within the SMC family. Genes Dev 9(5): 587-599.

Strunnikov, A.V., Larionov, V.L., and Koshland, D. 1993. SMC1: an essential yeast gene encoding a putative head-rod-tail protein is required for nuclear division and defines a new ubiquitous protein family. J Cell Biol 123(6 Pt 2): 1635-1648.

Su, T.T. and Jaklevic, B. 2001. DNA damage leads to a Cyclin A-dependent delay in metaphase-anaphase transition in the *Drosophila* gastrula. Curr Biol 11(1): 8-17.

Suau, P., Bradbury, E.M., and Baldwin, J.P. 1979. Higher-order structures of chromatin in solution. Eur J Biochem 97(2): 593-602.

Sullivan, B.A., Blower, M.D., and Karpen, G.H. 2001. Determining centromere identity: cyclical stories and forking paths. Nat Rev Genet 2(8): 584-596.

Sullivan, K.F. 2001. A solid foundation: functional specialization of centromeric chromatin. Curr Opin Genet Dev 11(2): 182-188.

Sullivan, K.F., Hechenberger, M., and Masri, K. 1994. Human CENP-A contains a histone H3 related histone fold domain that is required for targeting to the centromere. J Cell Biol 127(3): 581-592.

Sullivan, W., Ashburner, A., and Hawley, R.S. 2000. *Drosophila* Protocols. Cold Spring Harbor Laboratory Press.

Sumara, I., Vorlaufer, E., Gieffers, C., Peters, B.H., and Peters, J.M. 2000. Characterization of vertebrate cohesin complexes and their regulation in prophase. J Cell Biol 151(4): 749-762.

Sumara, I., Vorlaufer, E., Stukenberg, P.T., Kelm, O., Redemann, N., Nigg, E.A., and Peters, J.M. 2002. The dissociation of cohesin from chromosomes in prophase is regulated by Polo-like kinase. Mol Cell 9(3): 515-525.

Sumer, H., Craig, J.M., Sibson, M., and Choo, K.H. 2003. A rapid method of genomic array analysis of scaffold/matrix attachment regions (S/MARs) identifies a 2.5-Mb region of enhanced scaffold/matrix attachment at a human neocentromere. Genome Res 13(7): 1737-1743.

Sumner, A.T. 1992. Inhibitors of topoisomerases do not block the passage of human lymphocyte chromosomes through mitosis. J Cell Sci 103 (Pt 1): 105-115.

Sun, X., Le, H.D., Wahlstrom, J.M., and Karpen, G.H. 2003. Sequence analysis of a functional *Drosophila* centromere. Genome Res 13(2): 182-194.

Sun, X., Wahlstrom, J., and Karpen, G. 1997. Molecular structure of a functional *Drosophila* centromere. Cell 91(7): 1007-1019.

Sutani, T. and Yanagida, M. 1997. DNA renaturation activity of the SMC complex implicated in chromosome condensation. Nature 388(6644): 798-801.

Sutani, T., Yuasa, T., Tomonaga, T., Dohmae, N., Takio, K., and Yanagida, M. 1999. Fission yeast condensin complex: essential roles of non-SMC subunits for condensation and Cdc2 phosphorylation of Cut3/SMC4. Genes Dev 13(17): 2271-2283.

Swedlow, J.R. and Hirano, T. 2003. The making of the mitotic chromosome: modern insights into classical questions. Mol Cell 11(3): 557-569.

Swedlow, J.R., Sedat, J.W., and Agard, D.A. 1993. Multiple chromosomal populations of topoisomerase II detected in vivo by time-lapse, three-dimensional wide-field microscopy. Cell 73(1): 97-108.

Takemoto, A., Kimura, K., Yanagisawa, J., Yokoyama, S., and Hanaoka, F. 2006. Negative regulation of condensin I by CK2-mediated phosphorylation. Embo J.

Tavormina, P.A., Come, M.G., Hudson, J.R., Mo, Y.Y., Beck, W.T., and Gorbsky, G.J. 2002. Rapid exchange of mammalian topoisomerase II alpha at kinetochores and chromosome arms in mitosis. J Cell Biol 158(1): 23-29.

Thoma, F. and Koller, T. 1977. Influence of histone H1 on chromatin structure. Cell 12(1): 101-107.

Thoma, F., Koller, T., and Klug, A. 1979. Involvement of histone H1 in the organization of the nucleosome and of the salt-dependent superstructures of chromatin. J Cell Biol 83(2 Pt 1): 403-427.

Tomonaga, T., Nagao, K., Kawasaki, Y., Furuya, K., Murakami, A., Morishita, J., Yuasa, T., Sutani, T., Kearsey, S.E., Uhlmann, F., Nasmyth, K., and Yanagida, M. 2000. Characterization of fission yeast cohesin: essential anaphase proteolysis of Rad21 phosphorylated in the S phase. Genes Dev 14(21): 2757-2770.

Uemura, T., Ohkura, H., Adachi, Y., Morino, K., Shiozaki, K., and Yanagida, M. 1987. DNA topoisomerase II is required for condensation and separation of mitotic chromosomes in *S. pombe*. Cell 50(6): 917-925.

Uhlmann, F., Lottspeich, F., and Nasmyth, K. 1999. Sister-chromatid separation at anaphase onset is promoted by cleavage of the cohesin subunit Scc1. Nature 400(6739): 37-42.

Uhlmann, F., Wernic, D., Poupart, M.A., Koonin, E.V., and Nasmyth, K. 2000. Cleavage of cohesin by the CD clan protease separin triggers anaphase in yeast. Cell 103(3): 375-386.

Vagnarelli, P., Hudson, D.F., Ribeiro, S.A., Trinkle-Mulcahy, L., Spence, J.M., Lai, F., Farr, C.J., Lamond, A.I., and Earnshaw, W.C. 2006. Condensin and Repo-Man-PP1 co-operate in the regulation of chromosome architecture during mitosis. Nat Cell Biol 8(10): 1133-1142.

Van Hooser, A., Goodrich, D.W., Allis, C.D., Brinkley, B.R., and Mancini, M.A. 1998. Histone H3 phosphorylation is required for the initiation, but not maintenance, of mammalian chromosome condensation. J Cell Sci 111 (Pt 23): 3497-3506.

Vass, S., Cotterill, S., Valdeolmillos, A.M., Barbero, J.L., Lin, E., Warren, W.D., and Heck, M.M. 2003. Depletion of Drad21/Scc1 in *Drosophila* cells leads to instability of the cohesin complex and disruption of mitotic progression. Curr Biol 13(3): 208-218.

Vernos, I., Raats, J., Hirano, T., Heasman, J., Karsenti, E., and Wylie, C. 1995. Xklp1, a chromosomal Xenopus kinesin-like protein essential for spindle organization and chromosome positioning. Cell 81(1): 117-127.

Vogelauer, M., Rubbi, L., Lucas, I., Brewer, B.J., and Grunstein, M. 2002. Histone acetylation regulates the time of replication origin firing. Mol Cell 10(5): 1223-1233.

Waizenegger, I.C., Hauf, S., Meinke, A., and Peters, J.M. 2000. Two distinct pathways remove mammalian cohesin from chromosome arms in prophase and from centromeres in anaphase. Cell 103(3): 399-410.

Waldeyer, H.v. 1888. Über Karyokinese und ihre Beziehungen zu den Befruchtungsvorgängen. Archiv für mikroskopische Anatomie und Entwicklungsmechanik 32: 1-122.

Wallace, J.A. and Orr-Weaver, T.L. 2005. Replication of heterochromatin: insights into mechanisms of epigenetic inheritance. Chromosoma 114(6): 389-402.

Wang, J.C. 2002. Cellular roles of DNA topoisomerases: a molecular perspective. Nat Rev Mol Cell Biol 3(6): 430-440.

Warren, W.D., Steffensen, S., Lin, E., Coelho, P., Loupart, M., Cobbe, N., Lee, J.Y., McKay, M.J., Orr-Weaver, T., Heck, M.M., and Sunkel, C.E. 2000. The *Drosophila* RAD21 cohesin persists at the centromere region in mitosis. Curr Biol 10(22): 1463-1466.

Watrin, E. and Legagneux, V. 2005. Contribution of hCAP-D2, a non-SMC subunit of condensin I, to chromosome and chromosomal protein dynamics during mitosis. Mol Cell Biol 25(2): 740-750.

Wei, Y., Mizzen, C.A., Cook, R.G., Gorovsky, M.A., and Allis, C.D. 1998. Phosphorylation of histone H3 at serine 10 is correlated with chromosome condensation during mitosis and meiosis in Tetrahymena. Proc Natl Acad Sci U S A 95(13): 7480-7484.

Wei, Y., Yu, L., Bowen, J., Gorovsky, M.A., and Allis, C.D. 1999. Phosphorylation of histone H3 is required for proper chromosome condensation and segregation. Cell 97(1): 99-109.

Weiss, E. and Winey, M. 1996. The *Saccharomyces cerevisiae* spindle pole body duplication gene MPS1 is part of a mitotic checkpoint. J Cell Biol 132(1-2): 111-123.

Weitzer, S., Lehane, C., and Uhlmann, F. 2003. A model for ATP hydrolysis-dependent binding of cohesin to DNA. Curr Biol 13(22): 1930-1940.

Whittaker, A.J., Royzman, I., and Orr-Weaver, T.L. 2000. *Drosophila* double parked: a conserved, essential replication protein that colocalizes with the origin recognition complex and links DNA replication with mitosis and the down-regulation of S phase transcripts. Genes Dev 14(14): 1765-1776.

Widom, J. 1992. A relationship between the helical twist of DNA and the ordered positioning of nucleosomes in all eukaryotic cells. Proc Natl Acad Sci U S A 89(3): 1095-1099.

Williams, B.C., Karr, T.L., Montgomery, J.M., and Goldberg, M.L. 1992. The *Drosophila* l(1)zw10 gene product, required for accurate mitotic chromosome segregation, is redistributed at anaphase onset. J Cell Biol 118(4): 759-773.

Williams, S.P., Athey, B.D., Muglia, L.J., Schappe, R.S., Gough, A.H., and Langmore, J.P. 1986. Chromatin fibers are left-handed double helices with diameter and mass per unit length that depend on linker length. Biophys J 49(1): 233-248.

Wodarz, A., Hinz, U., Engelbert, M., and Knust, E. 1995. Expression of crumbs confers apical character on plasma membrane domains of ectodermal epithelia of *Drosophila*. Cell 82(1): 67-76.

Wood, K.W., Sakowicz, R., Goldstein, L.S., and Cleveland, D.W. 1997. CENP-E is a plus end-directed kinetochore motor required for metaphase chromosome alignment. Cell 91(3): 357-366.

Woodcock, C.L., Frado, L.L., and Rattner, J.B. 1984. The higher-order structure of chromatin: evidence for a helical ribbon arrangement. J Cell Biol 99(1 Pt 1): 42-52.

Wright, S.J. and Schatten, G. 1990. Teniposide, a topoisomerase II inhibitor, prevents chromosome condensation and separation but not decondensation in fertilized surf clam (Spisula solidissima) oocytes. Dev Biol 142(1): 224-232.

Yamazoe, M., Onogi, T., Sunako, Y., Niki, H., Yamanaka, K., Ichimura, T., and Hiraga, S. 1999. Complex formation of MukB, MukE and MukF proteins involved in chromosome partitioning in Escherichia coli. Embo J 18(21): 5873-5884.

Yanagida, M. 2000. Cell cycle mechanisms of sister chromatid separation; roles of Cut1/separin and Cut2/securin. Genes Cells 5(1): 1-8.

Yeong, F.M., Hombauer, H., Wendt, K.S., Hirota, T., Mudrak, I., Mechtler, K., Loregger, T., Marchler-Bauer, A., Tanaka, K., Peters, J.M., and Ogris, E. 2003. Identification of a subunit of a novel Kleisin-beta/SMC complex as a potential substrate of protein phosphatase 2A. Curr Biol 13(23): 2058-2064.

Yoshimura, S.H., Hizume, K., Murakami, A., Sutani, T., Takeyasu, K., and Yanagida, M. 2002. Condensin architecture and interaction with DNA: regulatory non-SMC subunits bind to the head of SMC heterodimer. Curr Biol 12(6): 508-513.

Yu, H.G. and Koshland, D.E. 2003. Meiotic condensin is required for proper chromosome compaction, SC assembly, and resolution of recombination-dependent chromosome linkages. J Cell Biol 163(5): 937-947.

Yu, J., Fleming, S.L., Williams, B., Williams, E.V., Li, Z., Somma, P., Rieder, C.L., and Goldberg, M.L. 2004. Greatwall kinase: a nuclear protein required for proper chromosome condensation and mitotic progression in *Drosophila*. J Cell Biol 164(4): 487-492.

Zhou, Y.B., Gerchman, S.E., Ramakrishnan, V., Travers, A., and Muyldermans, S. 1998. Position and orientation of the globular domain of linker histone H5 on the nucleosome. Nature 395(6700): 402-405.

PART VI

APPENDIXES

Appendix 1

Abbreviations

a.a. : aminoacids

APC/C: Anaphase-Promoting Complex/Cyclosome

ATM: ataxia telanctasia

ATR: ATM related

BDGP: Berkeley *Drosophila* Genome Project

bp: base pairs

BSA: Bovine Serum Albumin

Bub: budding uninhibited by benzimidazole

C. elegans: *Caenorhabditis elegans*

CAK: Cdk-activating kinase

CAP: Chromosome Associated Protein

Cdk: cyclin-depnedent kinase

Cenp: Centromere Protein

CID: Centromere identifier

CKI: Cdk-inhibitor

CTs: Chromosome Territories

***CyO**: Curly of Oster*

DAPI: 4',6'- diamidino-2-phenylindole

DCC: Dosage Compensation Complex

Df: deficiency

diMeK4: dimethylated lysine 4 of Histone H3

diMeK9: dimethylated lysine 9 of Histone H3

DNA: deoxyribonucleic acid

DSB: Double Strand Breaks

dsRNA : double stranded RNA

DTT: dithiothreitol

E. coli : Escherichia coli

ECL: Enhanced ChemiLuminescence

EDTA: Ethylenediaminetetracetic acid

EGFP: Enhanced Green Fluorescent Protein

EGFP: Enhanced-Green fluorescence protein

EM: Electron Microscopy

EST: Expressed Sequence Tag

FACS: Fluorescence-Activated Cell Sorting

FBS: Fetal Bovine Serum

FISH: fluorescence in situ hybridization

FITC: fluorescein isothiocyanate

FRAP: Fluorescence Recovery After Photobleaching

FSG: fish skin gelatine

G1: Gap phase 1

GFP: Green Fluorescent Protein

h: hours

HisH2Av: histone H2A variant

HP1: Heterochromatin Protein 1

HRP: Horse redish peroxidase

IB: immunobloting

ICC: Initiation of Chromosome Condensation

IF: immunofluorescence

IPTG: isopropyl-β-D-thiogalactoside

IPTG: isopropyl-β-D-thiogalactoside

kb: kilobase

kDa: kiloDalton(s)

L: Liter

LB: Luria-Bertani culture medium

M: Molar

mAb: monoclonal antibody

Mad: Mitotic-arrrest deficient

MFI: Mean Fluorescence Intensity

min: minutes

ml: mililiter

mM: milimolar

mRFP1: monomeric Red Fluorescence Protein

mRNA: messenger RNA

MT(s): Microtubule(s)

MTOC: Microtubule-organizing center

n: number of samples in the study

NEBD: Nuclear Envelope Breakdown

nm: nanometer

OD: Optical density

ORC: Origin Recognition Complex

ORF: Open Reading Frame

PAGE: Polyacrilamide Gel Electrophoresis

PBS: Phosphate-buffered saline

PEV: Position Effect Variegation

PH3: phosphorylated histone H3

RC: Replication Complex

RFI: Relative Fluorescence Intensity

RNA: ribonucleic acid

RNAi : RNA interference

ROI: Region of Interest

rpm: Rotations per minute

RT: room temperature

S phase: DNA synthesis phase

S. cerevisiae: *Saccharomyces cerevisiae*

S. pombe: *Schizosaccharomyces pombe*

S2: *Drosophila* Schneider 2 cell line

SARs: Scaffold Attachment Regions

SC: Synaptonemal Complex

SCF: Skp1-Cullin-F-Box-complex

SD: standard deviation

SDS: Sodium dodecyl sulphate

SDS-PAGE: Sodium dodecyl sulfate-Polyacrylamide Gel Electrophoresis

sec: seconds

SMC: Structural Maintenance of Chromosomes

SSB: Single Stranded Breaks

ssDNA: single stranded DNA

ssRNA: single stranded RNA

$\mathbf{t_{1/2}}$: half time

TopoII: Topoisomerase II

Tris: Tris(hidroximethyl)aminomethane

t-test: Student's *t* test

UAS: upstream activating sequence

UV: ultraviolet

w: mini-white gene

wt: wild type

X. laevis: *Xenopus laevis*

µg: microgram

µl: microliter

µm: micrometer

Appendix 2

Recipes

Protein Electrophoresis:

stacking gel: 4% acrilamide; 125 mM Tris-HCl, pH 6.8; 0.1% SDS;

separating gel: 7.5% acrialmide; 375 mM Tris-HCl, pH 8.8; 0.1% SDS;

running buffer: 25 mM Tris, pH 8.3; 250 mM Glycine; 0.1% SDS

Transfer Buffer:

40mM glycine
50mM Tris
0.04%SDS
20%methanol

Phosphate-Buffered Saline (PBS):

137 mM NaCl
2.7 mM KCl
10 mM KH_2PO_4
1.8 mM Na_2HPO_4

Enhanced Chemiluminescent (ECL):

Solution A - 10ml Tris 100mM pH 8.5, 44 µl cumaric acid (Sigma) 90mM and 100 µl luminol (FLUKA) 250mM;

Solution B: 10ml Tris 100mM pH 8.5 and 6 µl H_2O_2 30% (Merck)

Solution A and B are mixed and incubated with the membrane at the time of ECL detection.

PHEM

60 mM Pipes
25 mM Hepes pH7.0
10 mM EGTA
4 mM $MgSO_4$

Calcium-Treatment Buffer:

100 mM PIPES, pH 6.8
1 mM $MgCl_2$
0.1 mM $CaCl_2$
0.1% Triton X-100

2 x Hepes-Buffered Saline:

50 mM HEPES
1.5 mM Na_2HPO_4
280 mM NaCl, pH 7.1

EB Buffer:

10 mM Tris.Cl pH 7.5
80 mM Na-β-glyrerophosphate
20 mM EGTA
15 mM $MgCl_2$
2 mM Na_3VO_4 (sodium-vanadate)
1 mM $Na_2S_2O_5$ (sodium-metabisulfite)
1 mM Benzamidin
0.2 mM PMSF

KEB Sample Buffer:

10% Glycerol
2.7 M β-mercaptoethanol
3% SDS
0.5 x
185 mM Tris-HCl, pH 8.8
0.01% bromophenol blue
50 mM NaF
20 mM EGTA pH 8.0
2 mM Na_3VO_4
Na-meta-bisulfite
1 protease inhibitor coctail per 50 mL of KEB

LB Medium

1% tryptone
0.5% yeast extract
1% NaCl

Sonication Buffer:

20 mM phosphate buffer, pH 8.0;
0.5 M NaCl; 20 mM imidazole;
100 μg/mL lysozyme;
1% TritonX100

Purification Buffer:

20 mM phosphate buffer, pH 8.0;
0.5 M NaCl;
20 mM imidazole;
8M Urea

Appendix 3

Cloning details and plasmids

pSPT18-Barr

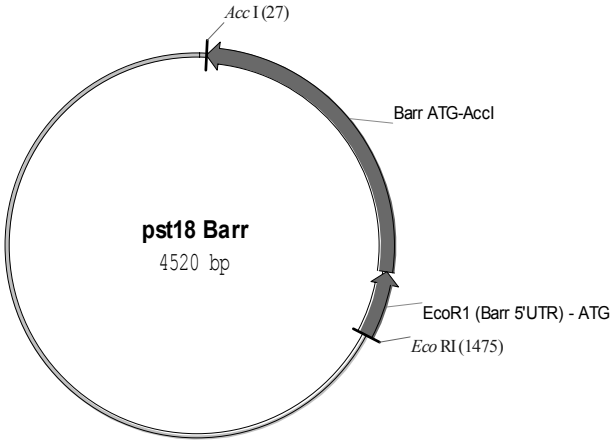

EcoR1-Acc1 fragment was obtained by digestion of the RE48802 clone.

This fragment was cloned into EcoR1/AccI cut pSPT 18 and pSPT 19 vectors (Roche).

Picture depicts pSPT18-Barr and pSPT19-Barr contains the insert in the opposite orientation.

Cloning was confirmed by sequencing analysis.

pSPT18-DmCAP-H2

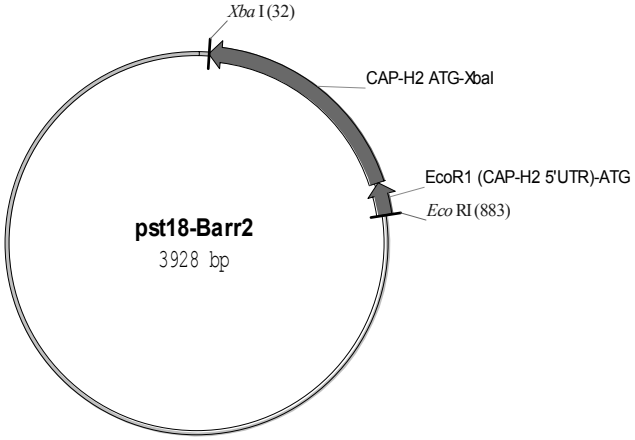

EcoR1-XbaI fragment was obtained by digestion of the SD09259 clone.

This fragment was cloned into EcoR1/XbaI cut pSPT 18 and pSPT 19 vectors.

Picture depicts pSPT18-DmCAP-H2 and pSPT19-DmCAP-H2 contains the insert in the opposite orientation.

Cloning was confirmed by sequencing analysis.

pEGFPN1-Barren

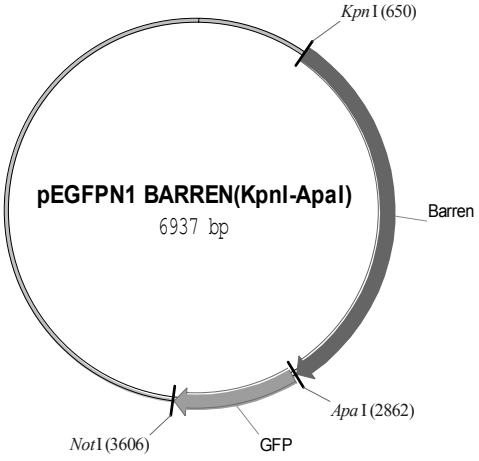

Barren cDNA was amplified by PCR from the cDNA (RE48802, BDGP).

Primers:

KpnI
ATAT GGTACC **ATG**
ACTCTGCCCCGCTTAGAAACTCCG

ApaI
TAAT GGGCCC A **ATC**
CAACACCTGGCGAATTTGAAAGTCCTC
C

The digested PCR product was cloned into KpnI/ApaI cut pEGFPN1 vector (Conetech). Proper Barren-EGFP fusion was confirmed by sequencing analysis.

pRmHa-3 Barren-EGFP

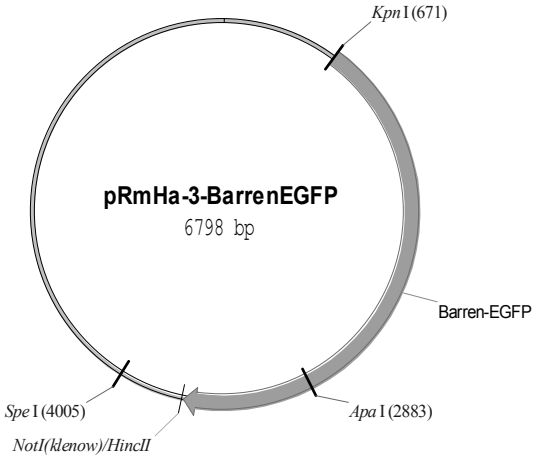

Barren-EGFP insert was obtained from the pEGFPN1-Barren vector, cut with NotI and filled with klenow and cut with KpnI.
This was cloned into the pRmHa-3 vector, cut with KpnI / HincII (blunt).

Proper ligation was confirmed by several restriction enzymes digestions.

pMTV-EGFP-Barren

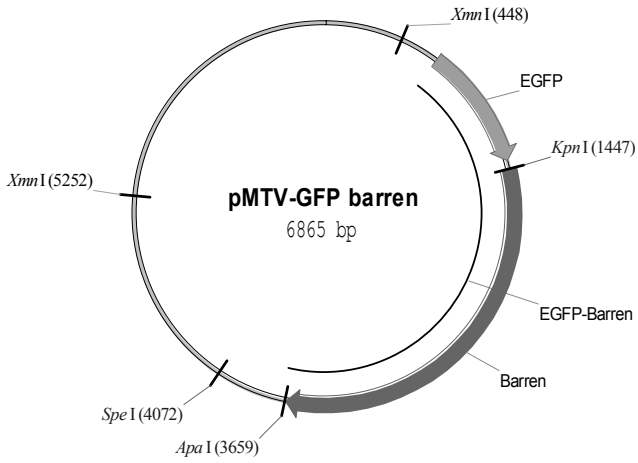

Barren cDNA was amplified by PCR from the cDNA (RE48802, BDGP) as described above.

The digested PCR product was cloned into KpnI/ApaI cut pMTV-EGFP vector.

Proper EGFP-Barren fusion was confirmed by sequencing analysis.

pmRFP1-N1

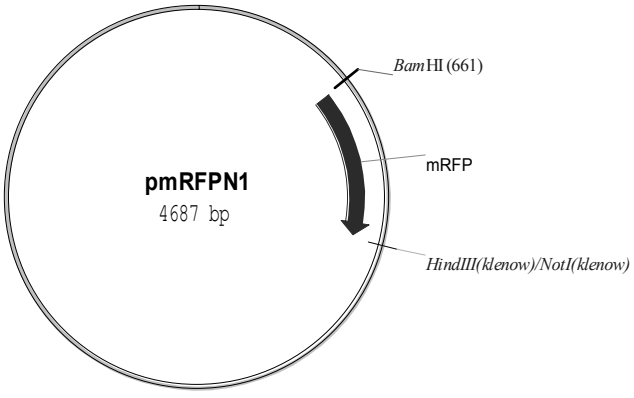

This plasmid was constructed by replacing the DsRed sequence from the pDSRedN1 (Clonetech) by the mRFP1 sequence (kindly given by R. Tsien, UCSD). mRFP1 sequence was obtained from the provided plasmid (pSET B) by digestion with HindIII, filling with Klenow and subsequent digestion with BamH1. This insert was then cloned in the pDsRedN1 vector that was cleaved with NotI filled with klenow and cleaved with BamH1 (which removes the DsRed seq). Confirmed by sequencing analysis.

pmRFPN1-Barren

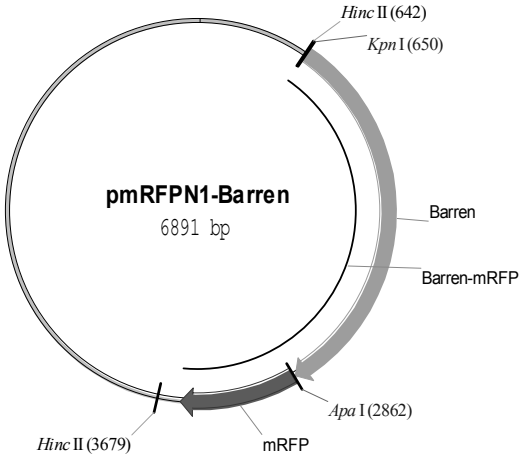

Barren cDNA was amplified by PCR from the cDNA (RE48802, BDGP) as described above.

The digested PCR product was cloned into KpnI/ApaI cut mRFPN1 vector.

Proper Barren-mRFP1 fusion was confirmed by sequencing analysis.

pRmHa3-mRFPN1-Barren

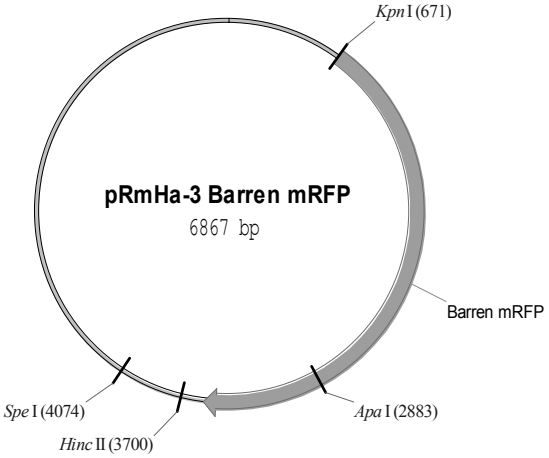

Barren-mRFP1 insert was obtained from the pmRFPN1-Barren vector,
cut with KpnI and HincII and cloned into the KpnI/HincII pRmHa-3 vector.

Proper ligation was confirmed by several restriction enzymes digestions.

pUASP - Barren-EGFP

The Barren-EGFP insert was obtained from the pRmHa-3-Barren-EGFP vector digested with KpnI and SpeI.

This was cloned into a pUASP vector cleaved with KpnI and XbaI.

(SpeI and XbaI have compatible cohesive ends)

pUASP - Barren-mRFP1

The Barren-mRFP1 insert was obtained from the pRmHa-3-Barren-mRFP1 vector digested with KpnI and SpeI.
This was cloned into a pUASP vector cleaved with KpnI and XbaI.
(SpeI and XbaI have compatible cohesive ends)

pUASP – EGFP- Barren

The EGFP-Barren insert was obtained from the pMTV-EGFP-Barren vector, digested with XmnI (blunt) and SpeI. This insert was cloned in the vector digested with KpnI (filled to blunt with klenow) and digested with XbaI.
(SpeI and XbaI have compatible cohesive ends)

pRmHa-3 DmCAP-H2(PC)-EGFP

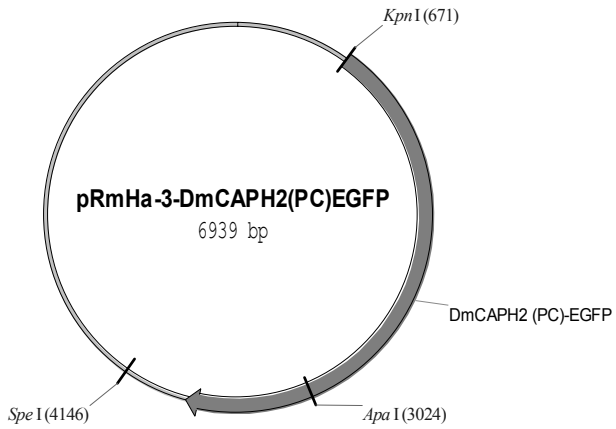

DmCAP-H2(PC) cDNA was amplified by PCR from the cDNA (SD09295, BDGP). Primers:

KpnI
ATAT GGTACC **ATG** TCGGACGA
CAAGCGCTTCAACGCGGCGG

ApaI
TAAT GGGCCC A **CTT** CAGGCGGG
CTGTCGATGCCAATGATGAGC

The digested PCR product was cloned into KpnI/ApaI cut pRmHa3-Barren-EGFP (removes Barren insert). Proper DmCAP-H2-EGFP fusion was confirmed by sequencing analysis.

Note: This cDNA is probably not a full length one as other EST predict the formation of two other isoforms of the protein which start in the exon 1 and therefore have ~ 180 a.a. more.

pRmHa-3 DmCAP-H2(PC)-EGFP

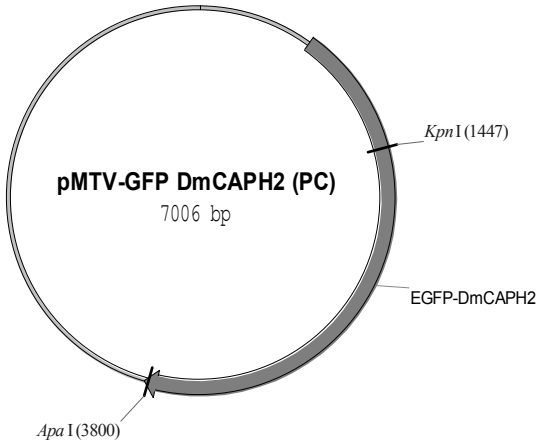

DmCAP-H2 cDNA was amplified by PCR from the cDNA (SD09295, BDGP) as described above.

The digested PCR product was cloned into KpnI/ApaI cut pMTV-EGFP vector.

Proper EGFP-CAP-H2 fusion was confirmed by sequencing analysis.

pUASP – DmCAP-H2-EGFP

The CAP-H2-EGFP insert was obtained from the pRmHa-3-CAP-H2-EGFP vector digested with KpnI and SpeI.

This was cloned into a pUASP vector cleaved with KpnI and XbaI.

(SpeI and XbaI have compatible cohesive ends)

pET 23a DmCAPH2 (PC) $_{1\text{-}419}$ $(His)_6$

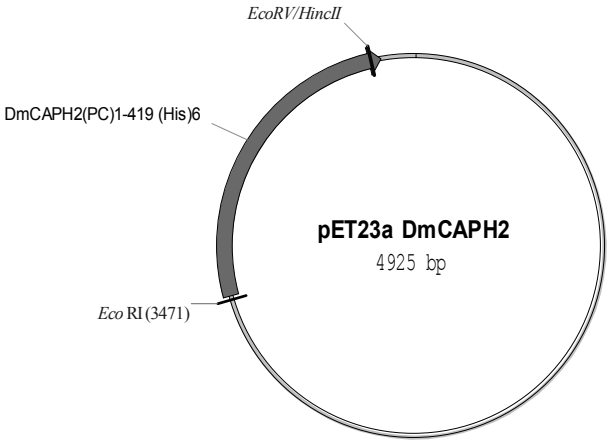

The insert DmCAP-H2 was obtained from the pRmHa3-DmCAP-H2-EGFP vector after digestion with EcoRI and EcoRV (blunt).

The insert was cloned into EcoRI/HincII cut pet23a vector (novagen).

Proper cloning was confirmed by sequencing analysis (T7promoter and T7terminator).

Appendix 4

Supplementary movies legends

Movie 1.2: Mitotic division of a control S2 cell stably expressing GFP-Tubulin recorded by time lapse fluorescence microscopy. Times are relative to nuclear envelope breakdown.

Movie 1.2: Mitotic division of a Barren/CAP-H depleted S2 cell stably expressing GFP-tubulin recorded by time lapse fluorescence microscopy. Times are relative to nuclear envelope breakdown. Note that this cell spends an extended period in prometaphase/metaphase state, before undergoing anaphase.

Movie 1.3: Mitotic division of a control S2 cell stably expressing GFP-Histone H2B recorded by time lapse fluorescence microscopy. Note that chromosomes rapidly congress to a well defined metaphase plate and initiate anaphase. Times are relative to anaphase onset.

Movie 1.4: Mitotic division of a Barren/CAP-H depleted S2 cell stably expressing GFP-Histone H2B recorded by time lapse fluorescence microscopy. This movie shows that DNA bridges are observed as soon as the two chromatin masses begin separation at anaphase. We never observed well defined sister chromatids at any stage of mitosis. Times are relative to anaphase onset.

Movie 1.5: Mitotic division of a Barren/CAP-H depleted S2 cell stably expressing GFP-Histone H2B recorded by time lapse fluorescence microscopy. This movie shows cell attempting anaphase onset while a large DNA bridge forms leading to regression chromosome segregation and formation of a polyploid cell. Times are relative to anaphase onset.

Movie 2.1: *In vivo* analysis of syncytial nuclear divisions in Barren-EGFP and HisH2Av-mRFP1 expressing embryos. This movie shows an embryo in which Barren-EGFP (green) and HisH2Av-mRFP1 (red) were maternally deposited undergoing three consecutive syncytial embryonic divisions (mitosis 11-13). Note that Barren-EGFP co-localizes with chromatin throughout mitosis.

Movie 2.2: *In vivo* analysis of post-blastoderm nuclear divisions in Barren-EGFP and HisH2Av-mRFP1 expressing embryos. This movie shows mitotic domains from a post-blastodermal embryo co-expressing Barren-EGFP (green) and HisH2Av-mRFP1 (red). Note than Barren-EGFP is associated with chromatin throughout mitosis.

Movie 2.3: *In vivo* analysis of the initial stages of a syncytial nuclear division in Barren-EGFP and Cid-mRFP1 expressing embryos. This movie shows an embryo in which Barren-EGFP (green) and Cid-mRFP1 (red) were maternally deposited undergoing mitosis 12. During interphase, Barren-EGFP

is excluded from the nuclear space. Cid-mRFP detects dot like structures located at the apical site of the nucleus corresponding to the centromeres. While the nuclei enter prophase, Barren-EGFP starts to be detectable inside the nuclear area specifically at the centromeric region (indicated by Cid-mRFP). Later on, Barren-EGFP signal is detectable throughout the nuclear area, suggesting Barren-EGFP localization all over chromosomal arms.

Movie 2.4: *In vivo* analysis of a syncytial division in DmSMC4-EGFP and HisH2Av-mRFP1 expressing embryos. This movie shows an embryo in which DmSMC4-EGFP (green) and HisH2Av-mRFP1 (red) were maternally deposited undergoing one syncytial embryonic division. Note that SMC4-EGFP co-localizes with chromatin throughout mitosis. However, segregate problems can be observed in some of the dividing figures, with chromatin bridges linking segregating chromatids.